Mechanism and Inhibition of Hypochlorous Acid-Mediated Cell Death in Human Monocyte-Derived Macrophages

---

A thesis
submitted in partial fulfilment
of the requirements for the Degree
of
Doctor of Philosophy
in Biochemistry

at the
University of Canterbury
New Zealand

Ya-ting (Tina) Yang

2009

TABLE OF CONTENTS

LIST OF FIGURES

List of Tables

ABBREVIATIONS

1,3-PGA	1,3-diphospho-glycerate
7,8-NP	7,8-Dihydroneopterin
γ-GCS	γ-Glutamylcysteine synthetase
A23187	4-bromo-calcium ionophore A23187
AAPH	2,2'-Azobis (2-amidino propane) dihydrochloride
ACAT	Acyl coenzyme A:cholesterol acyltransferase
Ac-DEVD-AMC	Acetyl-Asp-Glu-Val-Asp-7-Amido-4-methylcoumarin
AD	Alzheimer's disease
AO	Acridine orange
ADP	Adenosine diphosphate
AIF	Apoptosis inducing factor
AMP	Adenine monophosphate
ANOVA	Analysis of variance
ANT	Adenine nucleotide translocator
AP-1	Activator protein-1
Apaf-1	Apoptotic activating factor-1
AP-1 CAT	Activation protein-1 chloramphenicol acetyltransferase
APCs	Antigen presenting cells
ApoE	Apolipoprotein E
ATP	Adenosine triphosphate
BCA	Bicinchoninic acid
BH_4	5,6,7,8-tetrahydrobiopterin
BHT	Butylated hydroxytoluene
BSA	Bovine serum albumin
Ca^{2+}	Calcium ion
$CaCl_2$	Calcium chloride
CARD	Caspase recruitment domain
CCR2	Monocyte chemotactic protein receptor
cGMP	Cyclic guanosine monophosphate
CHAPS	3-[(3-Cholamidopropyl)dimethylammonio]-1-propanesulfonate
Cl^-	Chloride ion

CNTP	3-carboxylato-4-nitrothiophenolate
CSA	Cyclosporin A
CyP-D	Cyclophilin-D
dATP	Deoxyadenosine triphosphate
DDs	Death domains
DED	Death-effector domain
DEM	Diethyl maleate
DEVD	Asp-Glu-Val-Asp
DHE	Dihydroethidium
DIC	Differential interference contrast
DMEM	Dulbecco's modified eagle medium
DMSO	Dimethyl sulphoxide
DNA	Deoxyribonucleic acid
DOPA	3,4-dihydroxy-L-phenylalanine
DTT	1,4-Dithiothreitol
DTNB	5,5'-Dithiobis-2-nitrobenzoic acid
EBSS	Earle’s balanced salt solution
ECM	Extracellular matrix
ECs	Endothelial cells
EDTA	Ethylenediaminetetraacetic acid
EGTA	Ethlylene glycol-bis(2-aminoethylether)-N,N,N’,N’-tetracetic acid
ELISA	Enzyme-linked immunosorbant assay
EndoG	Endonuclease G
ER	Endoplasmic reticulum
ERK	Extracellular signal-regulated kinase
ETC	Electron transport chain
FADD	Fas-associated death domain
Fas	Fibroblast associated cell surface
FLIP	FLICE-inhibitory protein
Fluo-3-AM ester	Fluo-3-acetoxymethyl ester
FITC	Fluorescein isothiocyanate
GAP	Glyceraldehyde-3-phosphate
GAPDH	Glyceraldehydes-3-phosphate dehydrogenase
GM-CSF	Granulocyte-macrophage colony stimulating factor
GPXs	Glutathione peroxidases

GSH	Glutathione
GSSG	Disulfides
GTP	Guanosine triphosphate
GR	Glutathione reductase
GRXs	Glutaredoxins
GST	Glutathione S-transferase
H^+	Protons
H_2O_2	Hydrogen peroxide
HCl	Hydrochloric acid
HDL	High density lipoprotein
HEPES	4-(2-hydroxyethyl)-1-piperazineethane-sulfonic acid
HIHS	Heat-Inactivated Human Serum
HIV	Human immunodeficiency virus
HMDM	Human monocyte derived macrophage
HOCl	Hypochlorous acid
HPLC	High performance liquid chromatography
HRP	Horseradish peroxidase
IAP	Inhibitors of apoptosis
IκBα	Intracellular inhibitor
ICAM-1	Inter-Cellular Adhesion Molecule-1
IFN-γ	Interferon-γ
IL-12	Interleukin-12
IL-18	Interleukin-18
IMM	Inner mitochondrial membrane
IMS	Inter-membrane space
iNOS	Inducible nitric oxide synthase
JNKs	c-Jun NH2-terminal kinases
LDL	Low density lipoprotein
LPL	Lipoprotein lipase
LOs	Lipoxygenase
MCP-1	Monocyte chemotactic protein
MMPS	Matrix metalloproteinases
MHC	Major histocompatibility complex
mmLDL	Minimally modified LDL
MOMP	Mitochondrial outer membrane permeabilisation

MOPS	4-Morpholine-propanesulfonic acid
MPO	Myeloperoxidase
MPT	Mitochondrial permeability transition
MTT	3-[4,5-Dimethylthiazol-2-yl]-2,5-diphenyl-tetrazolium bromide
NAC	N-acetylcysteine
NAD^+	Nicotinamide adenine dinucleotide
$NADP^+$	Nicotinamide adenine dinucleotide phosphate
NaOH	Sodium hydroxide
NMDA	N-methyl-d-aspartate
NF-κβ	Nuclear factor-κβ
NO	Nitric oxide
NOS	Nitric oxide synthase
$O_2^{\bullet-}$	Superoxide anion
^-OCl	Hypochlorite
$OH^\bullet$	Hydroxyl radical
OMM	Outer mitochondrial membrane
$ONOO^-$	Peroxynitrite
oxLDL	Oxidised LDL
PBS	Phosphate Buffered Saline
PCA	Perchloric acid
PDTC	Pyrrolidine dithiocarbamate
PECAM-1	Platelet endothelial cell adhesion molecule-1
PI	Propidium iodide
PKC	Protein kinase C
PMA	Phorbol 12-myristate 13-acetate
PRXs	Peroxiredoxins
PS	Phosphatidylserine
PTPS	6-pyrovoyltetrahydropterin synthase
$RO_2^\bullet$	Peroxyl radical
ROS	Reactive oxygen species
RS	Reactive species
RSG	GSH S-conjugates
RPMI	Roswell Park Memorial Institute 1640
RyR2	Ryanodine receptor 2

SAPK	Stress-activated protein kinase
SDS	Sodium dodecyl sulphate
SDS-PAGE	Sodium dodecyl sulfate polyacrylamide gel electrophoresis
SMCs	Smooth muscle cells
SOD	Superoxide dismutase
SR	Sarcoplasmic reticulum
SRA	Scavenger receptors class A
TBA	2-Thiobarbituric acid
tBid	Truncated form of Bid
TCA	Trichloroacetic acid
TFA	Trifluoroacetic acid
TIMPs	The inhibitors of metalloproteinases
TMRM	Tetramethylrhodamine methyl ester
TNF- α	Tumor necrosis factor-α
TNFR	Tumor necrosis factor receptor
TRADD	TNF receptor-associated death domain
TRAIL	TNF-related apoptosis-inducing ligand
TRXs	Thioredoxins
VCAM-1	Vascular cell adhesion molecule-1
VDAC	Voltage-dependent anion channel
VSMCs	Vascular smooth muscle cells
VLDL	Very low density lipoprotein
WAF1/CIP1	wild-type activating fragment-1/cyclin-dependent kinase inhibitory protein-1

ABSTRACT

Hypochlorous acid (HOCl) is a powerful oxidant produced by activated phagocytes at sites of inflammation to kill a wide range of pathogens. Yet, it may also damage and kill the neighbouring host cells. The abundance of dead macrophages in atherosclerotic plaques and their colocalization with HOCl-modified proteins implicate HOCl may play a role in killing macrophages, contributing to disease progression. The first part of this research was to investigate the cytotoxic effect and cell death mechanism(s) of HOCl on macrophages. Macrophages require efficient defense mechanism(s) against HOCl to function properly at inflammatory sites. The second part of the thesis was to examine the antioxidative effects of glutathione (GSH) and 7,8-dihydroneopterin (7,8-NP) on HOCl-induced cellular damage in macrophages. GSH is an efficient scavenger of HOCl and a major intracellular antioxidant against oxidative stress, whereas 7,8-NP is secreted by human macrophages upon interferon-γ (IFN-γ) induction during inflammation and can also scavenge HOCl.

HOCl caused concentration-dependent cell viability loss in human monocyte derived macrophage (HMDM) cells above a specific concentration threshold. HOCl reacted with HMDMs to cause viability loss within the first 10 minutes of treatment, and it posed no latent effect on the cells afterwards regardless of the HOCl concentrations. The lack of caspase-3 activation, rapid influx of propidium iodide (PI) dye, rapid loss of intracellular ATP and cell morphological changes (cell swelling, cell membrane integrity loss and rupture) were observed in HMDM cells treated with HOCl. These results indicate that HOCl caused HMDM cells to undergo necrotic cell death. In addition to the loss of intracellular ATP, HOCl also caused rapid loss of GAPDH enzymatic activity and mitochondrial membrane potential, indicating impairment of the metabolic energy production. Loss of the mitochondrial membrane potential was mediated by mitochondrial permeability transition (MPT), as blocking MPT pore formation using cyclosporin A (CSA) prevented mitochondrial membrane potential loss.

HOCl caused an increase in cytosolic calcium ion (Ca^{2+}) level, which was due to both intra- and extra-cellular sources. However, extracellular sources only contributed significantly above a certain HOCl concentration. Preventing cytosolic Ca^{2+} increase significantly inhibited HOCl-induced cell viability loss. This suggests that cytosolic Ca^{2+} increase was associated with HOCl-induced necrotic cell death in HMDM cells, possibly via the activation of Ca^{2+}-dependent calpain cysteine proteases. Calpain inhibitors

prevented HOCl-induced lysosomal destabilisation and cell viability loss in HMDM cells. Calpains induced HOCl-induced necrotic cell death possibly by degrading cytoskeletal and other cellular proteins, or causing the release of cathepsin proteases from ruptured lysosomes that also degraded cellular components. The HOCl-induced cytosolic Ca^{2+} increase also caused mitochondrial Ca^{2+} accumulation and MPT activation-mediated mitochondrial membrane potential loss. MPT activation, like calpain activation, was also associated with the HOCl-induced necrotic cell death, as preventing MPT activation completely inhibited HOCl-induced cell viability loss. The involvement of both calpain activation and MPT activation in HOCl-induced necrotic cell death in HMDM cells implies a cause and effect relationship between these two events.

HMDM cells depleted of intracellular GSH using diethyl maleate showed increased susceptibility towards HOCl insult compared to HMDM cells with intact intracellular GSH levels, indicating that intracellular GSH played an important role in protecting HMDM cells against HOCl exposure. Intracellular GSH level in each HMDM cell preparation directly correlated with HOCl concentration required to kill 50% of population for each cell preparation, indicating intracellular GSH concentrations determine the efficiency of GSH in preventing HOCl-induced damage to HMDM cells. Intracellular GSH and cell viability loss induced by 400 μM HOCl were significantly prevented by 300 μM extracellular 7,8-NP, indicating that added 7,8-NP is an efficient scavenger of HOCl and out-competed intracellular GSH for HOCl. The amount of 7,8-NP synthesized by HMDM cells upon IFN-γ induction was too low to efficiently prevent HOCl-mediated intracellular GSH and cell viability loss.

HOCl clearly causes HMDM cells to undergo necrosis when the concentration exceeds the intracellular GSH concentrations. Above this concentration HOCl causes oxidative damage to the Ca^{2+} ion channels on cell and ER membranes, resulting in an influx of Ca^{2+} ions into the cytosol and possibly the mitochondria. The rise in Ca^{2+} ions triggers calpain activation, resulting in the MPT-mediated loss of mitochondrial membrane potential, lysosomal instability and cellular necrosis.

1 INTRODUCTION

1.1 Overview

It has been well documented that reactive oxygen species (ROS) play important roles in killing invading pathogens and in immune response. Yet, increasingly more literature has implicated that overproduction of ROS can cause extensive damage to surrounding tissues, leading to progression of a range of inflammatory diseases; including atherosclerosis, Alzheimer's and Parkinson's diseases.

One important ROS present during inflammation is hypochlorous acid (HOCl), which is secreted by phagocytes including neutrophils, monocytes and certain subtypes of macrophages via myeloperoxidase (MPO) enzyme. HOCl shows high reactivity with a range of biomolecules, including proteins, phospholipids and nucleic acids, which makes it an efficient bactericidal agent. However, it also means that HOCl is capable of damaging the surrounding host cells at inflammatory sites. For instance, dead macrophages that contributed to disease progression of atherosclerosis, were found colocalizing with HOCl-modified proteins and MPO in atherosclerotic plaques, implicating a role for HOCl in killing macrophages and atherosclerotic disease progression.

For macrophages to survive in the inflammatory environment, they must be able to neutralise ROS and other damaging biomolecules that they are exposed to. Glutathione (GSH) is considered the major intracellular antioxidant against ROS and is an efficient scavenger of HOCl. 7,8-dihydroneopterin (7,8-NP), synthesized by macrophages upon interferon-γ induction during inflammation, was previously found to scavenge HOCl. It is therefore possible that GSH and 7,8-NP play important roles in protecting macrophages against HOCl insult.

This research will examine the cell death mechanism ensued in human monocyte-derived macrophage (HMDM) cells after HOCl exposure, and determine whether GSH and 7,8-NP act as efficient antioxidants for protecting HMDM cells against HOCl insult.

1.2 Inflammation

Inflammation is the localised protective response of tissues against microbial infection or damaged host cells, involving the removal of such irritants by phagocytic cells. There are two types of inflammation: acute and chronic inflammation. When animal tissues are injured, an acute inflammatory response develops. This is characterised by the rapid migration of neutrophils from the circulation into inflamed areas, through the endothelial cell (EC) monolayer lining the blood vessels, in response to chemotactic factors formed in the inflamed areas. Subsequently, the invading microbes and dead or damaged cells are removed by neutrophils via phagocytosis. At a later stage of inflammation, monocytes are recruited to the inflamed areas and undergo differentiation into macrophages, regulated by the chemotactic factors and cytokines produced by the activated neutrophils and endothelial cells. Macrophages show increased contents of lysosomal enzymes, metabolic activity, motility and phagocytic and microbicidal capacity compared to monocytes. The inflammatory event usually ends here. However, if the bacteria are not completely eliminated or the tissue injury continues, chronic inflammation can develop (Halliwell and Gutteridge, 2007).

1.3 Atherosclerosis as an inflammatory disease

Atherosclerosis is a disease with inflammation mediators playing crucial roles in its progression and so is now recognised as a chronic inflammatory disease (see below). This disease is characterised by a local thickening of the artery wall, resulting from the accumulation of lipids, dead cells and fibrous elements in the intima. Complications such as cardiovascular disease, heart infarction and stroke may then occur, which are the most common causes of death in developed countries (Halliwell & Gutteridge, 2007).

Atherosclerosis is a progressive disease, beginning with changes to endothelial cells (ECs) that allow the attraction, adherence and transmigration of monocytes through the endothelium (Ross, 1993) (**Figure 1.1**). The changes can be initiated by the accumulation of low density lipoprotein (LDL) in the intima, which is oxidatively modified by reactive oxygen species (ROS) produced in ECs, resident macrophages or smooth muscle cells (SMCs) (Lusis, 2000; Steffens and Mach, 2004; Glass and Witztum, 2001) (See also **section 1.4**). The resulting “minimally oxidised” LDL (mmLDL) stimulates the overlying ECs to produce a number of pro-inflammatory molecules, chemotactic factors and growth

factors, which assist in recruiting the circulating monocytes and T cells into the intima and in the differentiation of monocytes into macrophages. Once mmLDL is oxidised further (now referred to as oxidised LDL or oxLDL), it is recognised and taken up by macrophages via the macrophage scavenger receptors, especially SR-A and CD36 (Glass and Witztum, 2001). This leads to the accumulation of cholesterol esters in the macrophage cytoplasm and subsequently the formation of foam cells (lipid-laden macrophages), which are the major component of the early stage arterial lesion often described as a fatty streak.

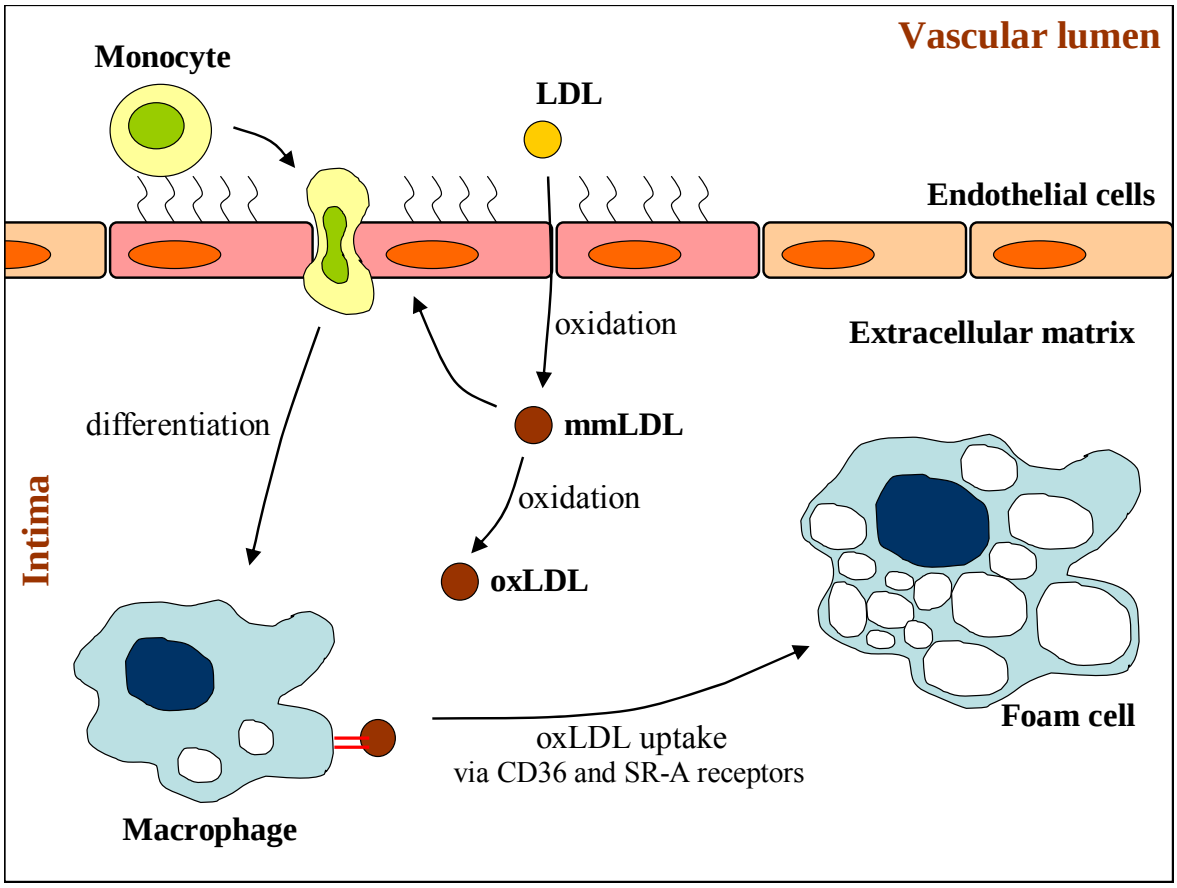

Figure 1.1 Initiating events in the development of a fatty streak lesion.
LDL is oxidatively modified in the sub-endothelial space to mmLDL, which is further oxidised to generate oxLDL. Endothelial cells were stimulated to express adhesion and chemotatic molecules by mmLDL, inflammatory cytokines and oxLDL, allowing monocytes to attach to endothelial cells and migrate into the intima through the tight junctions. The intimal monocytes then differentiate into macrophages, which express scavenger receptors, CD36 and SR-A. These scavenger receptors promote oxLDL uptake. The oxLDL cholesterol being taken up is subject to esterification and storage in lipid droplets, leading to foam cell formation.

In the intima, T cells and macrophages can be activated via many ways (Hansson *et al.*, 2006). For instance, T cells are activated by their ligation to the antigens (such as oxLDL) that are bound to the major histocompatibility complex (MHC) molecules on the surface of macrophages. The activated T cells then release pro-inflammatory cytokines such as interferon-γ (IFN-γ) and tumor necrosis factor (TNF), which stimulate the activation of macrophages. Interaction between CD40 receptor on T cells and CD40 on macrophages can also activate T cells. The end result of T cell and macrophage activation is the secretion of cytokines, growth factors and reactive species, which facilitate the recruitment of more inflammatory cells, migration of SMCs to the intima and proliferation of SMCs. These events allow a fatty streak to develop into a fibrous plaque. This more complicated plaque consists of a fibrous cap containing mostly SMCs and extracellular matrix (ECM) (Ross, 1999). ECM is composed mainly of collagen, elastin, proteoglycans, glycoproteins, fibrin and other forms of collagen (Halliwell and Gutteridge, 2007; Stary *et al.*, 1995). This fibrous cap covers an area rich in macrophages, SMCs and T cells. Often there is a deeper necrotic core, which contains debris from dead cells, extracellular lipid deposits and cholesterol crystals (Glass & Witztum, 2001). Calcification and neovascularisation may occur to make fibrous plaques more complicated and less stable (Lusis, 2000).

Plaque ruptures expose plaque lipids and tissue factor to blood components, initiating the coagulation cascade, platelet adherence, thrombosis and hence leads to the onset of an acute ischaemic event. This event is more likely to occur in lesions heavily infiltrated by foam cells, and those with thin fibrous caps and large necrotic cores (Davies *et al.*, 1993; Lee and Libby, 1997). Activated macrophages can contribute to thinning of fibrous caps by producing matrix metalloproteinases (MMPs), which degrade the connective tissue that strengthens the fibrous caps (Galis *et al.*, 1994; Brown *et al.*, 1995). The oxidised lipid in the necrotic core will be pro-inflammatory and cytotoxic, promoting further destabilisation of the plaque.

The appearance of macrophages and lymphocytes within atherosclerotic lesions exemplifies a site where both innate and adaptive immunity contribute towards the disease progression. The immediate site of plaque rupture or superficial erosion is rich in macrophages and to a lesser extent T lymphocytes, with abundant expression of HLA-DR antigens on both the inflammatory cells and the adjacent SMCs (Libby & Hansson, 1991; van der Wal *et al.*, 1994). HLA-DR antigens are class II major histocompatibility complex (MHC II) membrane bound glycoproteins that play an important role in the regulation of

immune response. The detection of inflammatory markers and antibodies in patients provides additional support for the inflammatory nature of the atherosclerotic lesion. Xu *et al.,* (1993) demonstrated a strong correlation between anti-heat shock protein 65 antibodies and carotid atherosclerosis. In addition, the level of the inflammatory marker C-reactive protein is elevated in early and late stages of atherosclerotic lesions (Patrick and Uzick, 2001) and in most of the patients with a diagnosis of unstable angina. Neopterin, another inflammatory marker, is also elevated in patients with vascular disease (Schumacher *et al*., 1992; Tatzber *et al*., 1991). IFN-γ is a molecule that stimulates the synthesis of 7,8-dihydroneopterin (the reduced form of neopterin) from macrophages, and it is detected in elevated levels in atherosclerotic plaques of both humans and mice (Hansson *et al*., 1989a; Zhou *et al*., 1998) (see **section 1.6.2**). Various infectious agents have also been shown to initiate or promote inflammatory atherogenesis. *Chlamydia pneumonia, Helicobacter pylori* and cytomegalo-virus have been identified in cardiovascular atheroma (Osterud & Bjorklid, 2003; Torgano *et al*., 1999).

1.4 ROS and atherosclerosis

ROS appear to play important roles in the development of atherosclerosis. It is a collective term that includes not only the oxygen radicals with unpaired electron(s) such as superoxide ($O_2^{\bullet -}$), peroxyl ($RO_2^{\bullet}$) and hydroxyl radicals ($OH^{\bullet}$), but also some non-radical derivatives such as hydrogen peroxide (H_2O_2), hypochlorous acid (HOCl) and peroxynitrite ($ONOO^-$) (Halliwell and Gutteridge, 2007). There are a number of sources of ROS that contribute to the progression of atherosclerosis. MPO enzyme is responsible for the HOCl production (Glass and Witztum, 2001), and both MPO enzyme and HOCl (detected as 3-chlorotyrosine) have been found colocalising in atherosclerotic plaques (Daugherty *et al.*, 1994; Malle *et al*., 2000; Sugiyama *et al*., 2001). Inducible nitric oxide synthase (iNOS) catalyses the generation of NO, which contributes to LDL oxidation *in vivo* (Glass and Witztum, 2001). Inhibitors of iNOS have been shown to decrease atherosclerosis in mice (Detmers *et al*., 2000).

ROS can contribute to lesion formation in many ways. Depending on the types and availability, ROS can oxidise lipid or protein (apolipoprotein B-100) components of LDL, hence transforming LDL to a high uptake form that is internalised by macrophages and resulting in foam cell formation. OxLDL taken up by macrophages may eventually impose

an oxidative stress on these cells and cause some foam cells to die by apoptosis or necrosis, which contributes to necrotic core formation. H_2O_2 can signal growth factor generation and cell proliferation, which have long been implicated in atherosclerosis (Cromheeke *et al.*, 1999; Stocker and Keaney, 2004). Moreover, ROS can induce the loss of nitric oxide, which is thought to be anti-atherogenic by inhibiting LDL peroxidation and deterring thrombosis, phagocyte adhesion to endothelium and nuclear factor κB (NF-κB) activation (Halliwell and Gutteridge, 2007). ROS can also cause endothelial dysfunction (Cai and Harrison, 2000) and destabilise atherosclerotic plaques. The presence of oxidation products of lipids and (lipo)proteins in atherosclerotic plaques further support the roles ROS play in the lesion development (Stocker and Keaney, 2004; Leeuwenburgh *et al.*, 1997) (see **section 1.5.4**).

1.5 Hypochlorous acid (HOCl)

Hypochlorous acid (HOCl) is a powerful 2-electron oxidizing agent and a weak acid with pKa approximately 7.5, hence it is present in equal mixture with its conjugate base hypochlorite ($^-$OCl) at pH 7.4. For the purpose of simplicity, HOCl/$^-$OCl will be referred to as HOCl in this thesis. HOCl also readily decomposes to liberate chlorine (Cl_2) gas. However, this only occurs at much lower pH (Pullar *et al.*, 2000). It has important antibacterial properties, but excessive or mis-directed production of HOCl has been implicated in several diseases, including atherosclerosis, arthritis and some cancers associated with inflammation (Klebanoff, 2005).

1.5.1 Sources of HOCl and phagocytosis

Phagocytes such as neutrophils, monocytes and macrophages play a crucial role in host defenses against microbial pathogens via phagocytosis. The ROS generated in these cells, including $O_2^{\bullet-}$, $OH^{\bullet}$, H_2O_2 and HOCl (**Figure 1.2**), together with microbicidal peptides and proteases, are proposed to constitute their antimicrobial arsenal. HOCl is suggested to be one of the major ROS generated in neutrophils for killing (Jiang *et al.*, 1997; Hazen *et al.*, 1996b; Wagner *et al.*, 1986; Foote *et al.*, 1983; Albrich *et al.*, 1981) or inhibiting cell growth (Mckenna and Davies, 1988) of phagocytosed bacteria. It is also produced in monocytes and certain types of macrophages (Halliwell and Gutteridge, 2007).

When coated with opsonins (generally complement or antibody), microorganisms bind to specific receptors on the surface of the neutrophil. Invagination of the neutrophil cell membrane then occurs until the microorganism is completely enclosed in an intracellular phagosome. This is followed by a burst of oxygen consumption, known as the respiratory burst. NADPH oxidases then use electrons derived from intracellular NADPH to convert most of the extra oxygen consumed to $O_2^{\bullet -}$. Concurrently, cytoplasmic granules fuse with the phagosomal membrane causing more ROS generation including HOCl production, which is catalysed by myeloperoxidase (MPO) enzyme (**Figure 1.2**). The degranulation and the generation of ROS result in the killing and degradation of the engulfed bacteria.

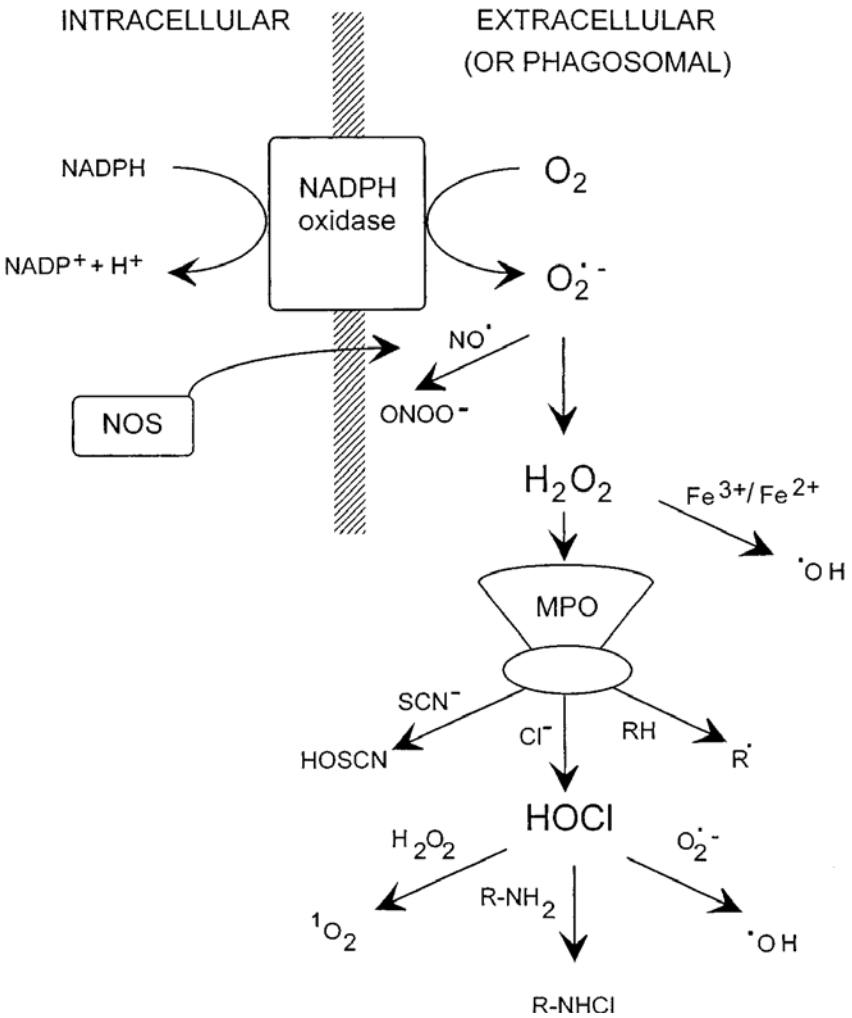

Figure 1.2 Possible ROS generating reactions with stimulated neutrophils.
During respiratory burst, most of the oxygen consumed is converted to $O_2^{\bullet -}$ via NADPH oxidase catalysis. $O_2^{\bullet -}$ then undergoes a dismutation reaction to form H_2O_2. HOCl is produced in the presence of MPO and chloride ions (Cl^-). $OH^\bullet$ can be formed via the $O_2^{\bullet -}$-driven Fenton reaction between H_2O_2 and an appropriate transition metal catalyst, and via the reaction of HOCl with $O_2^{\bullet -}$. Singlet oxygen could theoretically be produced from the reaction of HOCl and H_2O_2. Chloramines (R-NHCl) are generated indirectly through the reaction of HOCl with amines. HOCl can also oxidize SCN^- into hypothiocyanite ($OSCN^-$) which also has antibacterial effects. This scheme is adapted from Hampton *et al.* (1998b).

1.5.1.1 NADPH oxidase

NADPH oxidase is present in neutrophils, eosinophils, monocytes and macrophages. It is also found in vascular cells, but not identical to the ones found in leukocytes (Klebanoff, 2005). This oxidase is in an inactive form in resting cells as two membrane-bound and four cytosolic components (El-Benna *et al*., 2005). The NADPH binding site is located within the membrane-bound components. During activation, the cytoplasmic components of the NADPH oxidase form a complex with the membrane-bound components.

While phagocytic stimuli cause ROS production largely within the phagosome, soluble stimuli such as immune complexes, complement protein C5a, N-formyl peptides and tumour necrosis factor (TNF-α) cause the activation of NADPH oxidase over the surface of the plasma membrane (Goldstein *et al.*, 1975; Nathan, 1987). This can lead to the release of oxidants and granule proteins into the extracellular space. This extracellular release of products from activated neutrophils also occurs through a process called "frustrated phagocytosis", where the neutrophil is in contact with a non-ingestible, immune-complex coated surface (Chatham *et al.*, 1994; Blackburn *et al.*, 1995).

1.5.1.2 Myeloperoxidase (MPO)

MPO is a tetrameric and heavily glycosylated heme protein with a molecular weight of approximately 150 kDa. It is composed of two identical disulfide-linked dimers, each of which possesses a protoporphyrin-containing 59-64 kDa heavy subunit and a 14 kDa light subunit (Podrez *et al*., 2000). MPO is sequestered in azurophil granules of neutrophils, where it comprises 2 to 5% of total neutrophil proteins (Halliwell and Gutteridge, 2007). It is also present in monocytes and in certain subtypes of macrophages and has been found upregulated in disease state brain cells (Green *et al.*, 2004; Nagra *et al*., 1997).

Active MPO can lead to the formation of a range of oxidation products by catalysing the oxidation of a range of substrates and by the reaction of the oxidation products with other substrates. MPO uses H_2O_2 to oxidise halide ions such as chloride, bromide and iodide to form hypochlorous, hypobromous and hypoiodous acid, respectively (Harrison and Schultz, 1976; Halliwell and Gutteridge, 2007) (**Figure 1.3**). MPO can also oxidise thiocyanate anions into hypothiocyanite (Hampton *et al.*, 1998b). However, the high chloride ion concentrations in phagocyte cytoplasm and extracellular fluids suggest that HOCl is the major physiological product of MPO activity (Thomas and Fishman, 1986). Indeed, 28 to

70% of the H_2O_2 produced by neutrophils has been detected as HOCl (Foote *et al*., 1983; Weiss *et al.*, 1982). HOCl can subsequently react with $O_2^{\bullet-}$, amines and H_2O_2 to generate $OH^{\bullet}$, chloramines and singlet oxygen, respectively (Klebanoff, 2005). MPO also uses H_2O_2 to oxidize a variety of aromatic compounds (RH) (**Figure 1.3**), tyrosine residues (Klebanoff, 2005) and nitrite (Eiserich *et al*., 2002) to generate their respective radicals.

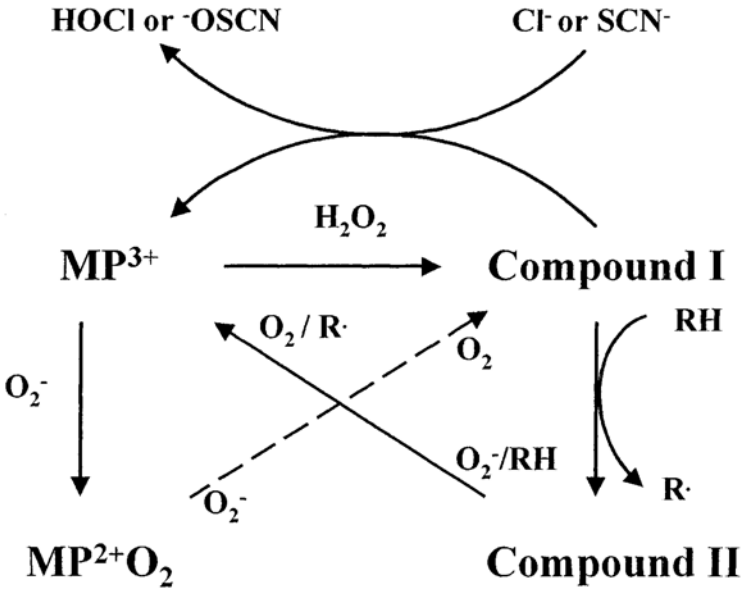

Figure 1.3 Reactions of MPO.
H_2O_2 reacts with the ferric iron of MPO (MP^{3+}) to form the redox intermediate compound I. Compound I oxidizes a halide (chloride, thiocyanate or bromide) by a single 2-electron transfer to produce the respective hypohalous acids (HOCl, HOSCN or HOBr), regenerating the native MP^{3+} state. MPO also oxidizes numerous organic substrates (RH) by two successive 1-electron transfers involving the enzyme intermediates, compound I and compound II. Compound II can be reduced to the active, native MP^{3+} state by $O_2^{\bullet-}$, as well as by a number of other reducing agents. $O_2^{\bullet-}$ can also react with the native MPO to form an unstable compound III (Winterbourn *et al.*, 1985), which is turned over by a second reaction with superoxide. The scheme is adapted from Hampton *et al.* (1998b).

MPO appears critical for oxidative killing of microorganisms in experimental systems. Neutrophils isolated from the blood of MPO-deficient individuals were inefficient in killing a variety of microorganisms (Lehrer and Cline, 1969; Kitahara *et al*., 1981). In addition, inhibitors of MPO such as azide, cyanide and salicylhydroxamic acid impair killing by normal cells (Klebanoff, 1970; Humphreys *et al.*, 1989). Furthermore, the cytoplasm of neutrophils that lack granule enzymes but generate H_2O_2, only kill bacteria if they are coated with MPO before ingestion (Hampton *et al.*, 1998b).

Following phagocytosis, neutrophils undergo degranulation and MPO is rapidly released into the phagosome. However, leakage or secretion of MPO to the outside of the cell through incomplete closure of the phagosome or "frustrated phagocytosis" also occurs (Vissers *et al.*, 1985) (see also **section 1.5.1.1**). This leakage of MPO can induce damage to surrounding tissue, and is thought to contribute to the pathogenesis of several diseases (Malle *et al.*, 2000; Daugherty *et al.*, 1994; Baldus *et al*., 2002).

1.5.2 Biological reactions of HOCl

HOCl is not known to be a substrate for any enzymatic scavenging system, but reacts with a range of biomolecules such as DNA, lipids, proteins and free thiols at different reactivity (see below). How vulnerable a particular target is towards HOCl also depends on what else is present to compete for HOCl, on relative concentrations and on its accessibility to HOCl.

HOCl can react with nucleotides and DNA, with the base moiety being the major target (Whiteman *et al.*, 1997; Spencer *et al*., 2000). HOCl reacts with both the heterocyclic (NH-groups) and exocyclic (-NH_2) amine groups of nucleotides, with the former at a faster rate than the latter (Prutz, 1998; Prutz, 1996). Reaction of HOCl with nucleotides is known to cause the formation of short-lived chloramine species (RNHCl and RR'NHCl) (Hawkins and Davies, 2001), which can lead to the dissociation of double-stranded DNA due to the disruption of hydrogen-bonding (Prutz, 1996). HOCl is also found to directly react with adenosine triphosphate (ATP) (Prutz, 1996).

Unsaturated fatty acids and cholesterol are also susceptible to HOCl, causing the formation of chlorohydrin derivatives by addition of HOCl to double bonds. However, this reaction is relatively slow, with chlorohydrins only being detected in cells after exposure to cytotoxic HOCl concentrations (Carr *et al.*, 1996; Vissers *et al*., 1998). Moreover, chlorohydrins were seen on LDL only at HOCl concentrations well above those required for protein modification (Hazell *et al*., 1994).

HOCl also reacts with a range of low molecular weight biomolecules and antioxidants. HOCl reacts with GSH and ascorbate with rate constants > 10^7 $M^{-1}s^{-1}$ and approximately 6×10^6 $M^{-1}s^{-1}$, respectively (Folkes *et al*., 1995). Phenols, hydroquinones (Pattison and Davies, 2001), taurine (Folkes *et al*., 1995), NADH, uric acid (Winterbourn, 1985), heme groups (Aruoma and Halliwell, 1987) and iron-sulfur centres (Rosen and Klebanoff, 1985)

are also oxidised by HOCl, though at much lower rates than GSH and ascorbate (Albrich *et al*., 1981; Winterbourn, 1985; Folkes *et al*., 1995).

In addition to high reactivity with free thiols such as GSH, HOCl can also oxidise protein thiols, though their reactivity may vary based on their accessibility and pKa (Pullar *et al*., 1999). HOCl can inactivate a range of thiol-containing enzymes, including glyceraldehyde 3-phosphate dehydrogenase (GAPDH), creatine kinase, lactate dehydrogenase (Pullar *et al*., 1999; Peskin and Winterbourn, 2006; Mckenzie *et al*., 1999), Na^+-K^+-ATPase (Kato *et al*., 1998) and Ca^{2+}-ATPase (Eley *et al*., 1991). HOCl can also induce the release of zinc from zinc finger proteins, in which the metal is bound to the sulfhydryl group of cysteine residues by thiolate bonds (Fliss and Menard, 1991).

HOCl reacts with amino acid side chains of proteins with the following preference order: Met > Cys >> cystine~His~α amino acid > Trp > Lys >> Tyr~Arg > backbone amides > Gln~Asn (Winterbourn, 1985; Pattison and Davies; 2001). Amino acids, peptides and proteins are likely to be the major targets of HOCl due to their abundance in biological systems and their high reactivity with HOCl (Pattison and Davies, 2001), with the exception of reaction with GSH and possibly ascorbate. Such reaction results in side-chain modification, backbone fragmentation and cross-linking. For instance, irreversible protein crosslinks have been observed in cell membranes of red cells exposed to low doses of HOCl (Vissers *et al*., 1998). HOCl can react with free tyrosine or tyrosine residues of proteins, resulting in the formation of 3-chlorotyrosine and 3,5-dichlorotyrosine (Domigan *et al*., 1995; Hazen *et al.*, 1996b; Kettle, 1996; Hazen *et al*., 1997; Fu *et al*., 2000).

The amino groups of lysine and the N-terminal amines react with HOCl to form chloramines. These products can undergo secondary reactions with thiols and thiol-containing proteins (Pullar *et al*., 2000), induce radical generation that may result in protein fragmentation or lipid peroxidation (Hawkins and Davies, 1999; Hazell *et al.*, 1999) or break down to form protein carbonyls in proteins (Handelman *et al*., 1998; Hazen *et al*., 1998a). Chloramine can also serve as a signalling molecule. Taurine chloramine, produced by HOCl reacting with taurine amino acid (Folkes *et al*., 1995), can activate extracellular signal-regulated kinase (ERK) (Midwinter *et al*., 2004). Glycine chloramine can oxidize the intracellular inhibitor (depicted as IκBα) of NF-κB (Midwinter *et al.*, 2006), which is a major transcription factor that regulates expression of a large number of genes that code for cytokines, adhesion molecules and other components of the inflammatory response.

1.5.3 Cytotoxicity of HOCl towards mammalian cells

HOCl has been implicated in exerting a cytotoxic effect on mammalian cells, as scavenging HOCl or inactivating MPO in stimulated neutrophils, monocytes or granulocytes prevented cytotoxicity to tumor cells and leukocytes (Clark and Klebanoff, 1975; Clark and Klebanoff, 1977; Slivka *et al*., 1980; Weiss and Slivka, 1982). Similarly, neutrophils lacking MPO or membrane NADPH oxidase complex were not cytotoxic to tumor cells (Clark and Klebanoff, 1975).

HOCl's cytotoxicity to mammalian cells is further supported by it killing a range of cell types including red cells (Vissers *et al*., 1994), endothelial cells (Tatsumi and Fliss, 1994), epithelial cells (Abernathy and Pacht, 1995) fibroblasts (Vile *et al*., 2000), T-cell lines (Slivka *et al*., 1980) and tumor cells (Schraufstatter *et al.*, 1990). These studies have demonstrated that HOCl caused necrotic cell death, as membrane integrity loss and cell lysis occurred. However, low concentrations of HOCl can also cause apoptotic cell death. Human hepatoma and fetal liver cells treated with HOCl showed mitochondrial permeability transition (MPT) -mediated mitochondrial membrane potential loss and caspase activation (see **section 1.7.3**), leading to apoptotic cell death (Whiteman *et al.*, 2005b). Human mesenchymal progenitor cells, upon HOCl treatment, showed Bax-dependent MPT activation, which led to apoptosis inducing factor (AIF)/endonuclease G (EndoG) -dependent apoptotic cell death without the involvement of caspases (Whiteman *et al.*, 2007). Vissers *et al.* (1999) demonstrated caspase-dependent apoptotic cell death in human endothelial cells upon HOCl treatment (see **section 1.7** for apoptosis and necrosis).

1.5.4 HOCl and atherosclerosis

HOCl is suggested to contribute to the development of atherosclerosis via many pathways. One such pathway involves HOCl oxidatively modifying LDL, transforming it into a high uptake form for macrophages and eventually leads to foam cell formation. Indeed, exposing LDL to HOCl resulted in preferential oxidation of lysine residues of apo B-100 (Hazell *et al.*, 1994). The subsequent exposure of mouse peritoneal macrophages to this HOCl-oxidised LDL led to an increase in intracellular concentrations of cholesterol and cholesteryl esters (Hazell and Stocker, 1993).

The detection of oxidative markers of HOCl, HOCl-modified epitopes and MPO in atherosclerotic lesions also implicates HOCl in the modification of LDL and general

plaque formation. The level of 3-chlorotyrosine, an oxidative marker of HOCl (Domigan *et al*., 1995; Kettle, 1996), was 6-fold higher in atherosclerotic tissue than in normal aortic intima and 30-fold higher in LDL isolated from atherosclerotic intima than in circulating LDL (Hazen and Heinecke, 1997). *o,o'*-Dityrosine levels, another oxidative marker of HOCl (Leeuwenburgh *et al*., 1997; Heinecke *et al*., 1993), were also detected to be 100-fold higher in LDL isolated from human atherosclerotic lesions than those in the circulation. However, dityrosine can also form during $OH^{\bullet}$-mediated LDL oxidation via the Fenton reaction (Bruce *et al*., 1999). In addition, HOCl-modified apolipoprotein B-100-containing lipoproteins have been identified in human lesions (Hazell *et al*., 1996). HOCl-modified epitopes, recognized by monoclonal antibodies that are raised against HOCl-modified LDL, are also found both inside and outside of macrophages in human lesions (Sugiyama *et al*., 2001). The immunoreactive MPO is found in human lesions as well, colocalizing with HOCl-modified epitopes (Daugherty *et al.*, 1994; Malle *et al*., 2000; Sugiyama *et al*., 2001). These findings provide convincing evidence that MPO-derived HOCl oxidizes LDL under *in vivo* conditions.

HOCl can also participate in the development of atherosclerosis via other pathways. HOCl can fragment components of ECM (Woods and Davies, 2003), which also occurs in atherosclerotic plaques (Woods *et al*., 2003). Moreover, HOCl can convert the pro-enzyme form of matrix metalloproteinases (MMPs) to the activated form (Weiss *et al*., 1985; Springman *et al*., 1990; Peppin and Weiss, 1986). MMPs will then degrade the ECM that strengthens the fibrous caps, accelerating plaque rupture (see **section 1.3**). HOCl can also indirectly activate MMPs by inhibiting the the activity of a class of proteins called "inhibitors of metalloproteinases" (TIMPs) (Shabani *et al*., 1998), which function by inhibiting MMP activity. HOCl itself can also solubilise collagen (Davies *et al*., 1993; Daumer *et al*., 2000) and degrade proteoglycan (Klebanoff *et al*., 1993), suggesting that HOCl may contribute to structural weakening of the fibrous cap and plaque rupture itself.

Furthermore, HOCl can induce growth arrest, apoptosis or necrosis of endothelial cells (Sugiyama *et al*., 2004; Vissers *et al.*, 1999), decrease adhesiveness of subendothelial matrix to endothelial cells (Vissers and Thomas, 1997) and increase endothelial cell permeability by causing rapid cytoskeletal shortening and cell retraction (Tatsumi and Fliss, 1994). These data imply that the local production of HOCl by MPO-positive macrophages in the sub-endothelium of human coronary atheroma may promote local endothelial desquamation that produces superficial erosion of the intima and increase thrombogenicity.

MPO-derived HOCl is also suggested to promote the net accumulation of cholesterol within the artery wall by disturbing the cholesterol efflux from macrophages. Cholesterol can be exported from macrophages through the plasma membrane, via a high density lipoprotein (HDL) -dependent process called reverse cholesterol transport (Jessup & Kritharides, 2000), to the extracellular acceptor HDL. MPO-derived HOCl is found to oxidise HDL, hence impairing its ability to promote reverse cholesterol transport (Shao *et al.*, 2006; Zheng *et al*., 2004; Zheng *et al*., 2005).

1.5.5 HOCl as a signalling molecule

HOCl has been speculated to regulate specific cell processes. Endothelial cells (Vissers *et al.*, 1999) and human skin fibroblasts (Vile *et al*., 2000) exposed to low doses of HOCl initiate a transient growth arrest. The latter has shown that the growth arrest was associated with an increase in the levels of the transcription factor p53 and the p53-dependent wild-type activating fragment-1/cyclin-dependent kinase inhibitory protein-1 (WAF1/CIP1). Furthermore, a sublethal dose of HOCl activated transcription of apurinic endonuclease, which reduced chromosomal aberrations caused by subsequent exposure to H_2O_2 (Grösch *et al.*, 1998). Low doses of HOCl have also been found to activate mitogen-activated protein kinases (Midwinter *et al*., 2001).

1.6 Antioxidant defenses

While small amounts of oxidants may mediate cell-signalling cascades via alteration of the reducing environment in cells (Schafer and Buettner, 2001; Cross and Templeton, 2004), the excessive production of oxidants oxidises proteins, lipids, DNA and so on. These events result in cell proliferation, adaption of the cells by upregulation of defence systems, cell injury, senescence or cell death (Finkel, 1999; Sato *et al.*, 1995; Halliwell and Gutteridge, 2007).

Cells maintain the reducing environment and survive in the presence of oxidants by possessing a wide range of antioxidant defenses that prevent oxidant-induced cellular damage and maintain the redox-state of the cell. These antioxidant defenses include 1) antioxidant enzymes that remove reactive species (such as catalase, superoxide dismutase, superoxide reductase and peroxidise enzymes), 2) Repair systems that repair oxidised compounds or remove the damaged proteins (such as thioredoxin, methionine sulphoxide

reductase and ubiquitination), 3) Sequestration of pro-oxidants, such as iron ions, copper ions or haem, by proteins (such as transferrins, metalloproteins, albumin and haem oxygenases) to minimise their availability and 4) low molecular weight molecules that scavenge oxidants (such as GSH, ascorbate, α-tocopherol and urate). The next section will examine the antioxidant roles of GSH amd 7,8-dihydroneopterin (7,8-NP) in cellular protection.

1.6.1 Glutathione (GSH)

1.6.1.1 Functions of GSH

GSH (**Figure 1.4**) is the predominant low molecular weight thiol in cells, with an intracellular concentration of 0.1-10 mM (Meister, 1988). More than 98% of the synthesized GSH exists in the thiol-reduced form. The most important function of GSH appears to be as an antioxidant defense removing oxidative stress and maintaining the thiol-redox status of the cell.

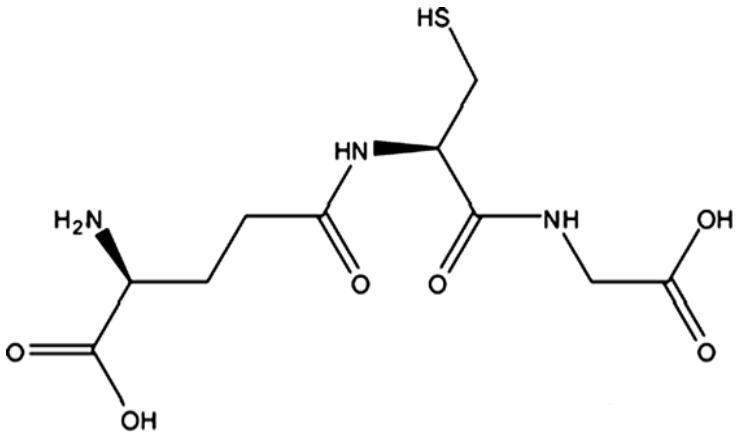

Figure 1.4 Structure of GSH (adapted from Forman *et al.*, 2009).

GSH can act as an antioxidant by directly reacting with a range of oxidants such as $OH^{\bullet}$, HOCl, $ONOO^{-}$, $RO^{\bullet}$, $NO_2^{\bullet}$ and less efficiently with $O_2^{\bullet-}$ (Halliwell and Gutteridge, 2007), resulting in the generation of GSSG. The GSH/GSSG couple is a major contributor to the redox state of the cell, with most cells having this couple at a ratio of 100:1 (Akerboom *et al.*, 1982). Changes in this couple appear to correlate with cell proliferation, differentiation, or apoptosis (Boggs *et al.*, 1998; Ballatori *et al.*, 2009). Hence, intracellular GSH levels

must be maintained for cells to function properly. GSSG can be converted back to GSH by glutathione reductase (GR) in the presence of NADPH (**reaction 1**).

$$GSSG + NADPH + H^{+} \xrightarrow{GR} 2GSH + NADP^{+} \qquad \textbf{(reaction 1)}$$

However, GSH reacting with an excess amount of HOCl favours the formation of higher oxidation products such as sulfonamide and thiosulfonate (Pullar *et al*., 2001; Winterbourn and Brennan, 1997), which cannot be converted back to GSH by GR. This will be discussed in more details in **sections 3.1 and 3.3**.

GSH can also react with exogenous xenobiotics or endogenous electrophilic molecules (both depicted as RX here), catalysed by glutathione S-transferase (GST) enzymes, to form GSH S-conjugates (RSG) (**reaction 2**).

$$RX + GSH \xrightarrow{GST} RSG + HX \qquad \textbf{(reaction 2)}$$

The above process can facilitate the detoxification of both exogenous xenobiotics and endogenous reactive intermediates and is critical for the formation of specific biological mediators (Wang and Ballatori, 1998). Some examples of xenobiotics that are metabolized by GSH in the presence of GST in animals are chloroform, adiamycin, DDT, naphthalene and paracetamol (Halliwell and Gutteridge, 2007). However, the presence of large amounts of such xenobiotics can decrease hepatic GSH concentrations, imparing the antioxidant defence capacity of the liver. Some examples of endogenous electrophilic molecules that form thioether conjugates with GSH are leukotrienes, prostaglandins, hepoxilin, nitric oxide, hydroxyalkenals, ascorbic acid, dopamine and maleic acid (Ballatori *et al.*, 2009).

GSH can also form mixed disulfides (by a process called protein-S-glutathionylation) with oxidized proteins (**reactions 3-5**).

$$\text{Protein-SH} \xrightarrow{R^{\bullet}} \text{Protein-S}^{\bullet} \qquad \textbf{(reaction 3)}$$

$$\text{Protein-S}^{\bullet} + GSH \longrightarrow \text{Protein-S-S}^{\bullet-}\text{G} \qquad \textbf{(reaction 4)}$$

$$\text{Protein-S-S}^{\bullet-}\text{G} + O_2 \longrightarrow \text{Protein-SSG} + O_2^{\bullet-} \qquad \textbf{(reaction 5)}$$

S-glutathionylation is a reversible process, which helps in removing the oxidative stress and may protect protein thiol groups from further oxidations to irreversible sulphinic (RSO_2H) and sulphonic (RSO_3H) acids. Most importantly, this process has been increasingly recognized as an important mechanism for dynamic, post-translational regulation of a variety of regulatory, structural and metabolic proteins, and for the regulation of signaling and metabolic pathways in intact cell systems (Dalle-Donne *et al*., 2007; Ghezzi and Simplicio, 2007; Mieyal *et al.*, 2008; Halliwell and Gutteridge, 2007).

GSH also serves as a cofactor for the glutathione peroxidase (GPX) or peroxiredoxins (PRXs) enzymes, which remove H_2O_2 and lipid hydroperoxides by coupling their reduction to H_2O, with oxidation of GSH (**reaction 6**). Furthermore, GSH is involved in deglutathionylation (hence maintaining the reduced state of protein thiols) via the enzymes glutaredoxins (GRXs) and thioredoxins (TRXs) (**Figure 1.5**).

$$\text{GSH} + \text{oxidants} \xrightarrow[\text{or PRX}]{\text{GPX}} \text{GSSG} \qquad \textbf{(reaction 6)}$$

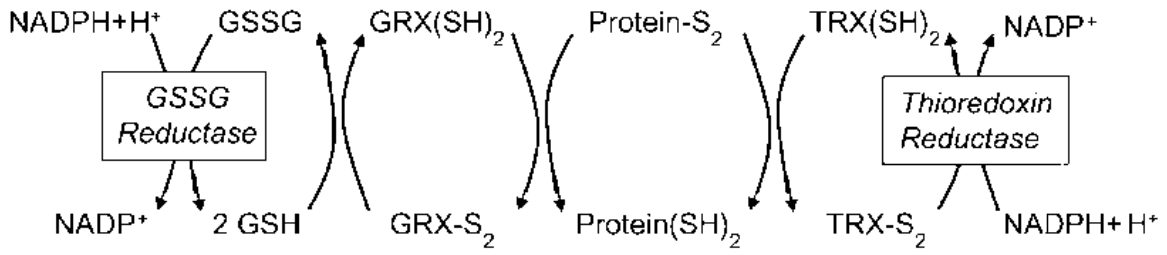

Figure 1.5 Involvement of GSH in redox reactions.
GSH is involved in maintaining the redox state of protein thiols via the enzymes glutaredoxins (GRXs) and thioredoxins (TRXs). The oxidized GSH (GSSG) and TRXs are converted back to the reduced state by the NADPH-dependent glutathione reductase and thioredoxin reductase, respectively. This scheme is adapted from Ballatori *et al*. (2009).

1.6.1.2 Biosynthesis, degradation and export of GSH

The maintainence of GSH homeostasis is crucially important for cell function and is regulated by controlling its rate of synthesis, exportation from cells and degradation. GSH levels are also influenced by agents or conditions, which alter the thiol redox state, cause the formation of glutathione S-conjugates or complexes and disrupt the distribution of GSH among intracellular organelles. Nutritional status, hormonal/stress levels and physiological states (such as pregnancy and exercise) can also alter GSH levels (Ballatori *et al.*, 2009).

GSH is synthesized in every cell of higher eukaryotes. Yet, GSH synthesis, its turnover rates, and intracellular GSH levels differ among cell types and tissues (Uhlig and Wendel, 1992). GSH is produced in the cytoplasm of cells from its precursor amino acids (glutamate, cysteine and glycine) in a series of reactions catalysed by ATP-dependent γ-glutamylcysteine synthetase (γ-GCS) and GSH synthetase (**reactions 7-8**) (Forman *et al.*, 2009). The expression and catalytic activity of γ-GCS and the availability of cysteine largely control the rate of GSH biosynthesis. Cysteine can be made from methionine, taken up from the surrounding fluids or taken up in the form of cystine that is reduced to cysteine by cells. Although GSH is present in many foods, only small amounts are absorbed intact by the gut; most is hydrolysed to other amino acids before absorption (Halliwell and Gutteridge, 2007).

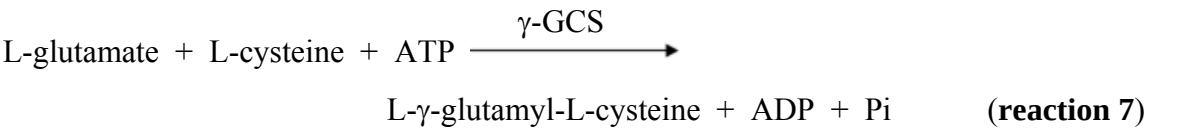

(**reaction 7**)

(**reaction 8**)

After its synthesis, GSH is delivered into intracellular compartments, including mitochondria, endoplasmic reticulum (ER), nucleus and the extracellular space (such as blood plasma and biles). GSH degradation occurs exclusively in the extracellular space, and in particular, on the surface of cells that express γ-glutamyl transpeptidase.

1.6.1.3 GSH deficiency and diseases

Changes in GSH levels and oxidation state have been reported in numerous human diseases (**Table 1.1**). GSH deficiency leads to increased susceptibility to oxidative stress and the resulting damage is considered a key step in the onset and progression of many disease states. Conversely, elevated GSH levels generally increase antioxidant capacity and resistance to oxidative stress. Elevated GSH levels are observed in various types of cancerous cells and solid tumors, which render them more resistant to chemotherapy (Balendiran *et al*., 2004; Ballatori *et al.*, 2009). Although in many cases these changes likely occur as a result of the underlying disease progression, in other cases these changes are closely linked to the onset and/or development of the disease.

GSH levels, turnover rates and oxidation state may be determined by inherited or acquired defects in the enzymes, transporters, signalling molecules, transcription factors that are involved in GSH homeostasis or from exposure to reactive chemicals or metabolic intermediates (Ballatori *et al*., 2009; Njalsson and Norgren, 2005; Ristoff and Larsson, 2007; Hirrlinger *et al.*, 2002a and b).

	GSH levels
Too much apoptosis	
Neurodegenerative disorders	
Parkinson's disease	Low
Alzheimer's disease	Low
Ischemic	
Myocardial infarction	Low
Immune	
AIDS	Low
Rheumatoid arthritis	Low
Insulin-dependent diabetes mellitus	Low
Multiple sclerosis	Low
Too little apoptosis	
Cancer	High

Table 1.1 Correlation between GSH levels and rate of apoptosis in human diseases. Adapted from Ballatori *et al*., 2009.

1.6.2 7,8-dihydroneopterin (7,8-NP) and neopterin

1.6.2.1 Biosynthesis of 7,8-NP and neopterin

The biosynthesis of 7,8-NP takes place in the pathway that leads to tetrahydrobiopterin (BH_4) formation (**Figure 1.6**). BH_4 serves as the electron donor in the hydroxylation of phenylalanine to tyrosine in the liver and of tyrosine to L-dopa and tryptophan in neuroendocrine tissue synthesising catecholamines or serotonin. It also serves as a cofactor for nitric oxide synthase (Walter *et al*., 2001). The pathway leading to BH_4 starts with the conversion of GTP to 7,8-dihydroneopterin triphosphate. This step is catalysed by GTP-cyclohydrolase I, with interferon-γ (IFN-γ) being the major trigger for this enzyme. In the presence of both Mg^{2+} ions and 6-pyrovoyltetrahydropterin synthase (PTPS), 7,8-dihydro-neopterin triphosphate is converted to 6-pyrovoyl-tetrahydropterin, which is then reduced to BH_4 in an NADPH-dependent reaction catalyzed by sepiapterin reductase (Hoffmann *et al*., 2003). The activity of PTPS in human and primate tissues and cell lines was found to be lower than that of other mammals, with lowest activities found in monocytes and macrophages (Werner-Felmayer *et al*., 1990; Werner *et al*., 1990). This results in an accumulation of 7,8-dihydroneopterin trisphosphate, which is subsequently cleaved by non-specific phosphatases to yield 7,8-NP. 7,8-NP diffuses out of the activated macrophages into the extracellular space and finally to the plasma.

7,8-NP can be oxidised to form two products depending on the types of oxidant present (**Figure 1.6**). 7,8-NP is oxidised to the highly fluorescent neopterin through the loss of hydrogen at carbon-7 and nitrogen-8 of 7,8-NP after oxidation by hypohalous acids such as HOCl (Gieseg *et al*., 2001; Widner *et al*., 2000). The non-fluorescent 7,8-dihydroxanthopterin can also be generated through the loss of the trihydroxylpropyl side chain at position 6 of 7,8-NP. This may occur by 7,8-NP reacting with $O_2^{\bullet-}$, $RO_2^{\bullet}$ and H_2O_2 (Gieseg *et al*., 2001; Murr *et al*., 1994; Widner *et al*., 2000).

1.6.2.2 Interferon-γ (IFN-γ)

The enzyme GTP-cyclohydrolase I can be activated upon IFN-γ induction to catalyse 7,8-NP synthesis. IFN-γ is a dimeric molecule produced by monocytes, macrophages and T cells during the innate and acquired immune response. IFN-γ production is controlled by cytokines, particularly interleukin-12 (IL-12) and interlekin-18 (IL-18), which are secreted

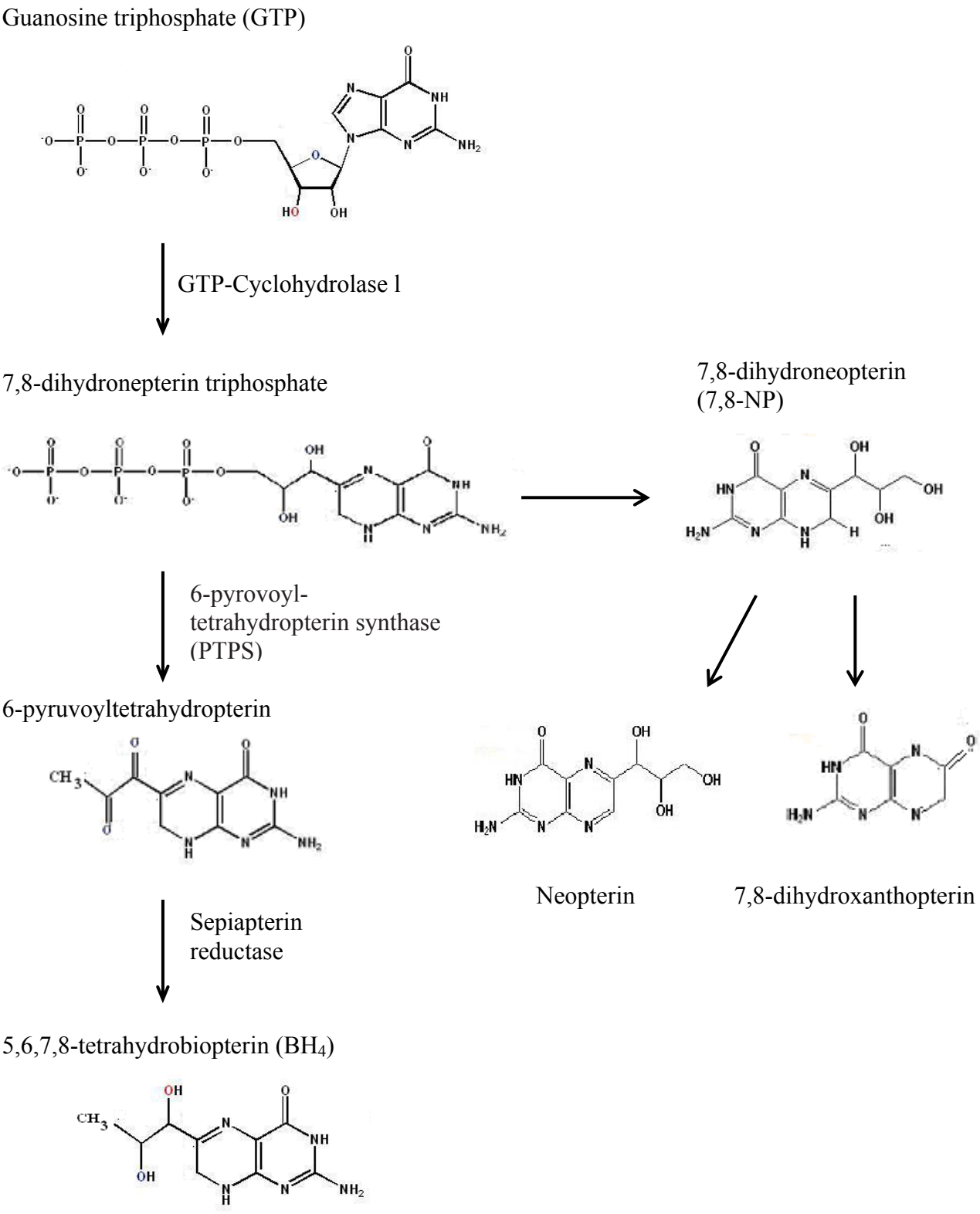

Figure 1.6 The biosynthesis and metabolism of 7,8-NP and neopterin.
Human monocytes/macrophages lack the PTPS enzyme that converts 7,8-dihydro-neopterin triphosphate to 6-pyrovoyltetrahydropterin, resulting in the accumulation of 7,8-dihydronepterin tri-phosphate. This species is then hydrolysed by phosphatases to produce 7,8-NP, which can be oxidised to neopterin or 7,8-dihydroxanthopterin depending on the types of oxidants present. This scheme is modified from Hoffmann *et al.,* (2003).

by antigen presenting cells (such as macrophages, monocytes and dendritic cells). Macrophage recognition of many pathogens induces secretion of IL-12 and chemokines. The chemokines attract natural killer (NK) cells to the site of inflammation, whereas IL-12 promotes IFN-γ synthesis in these cells. The combined stimulation of IL-12 and IL-18 further increases IFN-γ production in macrophages, NK and T cells (Schroder *et al*., 2004).

IFN-γ has shown both pro- and anti-atherogenic activities. The anti-atherogenic activities of IFN-γ include inhibiting the induction of E-selectin, P-selectin, platelet endothelial cell adhesion molecule-1 (PECAM-1), monocyte chemotactic protein (MCP-1) and its receptor monocyte chemotactic protein receptor (CCR2) (Leon & Zuckerman, 2005). These molecules assist in recruiting the circulating monocytes and T cells into the intima during the formation of a fatty streak lesion (see **section 1.3**). IFN-γ can also prevent human monocyte-mediated LDL oxidation by inhibiting 15-lipoxygenase synthesis (Folcik *et al*., 1997). In addition, IFN-γ can decrease intracellular cholesteryl ester accumulation and foam cell formation possibly by down-regulating SR-A and CD36 receptors (Geng & Hansson, 1992; Grewal *et al*., 2001; Nakagawa *et al*., 1998).

The pro-atherogenic activities of IFN-γ include up-regulation of antigen presenting components (like MHC), activation of macrophages, stimulation of respiratory burst (Hansson *et al*., 2006), induction of ceruloplasmin synthesis (Mazumder *et al*., 1997), promotion of T lymphocyte and monocyte recruitment by enhancing the release of endothelial-derived T cell α-chemoattractant (Cole *et al*., 1998) and increasing the expression of MCP-1 and the adhesion molecule vascular cell adhesion molecule-1 (VCAM-1) (Leon & Zuckerman, 2005). IFN-γ can also increase expression of the scavenger receptor SR-PSOX in human monocytes and THP-1 cells, which would increase oxLDL uptake by the cells (Wuttge *et al*., 2004). On the other hand, IFN-γ can inhibit LDL receptor expression in murine and human macrophages (Garner *et al*., 1997; LaMarre *et al*., 1993), very low density lipoprotein (VLDL) receptor expression in phorbol ester stimulated THP-1 and HL60 human macrophage cell (Kosaka *et al*., 2001) and reduces lipoprotein (a)/apoprotein (a) receptor expression (Skiba *et al*., 1994). IFN-γ also decreases cholesterol efflux and ATP binding cassette transporter-1 expression in murine and human macrophage-derived foam cells and cholesterol efflux in THP-1 cells (Panousis & Zuckerman, 2000; Reiss *et al*., 2004). Furthermore, IFN-γ decreases synthesis of lipoprotein lipase (LPL) (Garner *et al*., 1997; Jonasson *et al*., 1990), apolipoprotein E

(apoE) (Garner *et al*., 1997; Kalkan *et al*., 2005) and cholesterol 27-hydroxylase (Carpenter *et al*., 2001; Reiss *et al*., 2004). Decreases in LPL and apo E synthesis would reduce LDL and VLDL clearance from the circulation or lesion, whereas decreased synthesis of 27-hydroxylase would reduce clearance of cholesterol from foam cells as 27-hydroxylation represents the first step in extrahepatic cholesterol metabolism. Finally, IFN-γ increases acyl coenzyme A:cholesterol acyltransferase activity and expression in macrophages, which would be expected to promote cholesterol storage by increasing cholesterol ester synthesis thereby promoting foam cell formation (Panousis & Zuckerman, 2000).

1.6.2.3 Neopterin as a marker of inflammation

Neopterin concentrations have been used as a marker of immune cell activation in a wide range of diseases. The highly fluorescent nature of neopterin makes it easily detectable by HPLC methods (Rippin, 1992; Werner *et al*., 1987), although many clinical laboratories also use immuno-based methods such as radioimmunoassay or enzyme-linked immunosorbant assay (ELISA) (Wachter *et al*., 1989; Westermann *et al*., 2000).

For healthy individuals, mean neopterin concentrations in serum lie within 5.2 $\pm$ 2.7 nM and in urine it ranges between 100 and 200 μmol/mol creatinine (Wachter *et al*., 1989). It is difficult to analyse neopterin concentrations in other body fluids such as synovial fluid, saliva and cerebrospinal fluid, due to the invasive techniques required. Therefore, only minimal data are available from healthy controls, with neopterin concentrations from 1.0 to 9.0 nM (Hoffmann *et al.*, 2003). The neopterin/7,8-NP ratio remains nearly constant at 1:2 in urine, serum, or cerebrospinal fluid, suggesting that neopterin is not further metabolized after production (Hoffmann *et al.*, 2003).

Due to the stability of neopterin in biological fluids, with a half-life of approximately 90 minutes within the circulatory system (Fuchs *et al*., 1994), neopterin has become a useful tool to assess the intensity of immune cell activation in a wide range of diseases. High neopterin concentrations are a reliable measure of the severity of infections such as viral, bacterial, protozoic, parasitic or fungi-induced infections, and chronic diseases such as rheumatoid arthritis, insulin-dependent diabetes mellitus, systemic lupus erythematosus, multiple sclerosis, coeliac disease, and rheumatic fever (Hoffmann *et al*., 2003). Plasma neopterin is not generally used in the management of cardiovascular diseases, however,

there is a growing amount of evidence on its value. Higher serum concentrations of C-reative proteins and neopterin together with lower phospholipid concentrations are observed in patients with coronary heart disease (Rudzite *et al*., 2003). Serum neopterin concentration is also increased in patients with unstable angina and acute myocardial infarction (Schumacher *et al*., 1992; Schumacher *et al*., 1997; Tatzber *et al*., 1991). Moreover, neopterin concentrations in pus and plaque were found to be between 1 and 3 μM (Gieseg *et al*., 2007).

Neopterin production has also been shown to increase with increased production of ROS and in the presence of low serum concentrations of antioxidants like α-tocopherol (Schroecksnadel *et al*., 2004) and folic acid (Nathan, 1986). These results suggest that neopterin not only serves as a marker of the extent of cellular immune activation, but also a marker of the extent of tissue damage caused by ROS.

1.6.2.4 Physiological role of 7,8-NP and neopterin

The physiological role of 7,8-NP and neopterin during inflammation is controversial (Gieseg *et al*., 2007). Numerous *in vitro* studies suggested that these two species serve as pro-oxidants by enhancing oxidant production and cell death in combination with tumor necrosis factor (TNF). In contrast, 7,8-NP has also been shown to serve as an antioxidant by protecting macrophages from oxidants released during inflammation. In addition, 7,8-NP and neopterin are also involved in apoptosis, signal transduction and gene expression.

A) Antioxidant effect of 7,8-NP and neopterin

7,8-NP can scavenge free radicals such as $OH^{\bullet}$ (Heales *et al.*, 1988) $O_2^{\bullet-}$, H_2O_2 (Shen, 1994), aqueous peroxyl radicals (Oettl *et al*., 1997; Gieseg *et al*., 1995), lipid peroxyl radicals (Gieseg *et al*., 1995; Gieseg *et al*., 2003) and HOCl (Gieseg *et al*., 2001b). 7,8-NP is also an efficient scavenger of non-physiological radicals like 1,1-diphenyl-2-picrylhydrazyl and 2,2'-azino-di-(3-ethylbenz-thaizoline sulphonate) (Oettl & Reibnegger, 2002).

On a larger scale, the radical scavenging activity of 7,8-NP explains the inhibition of radical-induced damages to a variety of cellular substrates and cells in the presence of 7,8-NP. 7,8-NP inhibited metal ion- and aqueous peroxyl radical-mediated lipid peroxidation

on native LDL or linoleate by scavenging the propagating lipid peroxyl radicals (Gieseg *et al*., 1995; Gieseg and Cato, 2003; Gieseg *et al.*, 2003). THP-1 and HMDM cell-mediated LDL oxidation was also prevented completely by micromolar concentrations of 7,8-NP (Gieseg and Cato, 2003). 7,8-NP was further found to inhibit ROS-mediated damage to a range of other substrates and cells, including bovine serum albumin (Duggan *et al.*, 2001), erythrocytes (Gieseg *et al.*, 2001b) and the U937 monocytic cell line (Gieseg *et al.*, 2001a; Duggan *et al.*, 2002). These studies noted protection against damage that ranged from dityrosine and protein hydroperoxide formation to haemolysis, cell death and thiol oxidation. Similarly, 7,8-NP appears to prevent copper- and AAPH-induced protein hydroperoxide formation on LDL by scavenging the lipid-derived radicals that are suggested to promote protein peroxidation (Gieseg *et al.*, 2003). In addition to the above substrates, 7,8-NP has also been shown to prevent oxLDL-induced intracellular GSH loss in U937 cells by scavenging oxLDL-induced intracellular oxidants, which in turn maintained the intracellular redox environment and hence prevented cell viability loss (Baird *et al*., 2004; Baird *et al.*, 2005). 7,8-NP also appears to efficiently scavenge reactive nitrogen species, inhibiting 3-nitrotyrosine formation in a simple system of 7,8-NP, tyrosine and peroxynitrite (Widner *et al.*, 1998; Oettl *et al.*, 2004). 7,8-NP has also been shown to protect *Escherichia coli* from chloramine T- and HOCl-induced growth inhibition and cytotoxicity (Weiss *et al.*, 1993; Horejsi *et al.*, 1996; Wede *et al.*, 1999).

7,8-NP and neopterin were also demonstrated to inhibit TNF-α-mediated apoptosis in the U937 cell line (Baier-Bitterlich *et al.*, 1995). Furthermore, neopterin has been specifically confirmed to inhibit the activity of at least two other enzymes *in vitro* – the superoxide radical generators, NADPH oxidase and xanthine oxidase. Inhibition of the former occurs via neopterin competing with the NADPH substrate (Kojima *et al.*, 1993), where inhibition of the latter involves a reversible, non-competitive mechanism (Oettl *et al.*, 1997; Oettl & Reibnegger, 1999). Neopterin has also been found to inhibit MPO, leading to an increase in singlet oxygen but a decrease in all other ROS (Razumovitch *et al.*, 2004).

B) Pro-oxidant effect of 7,8-NP and neopterin and apoptosis

Although 7,8-NP is clearly a potent radical scavenger, it mostly exhibits strong pro-oxidant activity at high concentrations. 7,8-NP, at 5 mM concentration, was found to induce oxidative stress resulting in apoptotic cell death in U937 cells (Baier-Bitterlich *et al*., 1995), neuronal NT2/ HNT cells (Spottl *et al*., 2000), Jurkat cells (Enzinger *et al*., 2002a;

Wirleitner *et al*., 1998; Wirleitner *et al*., 2001) and the rat pheochromocytoma cell line PC12 (Enzinger *et al*., 2002b). At this concentration, 7,8-NP also superinduced TNF-α-mediated apoptosis in U937 cells (Baier-Bitterlich *et al*., 1995). Surprisingly, neopterin or 7,8-NP with concentrations as low as 10 μM also induced apoptosis and augmented TNF-α/IFN-γ-mediated apoptosis in rat alveolar epithelial cell line L2 cells (Schobersberger *et al*., 1996). The same study revealed that nitric oxide production was not involved in neopterin-mediated apoptosis in L2 cells. This was in contrast to neopterin- and 7,8-NP-induced apoptosis in vascular smooth muscle cells (VSMCs), where inhibition of iNOS suppressed the pro-apoptotic effects of neopterin in VSMCs (Hoffmann *et al*., 1998; Hoffmann *et al*., 1996).

One explanation for the observed pro-oxidant characteristic of 7,8-NP is related to its reducing nature (Gieseg *et al*., 2007). 7,8-NP may cause the reduction of redox-active metal ions within the buffers, which would increase the formation of various oxidants. For instance, 7,8-NP at high concentrations showed enhancement of copper-induced LDL oxidation, possibly due to the ability of 7,8-NP to reduce copper ion to its redox active state (Herpfer *et al*., 2002). 7,8-NP has also been shown to reduce another transition metal, iron, to the redox active ferrous ion state (Wirleitner *et al*., 2005). Moreover, it was reported that 7,8-NP enhanced the rate of $OH^{\bullet}$ generation in phosphate buffered saline (PBS) containing low levels of iron (Oettl *et al*., 1999). However, this oxidant generation only becomes significant at extremely high 7,8-NP concentrations and in protein-free media, as proteins are very effective radical scavengers. Therefore, the high concentration of soluble proteins within plaque may make these reactions unlikely, although still possible (Gieseg *et al*., 2007).

The pro-oxidant characteristic of 7,8-NP and neopterin can also be attributed to them enhancing ROS generation under certain conditions. For instance, neopterin and high concentrations of 7,8-NP intensify H_2O_2- and chloramine T-mediated luminol-dependent chemiluminescence assay, suggesting an enhancement of free radical formation (Murr *et al*., 1996; Weiss *et al*., 1993). Unlike 7,8-NP, the effects of neopterin were generally pH-dependent. For example, neopterin only promoted 3-nitrotyrosine formation at pH between 4 and 5.5 (Widner *et al*., 1998), whereas its enhancement of chloramine T- and H_2O_2-induced chemiluminiscence and cytotoxicity required a neutral or slightly alkaline pH (Weiss *et al*., 1993). In addition, the enhancement of neopterin on H_2O_2-induced chemiluminescence was found to be dependent on the presence of iron chelator complexes

(Murr *et al*., 1994). Antioxidants ranging form N-acetylcysteine to pyrrolidine dithiocarbamate, catalase and superoxide dismutase have been shown to significantly inhibit 7,8-NP-mediated apoptosis (Baier-Bitterlich *et al*., 1995; Baier-Bitterlich *et al*., 1996; Enzinger *et al*., 2002b; Hoffmann *et al*., 2003; Spottl *et al*., 2000). It therefore appears that the presence of excess 7,8-NP results in ROS generation, disrupting the oxidant/antioxidant balance and ultimately leading to cell death.

C) Gene expression and signal transduction

Disruption of the cellular redox balance not only promotes apoptosis, but may also account for the neopterin- and 7,8-NP-mediated activation of various redox-sensitive transcription factors. For instance, the transcription factor activator protein 1 (AP-1) is known to sense the intracellular redox state and regulate the expression of multiple genes involved in stress response. It is composed of proteins from the *Fos* and *Jun* families and is usually a c-*fos* /c-*jun* heterodimer. The activity of AP-1 is regulated by the amount of c-*fos* and c-*jun* made by cells and by phosphorylation of already-synthesised proteins (e.g. by mitogen-activated protein kinases (MAPKS)). Both processes can be altered by various ROS (Halliwell and Gutteridge, 2007).

Along this line it was observed that incubation of cells with neopterin, and to a greater extent 7,8-NP, together with cyclic guanosine monophosphate (cGMP) induces *c-fos* gene expression in a *c-fos*-CAT reporter transactivation system of NIH3T3 mouse fibroblasts (Uberall *et al*., 1994). In addition, 7,8-NP activates the redox-sensitive transcription factor, activation protein-1 chloram-phenicol acetyltransferase (AP-1-CAT) and amplifies TNF-α induced NF-κB activation in Jurkat cells (Baier-Bitterlich *et al*., 1997b) and enhances apoptosis in rat PC12 cells by up-regulating signalling cascades associated with MAPKs (Enzinger *et al*., 2001). Activation of p44/42 ERK was mediated by 7,8-NP alone, while strong activation of stress-activated protein kinase (SAPK) required co-incubation with TNF-α (Enzinger *et al*., 2002b). These data suggests that neopterin and 7,8-NP may alter gene expression by modulating the intracellular redox state. Interestingly, there is no documentation to date reporting on the specific pteridine receptor.

Neopterin also enhances inducible nitric oxide synthase (iNOS) gene expression and nitric oxide release in rat vascular SMCs (Schobersberger *et al*., 1995) and amplifies the secretion of TNF-α in peripheral blood mononuclear cells induced by IFN-γ and IL-2

(Barak & Gruener, 1991). In VSMCs, neopterin is a potent stimulus of TNF-α gene expression and TNF-α protein release (Hoffmann *et al*., 1998). Furthermore, this laboratory has demonstrated that 7,8-NP down-regulated certain isoforms of CD36 protein, an oxLDL scavenger receptor (Amit, 2008, PhD thesis).

In transfected Jurkat cells, 7,8-NP has been shown to induce trans-activation of IFN-γ, as well as the type I human T-cell leukaemia virus long terminal repeat sequence and HIV-1 promoter (Baier-Bitterlich *et al*., 1996; Baier-Bitterlich *et al*., 1997a). Neopterin also induced inter-cellular adhesion molecule-1 (ICAM-1) gene expression and protein synthesis in type II-like alveolar epithelial cells (Hoffmann *et al*., 1999). As mentioned earlier, the increased production of ICAM-1 promotes the recruitment of immune cells into the intima. Infectious diseases of the lungs including sarcoidosis, lung tumours, fibrosis and adult respiratory distress syndrome are also associated with elevated neopterin concentrations in serum and an increased production of ICAM-1 (Wirleitner *et al*., 2005).

The pteridines also influence secondary messengers. For instance, both neopterin and 7,8-NP were shown to induce an intracellular calcium influx in THP-1 cells (Woll *et al*., 1993) and inhibit ATP-induced calcium release from alveolar epithelial cells (Hsieh *et al*., 2001). Neopterin was also shown to cause cardiac contractile dysfunction in isolated perfused rat hearts (Balogh *et al*., 2005). These results imply the adverse clinical effect of neopterin, as calcium deposition represents a serious deterioration in patient prognosis due to the increasing complexity of the plaque tissue.

1.7 Cell death mechanisms

Cells die in response to a variety of stimuli and cell death can commonly occur by two mechanisms, necrosis and apoptosis. Yet, sometimes death with features of both pathways can occur (Halliwell & Gutteridge, 2007).

Necrotic cell death is ATP-independent and is characterised by swelling of the cell and internal organelles, loss of cellular ion homeostasis, loss of integrity of mitochondrial, peroxisomal and lysosomal membranes, and eventual rupture of the plasma membrane releasing cell contents into the surroundings that may affect adjacent cells (Lelli *et al*., 1998). The released contents can be antioxidants such as superoxide dismutase (SOD), catalase or GSH, pro-oxidants such as haem, iron and copper ions and other damaging

agents, such as activated calpains (Halliwell and Gutteridge, 2007). Another hallmark of necrosis is inflammation, where cells of the immune system ingest the necrotic cells to help limit infection and clear away debris. However, the activities and secretions of the phagocytes can also damage normal tissue in the vicinity, sometimes extensively (Duke *et al*., 1996). Severe damage to cytoskeletal proteins by calpain enzymes or cathepsins can cause irreversible membrane blebbing and eventually necrosis. This will be discussed in detail in **Chapter 5**. Dramatic intracellular ATP loss can also lead to necrosis, which will be discussed in **Chapter 4**.

The earliest visible morphological changes in apoptotic cell death are cell shrinkage and bleb formation on the surface of the cell membrane without the membrane losing its integrity (Haunstetter & Izumo, 1998). Internal organelles retain their structure, but chromatin condensation and nuclear fragmentation occur (Yuan *et al*., 2000). Eventually, the cell breaks into small membrane-surrounded fragments (called apoptotic bodies), without rupture of organelle membranes (Haunstetter & Izumo, 1998). The apoptotic bodies are then cleared by phagocytosis without inciting an inflammatory response. The redistribution of phosphatidylserine (PS) to the outer surface of plasma membrane is also a hallmark of apoptosis, which enables the recognition of apoptotic bodies by phagocytic cells (van Engeland *et al*., 1998). If the apoptotic bodies are not phagocytosed, a process known as secondary necrosis will occur, in which the membranes of apoptotic bodies lyse and the contents of the bodies are released (Skepper *et al*., 1999; Tabas, 2005).

1.7.1 Molecular mechanism of apoptosis

Apoptosis is a tightly regulated cell death program involving a complex cascade of events. Apoptosis can be triggered by various stimuli from either outside or inside the cell, such as by ligation of cell surface receptors, DNA damage as a cause of defects in DNA repair mechanisms, treatment with cytotoxic drugs or irradiation, contradictory cell cycle signalling or by developmental death signals. Two major pathways, the extrinsic and intrinsic pathways, leading to apoptotic cell death have been described, and caspases are heavily involved in both pathways.

1.7.1.1 Caspases

Caspases are a family of at least 14 cysteine proteases that have been described as 'the central executioners' of apoptosis. Their full name 'cysteine-aspartyl-specific proteases' reflects their active cysteine group and the characteristic cleavage of protein substrates at aspartate residues (Chandra & Orennius, 2002; Hampton & Orennius, 1997). Caspases can be functionally classified into two classes; (i) the initiator caspases that are involved in recruitment and activation, and are characterised by long prodomains containing either death-effector domain (DED) (caspase-8 and caspase-10) or a caspase recruitment domain (CARD) (caspase-2, and caspase –9); and (ii) the executioner or effector caspases containing short prodomains (caspase-3, caspase-6 and caspase-7) (Grutter, 2000). Not all caspases are involved in cell death. For instance, caspases-1, -4 and -5 (possessing large terminal domains) in humans are involved in the processing of pro-inflammatory cytokines such as pro-IL-1β and -18 (Kroemer and Martin, 2005).

In resting cells, caspases are present as inactive zymogens, the so called pro-caspases. Activation requires that the N-terminal domain of a pro-caspase be removed by proteolytic cleavage, leaving proteolytic active ~20 kDa and ~10 kDa subunits. The effector caspases are proteolytically activated by the initiator caspases. The hypothesized mechanism of initiator caspase activation is described in **section 1.7.1.2**. The active enzyme consists of heterotetramers composed of two large and two small subunits, with two active sites per molecule (Thornberry and Lazebnik, 1998). The cysteine and histidine residues at the active site are harbored within the large subunit.

1.7.1.2 The extrinsic, intrinsic and other apoptotic pathways

In the extrinsic pathway, apoptotic signal can be initiated by direct interaction of specific ligands with their respective receptors on cell membranes (**Figure 1.7**). These receptors are called death receptors, which belong to the tumour necrosis factor receptor (TNFR) gene superfamily, including TNFR-1, Fas/CD95 (fibroblast associated cell surface) and the TNF-related apoptosis-inducing ligand (TRAIL) receptors DR-4 and DR-5 (Ashkenazi, 2002). All members of the TNFR family consist of cysteine-rich extracellular subdomains that allow them to recognise specific ligands, resulting in the trimerisation and activation of the respective death receptor. The activated death receptors on the cytoplasmic side then recruit adapter proteins, such as Fas-associated death domain (FADD) and TNF receptor-associated death domain (TRADD), to their cytosolic death domains (DDs). TRADD and

FADD contain both DDs and death effector domains (DEDs). While their DDs bind to cytosolic DDs of TNFR, their DEDs bind to DED-containing pro-caspases, particularly pro-caspase-8 (or pro-caspase-10). This results in recruitment of pro-caspase-8 to liganded death receptor complexes and activation of caspase-8 through the induced proximity mechanism (Ashkenazi, 2002). This mechanism suggests that the zymogen forms of unprocessed caspases are not entirely inactive but rather possess weak protease activity (measured in some cases at ~1% of the fully active enzymes). When brought into close proximity during recruitment, the zymogens can *trans*-process each other, producing the fully active proteases (Reed, 2000). The activated caspase-8 in turn cleaves and activates the downstream effector caspases-3, -6 and -7.

Activation of effector caspases put in motion the cellular events characteristic of apoptosis. These include modification of the function of the target proteins, which results in the disabling of homeostatic and repair processes (such as activation of the caspase-activated DNAse that fragments DNA), the stopping of cell cycle progression, the inactivation of apoptotic inhibitors, the disassembly of the cell (such as activation of enzymes that remodel the cytoskeleton and cause blebbing) and the marking of the dying cell for disposal (Reed, 2000; Grutter, 2000). Caspase-3 is also responsible for cleaving poly-ADP ribose polymerase specifically at Asp-Glu-Val-Asp (DEVD) sequence (Nicholson *et al*., 1995).

The intrinsic apoptosis pathway is activated by a variety of extracellular and intracellular stresses, such as oxidative stress and treatment with cytotoxic drugs. Generally, the signal derived from the activated death receptor is not sufficient to stimulate the direct activation of apoptotic effector caspases and subsequently to execute cell death. Hence, the signal needs to be amplified via the mitochondria-dependent apoptotic pathway (**Figure 1.7**). This occurs when activated caspase-8 cleaves the pro-apoptotic protein Bid of the Bcl-2 family into its truncated form (tBid) (see also **section 1.7.2**), which translocates to the mitochondria. tBid then acts in concert with Bax and Bak of the pro-apoptotic Bcl-2 family to facilitate the mitochondrial outer membrane permeabilisation (MOMP) and release of factors from the inter-membrane space to the cytosol, such as cytochrome c (Luo *et al*., 1998; Halliwell and Gutteridge, 2007). Earlier data suggested that loss of mitochondrial membrane potential and opening of the mitochondrial membrane permeability (MPT) pore are necessary for cytochrome *c* release (Kluck *et al*., 1999; Liu *et al*., 1996). However, recent data suggested that both events are not needed (Ly *et al*., 2003; Stridth *et al*., 1998;

Waterhouse *et al*., 2002). MOMP may also release SMAC (alternatively called DIABLO) (Luo *et al*., 1998; Halliwell and Gutteridge, 2007). SMAC is a protein that binds and inhibits endogenous caspase blockers (IAP) (Adam *et al*., 2000; Verhagen *et al*., 2000).

Cytochrome *c* is a 14 kDa soluble protein attached to the inner membrane of the mitochondria and its traditional role is to shuttle electrons between complexes III and IV of the electron transport chain (ETC) on the inner mitochondrial membrane. The release of cytochrome c may result in breakdown in electron flow, generating ROS such as $O_2^{\bullet-}$ and reduces the supply of adenosine triphosphate (ATP) (Cai & Jones, 1998; Stridth *et al*., 1998). Once in the cytosol cytochrome c, as well as ATP/ deoxyadenosine triphosphate (dATP), binds to the cytosolic caspase adaptor Apaf-1 (apoptotic proteinase activating factor 1) to form the apoptosome. This complex binds pro-caspase-9 and facilitates *trans*-processing of caspase-9 zymogens via the induced proximity mechanism (Reed, 2000) (see above). The activated caspase-9 in turn activates caspases-3 and -6 (Halliwell and Gutteridge, 2007).

Another way of triggering apoptosis is to introduce an agent that directly activates caspases and/or mitochondrial pro-apoptotic proteins. For example, tributylin targets mitochondria, causing swelling and cytochrome *c* release. The cytotoxic T lymphocytes can deliver a pore-forming protein (perforin) and a set of proteolytic enzymes (granzymes) into their target cells. Granzyme B can directly activate the target cell's caspases and by doing so, induce apoptosis. Granzyme B can also bypass caspases by directly cleaving inhibitors of caspase-3-activated DNase (ICAD), Bid and caspase-3. The ER stress response can also lead to apoptosis (Halliwell & Gutteridge, 2007).

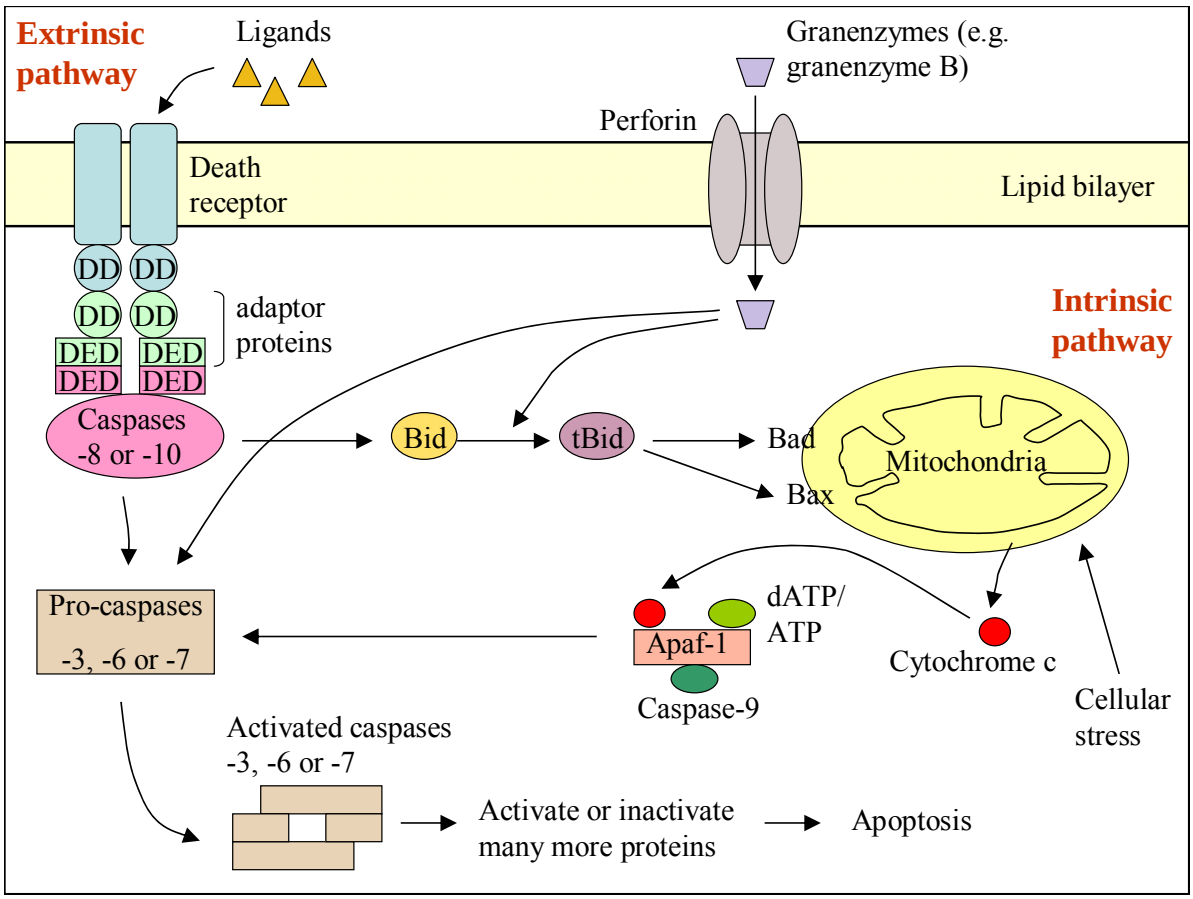

Figure 1.7 Some major caspase-dependent apoptotic pathways (simplified scheme). Refer to the text in **section 1.7.1.2** for the description of the pathways.

1.7.1.3 Caspase-independent apoptotic pathways

Some of the mitochondrial proteins released as a result of MOMP, such as apoptosis inducing factor (AIF) and HtrA2/Omi (a mitochondrial serine protease), can also promote caspase-independent apoptotic death by causing chromatin condensation, ROS generation and DNA damage (Kroemer and Martin, 2005). oxLDL was previously found to activate a caspase-independent apoptotic pathway mediated by the release of AIF (Zhang *et al.*, 2004; Vindis *et al.*, 2005). Moreover, microinjection of AIF-specific antibodies can prevent caspase-independent neuronal death induced by DNA damage or excitotoxins (Cregan *et al.*, 2002; Wang *et al.*, 2004). HtrA2/Omi-specific inhibitor ucf-101 inhibits the nephrotoxic and the pro-apoptotic effect of cisplatin *in vivo* (Cilenti *et al.*, 2005).

Caspase-independent apoptotic death can also result from stimuli that cause calpain enzyme activation and lysosomal membrane permeabilization with the consequent release of cathepsin proteases (Kroemer and Martin, 2005). This will be discussed in more detail in **Chapter 5**.

1.7.2 Bcl-2, ROS and redox regulation of apoptosis

The Bcl-2 family of proteins serve as either anti- or pro-apoptotic factors regulating the mitochondrial membrane potential, outer membrane permeability and hence the release of pro-apoptotic factors (Reed, 1997; Reed, 1998). There are over 30 protein members in the Bcl-2 family, which can be characterised by the presence of particular conserved sequence motifs, known as Bcl-2 homology domains (BH1 to BH4). The anti-apoptotic proteins including Bcl-2, Bcl-X_L, Bcl-w and Bcl-B posses the domains BH1, BH2, BH3 and BH4. The pro-apoptotic proteins can be divided into two subgroups: the Bax-subfamily (consists of Bax, Bak and Bok) that all possess the domains BH1, BH2 and BH3; the BH3 only proteins (Bid, Bim, Bik, Bad, Bmf, Hrk, Noxa, Puma, Blk, BNIP3 and Spike) have only the short BH3 motif (Cory & Adams, 2005). The relative ratios of these pro- and anti-apoptotic members are more important to the survival of a cell than the expression of any member in particular (Carmody & Cotter, 2001).

The Bcl-2 family proteins regulate apoptosis via many pathways. Bax, Bcl-Xs, Bid, Bim and Bak occur as dimers or oligomers in the cytosol and form ion-conducting channels in the mitochondrial outer membrane (Kroemer & Reed, 2000). They also form pores in the membranes of the ER and nucleus. These channels/pores probably induce mitochondrial membrane permeability and cytochrome *c* release from the mitochondria, intervene in calcium ion (Ca^{2+}) signalling by inducing Ca^{2+} release from the ER and modulate nuclear membrane. The pro-apoptotic effect to some extent also depends on caspases. For example, caspases-1 and -3 degrade Bcl-X_L and Bcl-2, respectively, converting anti-apoptotic proteins into pro-apoptotic mediators (Kirsch *et al*., 1999).

Bcl-2 also appears to function as an antioxidant. For instance, Bcl-2 was previously shown to prevent lipid peroxidation associated with apoptosis, suggesting that Bcl-2 may indirectly regulate antioxidant defences to prevent cell death (Hockenbery *et al*., 1993). There is also a strong link between Bcl-2 and the endogenous antioxidant GSH, as the analysis of multiple lymphoid systems showed that increased Bcl-2 protein levels were related to increased intracellular GSH levels. Moreover, the resistance of cells to apoptosis-inducing stimuli conferred by elevated Bcl-2 expression was significantly decreased following depletion of intracellular GSH (Mirkovic *et al*., 1997). Bcl-2 has also been found to prevent mitochondrial permeability transition and cytochrome c release via maintenance of reduced pyridine nucleotides (Kowaltowski *et al.*, 2000).

The role of ROS and redox in apoptosis is not clearly defined since it is difficult to distinguish whether oxidative events are a consequence of damage or cause of cell death. The ability of antioxidants to prevent apoptosis provides evidence for a role of ROS in apoptotic signal transduction (Carmody & Cotter, 2001). Oxidative stress can lead to apoptosis, often by inducing the MPT and causing release of pro-apoptotic factors. However, caspases have exposed sulfhydryl (–SH) groups, which can be readily inactivated by H_2O_2, HOCl, $OH^{\bullet}$, $ONOO^-$ and other reactive species (RS) (Hampton *et al*., 2002; Hampton & Orennius, 1997). Thus, high levels of RS can delay or halt apoptosis, but often cell death continues by a necrotic or intermediate pathway. Alternatively, apoptosis triggered by other mechanisms (such as ligand binding to death receptors) is accompanied by oxidative stress. For example, release of cytochrome c and caspase-dependent cleavage of complex I of the mitochondrial ETC disrupt the ETC, causing more $O_2^{\bullet-}$ formation (Halliwell and Gutteridge, 2007).

1.7.3 Mitochondrial membrane permeability transition (MPT)

Mitochondrial membrane potential loss is considered a common pathway leading to both apoptotic and necrotic cell death (Kim *et al.*, 2003a; Lemasters, 1999). The level of its loss affects cellular ATP levels, which determine whether cells undergo necrosis or caspase-dependent apoptosis (Eguchi *et al*., 1997), since caspase activation requires ATP.

The mitochondrion is encompassed by two membranes, and the electron transport chain (ETC) at the inner mitochondrial membrane (IMM) is where oxidative phosphorylation and hence most of the cellular ATP generation take place (**Figure 1.8**). The mitochondria of healthy cells maintain an electrochemical gradient across the IMM, which is created by pumping protons (H^+) from the matrix to the inter-membrane space (IMS) of the mitochondria in conjunction with electron transport through the ETC at the IMM. Influx of H^+ back into the matrix through the F_0F_1-ATPase/H^+ pump at the IMM drives the conversion of adenosine diphosphate (ADP) and PO_4^{3-} (Pi) to ATP (Matsuyama and Reed, 2000).

In order to maintain this crucial gradient, transport across the IMM is tightly regulated by many specific transporters for the metabolites that need to cross the IMM, such as the H^+/K^+ antiporter, Na^+/H^+ exchanger, Cl^-/HCO_3^- antiporter, uncoupling proteins and the Pi/OH^- exchanger. The IMM also contains protein import channels, as well as the adenine

nucleotide translocator (ANT) that exchanges ADP and ATP between the mitochondrial matrix and the IMS.

In contrast to the IMM, the outer mitochondrial membrane (OMM) is completely porous to H^+, presumably due to the presence of the voltage-dependent anion channel (VDAC). VDAC is a β-sheet-type transmembrane channel protein involved in transporting metabolites, including ADP and ATP, between mitochondria and cytosol (**Figure 1.8**). It is permeable to molecules of up to 5000 daltons in its open configuration (Mannella, 1992; Harris and Thompson 2000). Even in its "closed" configuration, it creates a pore of approximately 1.8 angstroms in diameter, which is adequate for passage of H^+ and other biologically relevant ions (Matsuyama and Reed, 2000). The IMS is where many of the characterized apoptosis-inducing proteins reside, including cytochrome c, apoptosis inducing factor (AIF) and some pro-caspases.

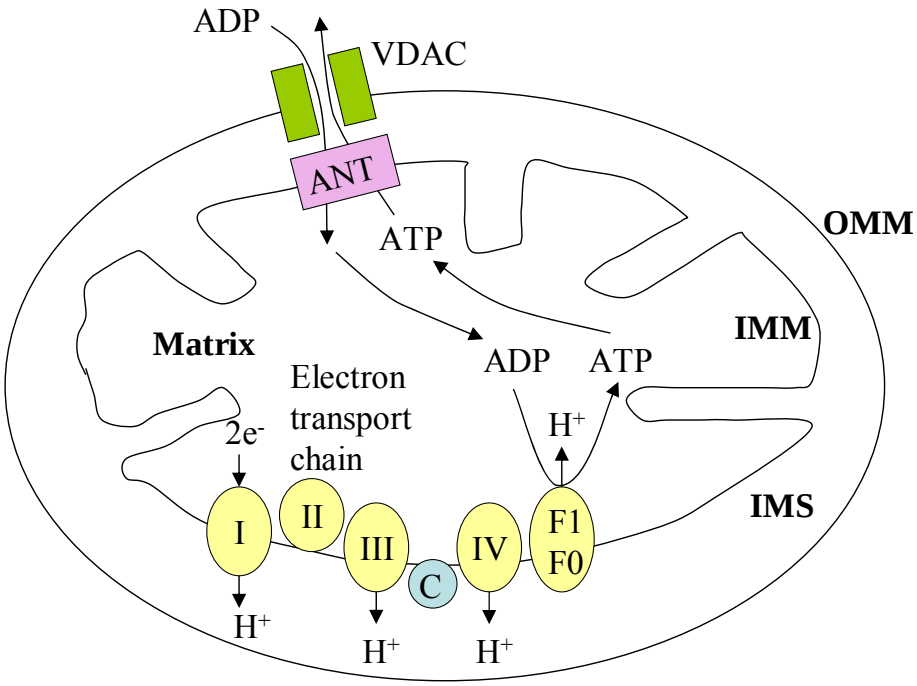

Figure 1.8 ATP generation and transport in mitochondria.
Oxidative phosphorylation occurs across the inner mitochondrial membrane (IMM) via the electron transport chain, including cytochrome c (C), and the F1F0-ATPase (F1F0). Protons (H^+) are pumped into the inter-membrane space (IMS) of mitochondria and flow back into the matrix through the the F1F0-ATPase. ATP produced in the matrix is exchanged for cytosolic ADP through the adenine nucleotide translocator (ANT) in the IMM and the voltage dependent anion channel (VDAC) in the outer mitochondrial membrane (OMM).

Many models for the mitochondrial membrane potential loss have been proposed, which may occur either before or after caspase activation, depending on the stimuli (Matsuyama and Reed, 2000; Harris and Thompson 2000). One of the popular models involves the opening of the high conductance membrane permeability transition (MPT) pore in the IMM (Kroemer, 1998), which is proposed to be a large multi-protein complex composed of VDAC, the ANT, creatine kinase, hexokinase, the benzodiazapine receptor and cyclophilin D (Zoratti and Szabo, 1995; Crompton, 1999). This multi-protein complex forms a large channel (2.0 ± 2.6 nm diameter) between the cytosol and the mitochondrial matrix, allowing passage of proteins up to 1.5 kD, in response to a number of mitochondrial stresses including Ca^{2+} (Zoratti and Szabo, 1995).

Mitochondria are known to import Ca^{2+} from the cytosol to the electronegative matrix via the Ca^{2+} uniporter in the IMM, in response to elevations of cytosolic Ca^{2+}. This creates transient depolarizations of the IMM, followed by efflux of H^{+} and restoration of mitochondrial membrane potential (Loew *et al*., 1994). Typically, mitochondria can tolerate a few to several pulses of Ca^{2+}, but eventually their capacity to adapt to Ca^{2+} loads is overwhelmed and the mitochondria depolarize irreversibly due to a profound change in the inner membrane permeability representing the so-called "permeability transition" (Bernardi *et al*., 1998). This phenomenon leads to the MPT pore opening, allowing free passage of protons and ions across the IMM, osmotic disequilibrium and eventually swelling of the matrix. Since the IMM is folded into cristae that have a larger surface area than the surrounding OMM, matrix swelling would eventually exceed the surface area of the OMM and cause OMM to rupture, thereby spilling the contents of the IMS into the cytosol. This Ca^{2+}-based mechanism for cell death may be particularly relevant to ischemia-reperfusion injury and neuroexcito-toxicity involving NMDA-family receptors, a family of plasma membrane Ca^{2+} channels that open in response to glutamate and related neurotransmitters and that have been implicated in cell death during stroke and several other neurological diseases (Matsuyama and Reed, 2000). MPT opening is also regulated by the intracellular redox environment, mitochondrial calpain activation and cathepsin proteases, which will be discussed in detail in **Chapter 5**.

Whether depolarization is the initial event leading to apoptosis is under debate, as many reports suggest that mitochondrial hyperpolarization and subsequent matrix alkalinization are earlier events in apoptosis (Harris and Thompson, 2000), though depolarization eventually occurs in apoptosing cells.

1.8 Calpain enzymes

Calpains are Ca^{2+}-dependent cysteine proteinases, which form a family consisting of at least six distinct members (Sorimachi *et al*., 1989; Sorimachi *et al*., 1993; Sorimachi *et al*., 1994). The family can be divided into two groups on the basis of distribution- ubiquitous and tissue specific. Within mammals, calpains 1, 2, 4, 5, 7, 10, 12 and 13 are ubiquitously expressed, whereas calpains 3, 6, 8, 9 and 11 have more tissue-specific distributions (Huang and Wang, 2001), implicating a diverse set of roles for calpain family members. However, the current knowledge about the enzymological and biological properties of calpains applies mainly to the ubiquitous isozymes, μ- and m-calpains (or calpains I and II, respectively). μ-Calpain is activated in the presence of μM levels of Ca^{2+}, whereas m-calpain requires mM levels of Ca^{2+} (Croall and DeMartino, 1991; Saido *et al*., 1994a). They localize mainly in cytoplasm, but are also found in mitochondria, Golgi and ER membranes (Arrington *et al*., 2006; Tavares and Duque-Magalhaes, 1991).

All the ubiquitous calpain isozymes are heterodimers consisting of one large subunit and one small subunit (Saido *et al*., 1994b). It is suggested that calpain is activated via autolysis of the subunits in the presence of sufficient Ca^{2+} (Saido *et al*., 1992). Autolysis removes the amino-terminal pro-peptide portion that presumably suppresses the protease activity or may cause a conformational change in the molecule, leading to the enzyme activation (Saido *et al*., 1994b). However, Brown and Crawford (1993) suggested that autolysis might be a post-activation process. Phosphatidylserine and phosphatidylinositol were found to lower the Ca^{2+} concentration required for calpain autolysis (Coolican and Hathaway, 1984), leading to the hypothesis that the enzyme is activated at cell membranes where these phospholipids are localized (Suzuki *et al*., 1987).

Calpains are linked to the pathogenesis of Alzheimer's disease, cataracts, limb girdle muscular dystrophy, gastric carcinoma and Type II diabetes (Goll *et al*., 2003; Saito *et al*., 1993). Unlike caspases that require specific amino acid sequences for the cleavage, calpains show no obvious sequence preferences (Sorimachi *et al*., 1997). The substrates of calpains are diverse such as cytoskeletal proteins (Liu and Schnellmann, 2003; Muguruma *et al*., 1995; Ringger *et al*., 2004; Taylor *et al*., 1995), receptors (Gregoriou *et al*., 1994), ion channels (Bi *et al*., 1996; Hell *et al*., 1996), proteases (Bizat *et al*., 2003; Blomgren *et al*., 2001; Chua *et al*., 2000), oncogenic proteins (Pariat *et al*., 1997), cell signalling molecules (Sato and Kawashima, 2001; Tremper-Wells and Vallano, 2005), lens proteins (Fukiage *et al*., 1997) and extracellular matrix components such as proteoglycans and

fibronectin (Goll *et al*., 2003). Calpains are also thought to participate in the induction of cellular necrosis in various cell types (Inserte *et al.*, 2004; Shi *et al.*, 2000; Wang *et al.*, 2004) and in the regulation of apoptosis through interactions with p53, Bid and caspase 3 (Bizat *et al*., 2003; Chen *et al*., 2001; Pariat *et al*., 1997). Furthermore, calpains induce morphological changes in thrombocytes (Wolf *et al*., 1999) and neuronal cells (Yap *et al.*, 2006), resembling a caspase-mediated apoptotic cell death. Unfortunately, in many cases, the specific calpain responsible for these cellular actions and disease processes has not been identified. Consistent with the observation that calpain activation takes place at cell membranes (see above), a large portion of the substrates are proteins that are closely associated with membranes (Saido *et al*., 1994b).

The nature of calpain-catalyzed proteolysis usually proceeds in a limited manner and results in alteration, rather than simple destruction, of the substrate proteins. For example, limited proteolysis, by both μ- and m-calpains, at the hinge region between the regulatory (inhibitory) and catalytic domains of protein kinase C produces an active fragment. The activity of this active fragment is independent of cofactors such as phospholipids and phorbolester that are normally required for activation of the intact molecule (Kishimoto *et al*., 1989). In addition, limited proteolysis of a given protein by calpains is likely to cause destabilization of its structural rigidity as well, making it more sensitive to attack by various cellular proteases.

1.9 Research programme

There are two major aims of this PhD project:

1) To examine the antioxidative effect of intracellular GSH and 7,8-NP on HOCl-induced damage to HMDM cells;
2) To investigate the cell death mechanisms of HMDM cells upon HOCl exposure.

Chapter 3 will discuss the cytotoxic effect of HOCl on HMDM cells and the protective effects of intracellular GSH and 7,8-NP on HMDM cells against HOCl. The cytotoxic effect of HOCl on HMDM cells will be determined by examining cell viability loss, cell morphological changes and intracellular GSH loss in HOCl-treated HMDM cells. The protective effect of intracellular GSH on HMDM cells upon HOCl insult will be studied by examining the HOCl-induced cell viability loss in HMDM cells depleted of intracellular GSH and examining HOCl LD_{50} levels of different HMDM cell preparations against their

GSH levels. The effect of 7,8-NP in protecting HMDM cells against HOCl will be investigated by examining cell viability and intracellular GSH loss in HOCl-treated HMDM cells in the presence of extracellular 7,8-NP, or 7,8-NP produced by HMDM cells upon IFN-γ stimulation.

Chapter 4 will discuss the mode of cell death that HMDM cells undergo upon HOCl treatment and the effects of HOCl on proteins and metabolic energies in HMDM cells. Caspase-3 enzyme activation and cellular membrane integrity will be investigated to determine whether HMDM cells undergo apoptotic or necrotic cell death upon HOCl exposure. Effects of HOCl on tyrosine residues, intracellular ATP, GAPDH enzyme activity, mitochondrial membrane potential and $O_2^{\bullet-}$ generation will also be examined. The role of MPT activation in HOCl-mediated death will be examined using the MPT inhibitor, cyclosporin A.

Chapter 5 will discuss the role Ca^{2+} plays in HOCl-induced HMDM cell death. The effect of HOCl on cytosolic Ca^{2+} levels and the sources of these changes will be studied using fluorescent dyes and a range of Ca^{2+} channel blockers and a Ca^{2+} chelator. The effect of HOCl-induced cytosolic [Ca^{2+}] rise on HMDM cell viability will also be examined. Calcium ions are known to cause calpain and MPT activation. Calpain activation and its association with cell death will be studied using calpain inhibitors in HOCl-treated HMDM cells. The effect of HOCl-induced cytosolic Ca^{2+} level increase on MPT-mediated mitochondrial membrane potential loss will also be examined by reducing the cytosolic Ca^{2+} level increase and by preventing cytosolic Ca^{2+} uptake by mitochondria.

2. MATERIALS AND METHODS

2.1 Materials

2.1.1 Reagents

All reagents used were of analytical grade or better. All solutions were prepared using ion-exchanged ultra filtered water, produced using a NANOpure ultrapure water system from Barnstead/Thermolyne (IA/USA).

β-mercaptoethanol	Sigma-Aldrich Chemical Co., Missouri, USA
1,4-Dithiothreitol (DTT)	Boehringer, Mannheim, Germany
3-[(3-Cholamidopropyl)dimethylammonio]-1-propanesulfonate (CHAPS)	Sigma-Aldrich Chemical Co., Missouri, USA
3-[4,5-Dimethylthiazol-2-yl]-2,5-diphenyl-tetrazolium bromide (MTT)	Sigma Chemical Co., Missouri, USA
4-bromo-calcium ionophore A23187 (Br-A)	Sigma Chemical Co., Missouri, USA
4-(2-hydroxyethyl)-1-piperazineethane-sulfonic acid (HEPES)	Sigma Chemical Co., Missouri, USA
4'6-diamidino-2-phenylindole (DAPI)	Aldrich Chemical Co., Wisconsin, USA
4-morpholine-propanesulfonic acid (MOPS)	Sigma Chemical Co., Missouri, USA
5,5'-dithiobis-(2-nitrobenzoic acid) (DTNB)	Sigma Chemical Co., Missouri, USA
7-amino-4-methyl-coumarin (AMC)	Sigma-Aldrich Chemical Co., Missouri, USA
7,8-Dihydroneopterin (7,8-NP)	Schircks Laboratory, Switzerland
Acetic acid	Merck Ltd, Poole, England
Acetone	Merck Ltd, Poole, England
Acetonitrile	J.T.Baker (USA)
Acetyl-Asp-Glu-Val-Asp-7-amido-4-methylcoumarin (Ac-DEVD-AMC)	Sigma-Aldrich Chemical Co., Missouri, USA
Acridine orange (AO)	Invitrogen, California, USA
Adenosine diphosphate (ADP)	Sigma-Aldrich Chemical Co., Missouri, USA
Adenosine monophosphate (AMP)	Sigma-Aldrich Chemical Co., Missouri, USA
Adenosine triphosphate (ATP)	Sigma-Aldrich Chemical Co., Missouri, USA
Ammonium phosphate dibasic	Sigma Chemical Co., Missouri, USA
Anchor non fat milk powder	Fonterra Brand New Zealand, Ltd, N
Annexin V Apoptosis Kit	Santa Cruz Biotechnology Inc., (USA)
Argon gas	BOC Gasses; Auckland, NZ
Ascorbic acid	Sigma Chemical Co., St. Louis, USA
Bicinchoninic acid (BCA) protein determination kit	Pierce, Illinois, USA
Bovine serum albumin (BSA)	Sigma Chemical Co., Missouri, USA
Bromophenol blue	Sigma Chemical Co., Missouri, USA
Butylated hydroxytoluene (BHT)	Sigma Chemical Co., Missouri, USA
Calcium chloride ($CaCl_2$)	BDH lab supplies Ltd., Poole, England
Calpeptin	Merck, Darmstadt, Germany
Chelex 100 resin	Bio-Rad Laboratories, California, USA
Coumassie blue	Bio-Rad Laboratories, California, USA
Cyclosporin A (CSA)	Merck, Darmstadt, Germany
Dantrolene	Sigma Chemical Co., Missouri, USA
Diethyl ether	Merck, Darmstadt, Germany

Diehtyl maleate	Sigma Chemical Co., Missouri, USA
Dihydroethidium (DHE)	Merck, Darmstadt, Germany
Dimethyl sulphoxide (DMSO)	BDH lab supplies Ltd., Poole, England
DL-Buthionine-[S,R]-Sulfoximine (BSO)	Sigma Chemical Co., Missouri, USA
DL-O-tyrosine	Sigma Chemical Co., Missouri, USA
Ethanol	BDH lab supplies Ltd., Poole, England
Ethylenediaminetetraacetic acid (EDTA)	BDH lab supplies Ltd., Poole, England
Ethlylene glycol-bis(2-aminoethylether)-N,N,N',N'-tetracetic acid (EGTA)	Sigma Chemical Co., Missouri, USA
Flunarizine dihydrochloride	Sigma Chemical Co., Missouri, USA
Fluo-3-acetoxymethyl (AM) ester	Merck Darmstadt, Germany
Glyceraldehyde-3-phosphate (GAP)	Sigma Chemical Co., Missouri, USA
Glycerol	Sigma Chemical Co., Missouri, USA
Glycine	Bio-Rad Laboratories, California, USA
Glutathione (reduced form)	Sigma Chemical Co., Missouri, USA
Guanabenz acetate salt	Sigma Chemical Co., Missouri, USA
Hydrochloric acid (HCl)	BDH lab supplies Ltd., Poole, England
Idazoxan hydrochloride	Sigma Chemical Co., Missouri, USA
Iodine	BDH lab supplies Ltd., Poole, England
Interferon-γ (IFN-γ)	Imukin®; Boehringer Ingelheim Pty Ltd, New South Wales, Australia
Lymphoprep	Axis-Shield PoC AS, Oslo, Norway
Methanol	Merck Darmstadt, Germany
Molecular Weight Marker	Fermentas International Inc, Ontario, Canada
Monobromobimane	Sigma-Aldrich, Steinheim, Switzerland
Neopterin	Schircks Laboratory, Switzerland
Nicotinamide adenine dinucleotide (NAD^+)	Sigma Chemical Co., Missouri, USA
Nicotinamide adenine dinucleotide phosphate ($NADP^+$)	Sigma Chemical Co., Missouri, USA
Nifedipine	Sigma Chemical Co., Missouri, USA
Nitrogen gas	BOC Gasses, Auckland, NZ
NP-40	Sigma Chemical Co., Missouri, USA
Perchloric acid	BDH lab supplies Ltd., Poole, England
Phenol	Sigma Chemical Co., Missouri, USA
Phosphoric acid	BDH lab supplies Ltd., Poole, England
Ponceau S	Sigma Chemical Co., Missouri, USA
Potassium carbonate (K_2CO_3)	Merck Darmstadt, Germany
Potassium chloride (KCl)	Merck Darmstadt, Germany
Potassium iodide (KI)	May & Barker Ltd, Dagenham, England
Ruthenium red	Sigma Chemical Co., Missouri, USA
SJA6017	Merck Darmstadt, Germany
Sodium arsenate	BDH lab supplies Ltd., Poole, England
Sodium chloride (NaCl)	BDH lab supplies Ltd., Poole, England
Sodium dihydrogen orthophosphate	Merck Darmstadt, Germany
Sodium dodecyl sulphate (SDS)	Sigma-Aldrich Chemical Co., Missouri, USA
Sodium hydrogen carbonate ($NaHCO_3$)	Merck, Darmstadt, Germany
Sodium hydroxide (NaOH)	Merck, Darmstadt, Germany
Sodium hypochlorite (NaOCl)	Clorogene Supplies, Petone, NZ
Sucrose	Chelsea Sugar Refinery, Auckland, NZ
Supersignal West Dura chemiluminescence	Pierce Biotechnology Inc., Illinois, USA
Tetrabutylammonium bisulfate	Merck Darmstadt, Germany
Tetramethylrhodamine methyl ester (TMRM)	Merck Darmstadt, Germany
Thimerosal	Sigma Chemical Co., Missouri, USA
Trichloroacetic acid (TCA)	Sigma Chemical Co., Missouri, USA
Trifluoroacetic acid (TFA)	Sigma Chemical Co., Missouri, USA
Tris(hydroxymethyl)aminomethane (Tris)	Roche Diagnostics GmbH, Mannheim, Germany

Triton X-100	Sigma Chemical Co., Missouri, USA
Trypan blue solution (0.4%)	Sigma Chemical Co., Missouri, USA
Tween-20	Sigma Chemical Co., Missouri, USA
Verapamil hydrochloride	Sigma Chemical Co., Missouri, USA

2.1.2 Antibodies

Goat anti-mouse IgM HRP-conjugated	Santa Cruz Biotechnology Inc., USA
Mouse monoclonal against β-Actin	Sigma-Aldrich Chemical Co., USA
Mouse monoclonal IgG2a caspase-3 (E-8)	Santa Cruz Biotechnology Inc., USA
Sheep Anti-mouse IgG HRP-conjugated	Amersham Biosciences, England

2.1.3 Media and buffer

Earle's balanced salt solution (EBSS)	Invitrogen, California, USA
Heat-inactivated foetal calf serum	Invitrogen, California, USA
Penicillin/streptomycin liquid (containing 5000 units of penicillin and 5000μg of streptomycin/ml)	Invitrogen, California, USA
Roswell Park Memorial Institute (RPMI)-1640 media, with phenol red	Sigma-Aldrich Chemical Co., Missouri, USA
RPMI-1640 media, without phenol red	Sigma-Aldrich Chemical Co., Missouri, USA

2.1.4 General Solutions, Buffers and Media

2.1.4.1 Phosphate Buffered Saline (PBS)

Phosphate buffered saline (PBS; 150 mM NaCl and 10 mM sodium dihydrogen orthophosphate, pH 7.4) was stirred with 1 g of washed Chelex 100 resin for at least 4 hours to remove metal ions, followed by vacuum filtration using a 0.45 μm Phenex filter membrane (Phenomenex).

2.1.4.2 RPMI-1640 media (with or without phenol red)

The media was prepared as per manufacturer's instructions. Powdered RPMI-1640 (with or without phenol red) was dissolved in nanopure water, followed by addition of sodium bicarbonate and pH adjustment to 7.4 with 1 M NaOH. The media was filter-sterilised using a peristaltic pump (CP-600, Life Technologies) and a 0.22 μm Millex®-GP_{50} filter (Molsheim, SA). Once transferred into sterile bottles, media was stored at 4°C but warmed to 37°C before use.

2.1.4.3 7,8-Dihydroneopterin (7,8-NP) and interferon-γ (IFN-γ) solutions

A 2 mM stock of 7,8-dihydroneopterin (7,8-NP) was prepared fresh prior to each experiment. It was dissolved in degassed ice cold RPMI-1640 medium or EBSS buffer with 0.68 mM $CaCl_2$ during a 5-minute sonication. 7,8-NP was then filtered through a 0.20 μm membrane filter (Sartorius AG, Goettingen, Germany), and diluted to working concentrations in warm HMDM culture medium or EBSS with 0.68 mM $CaCl_2$. A 10,000 unit/ml IFN-γ stock solution was diluted to working concentrations (0-750 unit/ml) in warm HMDM culture medium.

2.1.4.4 Diethyl maleate (DEM) solution

A 100 mM diethyl maleate (DEM) stock solution was prepared in DMSO, which was then diluted to 2 mM in RPMI-1640 medium and filtered using a 0.20 μm membrane filter. The 2 mM stock was diluted to working concentrations (0-500 μM) in HMDM culture medium.

2.2 Methods

2.2.1 Cell culture

All cell experiments and preparation were carried out under aseptic conditions in a Class II biological safety cabinet (Clyde-Apex BH 200). Sterile plastic wares were supplied by Bector Dickinson & Co., Falcon, Nunc, Terumo, Unomedical, and Greiner Bio-one. Media and solutions were sterilised either by autoclaving or by filtration through a sterile 0.22 μm membrane filter. Any equipments and tissue culture products were sprayed with 70% ($^{v}/_{v}$) ethanol before being transferred into the Class II biological safety cabinet.

Experiments were conducted on both the THP-1 monocyte-like cell line and primary HMDM cells. Those cells were incubated at 37°C in a humidified incubator, with an atmosphere calibrated to 5% carbon dioxide: 95% air (Nuaire™ IR Autoflow).

2.2.1.1 Cell culture media

RPMI-1640 medium (with phenol red) containing 100 units/ml penicillin G and 100 μg/ml streptomycin was supplemented with either 10% ($^{v}/_{v}$) heat-inactivated human serum (HIHS)

(see **section 2.2.1.2**) or 5% ($^{v}/_{v}$) heat-inactivated foetal calf serum for culturing HMDMs or THP-1 cells, respectively. These two growth media for HMDM and THP-1 cells are referred to in the thesis as HMDM culture medium and THP-1 culture medium, respectively.

2.2.1.2 Preparing Human Monocyte-Derived Macrophages (HMDMs)

Ethics approval for the use of human blood was granted by the Canterbury Ethics Committee (protocol number 98/07/069). The isolation procedure for HMDMs was adapted from Firth (2006; PhD thesis) and carried out at room temperature. All the media and solutions were warmed up to room temperature prior to use, except for the HMDM culture medium, which was warmed up to 37°C.

Unlinked blood was collected from consenting haemochromatosis patients into 600 ml autologous bags containing the anticoagulant citrate-phosphate-dextrose-adenine (CPDA-1) by the NZ Blood Bank (Riccarton Road, Christchurch). Upon arrival at the Free Radical Biochemistry Laboratory, the blood was centrifuged (Multifuge 1 S-R, Heraeus) for 20 minutes in 50 ml Falcon tubes at 3000 g, with slow deceleration. The resulting buffy coat was collected using a mixing cannula attached to a 10 ml syringe, transferred into new Falcon tubes at 15 ml per tube, and mixed well with PBS at 20 ml per tube. The mixture was then underlaid with 15 ml of Lymphoprep, and centrifuged at 1000 g for 20 minutes with the brake on.

After centrifugation, a white layer of monocytes/lymphocytes appearing about half-way down the Falcon tube was transferred to new centrifuge tubes (50 ml/tube). Each tube was topped up to 45 ml with sterile PBS and centrifuged at 500 g for 15 minutes. The resulting cell pellet was washed in 45 ml of PBS (at 500 g for 10 minutes) 3 times. The cell pellet was subsequently re-suspended in serum-free RPMI-1640 media (at 5×10^{6} cells/ml) (see **section 2.2.5.2** for monocytic cell density determination), followed by incubation in 6-well Falcon suspension culture plates for approximately 40 hours. Under these conditions, any T cells contaminating the cell suspension are unable to survive and platelets adhere to the surface of the plates, while monocytes remain viable in suspension.

After 40 hours, the viable monocytes were centrifuged at 500 g for 15 minutes and re-suspended in HMDM culture medium supplemented with approximately 150 ng/ml

granulocyte macrophage colony-stimulating factor (GMCSF), at a concentration of 5×10^6 cells/ml. The cells were then plated at 5×10^6 cells/well in 12-well adherent plates. GMCSF was a gift from the Haemotology Research lab at the Christchurch School of Medicine, University of Otago.

The cells were also plated on coverslips using the method adapted from Amit (2008; PhD thesis). Coverslips (22×22mm; Marienfeld) were sterilised by immersing in 96% ethanol under aseptic conditions. This was followed by UV sterilisation for 15 minutes, during which they were left to dry. The sterilised coverslips were then placed into 6-well suspension culture plates (1 coverslip/well) and the cells were plated on top of the coverslip at 5×10^6 cells/coverslip. The plate was left undisturbed at room temperature for 1 hour, allowing the cells to attach to the coverslip, before adding 1 ml of HMDM culture medium into each well. Both 6-well and 12-well plates were then incubated at 37°C.

The HMDM culture medium was replaced every three to four days. Experiments were conducted once more than 70% of monocytes had matured to macrophages, which usually took 14 days after plating.

2.2.1.3 Preparation of heat-inactivated human serum (HIHS)

Unlinked blood from consenting haemochromatosis patients was collected into 600 ml dry bags by the NZ Blood Bank (Riccarton Road, Christchurch). The blood bag was incubated in an upright position at room temperature for 1 hour and then at 4°C overnight. This treatment allowed the blood to clot and the serum to separate from the blood clot. The serum was subsequently collected into 50 ml centrifuge tubes and centrifuged at 1500 rpm for 15 minutes to pellet any remaining blood cells. The resulting serum was transferred into new 50 ml centrifuge tubes, heat inactivated in a water bath at 56°C for 30 minutes, and then stored at –80 ºC.

2.2.1.4 Preparation of THP-1 cell line

The THP-1 cell line was originally obtained from a patient with acute monocytic leukaemia and has been confirmed to possess monocytic properties (Tsuchiya *et al.*, 1980). Our THP-1 cells were obtained from the Haemotology Research lab at the Christchurch School of Medicine, University of Otago.

Two vials of 20×10^6 cells/mL THP-1 cells, at 1 mL per vial, were removed from the liquid nitrogen storage and defrosted in a 37°C water bath until only a small piece of frozen liquid remained in the vials. The liquid in both vials was then poured into 30 ml of THP-1 culture medium in a 50 ml centrifuge tube, followed by centrifugation at 500 g for 5 minutes to remove the DMSO freezing medium. The resulting cell pellet was re-suspended in 10 ml of THP-1 culture medium in a 25 cm^2 tissue culture flask. Cell density was determined by Trypan blue assay (see **section 2.2.5.2**) and maintained at $0.3\text{-}1\times10^6$ cells/ml by passaging in 75cm^2 tissue culture flasks every 3 days.

2.2.2 Measurement of HOCl concentration

The concentration of sodium hypochlorite (NaOCl), stored at 4°C, was measured using the method described by van den Berg and Winterbourn (1994). A pH 12 buffer containing 25 ml of 0.2 M KCl and 6 ml of 0.2 M NaOH diluted to 100 ml with nanopure water was prepared. The buffer was then used to dilute the stock NaOCl 500-fold, and the absorbance at 292 nm measured on a Shimadzu UV-1601PC UV-visible spectrophotometer (Shimadzu Corporation, Japan). The concentration was determined using the extinction coefficient (350 $M^{-1}cm^{-1}$) of HOCl at pH 12 (Gazda and Margerum, 1994).

2.2.3 HOCl experimental setup

NaOCl was diluted to working concentrations in Earle's balanced salt solution (EBSS) containing 0.68 mM $CaCl_2$, unless otherwise stated. At pH 7.4, the HOCl solution contained about equimolar concentrations of HOCl and OCl^- (pka = 7.5) (Morris, 1966); however we have referred to it in the thesis as HOCl for simplicity. All the media and solutions were warmed up to 37°C prior to experiments.

HMDMs (5×10^6 cells/ml) were washed three times in PBS, followed by incubation with 0-500 μM HOCl (at 1ml/well) at 37°C for 10 minutes, unless otherwise stated. After treatment, the HOCl medium was removed and the cells were washed twice with PBS. Any cells dislodged during the HOCl treatment and washing steps were collected in 1.7 ml microtubes (Axygen, Scientific, USA) and the solutions were centrifuged for 7 minutes at 500 g. The resulting pellet was mixed with the corresponding adherent cells in each well.

The above processes were carried out before any analyses mentioned below, unless otherwise stated.

2.2.4 Incubation of THP-1 cells with 6% ethanol

Two millilitres of 1×10^6 cells/ml THP-1 cells were transferred to each well of a 12-well suspension culture plate. Cells were subsequently treated with or without 6% ethanol for 5 hours before transferring the cells to 15 ml centrifuge tubes and centrifugation at 400 g for 5 minutes at room temperature. The cell pellet was washed twice more with cold PBS at 2600 g for 5 minutes at 4°C, followed by storage at -80°C until analysis.

2.2.5 Cell viability assays

2.2.5.1 MTT reduction assay

The 3-(4,5-dimethylthiazol-2-yl)-2,5-diphenyl tetrazolium bromide (MTT) assay provides an indirect measure of cell viability. Metabolically active cells can endocytose and metabolise the yellow MTT compound, via the action of cellular NAD(P)H dehydrogenases, into a purple insoluble MTT-formazan product that can be quantified spectrophotometrically (Mosmann, 1983). The colour intensity provides an indication of the concentration of cells and their metabolic activity.

MTT was dissolved in RPMI-1640 medium (without phenol red), at a concentration of 5 mg/ml. The mixture was then sterilised through a 0.2 μm membrane filter (Sartorius AG, Germany) and stored at –20°C in the dark. 10% ($^{w}/_{v}$) sodium dodecyl sulphate (SDS) in 0.01 M hydrochloric acid (HCl) was stored at room temperature.

After treatment (see **section 2.2.3**), HMDMs in each well were incubated at 37°C with 1 ml of RPMI-1640 without phenol red containing 0.5 mg/ml MTT for 1 hour. The insoluble purple crystals developed in each well were then dissolved by mixing with 1 ml of 10% ($^{w}/_{v}$) SDS. The absorbance was read at 570 nm, against a blank lacking cells but containing all other reagents.

2.2.5.2 Trypan Blue Exclusion Staining

Trypan blue exclusion staining measures cell viability by analysing cell membrane integrity (Moldeus *et al.*, 1978). Viable cells have intact membranes that are impermeable to the dye and, as a consequence, appear opaque when viewed under a microscope. Dead cells have compromised membrane integrity and stain a deep blue colour due to trypan blue uptake.

Trypan blue stain (200 µl) was added directly to HMDMs in each well. After 1 minute, the dye in each well was replaced with 1 ml of PBS buffer. An inverted microscope was subsequently used to randomly examine five fields of view across each well. The proportion of viable cells in that well was calculated by dividing the number of viable cells from all five fields of view by the total number of cells (both alive and dead) from all five fields of view.

This method is also used to count monocytes and THP-1 cells on a haemocytometer (Marienfeld, Germany). Monocytes and THP-1 cells were mixed with the stain at 1:10 and 1:1 ratios, respectively. Subsequently, a light microscope was used to count the number of opaque (alive) cells in defined regions of a haemocytometer.

2.2.6 Total thiol determination by the DTNB assay

Cellular free thiol concentrations were measured using an assay described by Ando and Steiner (1973) and modified by Soszynski *et al.* (1997). 5,5'-Dithiobis-2-nitrobenzoic acid (DTNB or called Ellman's reagent) reacts with free thiols at 1:1 stoichiometry. The resulting product, 3-carboxylato-4-nitrothiophenolate (CNTP), is a coloured anion with a peak absorbance at 412 nm. DTNB (MW 396.3 g/mol) was dissolved in PBS to give a stock concentration of 3 mM, which was stored at 4°C in the dark for up to 1 month. 1% ($^{w}/_{v}$) SDS was made up by dissolving SDS in PBS and stored at room temperature.

HMDMs in each well were solubilised by adding 1 ml of 1% ($^{w}/_{v}$) SDS to each well. The resulting cell lysate was transferred to 1.7 ml microtube and sonicated for 15 seconds. Cell lysate (50 µl) was taken for protein assay (see **section 2.2.10**) before adding 500 µl of cold 3 mM DTNB solution to each sample (final concentration 1 mM). The samples were subsequently incubated at room temperature in a heated shaking block (Eppendorf Thermomixer 5436) for 30 minutes. The absorbance was then measured at 412 nm, against

blanks containing 1% ($^{w}/_{v}$) SDS with DTNB and also cell lysate lacking DTNB. Absorbance values were converted into thiol concentrations using an extinction coefficient of 13,600 $M^{-1}cm^{-1}$ (Boyne & Ellman, 1972).

2.2.7 HPLC analyses

High Performance Liquid Chromatography (HPLC) is a widely used system for separating, identifying and quantifying compounds. The HPLC system (Shimadzu Corporation, Japan) used in this research consisted of a controller (LC-20AD), a fluorescence detector (RF-10AXL), a UV-Vis detector (SPD-M20A), an auto sampler (SIL-20AC HT), a column oven (CTO-20A), inline vacuum degasser (DGU-$20A_5$), and a communication bus module (CBM-20A). Peak areas were quantified using the Shimadzu CLASS-VP software package.

All the mobile phases used were sonicated (Alphatech Systems Ltd & Co., Auckland) for 10 minutes prior to pumping through the HPLC system. Analytes in samples were standardised against particular standards with known concentrations to determine their concentrations.

2.2.7.1 Intracellular GSH analysis

Monobromobimane (MBB) is a cell-permeable fluorescent dye that binds thiol groups, specifically those of GSH. The GSH-MBB adducts can then be detected by the HPLC system after protein precipitation (Cotgreave and Moldeus, 1986). The procedures were carried out under minimum exposure of light, as MBB is light sensitive.

MBB (MW 271.1) was dissolved in acetonitrile to give a 40 mM stock, which was stored in darkness at 4°C for up to 2 weeks. Reduced GSH (MW 307.3 g/mol), at 5 and 10 μM concentrations, was prepared in cold PBS immediately before HPLC analysis to serve as standards.

For analysis, the media was removed and 400 μl of PBS, 9 μl of 0.1 M NaOH (to bring up the pH to 8), and 10 μl of 40 mM MBB were added to each well of HMDM cells, in this order. After 20 minutes of incubation in the dark at room temperature, 20 μl of 100% ($^{w}/_{v}$) trichloroacetic acid (TCA) was added to lyse the cells and precipitate cellular proteins. The cell lysate was collected and centrifuged in 1.7 ml microtubes at 900 g for 5 minutes. Five

µl of the resulting supernatant was injected onto the Phenosphere reverse phase C-18, 150×4.6 mm, 5 µm column (Phenomenex, Auckland, NZ), heated to 35°C. GSH-MBB adducts were detected by the fluorescence detector with excitation and emission wavelengths set at 394 nm and 480 nm, respectively. Mobile phase A (consisting of 0.25% acetic acid in nanopure water) and mobile phase B (consisting of 100% acetonitrile) were pumped through the column at a flow rate of 1.5 ml/minute with the following gradient program:

Time (minutes)	**Mobile phase A (0.25% acetic acid)**	**Mobile phase B (100% acetonitrile)**
0	90 %	10 %
10	90 %	10 %
11	0 %	100 %
15	0 %	100 %
16	95 %	5 %
20	95 %	5 %

2.2.7.2 Pterin analysis

This method was adapted from Flavall (2007; master thesis) and can measure pterin level in the cell-conditioned medium, cell-free medium, and in cells. 7,8-dihydroneopterin (7,8-NP) does not fluoresces, whereas neopterin (the oxidised form of 7,8-NP) can be detected by its native fluorescence. Total pterins (neopterin plus 7,8-NP) can therefore be detected by oxidising 7,8-NP to neopterin, and the initial 7,8-NP concentration can be calculated by subtracting neopterin level from total pterin level.

The acidic iodide solution (5.4% ($^{w}/_{v}$) iodine and 10.8% ($^{w}/_{v}$) potassium iodide in 1 M HCl) was prepared by dissolving 5.4 g of potassium iodide and 2.7 g of solid iodine in 35 ml of nanopure water, followed by adding 4.37 ml of 100% HCl. The solution was then made up to a final volume of 50 ml. Ascorbic acid (MW 176) at a concentration of 0.6 M in nanopure water was made fresh on the day of analysis.

HMDMs in each well were scraped off the wells and lysed in 300 µl of cold nanopure water and acetonitrile (1:1 ratio). One hundred µl of cell lysate was aliquoted to two sets of 1.7 ml microtubes; one for neopterin measurement and the other one for total pterin

measurement. As for cell-conditioned or cell-free medium, 100 µl of the medium was transferred to two sets of 1.7 ml microtubes and mixed well with 100 µl of acetonitrile.

The 100 µl samples prepared for neopterin measurement were vortexed thoroughly and centrifuged at 20,800 g for 10 minutes at 4°C. To 100 µl samples for total pterin measurement, 40 µl of the acidic iodide solution was added before vortexing for a few seconds. The reaction mixture was then incubated at room temperature for 15 minutes in the dark. Forty µl of 0.6 M ascorbic acid in water was subsequently added and mixed by vortexing briefly to oxidise the remaining iodine. The reaction mixture was then centrifuged at 20,800g for 10 minutes at 4°C. As a result, the reaction mixture for total pterin measurement contained only 40% acetonitrile, which was different from the 50% acetonitrile present in the neopterin standard (see below). However, the preliminary test showed that the elution times of neopterin peaks for the total pterin samples and the neopterin standard were very similar, indicating that this acetonitrile percentage differences did not affect the elution time of neopterin peak.

Ten µl of the supernatant from both neopterin and pterin samples was injected onto a reverse phase Synergi Hydro-RP 80A, 250 × 4.6 mm, 4 µm column (Phenomenex, Auckland, NZ), maintained at 35°C. The column was developed with a mobile phase of 95% ($^{v}/_{v}$) of 20 mM ammonium phosphate (pH 6) and 5% ($^{v}/_{v}$) methanol, pumped at a flow rate of 1 ml/minute. Twenty mM ammonium phosphate (MW 132.06) in nanopure water was adjusted to pH 6 by adding 10 M phosphoric acid. Neopterin was detected by a fluorescence detector using excitation and emission wavelengths set at 353 nm and 438 nm, respectively. A neopterin (MW 253) standard of 25 nM to 2 µM concentrations, made up in acetonitrile and 20 mM ammonium phosphate (pH 6) (1:1 ratio), was used to quantify the elution time and peak size of neopterin.

2.2.7.3 Protein tyrosine residue oxidation

Tyrosine residue oxidation serves as an indicator of protein damage by free radical exposure (Gieseg *et al.*, 1993; Gieseg *et al.*, 2003). In this research, cellular tyrosine residue loss upon HOCl insult was examined by measuring cellular tyrosine residue levels via acid hydrolysis of cellular proteins and HPLC analysis.

To each well of HMDMs, 1 ml of cold nanopure water, 50 µl of 100 mg/ml ethylene-diaminetetraacetic acid (EDTA), and 50 µl of 20 mg/ml butylated hydroxytoluene (BHT) in methanol were added in this order. The cells were then scraped off the wells, transferred to 1.7 ml microtubes, and sonicated for 5 minutes. The cell lysate (200 µl) was then transferred to a glass durham tube with a diameter of 7.5 mm and mixed with 10 µl of 100 mg/ml EDTA and 10 µl of 20 mg/ml BHT. The protein was then precipitated by adding 800 µl of ice cold acetone and incubating on ice for 10 minutes before centrifugation at 7000 g at 4ºC for 15 minutes. After removing the supernatant, the pellet was washed with 500 µl of ice cold diethyl ether with centrifugation to remove any remaining lipids.

For the acid hydrolysis of proteins, the resulting pellet was dried under vacuum for 1 hour and then placed into a Pico-Tag vial (Millipore, USA) containing 1 ml of 6M HCl with 1% ($^{w}/_{v}$) phenol and 50 µl of β-mercaptoethanol. Argon gas was flushed through the Pico-Tag vial for 5 minutes to remove oxygen. The vial was then evacuated by connecting to a high vacuum line for 2 seconds (the Vac. gauge pressure was maintained below 200mm Torr). Subsequently, the vial was incubated in a 110ºC oven for 16 hours, followed by gradual cooling down to 4ºC. Next, the sample was centrifuged under vacuum using the Speed Vac for 2 hours before re-solubilising the pellet with 200 µl of 0.1% trifluoroacetic anhydride (TFA) (pH 2.5). The sample was then centrifuged at 20,800 g for 5 minutes at 4ºC before transferring 100µl of the resulting supernatant to an auto sampling vial. Ten µl was injected onto a reverse phase Aqua C18, 250 x 4.6 mm, 5µm column (Phenomenex). The column was developed with mobile phase A (0.1% ($^{v}/_{v}$) TFA at pH 2.5) and mobile phase B (100% acetonitrile), pumped at a flow rate of 1 ml/minute using the following gradient program. TFA with a concentration of 0.1% ($^{v}/_{v}$) at pH 2.5 was prepared by adding 1 ml of TFA to 800 ml of nanopure water, adjusting the pH to 2.5 with 10 M NaOH, and making up to a final volume of 1 L. Tyrosine was detected by a fluorescence detector using excitation and emission wavelengths set at 280 nm and 320 nm, respectively. A tyrosine (MW 181.2) standard of 1 µM concentration, made up in 0.1% ($^{v}/_{v}$) TFA (pH 2.5), was used to quantify the elution time and peak size of tyrosine residue.

Time (minutes)	Mobile phase A (0.1% TFA, pH 2.5)	Mobile phase B (100% acetonitrile)
0	99 %	1 %
10	95 %	5 %
14	90 %	10 %
16	50 %	50 %
21	50 %	50 %
30	99 %	1 %

2.2.7.4 Measurement of intracellular ATP

The effect of HOCl on ATP in HMDMs was examined by measuring intracellular ATP levels upon HOCl exposure via HPLC analysis. For sufficient signal to be detected by the HPLC system, 3 wells of 5×10^6 cells/ml HMDMs were combined together by scraping using a total of 125 µl cold 0.07 M perchloric acid (PCA) in nanopure water. The cell lysate was then sonicated for 1 minute, left on ice for 30 minutes, and centrifuged at 20,800 g for 5 minutes at 4°C to remove proteins. The supernatant was neutralised with 12.5 µl of 2 M potassium carbonate (MW 138.21) in nanopure water (the ratio between 0.07 M PCA and 2 M potassium carbonate was 10:1) and centrifuged as above. The supernatant (40 µl) was injected onto a reverse phase 5 µm ODS (C18), 250 x 4.6 mm, 5 µm column (Phenomenex). This column was developed with mobile phase A (consisting of 6.9 g/L of sodium phosphate (MW 137.99) and 2 g/L of tetrabutylammonium bisulfate (MW 339.54) in nanopure water, pH adjusted to 5.5 using 10 M NaOH) and mobile phase B (consisting of mobile phase A and acetonitrile at a ratio of 75:25), pumped at a flow rate of 1 mL/minute using the following gradient program;

Time (minutes)	Mobile phase A (pH 5.5)	Mobile phase B
0	100 %	0 %
5	100 %	0 %
25	30 %	70 %
28	30 %	70 %
30	100 %	0 %
50	100 %	0 %

ATP was quantified by reverse phase ion pair-HPLC UV/Vis detection at 254 nm (Tuckey, 2008; PhD thesis). An ATP stock of 1 mM concentration was prepared in 50 mM NaH_2PO_4 (pH 7.2) and stored at -20°C. The stock was diluted to 25 µM in cold nanopure water immediately before use to serve as a standard for quantifying the elution time and peak size of ATP.

2.2.8 GAPDH activity measurement

Glyceraldehyde-3-phosphate dehydrogenase (GAPDH) is a glycolytic enzyme that catalyses the oxidative phosphorylation of glyceraldehyde-3-phosphate (GAP) to 1,3-diphospho-glycerate (1,3-PGA). In the process, the NAD^+ cofactor is reduced to NADH, which has a strong absorbance at 340nm. The activity of GAPDH can hence be monitored spectrophotometrically by measuring the rate of NADH formation using an assay modified from Steck and Kant (1974).

Thirty mM NaH_2PO_4 (pH adjusted to 8 with 10 M NaOH) in nanopure water, 0.2M sodium arsenate (MW 312.01) in nanopure water, and 0.2% ($^v/_v$) Triton X-100 in 30 mM NaH_2PO_4 (pH 8) were all stored at room temperature. A 294 mM GAP (MW 170.6) stock in nanopure water was stored at -80°C, which was diluted to the 15 mM working concentration in nanopure water. 20 mM NAD^+ (MW 663.43) was made up fresh on the day of analysis in cold nanopure water. Both substrates were stored on ice during use.

HMDM cells in each well were scraped off using cell scrapers (Greiner bio-one, Germany) and 1 ml of cold PBS. The resulting cell mixture was transferred to a 1.7 ml microtube and stored on ice. One hundred µl of cell lysate and 100 µl of 0.2% ($^v/_v$) Triton X-100 were mixed in a semi-micro cuvette, which was then incubated for 1 minute in the spectrophotometer at 37°C. To this was added 600 µl of 30 mM NaH_2PO_4 (pH 8) that had already been equilibrated to 37°C, 50 µl of 0.2 M sodium arsenate, 50 µl of 20 mM NAD^+, and 100 µl of 15 mM GAP in this order, followed by mixing. The absorbance was recorded at 0.1-minute intervals over 3 minutes at 294 mM. The molar extinction coefficient of NADH (6220 $M^{-1}cm^{-1}$) was used to calculate the rate of NADH release in µM/minute.

2.2.9 SDS-PAGE and Western blot analysis

2.2.9.1 Solutions for SDS-PAGE and Western blot analysis

The cracker buffer was prepared by dissolving SDS (MW 288.38), glycerol (MW 92.10), bromophenol blue (MW 670.02) in 0.5 M tris-HCl in nanopure water (pH adjusted to 6.8 using 11.4 M HCl) and making up to a final volume of 50 ml. Prior to use, 1 ml of the above solution was mixed with 20 µl of β-mercaptoethanol and 2 ul of 100 mg/ml ethylenediaminetetraacetic acid (EDTA). The final cracker buffer hence consisted of 0.125 M Tris-HCl (pH 6.8), 1% ($^{w}/_{v}$) SDS, 20% ($^{w}/_{v}$) glycerol, 0.1% ($^{w}/_{v}$) bromophenol blue, 2% ($^{v}/_{v}$) β-mercaptoethanol, and 0.5 mM EDTA.

Lysis buffer consisted of 40 mM of HEPES (MW 238.31), 50 mM of NaCl (MW 58.44), 1 mM EDTA (MW 372.24), and 1 mM EGTA (MW 380.4) in nanopure water, with pH adjusted to 7.4 using 10 M NaOH and stored at 4°C. Prior to use, Complete, Mini protease inhibitor stock (7×) was added to lysis buffer. The 7× stock protease inhibitor solution was prepared as per manufacturer's instructions. One Complete, Mini protease inhibitor cocktail tablet (Roche, Germany) was dissolved in 1.5 ml of nanopure water to give a 7× stock solution. The completed lysis buffer was stored on ice until use.

MOPS (4-morpholine-propanesulfonic acid) buffer consisted of 50 mM MOPS, 50 mM tris base, 0.1% ($^{w}/_{v}$) SDS, and 1 mM EDTA in nanopure water, with the pH adjusted to 7.7 by adding concentrated HCl.

Transfer buffer for Western blot analysis consisted of 25 mM tris, 192 mM glycine (MW 75.07), and 20% ($^{v}/_{v}$) methanol in nanopure water, which was stored at 4°C until use. Ponceau S stain consisted of 0.01% ($^{w}/_{v}$) Ponceau S and 5% ($^{v}/_{v}$) acetic acid.

The TBS washing solution consisted of 40 mM Tris-HCl (pH 7.5), 150 mM NaCl, 0.05% Tween-20 ($^{w}/_{v}$), and 0.01% ($^{w}/_{v}$) thimerosal (contains Hg) in nanopure water. The 5% ($^{w}/_{v}$) blocking solution (TBSM) was prepared by dissolving 10 g of Anchor non-fat milk powder in 200 ml of TBS and was stored at 4°C. 1 and 2% TBSM, were made up by diluting the 5% TBSM with TBS.

2.2.9.2 Cell processing for HMDM and THP-1 cells

One hundred and fifty µL of ice cold complete lysis buffer was used to scrape HMDMs off the plate or lyse THP-1 cell pellet (see **section 2.2.4**). The cell lysate was then transferred into a 1.7 ml microtube and incubated on ice to properly lyse the cells. After 30 minutes, the cell lysate was vortexed briefly and 5 µl was taken for protein assay (see **section 2.2.10**), while the rest was stored at -80°C until use.

After protein analysis, the volume of cell lysate containing 90 µg of protein was transferred to a new 1.7ml microtube. Ice cold acetone was then added to precipitate the proteins (the ratio of cell lysate to acetone was 1:10). After incubation on ice for 5 minutes, the sample was centrifuged at 20,800 g for 5 minutes at 4°C. The resulting protein pellet was dissolved in "cracker" buffer for SDS-PAGE analysis (see **section 2.2.9.3**).

2.2.9.3 Sodium dodecyl sulfate polyacrylamide gel electrophoresis (SDS-PAGE) analysis

Cracker buffer (90 µl) was used to dissolve the acetone-precipitated protein pellet described above to give a final protein concentration of 1 µg/µl. The sample was then heated in a heating block at 95ºC for 3 minutes and centrifuged for 5 minutes at 20,800 g at room temperature to remove any cell debris.

A gradient polyacrylamide gel, 4-12% (Bis-Tris Gel, Invitrogen, Carslband, CA, USA), was placed in the XCell SureLock™ Mini-Cell system (Invitrogen, US) and the MOPS running buffer added to the buffer reservoir. Five µl of Fermentas pre-stained molecular weight marker mix (Fermentas International Inc, Canada) and 15 µL of samples (containing 15 µg proteins) were loaded into the wells of the gel, before electrophoresis at 200 V for approximately 1 hour until the loading buffer dye reached the bottom of the gel.

2.2.9.4 Western blot analysis

After SDS-PAGE, the separated proteins on the SDS-PAGE gel were electrophoretically transferred onto a nitrocellulose membrane with 0.45 µm pore size (Invitrogen, USA) using a Hoefer^{TM} TE22 tank transfer unit (USA) filled with cold transfer buffer, with voltage set at 70 V using the PowerPac 300 power supply (BioRad). After approximately

15 hours, the nitrocellulose membrane was stained with Ponceau S stain for 1 minute to ensure that the transfer was successful.

The following membrane washing and incubation took place on a rocking platform mixer (Ratex Instruments, Australia). After briefly rinsing with water, the membrane was blocked using 5% TBSM for 2 hours, followed by three consecutive 5-minute washes in TBS. The membrane was then probed with the primary mouse monoclonal IgG2a antibodies against caspase-3 (E-8) (Santa Cruz Biotechnology Inc, USA) in 1:1000 dilution using 1% TBSM. After 1.5 hours, the membrane was washed 5 times in TBS 5 minutes each, followed by 1 hour incubation in the secondary antibody goat anti-mouse IgM-HRP (Santa Cruz Biotechnology Inc, USA) diluted to 1:1000 with 1% TBSM. The membrane was then washed as above, followed by brief washing in nanopure water twice to remove any residual TBS. TBS contains Tween-20, which inhibits the peroxidase from reacting with the chemiluminescence substrates, and hence interferes with visualisation (see **section 2.2.9.5**). The membrane was then left in nanopure water and taken for visualisation immediately.

2.2.9.5 Visualisation

Detection of the secondary HRP-coupled antibody was conducted using "Supersignal West Dura chemiluminescence" substrates (Pierce, USA), which consist of the luminol solution and the peroxide solution. These two solutions were mixed at 1:1 ratio to give the working solution immediately before use. When applied to the membrane, the luminol in the working solution reacts with the horseradish peroxidase (HRP) on the secondary antibody on the membrane and hydrogen peroxide in the working solution to generate 3-aminophthalate plus the emission of light at 425 nm.

The working solution (0.5 ml) was evenly applied to the membrane and the image was recorded for 12 minutes on a Syngene Chemigenius-2 bioimaging system using Genesnap software (Global, NZ). The membrane was then stored in TBS at 4ºC for β-actin detection (see **section 2.2.9.6**).

2.2.9.6 β-actin detection

The membrane (see **section 2.2.9.5**) was re-probed for β-actin as an internal control to confirm equal loading of proteins. The membrane was incubated for 1.5 hours with the primary mouse monoclonal antibodies against β-actin (Sigma-Aldrich Chemical Co., USA) diluted to 1:10000 in 1% TBSM. The procedures and visualisation were the same as those mentioned in **sections 2.2.9.4** and **2.2.9.5.** The two exceptions were that the secondary antibody used was peroxidase-conjugated sheep anti-mouse IgG (Amersham Biosciences, England) diluted to 1:10000 in 1% TBSM, and the exposure time for visualisation was 2 minutes.

2.2.10 Determination of protein concentration

Protein concentration was determined using the bicinchoninic acid (BCA) protein determination kit from Pierce (supplied by Global Scientific). The working reagent was prepared by mixing Reagent A (sodium carbonate, sodium bicarbonate, BCA and sodium tartrate in 0.1 M sodium hydroxide) and Reagent B (4% $CuSO_4.5H_2O$) at a 50:1 ratio immediately before use.

Fifty µl of sample and/or 0-250 µg/ml bovine serum albumin (BSA) were mixed with 1 ml of working reagent and incubated at 60°C for 30 minutes with gentle shaking in a heated shaking block before measuring the absorbance at 562 nm against water blank. Protein concentration was determined using the BSA standard curve.

2.2.11 Measurement of cellular caspase-3 activity

2.2.11.1 Solutions required for caspase-3 activity measurement

Caspase-3 binds to the synthetic substrate, acetyl-Asp-Glu-Val-Asp-7-Amido-4-methylcoumarin (Ac-DEVD-AMC), and enzymatically cleaves the substrate to release the fluorescent AMC, which can be detected by the fluorometer.

A buffer consisting of 100 mM of HEPES, 10% ($^{w}/_{v}$) sucrose, 0.1% ($^{w}/_{v}$) CHAPS, and 10^{-4} % ($^{w}/_{v}$) NP-40 was prepared in nanopure water, with the pH adjusted to 7.25 with 10 M NaOH and stored at -20°C.

Ac-DEVD-AMC (50 mM) in 100% DMSO was stored at -20°C. Dithiothreitol (DTT) (1 M) was prepared in nanopure water and kept on ice in the dark for no more than 24 hours. AMC (0-1000 nM) was prepared in dimethyl sulphoxide (DMSO) as standards. Working solution was made up of 1 ml of buffer, 5 µl of 1 M DTT, and 1 µl of 50 mM Ac-DEVD-AMC. It was kept at room temperature in the dark and only the required volume was prepared.

2.2.11.2 Measurement of caspase-3 activity in THP-1 cells

THP-1 cell pellet (see **section 2.2.4**) was mixed well with 200 µl of working solution and immediately measured for the rate of AMC release using the fluorescence spectrophotometer (Cary Eclipse), with the excitation and emission wavelengths set at 370 and 440 nm, respectively. The kinetics were measured at 0.1-minute intervals for 2 minutes using the Kinetics software (Cary Eclipse). The rate of AMC release was expressed as pmol/min by comparing the fluorescence (unit/min) to the standard curve. The fluorescence unit of the standard curve was monitored using the Advanced Reads software (Cary Eclipse). The cell lysate was then used for protein determination.

2.2.11.3 Measurement of caspase-3 activity in HMDM cells

HMDMs were scraped off each well using 70 µl of ice cold lysis buffer without the protease inhibitors (see **section 2.2.9.1**), transferred to a 1.7 ml microtube, and left on ice for 30 minutes to lyse cells. Five µl of the resulting cell lysate was taken for protein assay, while 60 µl of the cell lysate was mixed well with 200 µl working solution. The rate of AMC release was immediately measured as described in section **2.2.11.2**.

2.2.12 Fluorescence microscopy

Cytosolic calcium ion (Ca^{2+}) level, intracellular superoxide production, mitochondrial membrane potential and lysosomal stability in HMDMs were monitored by probing the cells with particular fluorescent dyes followed by examination by fluorescence microscopy.

HMDMs on coverslips (see **section 2.2.1.2**) were incubated with fluorescence dyes either before or after HOCl treatment depending on the type of fluorescence dye used, but always at 37ºC in the dark. The cells were then washed twice with warm PBS, placed onto a

microscope slide (25.4×76.2 mm, 1mm-1.2mm thick, Sail brand) containing about 50 µl of EBSS with 0.68 mM $CaCl_2$ with cells facing down.

The cells were viewed using a Zeiss AxioImager.M1 epifluorescent microscope (Carl Zeiss (NZ) Ltd, Auckland, New Zealand), equipped with a Differential Interference Contrast (DIC) condenser and fitted with an HBO 100 W mercury vapour lamp. Cells were viewed using 40× Plan-NEOFLUAR objective. Different fluorescent filters were used depending on the fluorescent dyes employed. The images were captured using a Zeiss AxioCam HRc CCD camera with AxioVision Rel. 4.5 software (1300 × 1030 pixel resolution) and processed with Adobe Photoshop 8.0. To ensure accuracy within experimental treatments and to avoid fluorescent dye quenching, the time for sample irradiation and image capture was kept constant. The concentration and volume applied, incubation period, excitation and emission wavelengths, and fluorescent filters used for each fluorescent dye are described in **sections 2.2.12.1** to **2.2.12.5**.

The resulting fluorescence intensities for the detection of mitochondrial membrane potential and cytosolic calcium were converted to numerical values using the online software Image J. The fluorescence intensities of 20 cells per treatment were converted and averaged using Microsoft Excel software.

2.2.12.1 Dihydroethidium (DHE)

Dihydroethidium (DHE) has been widely used for detecting intracellular superoxide anions. This cell permeable dye reacts with superoxide resulting in the formation of a two-electron oxidised product, ethidium (E^+), which binds to DNA and leads to enhancement of red fluorescence ($\lambda ex/\lambda em$ = 510/605 nm) (Budd *et al.*, 1997; Zhao *et al*., 2003). DHE (MW 315.4) stock was prepared in DMSO and stored at -20ºC.

After HOCl treatment and PBS washing, HMDMs were incubated with 200 µl of 10 µM DHE in EBSS with 0.68 mM $CaCl_2$ for 20 minutes. The fluorescent filter used for DHE was Zeiss filter set 00 (excitation: band path 530-585; beam-splitter: FT600; emission: LP615).

2.2.12.2 Acridine orange (AO)

Acridine orange (AO) can accumulate in acidic compartments, such as lysosomes. Upon excitation by blue light (λex 487 nm), the highly concentrated AO in lysosomes emits a red fluorescence, whereas less concentrated AO in cytosol emits a green fluorescence. It hence can be used to monitor lysosomal stability (Yap *et al.*, 2006). AO (MW 301.8) stock in nanopure water was stored at 4ºC.

After HOCl treatment and PBS washing, HMDMs on coverslips were incubated with 250 µl of 10 µg/ml AO in EBSS with 0.68 mM $CaCl_2$ for 20 minutes. The fluorescence filter used for AO was the Chroma multiband filter set 82000, using the single band blue exciter for FITC.

2.2.12.3 Fluo-3-acetoxymethyl (AM) ester

Fluo-3-acetoxymethyl (AM) ester is used to detect cytosolic free calcium and it is cell permeable due to its AM ester structure. After entering the cells, it is cleaved by intracellular esterases to form Fluo-3 and AM. Upon excitation by blue light (λex 488 nm), Fluo-3 emits a green fluorescence (λem 530 nm) when bound to free calcium ions in the cytosol (Minta *et al.*, 1989; Kao *et al*., 1989). Fluo-3-AM ester (MW 1129.9) stock was prepared in DMSO and stored at -20ºC.

HMDMs on coverslips were pre-incubated with 200 µl of 10 µM fluo-3-AM in EBSS with 0.68 mM $CaCl_2$ for 40 minutes, followed by PBS washing and HOCl treatment. The fluorescence filter used for fluo-3 was the Zeiss filter 38HE (FITC).

2.2.12.4 Tetramethylrhodamine methyl ester (TMRM)

Tetramethylrhodamine methyl ester (TMRM) is used to monitor mitochondrial membrane potential. It is a lipophilic cation, which accumulates in mitochondria in proportion to the mitochondrial membrane potential. The cationic nature of TMRM will cause intense fluorescence at more negative membrane potentials, losing its fluorescence as the membrane potential becomes more positive (Russell *et al*., 1999). TMRM (MW 500.9) stock in methanol was stored at -20ºC.

HMDMs on coverslips were pre-incubated with 300 µl of 100 nM TMRM in EBSS with 0.68 mM $CaCl_2$ for 30 minutes, followed by PBS washing and HOCl treatment. The fluorescence was immediately observed (λex/λem = 548/574 nm) using the Chroma multiband filter set 82000, with the single band green exciter for TRITC/Cy3.

2.2.12.5 Propidium iodide (PI)

The use of propidium iodide (PI) allows detection of necrotic cells. The cell membrane integrity excludes PI in viable and apoptotic cells, whereas necrotic cells are permeable to PI. The cells were processed following manufacturer's instructions (BD Biosciences Clontech, USA) and under minimal exposure of light. HMDM cells on coverslips, after HOCl treatment, were washed twice in warm RPMI-1640 media and left in 0.5 ml of binding buffer (10 mM HEPES adjusted to pH 7.4 with NaOH, 140 mM NaCl and 2.5 mM $CaCl_2$) for 1 minute. Next, the cells were incubated with 200 µl of binding buffer containing 4 µg/ml PI at room temperature in the dark for 30 minutes. The cells were then washed twice in binding buffer, followed by placing the coverslip, with cells facing down, on a microscope slide containing 50 µl of binding buffer. The fluorescent filter used for PI was a Zeiss filter set 00.

2.2.13 Statistical analysis

Data was graphed and statistically analysed using the Prism software program (version 4.0; GraphPad Software, USA). Significance was confirmed by a one-way analysis of variance (ANOVA), followed by Tukey's multiple comparison test to provide a more quantitative indication of significance between treatments and/or time points. Where appropriate, linear regression and correlation analyses were also applied with r^2 values calculated assuming a Gaussian distribution. Significance levels are indicated in the following manner: * $p \leq 0.05$; ** $p \leq 0.01$; *** $p \leq 0.001$.

Results displayed in this thesis are taken from one experiment, which is representative of at least three separate experiments. The means and standard errors of the mean (SEM) shown within each experiment were calculated from triplicate samples.

3. HOCL-INDUCED HMDM CELL DEATH AND DEFENSE MECHANISMS BY GSH AND 7,8-NP

3.1 Introduction

Hypochlorous acid (HOCl) is a powerful oxidant generated by neutrophils, monocytes, and certain types of macrophages at sites of chronic inflammation via the myeloperoxidase (MPO) enzyme-catalysed oxidation of Cl^- ions by H_2O_2. Previous studies have shown that 20-400 μM HOCl can be generated through the MPO/H_2O_2/Cl^- system per hour (Weiss *et al.*, 1982; Foote *et al.*, 1983).

HOCl plays a central role in the killing of microorganisms at sites of inflammation (Albrich *et al*., 1981; Barrette *et al*., 1987; McKenna and Davies, 1988; Albrich and Hurst, 1982). However, its high reactivity with a range of biomolecules (Pullar *et al*., 2000) suggests that it can also cause injury to the surrounding tissues. Exposing a variety of cell types to HOCl results in cell death either by necrosis (Vissers *et al*., 1994; Vissers *et al*., 1998; Hawkins *et al*., 2001; Tatsumi and Fliss, 1994; Abernathy and Pacht, 1995; Vile *et al*., 2000; Slivka *et al*., 1980; Schraufstatter *et al*., 1990) or apoptosis (Vissers *et al*., 1999; Wagner *et al*., 2000; Yap *et al*., 2006; Salunga *et al*., 2007; Whiteman *et al*., 2007; Whiteman *et al*., 2005b). HOCl can induce cytotoxicity either by reacting with cell membrane components (Schraufstatter *et al*., 1990; Barrette *et al*., 1989; Albrich *et al*., 1986), or by passing through cell membranes to react with intracellular components (Carr and Winterbourn, 1997; Vissers and Winterbourn, 1995; Pullar *et al*., 1999).

The necrotic core of advanced atherosclerotic plaques is rich in cell debris of macrophages (Ball *et al*., 1995; Berberian *et al*., 1990; Stary *et al*., 1995). These findings imply that macrophages within plaques undergo cell lysis, contributing to advanced plaque formation. HOCl may be responsible for the killing of macrophages during the progression of plaque formation, since macrophages, MPO enzyme and 3-chlorotyrosine (a biomarker of HOCl) were found colocalizing in advanced lesions (Daugherty *et al.*, 1994; Malle *et al*., 2000; Sugiyama *et al*., 2001). The abundance of macrophage cells and the absence of neutrophils in the lesions (Sugiyama *et al*., 2001) indicate that macrophages may be the primary cells producing HOCl in the lesions, and may be under threat of HOCl insult. Moreover, the

same study documents increased numbers of MPO-expressing macrophages in eroded or ruptured plaques, causing acute coronary syndromes. Human macrophages are therefore chosen in this thesis to study the cytotoxic effect of HOCl to better understand the roles HOCl and macrophages play in the progression of atherosclerotic disease.

For macrophages to function properly at inflammation sites, including in atherosclerotic lesions, they need to possess antioxidative mechanisms defending themselves against HOCl insult. Glutathione (GSH) is the major intracellular antioxidant and its deficiency has been implicated in a number of diseases; possibly due to the increased susceptibility of cells/tissues to oxidative stress (Ballatori *et al.*, 2009). Moreover, GSH is significantly lost in red cells (Vissers and Winterbourn, 1995) and neutrophils (Carr and Winterbourn, 1997) before cell lysis occurs, indicative of its role in defending cells against HOCl.

Winterbourn and Brennan (1997) have proposed a reaction scheme of GSH with HOCl (**Figure 3.1**). GSH reacts with OCl^- (reaction 1) to produce sulphenyl chloride (GSCl), which will readily react with more GSH (reaction 2) to form disulfides (GSSG). Reaction 3 will occur by HOCl competing for GSCl to produce sulphonyl chloride (GSO_2Cl). GSO_2Cl can react with more GSH to give thiolsulphonate (GSO_2SG) (reaction 4), which is more favourable at high GSH concentrations. GSO_2Cl can also undergo an internal HCl elimination to give the putative sulphonamide (reaction 5). Amines (RNH_2) can also compete for GSCl (reaction 6) giving chloramines (RNHCl), which then oxidize GSH to generate GSSG (reaction 7). As the products of reaction 7 react rapidly with each other, the chloramine is likely to be formed only as a transient species.

Human macrophages can synthesize and release neopterin and its reduced form, 7,8-dihydroneopterin (7,8-NP), upon induction by interferon-γ (IFN-γ) (Wachter *et al.*, 1989; Wachter *et al.*, 1992). 7,8-NP may be produced and play a role within the lesions, since IFN-γ (both mRNA and protein) has been detected in atherosclerotic lesions of humans and mice (Hansson *et al.*, 1989a; Libby, 1995; Zhou *et al.*, 1998). In addition, the neopterin levels are found to be significantly elevated in patients with vascular disease (Schumacher *et al.*, 1992; Tatzber *et al.*, 1991; Rudzite *et al.*, 2005).

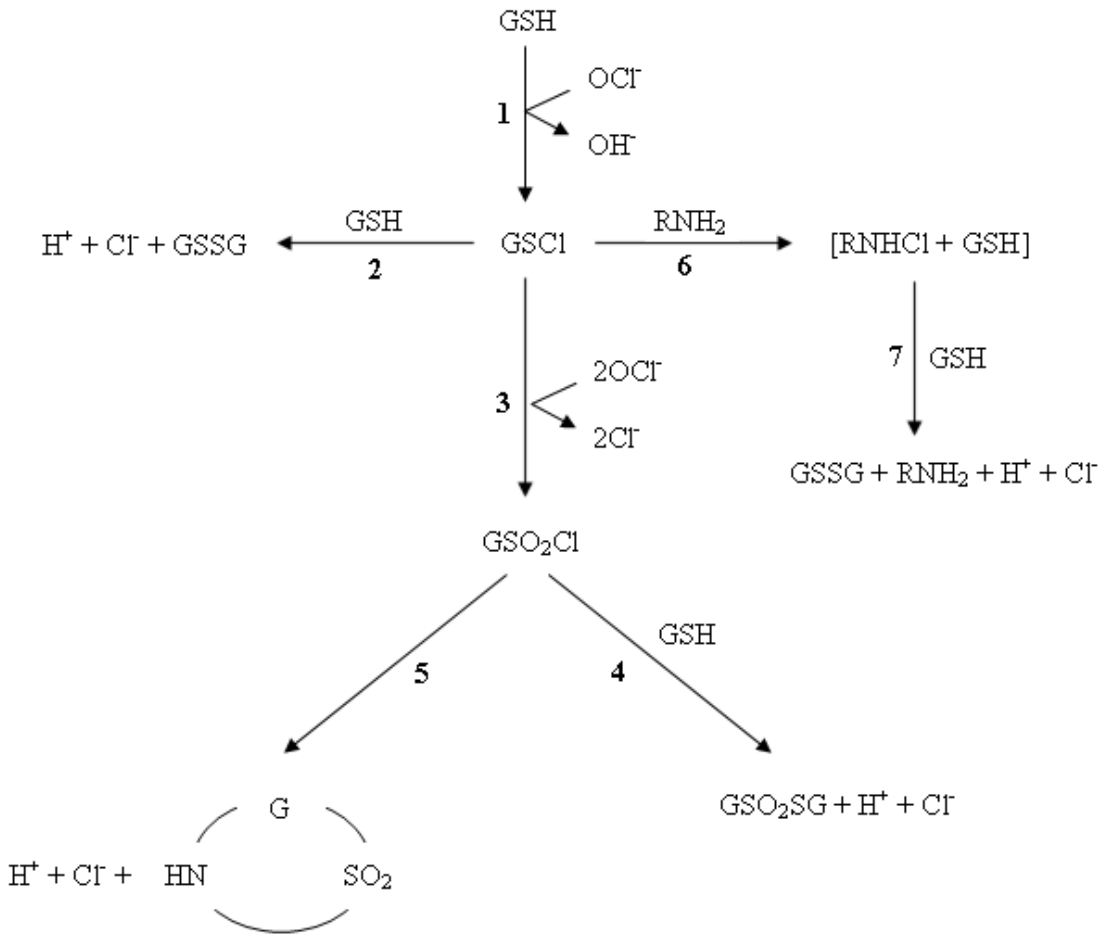

Figure 3.1 Proposed reaction of GSH with HOCl.
This reaction scheme is adapted and modified from Winterbourn and Brennan, 1997.

The purpose of γ-IFN-stimulated 7,8-NP production by macrophages is not yet fully understood. It has been found to act as either a pro-oxidant or antioxidant depending on its concentration (see also **sections 3.3** and **1.6.2**). Gieseg *et al*. (2007) have hypothesized that 7,8-NP is synthesised by γ-interferon-stimulated macrophages to protect cells against the oxidants encountered within an inflammatory site such as atherosclerotic lesion. This laboratory has previously shown that low μM concentrations of 7,8-NP is a very potent antioxidant. It protects erythrocytes from lysis induced by peroxyl radicals, hydrogen peroxide and HOCl (Gieseg *et al*., 2001b). Moreover, 7,8-NP has been demonstrated to protect free proteins, cellular proteins and protein thiols from oxidant damage (Duggan *et al*., 2001; Duggan *et al*., 2002). 7,8-NP was also shown to dramatically increase the lag time of LDL oxidation mediated by copper and peroxyl radical (Gieseg *et al*., 1995). In addition, 7,8-NP prevented cell-mediated LDL oxidation (Firth, 2006, PhD thesis; Gieseg & Cato, 2003) and effectively protected U937 cells from oxLDL-induced death at μM

concentrations (Baird *et al*., 2005). In contrast, neopterin and high concentrations of 7,8-NP could result in ROS generation, disrupt the oxidant/antioxidant balance and ultimately lead to cell death (Weiss *et al*., 1993; Murr *et al*., 1994; Baier-Bitterlich *et al*., 1995; Baier-Bitterlich *et al*., 1996a; Spottl *et al*., 2000; Enzinger *et al*., 2002a and b; Hoffmann *et al*., 2003). 7,8-NP was also found to upregulate the production of IFN-γ, thereby establishing an autocrine feed-back loop (Baier-Bitterlich *et al*., 1996b).

This first part of the chapter examines the cytotoxicity of HOCl on HMDM cells by examining the HOCl-mediated cell viability loss and morphological changes. The second part of the chapter studies the efficiency of intracellular GSH in protecting HMDM cells against HOCl insult. This is carried out by examining the degree of HOCl-induced cell viability loss in HMDM cells with intact or depleted intracellular GSH. The correlation between initial intracellular GSH level and the HOCl concentration required to kill 50% of a cell population will also be examined. The third part of the chapter studies the efficiency of 7,8-NP in preventing HOCl-mediated cytotoxicity to HMDM cells. This is carried out by examining the effect of extracellular and IFN-γ-induced 7,8-NP in preventing HOCl-mediated intracellular GSH and cell viability losses.

3.2 Results

3.2.1 Effect of HOCl on HMDM cell viability

The cytotoxicity of HOCl on HMDM cells was examined by exposing HMDM cells to HOCl for 10 minutes, followed by incubation in the RPMI-1640 medium containing 10% HIHS (referred to as HMDM culture medium in this thesis for simplicity) for 20 hours. The cell viability was measured by the MTT reduction assay (**Figure 3.2a**). No statistically significant cell viability loss was observed at 50 μM HOCl. In contrast, 100, 150, 200, and 300 μM HOCl reduced cell viability by approximately 10, 40, 55 and 81% of the control, respectively. The degree of cell viability loss measured by the trypan blue exclusion assay was similar to that measured by MTT assay ($r^2 = 0.9760$) (**Figure 3.2b**).

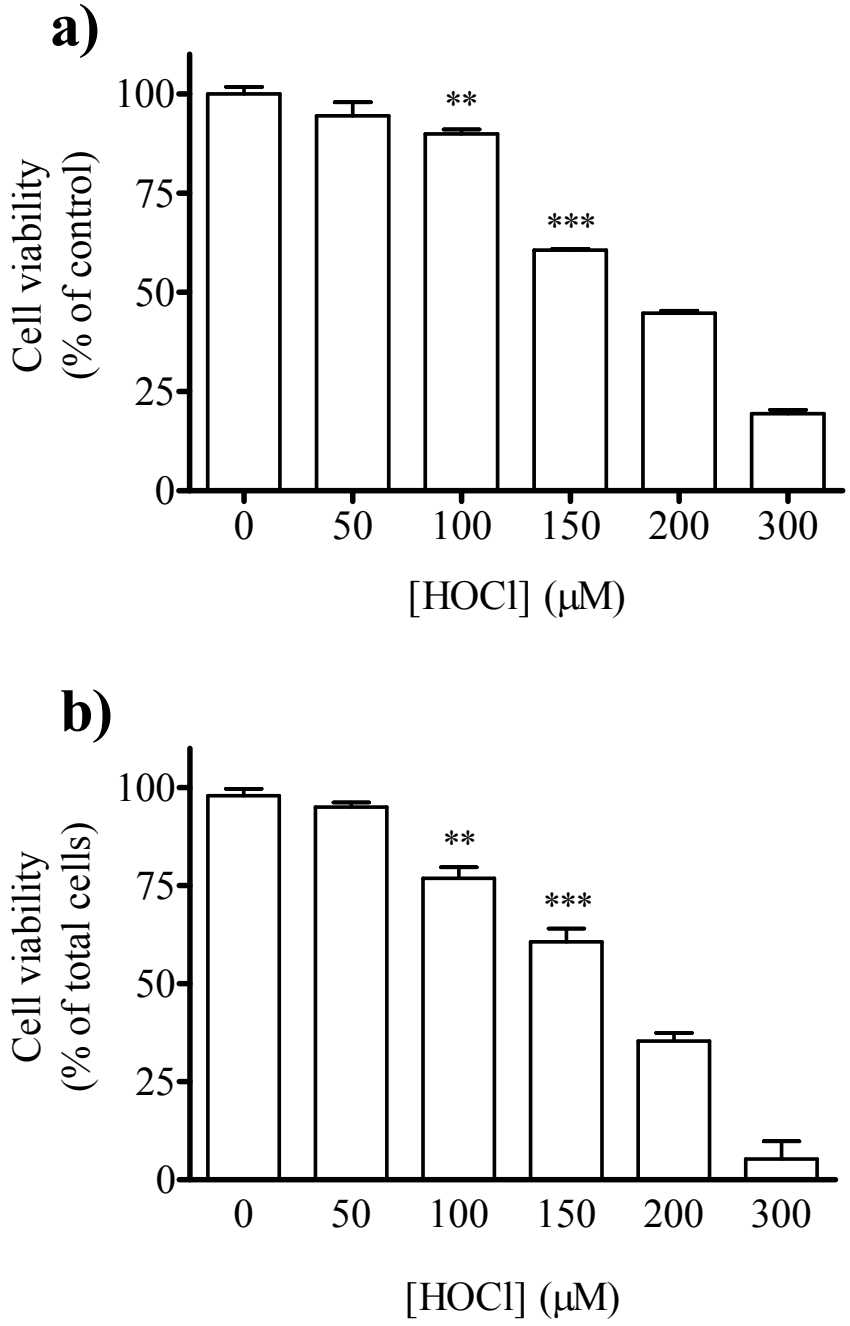

Figure 3.2 HMDM cell viability loss occurred after HOCl treatment.
HMDM cells (5×10^6 cells/ml) were treated with increasing HOCl concentrations for 10 minutes, followed by incubation in HMDM culture medium for 20 hours. The cells were subsequently analysed for cell viability using **a)** the MTT reduction assay and **b)** the trypan blue exclusion assay. The data are expressed as a percentage of the respective control values with no HOCl added. Significance is indicated from control with 0 μM HOCl. Results are displayed as mean ± SEM of triplicates from a single experiment, representative of three separate experiments.

To examine how fast HOCl exerted its cytotoxic effect on HMDM cells, the cells were incubated with increasing concentrations of HOCl for 10, 30, or 60 minutes and cell viability was determined after 20 hours (**Figure 3.3**). An HOCl concentration of 50 μM did not induce significant cell viability loss regardless of the length of the incubation. HMDM cells treated with 100, 150, 200, and 500 μM HOCl for 10 minutes showed cell viability loss of approximately 50, 70, 80, and 75% of the control, respectively. HMDM cells treated with the respective HOCl concentrations for 30 or 60 minutes showed similar degrees of cell viability loss. This suggests that the cytotoxic effect of HOCl on HMDM cells was rapid and completed within 10 minutes. Hence, HMDM cells were treated with HOCl for 10 minutes for all the future experiments.

A time course of HOCl-induced HMDM cell viability loss was examined by measuring cell viability at time intervals up to 24 hours in HMDM cells initially treated with HOCl for 10 minutes (**Figure 3.4**). Initially (0 hr post HOCl treatment), HMDM cells treated with 100, 150, and 200 μM HOCl showed viability loss of approximately 35%, 50%, and 75% of the control, respectively. No further significant cell viability loss were observed over time at 100 and 200 μM HOCl. At 150 μM HOCl, HMDM cells showed further decrease in viability at 6 hr and 12 hr by approximately 13% and 22%, respectively (compared to the respective 0 hr cell viability loss). However, the cell viability loss observed at 24 hr was similar to that at 0 hr. These results showed that HOCl caused rapid HMDM cell death and had no latent effect on the cells if they were not killed in the initial treatment.

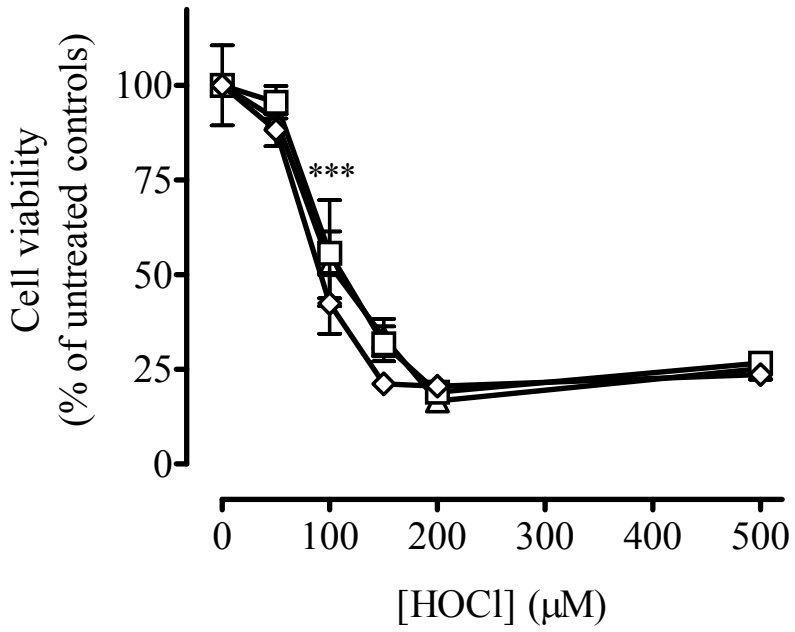

Figure 3.3 HMDM cell viability loss occurs after 10-minute exposure to HOCl.
HMDM cells (5×10^6 cells/ml) were treated with varying HOCl concentrations for 10 minutes (△), 30 minutes (□), or 60 minutes (◇), followed by incubation in HMDM culture medium for 20 hours. The cells were subsequently analysed for cell viability using the MTT reduction assay, with data expressed as a percentage of the respective controls with no HOCl added. Each data point was subtracted from blank controls. Significance is indicated from the respective controls with 0 μM HOCl.

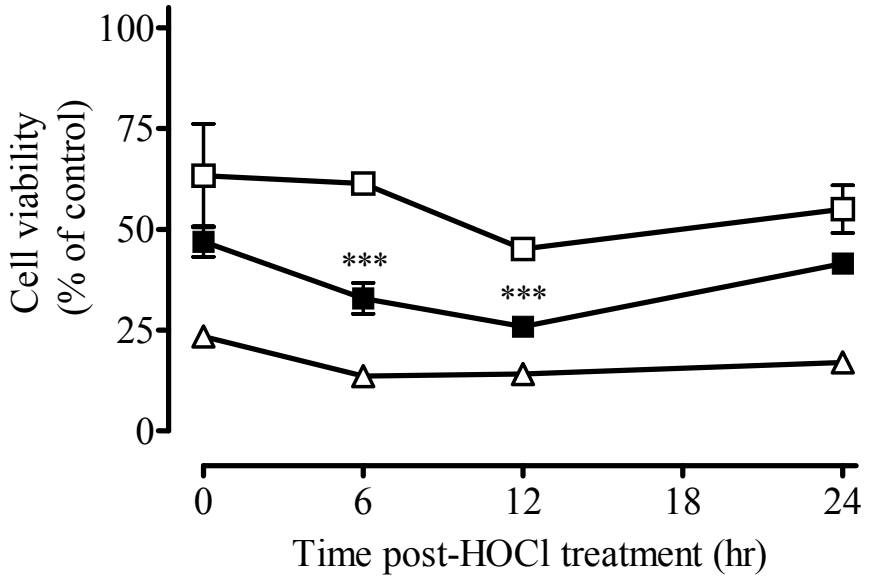

Figure 3.4 Time course of HMDM cell viability loss after HOCl treatment.
HMDM cells (5×10^6 cells/ml) were incubated with 100 (□), 150 (■) and 200 μM (△) HOCl for 10 minutes, followed by incubation in HMDM culture medium. Cell viability was determined at time intervals using the MTT reduction assay. Each data point is expressed as a percentage of the respective controls with 0 μM HOCl. Significance is indicated from the respective 0-hour values.

3.2.2 Effect of HOCl on HMDM cell morphology

Morphological changes of HMDM cells after HOCl treatment were also examined (**Figure 3.5**). The control cells showed a poached egg-like appearance, which is the classic morphology of macrophage cells. HMDM cells treated with 50 μM HOCl did not show significant morphological changes, while HMDM cells treated with 100 μM HOCl appeared rounder, more disk-like, and marginally enlarged compared to the control cells. HOCl at concentrations of 150 and 200 μM caused the cells to enlarge with bleb formation, which was detectable straight after the HOCl treatment and did not disappear 1 hour after treatment. The cellular membranes looked distorted and disrupted, and cell debris was detected. A number of cells were also found detached and floating in the medium. These morphological changes appeared to be characteristics of necrotic cell death.

3.2.3 Effect of HOCl on intracellular GSH

Intracellular GSH is a very potent antioxidant and can efficiently scavenge a range of oxidants and radicals including HOCl (Halliwell and Gutteridge, 2007). Hence, the antioxidative effect of intracellular GSH in scavenging HOCl and protecting HMDM cells from HOCl insult was examined. HMDM cells were treated with HOCl, followed by incubation in HMDM culture media for 3 hours (**Figure 3.6**). At 50 μM HOCl, HMDM cells showed a 15% decline in intracellular GSH level compared to the control (34.6 ± 0.4 nmol/mg protein), though this decrease was statistically insignificant ($p > 0.05$). At 100, 150, 200 and 300 μM HOCl, HMDM cells showed dramatic loss of 60, 70, 72 and 100% intracellular GSH compared to the control, respectively.

Cell viability was also measured concurrently with the intracellular GSH (**Figure 3.6**). At 50 and 100 μM HOCl, there were approximately 8% and 15% loss of cell viability, respectively. However, these decreases were statistically insignificant compared to the control. At 150, 200 and 500 μM HOCl, the cell viability decreased by approximately 50, 60 and 84% of the control, respectively. Taken together, there was significant intracellular GSH loss (i.e. at 100 μM HOCl) before significant cell viability loss occurred (i.e. at 150 μM HOCl).

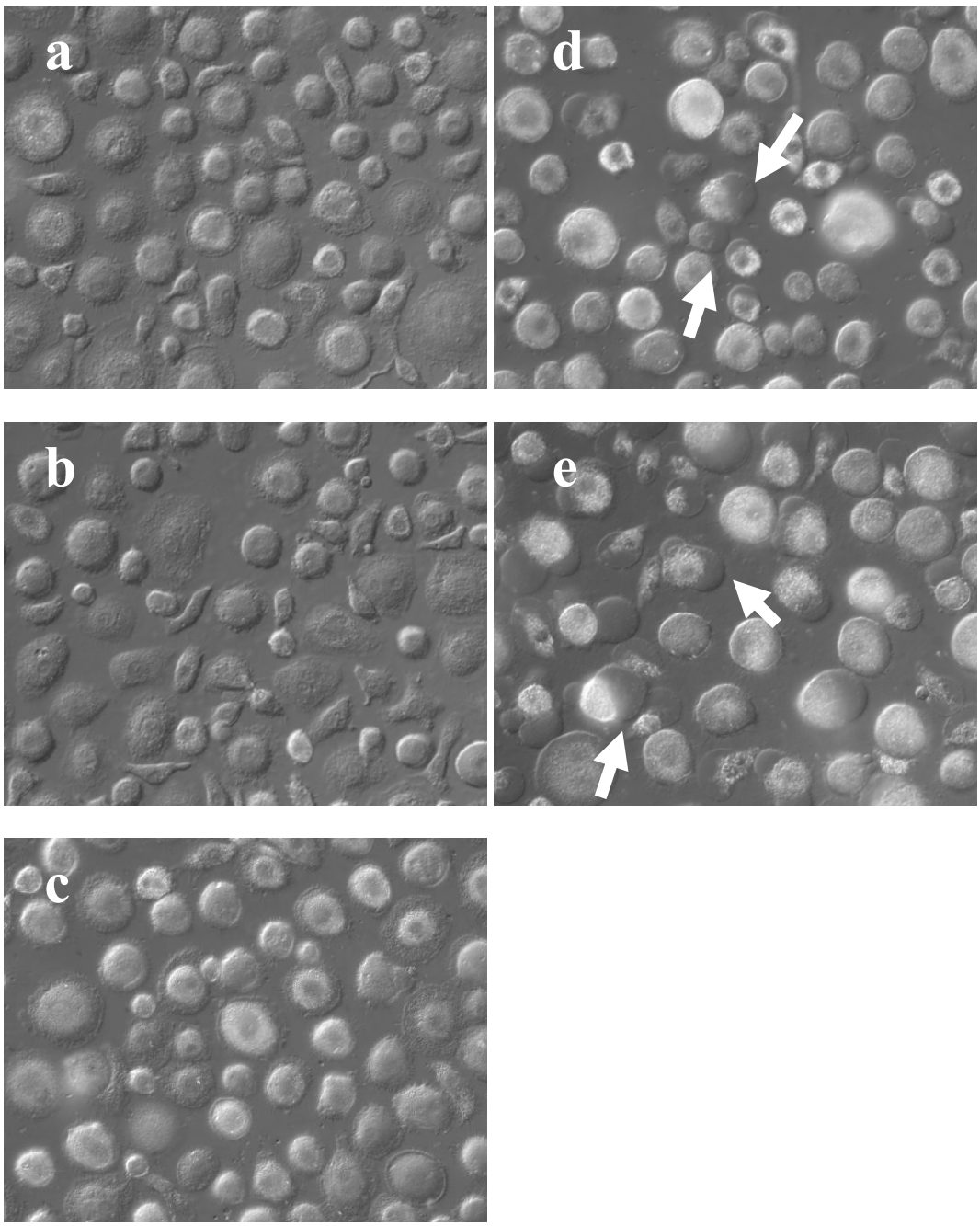

Figure 3.5 Morphological changes of HMDMs after HOCl treatment.
HMDM cells (5×10^6 cells/ml) grown on coverslips were treated with **a)** 0, **b)** 50, **c)** 100, **d)** 150 and **e)** 200 μM HOCl for 10 minutes, followed by incubation in HMDM culture medium for 1 hour. The cells were subsequently viewed *in situ* on microscope slides using an inverted microscope (40× magnification). Differential interference contrast (DIC) photos were taken using a digital camera. Cells with distorted cellular membranes are marked with white arrows.

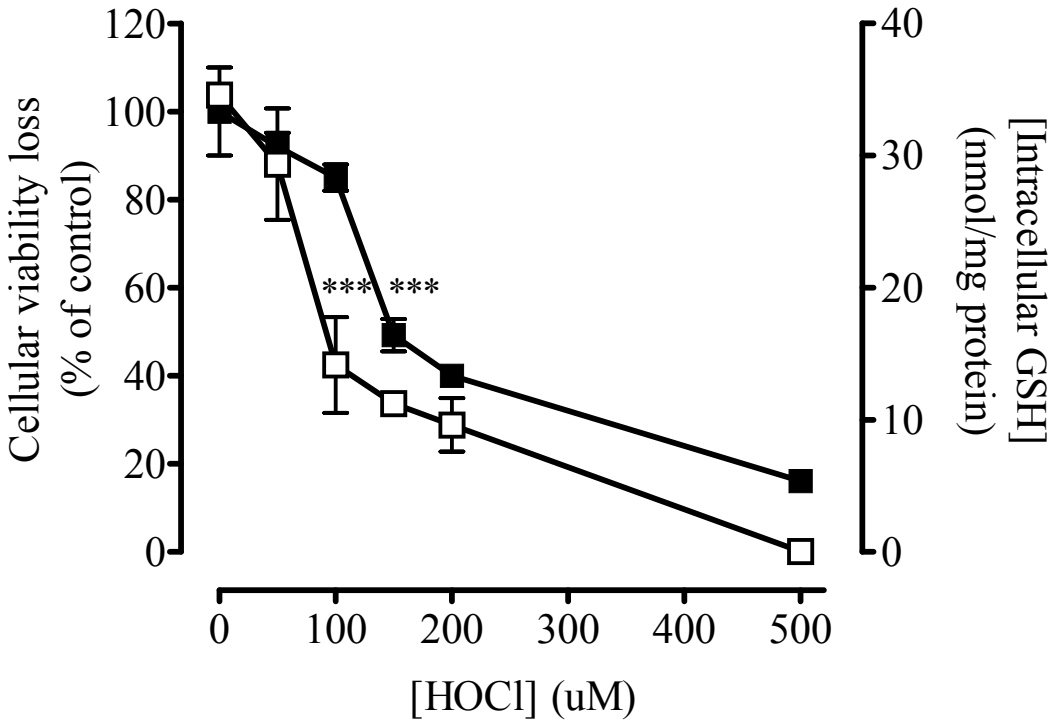

Figure 3.6 Intracellular GSH loss occurred before cell viability loss in HMDM cells upon HOCl treatment.
HMDM cells (5×10^6 cells/ml) were treated with increasing HOCl concentrations for 10 minutes, followed by incubation in HMDM culture medium for 3 hours. The cells were then analysed for cell viability (■) and intracellular GSH level (□) using the MTT reduction assay and HPLC analysis, respectively. Cell viability is presented as a percentage of the respective controls with no HOCl. Significance is indicated from the respective controls with 0 μM HOCl.

3.2.4 Effect of intracellular GSH in protecting HMDM cells against HOCl damage

The observation that intracellular GSH level declined significantly before significant cell viability loss occurred (**Figure 3.6**) implied that intracellular GSH might have played an important role in protecting HMDM cells from HOCl cytotoxicity. This hypothesis was investigated by depleting HMDM cells of intracellular GSH prior to HOCl treatment, followed by cell viability measurement. Diethyl maleate (DEM) has been commonly used as an intracellular GSH depleting agent, which binds to GSH either directly or via S-transferase (Mitchell *et al*., 1983; Bizzozero *et al*., 2006; Yamamoto *et al*., 2005; Chen *et al*., 2005; Yang *et al*., 2004).

Prior to this study, a suitable concentration of DEM and the optimal time period for DEM incubation needed to be determined. HMDM cells incubated with increasing concentrations of DEM for 4 hours showed a concentration-dependent decrease in intracellular GSH level **(Figure 3.7)**. The control cells had an intracellular GSH level of 28.8 ± 1.2 nmol/mg protein. At 50 and 100 μM DEM, the intracellular GSH levels were reduced to 8.2 ± 1.6 (70% decrease) and 2.5 ± 0.4 nmol/mg protein (90% decrease), respectively. There was no statistically significant decrease in cell viability with increasing DEM concentrations (**Figure 3.7**).

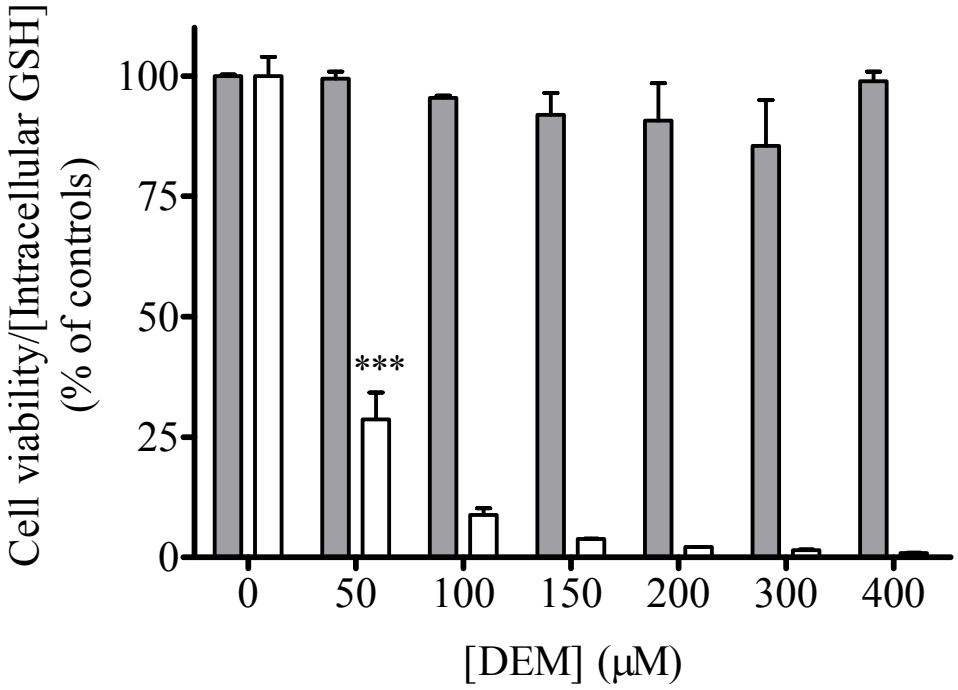

Figure 3.7 Diethyl maleate (DEM) blocked intracellular GSH without affecting HMDM cell viability.
HMDMs (5×10^6 cells/ml) were incubated with increasing concentrations of DEM at 37°C in the dark for 4 hours. The cells were subsequently analysed for cell viability (gray bars) and intracellular GSH (white bars) using the MTT reduction assay and HPLC analysis, respectively. Cell viability and GSH level are presented as percentage of the respective controls with no DEM added. Significance is indicated from the respective controls with 0 μM DEM.

To confirm that DEM did not react with cellular protein thiols, concurrent measurement of intracellular GSH and cellular protein thiols were carried out in HMDM cells treated with DEM for 4 hours (**Figure 3.8**). The protein thiol and intracellular GSH levels of the control were 703.7 ± 19.7 and 98.3 ± 3.2 nmol/mg protein, respectively. At 100, 200, and 300 μM DEM, the intracellular GSH levels were reduced to 19.5 ± 1.7 (80% decrease), 7.1 ± 1.7 (93% decrease), and 2.7 ± 0.1 nmol/mg protein (97% decrease), respectively. In contrast, there were no statistically significant decreases in protein thiol levels with the increasing DEM concentrations. DEM at a concentration of 100 μM was chosen for further experiments, as this concentration caused about 80-90% depletion of GSH in HMDM cells (**Figures 3.7** and **3.8**).

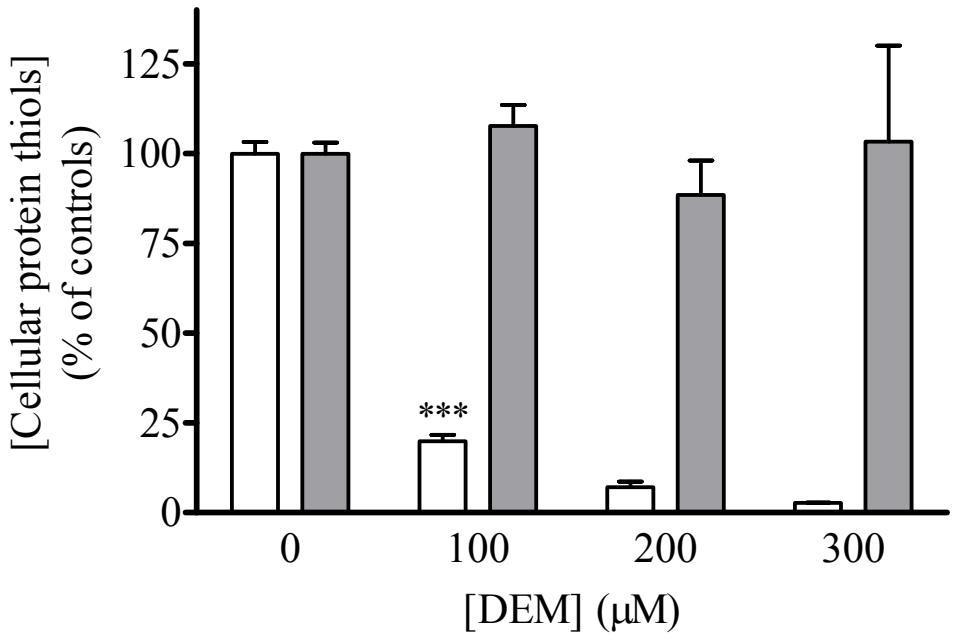

Figure 3.8 Diethyl maleate (DEM) did not remove protein thiols.
HMDM cells (5×10^6 cells/ml) were incubated with increasing concentrations of DEM at 37°C in the dark for 4 hours. Protein thiol levels (gray bars) and intracellular GSH levels (white bars) were then determined using the DTNB assay and HPLC analysis, respectively. Protein thiol and GSH levels are presented as percentage of the respective controls with 0 μM DEM. Significance is indicated from the respective controls.

The shortest incubation time period with DEM for maximal GSH depletion in HMDM cells was determined. HMDM cells incubated with 100 μM DEM were analysed for intracellular GSH at time intervals of up to 4 hours (**Figure 3.9**). The control HMDM cells showed an intracellular GSH level of 33.5 ± 2.8 nmol/mg protein. There was no observable decline in intracellular GSH level straight after DEM addition (i.e. 0 hr post DEM incubation) compared to the control. After 1, 2, 3 and 4 hours of incubation with DEM, HMDM cells showed decreased intracellular GSH levels by approximately 30, 38, 60 and 70% of the control, respectively. The decrease in intracellular GSH level was statistically significant ($p < 0.05$) between 2 and 3 hours, while statistically insignificant between 3 and 4 hours ($p > 0.05$). Based on this data, HMDM cells were incubated with 100 μM DEM for 3 hours for the future related experiments.

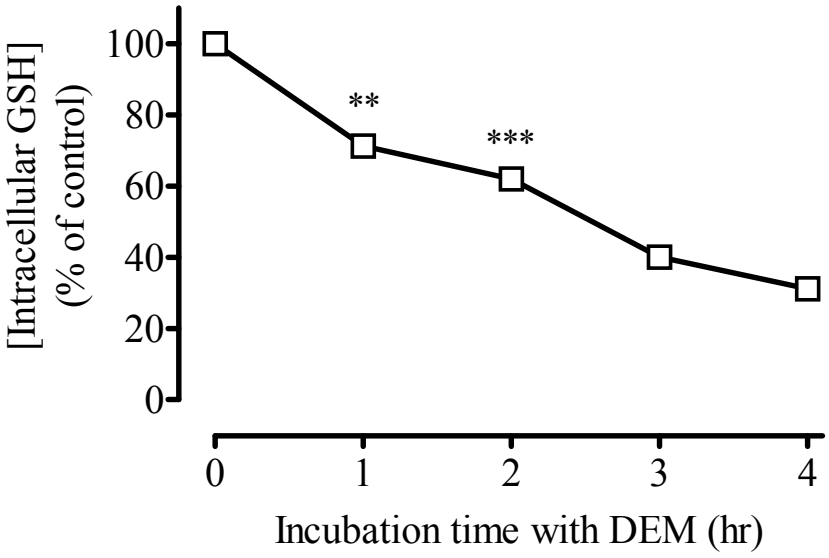

Figure 3.9 Time course of GSH depletion in HMDMs incubated with DEM.
HMDM cells (5×10^6 cells/ml) were incubated with or without 100 μM DEM at 37°C in the dark, followed by measuring intracellular GSH levels at time intervals by HPLC analysis. GSH levels are presented as percentage of the non-DEM-treated control. Significance is indicated from the same control.

To study the effect of intracellular GSH in protecting HMDM cells against HOCl cytotoxicity, HMDM cells were pre-incubated with 100 μM DEM for 3 hours prior to HOCl treatment and cell viability measurement (**Figure 3.10**). HMDM cells with intact intracellular GSH (i.e. without DEM treatment) showed approximately 20% ($p < 0.05$), 38% ($p < 0.001$) and 70% ($p < 0.001$) decreases in cell viability compared to the control

after treatment with 100, 150 and 200 μM HOCl, respectively. In contrast, HMDM cells depleted of approximately 90% of intracellular GSH showed a 20% decrease in cell viability after treatment with 50 μM HOCl ($p < 0.001$), while treatment with 100, 150 and 200 μM HOCl caused 59%, 64% and 47% of cell viability loss, respectively. At HOCl concentrations below 200 μM, the HOCl-induced viability loss in HMDM cells with depleted intracellular GSH was significantly greater than those in the respective HMDM cells with intact intracellular GSH. This suggests intracellular GSH played an important role in protecting HMDM cells against HOCl insult. However, there were no significant differences in cell viability loss between HMDM cells with intact or depleted intracellular GSH when HOCl concentrations were above 200 μM HOCl.

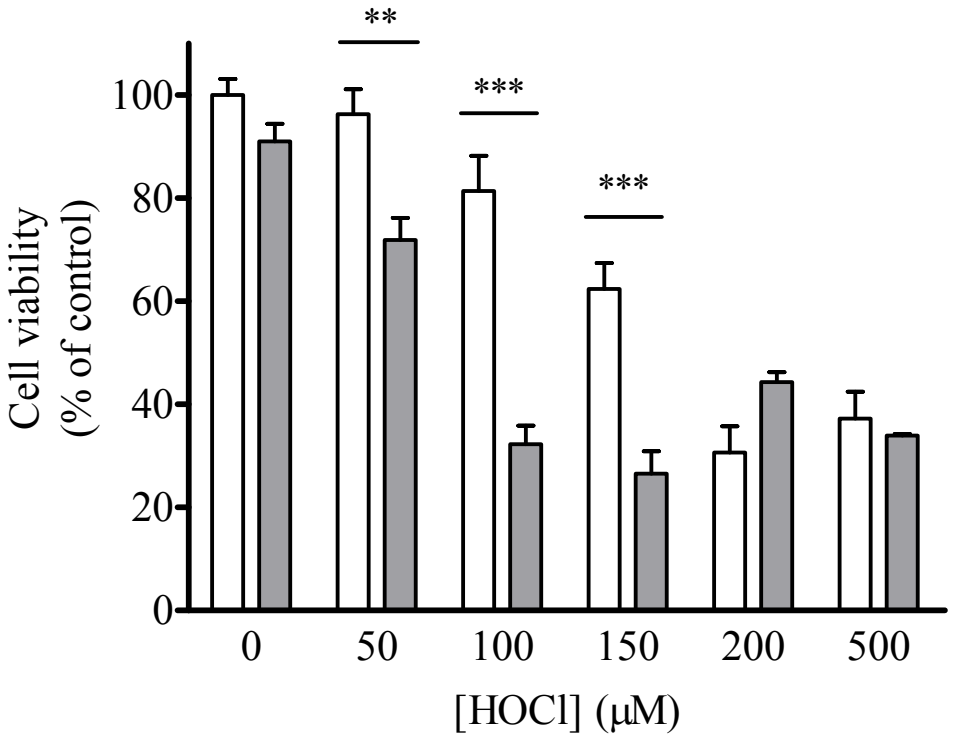

Figure 3.10 HMDM cells depleted of intracellular GSH are more sensitive to HOCl exposure.
HMDM cells (5×10^6 cells/ml) were pre-treated with (gray bars) or without (white bars) 100 μM DEM for 3 hours, followed by exposing the cells to increasing HOCl concentrations for 10 minutes. The cells were then incubated in HMDM culture medium for 1 hour prior to cell viability analysis using the MTT reduction assay. Cell viability is presented as a percentage of the DEM- and HOCl-non-treated control. * indicates the significance between HMDM cells treated with and without DEM.

3.2.5 Correlation between intracellular GSH levels of different HMDM cell preparations and the cells' resistance to HOCl exposure

A confounding factor in this research was that different HMDM cell batches showed varying levels of resistance towards HOCl cytotoxicity. HMDM cells prepared from different blood donors had similar initial MTT absorbance values ($p > 0.05$), i.e. they had similar initial metabolic activities. Yet, they had different levels of cell viability loss after treatment with increasing HOCl concentrations (**Figure 3.11**). The different levels of cell viability loss might be caused by varying experimental conditions on different days. To examine whether this was the case, two different HMDM cell preparations were exposed to the same HOCl preparation simultaneously (**Figure 3.12**). They showed statistically the same initial MTT absorbance values of approximately 1.0 ($p > 0.05$), but significantly different values after treatment with 150 μM HOCl ($p < 0.001$). These results indicate that the varying resistance of each HMDM preparation towards HOCl cytotoxicity was likely not caused by variation in experimental conditions. The similar initial metabolic activities within different cell preparations indicated that they could not have been a contributing factor either.

Based on earlier result (**Figure 3.10**), the varying level of resistance of HMDM cells towards HOCl insult might be attributed to the varying intracellular GSH level in each cell batch. To investigate this, each different HMDM cell batch was measured for its initial intracellular GSH value, initial protein concentration (in mg/5×10^6 cells), and cell viability after HOCl treatment. The HOCl concentration required to kill 50% of cell population in each cell preparation was directly related to their intracellular GSH level, as shown by the correlation analysis (**Figure 3.13a**). An r^2 value of 0.6808 suggests that 68% of the variant in LD_{50} (i.e. HOCl concentration required for killing 50% cell population in each cell batch) was predicted by the initial GSH level in each cell batch. This indicates that intracellular GSH provides approximately 70% protection against HOCl insult.

Furthermore, the correlation analysis between the initial protein concentration and the HOCl concentration required to kill 50% of cell population in each cell preparation showed an r^2 value of 0.063 (**Figure 3.13b**). Assuming the initial protein level of each cell preparation is directly proportional to the cell number, this result suggests that cell number was relatively consistent in each cell batch and was not responsible for the varying level of resistance in different cell preparations against HOCl insult.

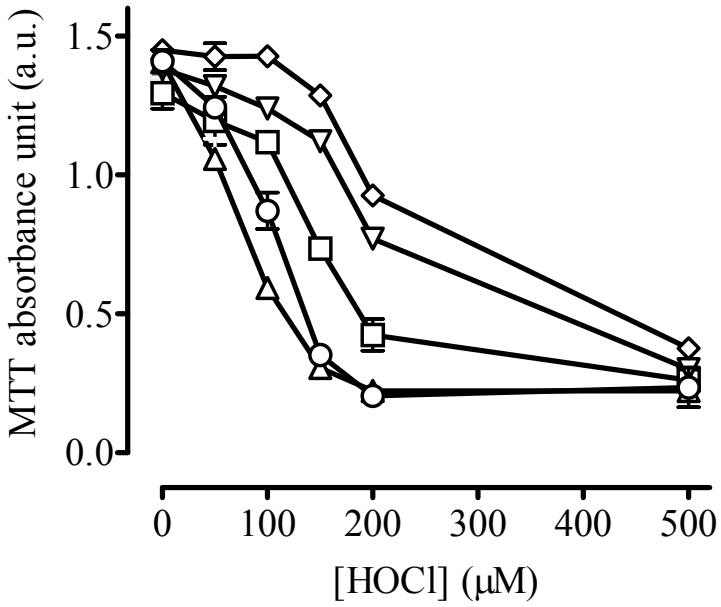

Figure 3.11 Different HMDM cell preparations showed varying resistance towards HOCl insult.
HMDM cells (5×10^6 cells/ml) prepared from different blood donors were treated with increasing HOCl concentrations for 10 minutes, followed by incubation in HMDM culture medium for 20 hours. The cells were then analysed for cell viability using the MTT reduction assay. Cell viability is presented in MTT absorbance units. Each line represents a different cell preparation from a different donor.

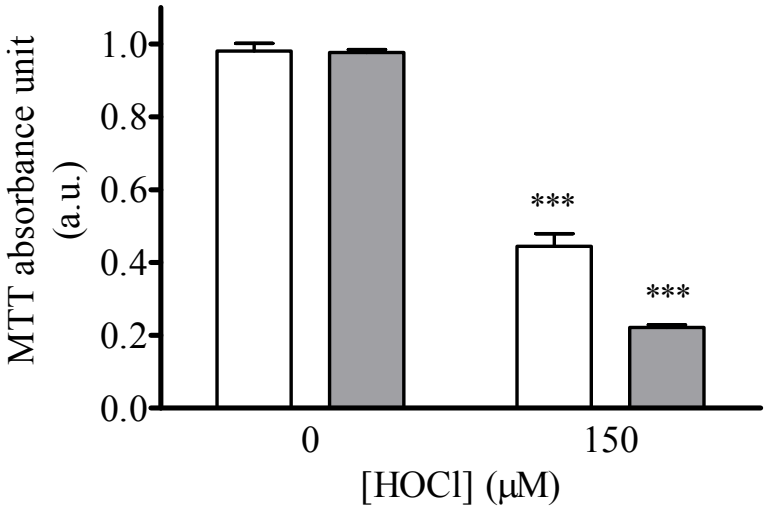

Figure 3.12 Two different HMDM cell preparations showed varying resistance towards the same HOCl insult.
HMDM cells (5×10^6 cells/ml) prepared from blood donors A (white bar) and B (gray bars) were treated with or without 150 μM HOCl for 10 minutes, followed by incubation in HMDM culture medium for 20 hours. The cells were then analysed for cell viability using the MTT reduction assay. Cell viability is presented in MTT absorbance units. Significance is indicated from the respective controls with 0 μM HOCl.

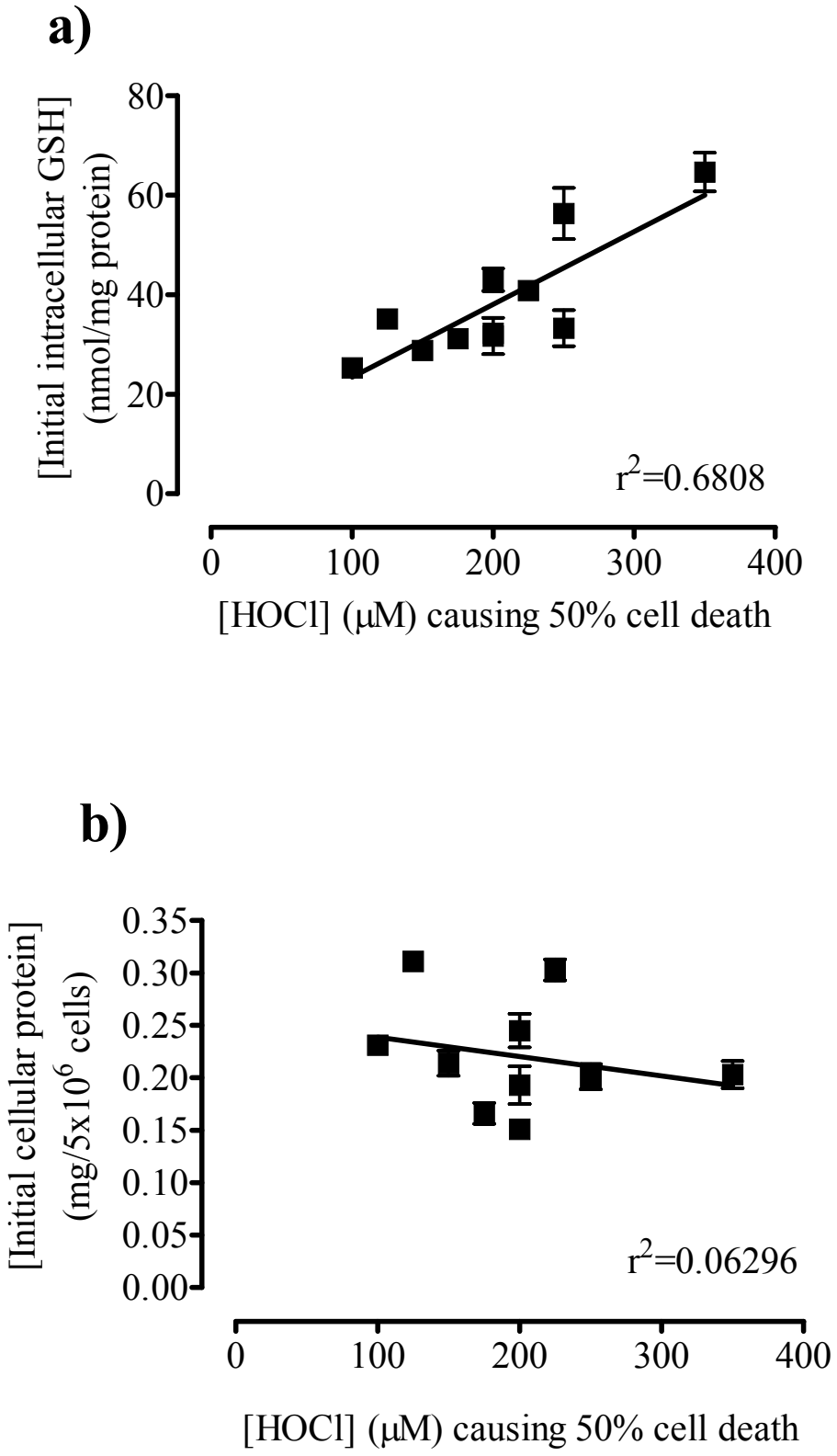

Figure 3.13 Intracellular GSH levels, not cellular protein levels, are the primary cause of varying resistance of different HMDM batches against HOCl damage.
The HOCl concentration required to kill 50% of the cell population in each HMDM cell batch was compared with **a)** the initial intracellular GSH and **b)** the initial cellular protein concentrations using a trend line to illustrate the correlation.

3.2.6 HOCl-mediated GSH loss in HMDM cells over time

Whether HOCl-treated HMDM cells were able to replenish their oxidised GSH pool was also studied. After the 10-minute exposure to HOCl, the intracellular GSH levels in HMDM cells were measured up to 24 hours **(Figure 3.14)**. The intracellular GSH level of control cells (with no HOCl addition) was approximately 60.9 ± 5.3 nmol/mg protein. At 50 μM HOCl, the intracellular GSH level remained statistically similar to the control value over time ($p > 0.05$). At 100 μM HOCl, the intracellular GSH level decreased initially to 40.5 ± 3.3 nmol/mg protein (25% decrease), which remained at this level for the next 10 hours and recovered to the control value at 24 hours. At 200 μM HOCl, the intracellular GSH level decreased initially to 29.9 ± 2.1 nmol/mg protein (50% decrease). There was a further progressive decrease in intracellular GSH level over the next 10 hours, which was not recovered at 24 hours. At 500 μM HOCl, the intracellular GSH level was completely depleted initially and was not recovered over time. The significance of this time course study will be discussed in **section 3.3**.

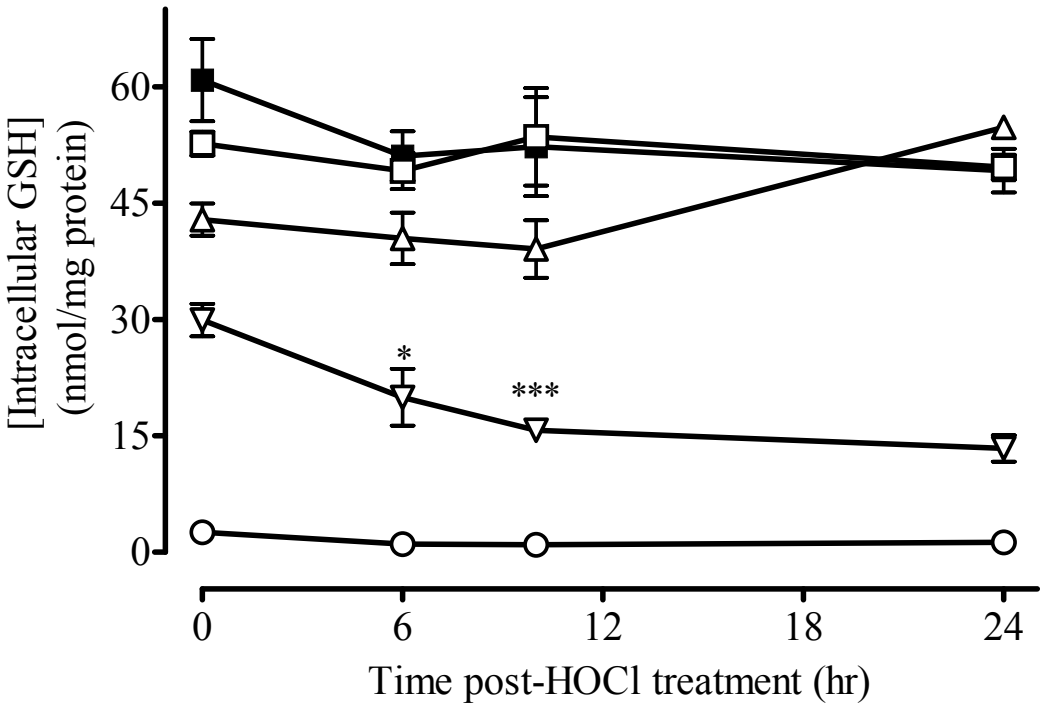

Figure 3.14 Time course of HOCl-induced GSH loss in HMDM cells.
HMDM cells (5×10^6 cells/ml) were treated with 0 (■), 50 (□), 100 (△) , 200 (▽), and 500 μM (○) HOCl for 10 minutes, followed by incubation in HMDM culture medium. The cells were subsequently collected at time intervals and analysed for GSH using HPLC analysis. Significance is indicated from the respective 0 hr controls.

3.2.7 Effect of extracellular 7,8-NP in preventing HOCl-mediated HMDM cell damage

7,8-NP has previously been shown to prevent loss of U937 viability (Gieseg *et al*., 2001a) and erythrocyte lysis (Gieseg *et al*., 2001b). This protection by 7,8-NP was possibly due to its scavenging of HOCl, as Widner *et al*. (2000) demonstrated that 7,8-NP scavenges HOCl efficiently to form neopterin. To study whether 7,8-NP is an effective cellular antioxidant against HOCl insult to HMDM cells, cells were treated wtih 400 μM HOCl in the presence of 7,8-NP in the reaction medium. The degree of protection extracellular 7,8-NP gives to the cells was then quantified by measuring cell viability and intracellular GSH loss concurrently (**Figure 3.15**). HOCl at 400 μM alone caused intracellular GSH to decrease by 90% (it decreased from a control value of 41.2 ± 2.7 to 3.7 ± 0.04 nmol/mg protein) and cell viability by 60%. In the presence of 100 μM 7,8-NP, the intracellular GSH level decreased by approximately 50% (the GSH level measured was 20.0 ± 2.5 nmol/mg protein) and cell viability by 10%, compared to the respective controls. In the presence of 200 μM 7,8-NP, the intracellular GSH level decreased by approximately 10% (the GSH level measured was 31.3 ± 2.3 nmol/mg protein) and no significant cell viability loss was observed, compared to the respective controls. At 300 μM 7,8-NP, there were no significant loss in either intracellular GSH level or cell viability. These results suggest that 7,8-NP in the medium efficiently prevented HOCl-induced intracellular GSH and HMDM cell viability loss.

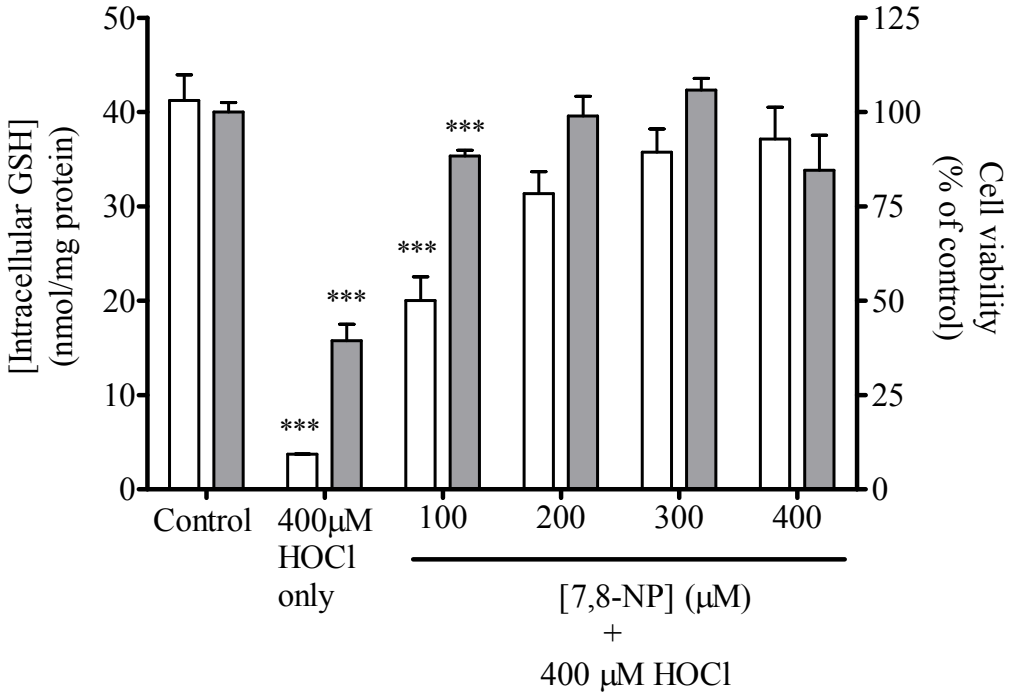

Figure 3.15 7,8-dihydroneopterin (7,8-NP) added to the reaction medium prevented GSH and cell viability losses in HMDM cells upon HOCl insult.
HMDM cells (5×10^6 cells/ml), pre-incubated in the presence or absence of increasing 7,8-NP concentrations in the dark at 37°C for 5 minutes, were treated with or without 400 μM HOCl for 10 minutes. The cells were then incubated in HMDM culture medium for 1 hour, followed by measuring cell viability (gray bars) and intracellular GSH (white bars) using the MTT reduction assay and HPLC analysis, respectively. Significance is indicated from the respective 0 μM HOCl controls.

3.2.8 Effect of IFN-γ-stimulated production of 7,8-NP in preventing HOCl-mediated HMDM cell damage

7,8-NP is synthesized in human macrophages in response to IFN-γ production (Wachter *et al*., 1989; Wachter *et al*., 1992). This section aims to study whether IFN-γ-induced 7,8-NP production in HMDM cells was enough to protect the cells from HOCl insult. This was carried out by synthesizing 7,8-NP *de novo* by incubating HMDM cells with IFN-γ, followed by exposing the cells to HOCl. 7,8-NP is non-fluorescent, while its oxidized form neopterin fluoresces and can be detected via HPLC analysis (λex/λem = 353/438 nm) with an elution time of approximately 4.1 min (**Figure 3.16**). The initial 7,8-NP level was calculated by subtracting the initial neopterin level (**Figure 3.16a**) from the total pterin level (the initial neopterin plus the initial 7,8-NP that had been oxidized to neopterin using the acidic iodide solution) (**Figure 3.16b**) (Flavall, 2007, Masters thesis).

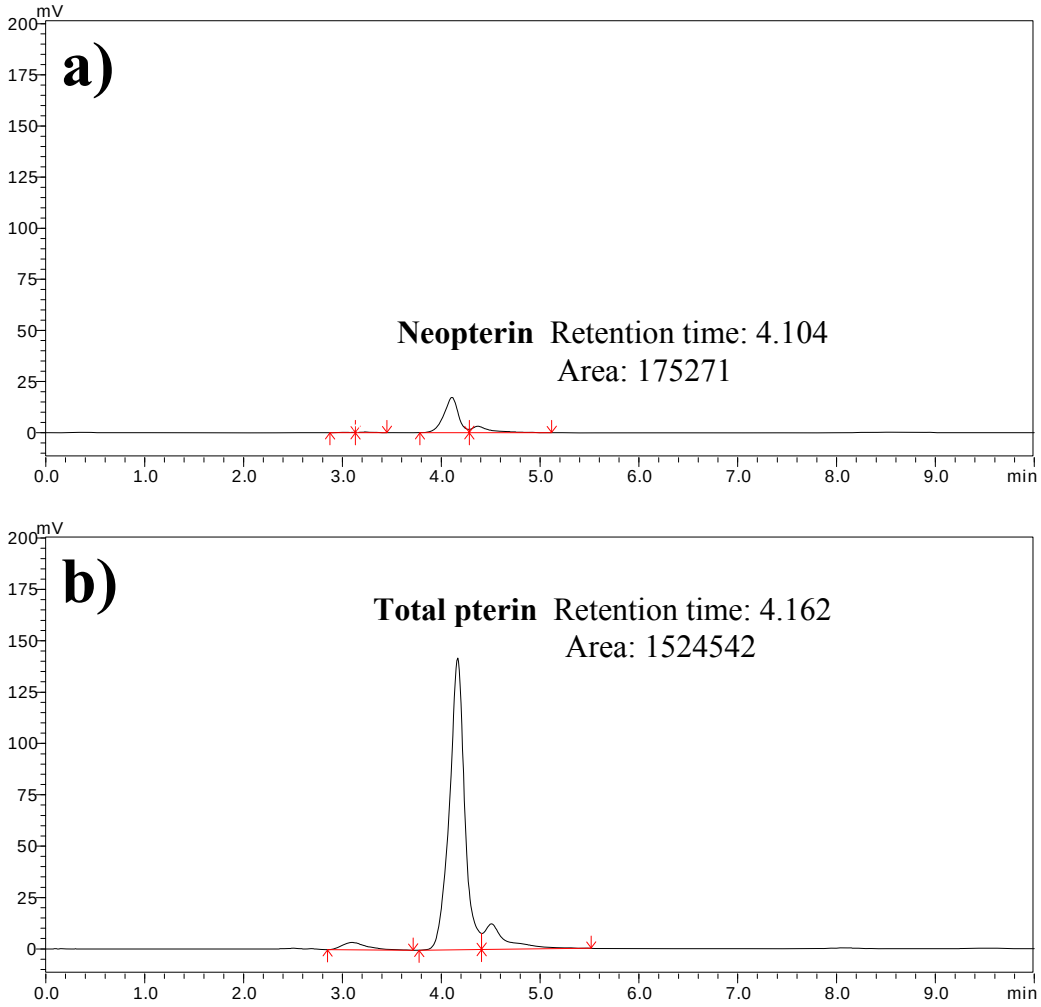

Figure 3.16 HPLC neopterin and total pterin traces of HMDM cells.
HMDM cells (5×10^6 cells/ml) were lysed in cold water and acetonitrile (1:1 ratio). **a)** Half of the cell lysate was centrifuged to precipitate down proteins and the resulting supernatant was analysed for neopterin by HPLC analysis. **b)** The other half of the cell lysate was mixed with the acidic iodide solution to oxidise all 7,8-NP to neopterin, followed by reducing the excess iodine using 0.6 M ascorbic acid. After centrifugation, the resulting supernatant was analysed for total pterin (neopterin and 7,8-NP that has been oxidised to neopterin) by HPLC analysis.

Prior to carrying out the above study, a suitable IFN-γ concentration and incubation period needed to be decided. HMDM cells were incubated with increasing IFN-γ concentrations in RPMI culture medium for 24 or 48 hours. The total 7,8-NP synthesised was calculated by measuring 7,8-NP levels in both cells and media, as 7,8-NP can diffuse out of the activated macrophages into the extracellular spaces (Gieseg *et al.*, 2007). The control cells at 24- and 48-hour showed total 7,8-NP levels of approximately 38.3 ± 3.2 and 39.3 ± 3.5 pmol/5×10^6 cells, respectively. At 24 hour, 250, 500 and 750 U/ml IFN-γ induced 7,8-NP

production in HMDM cells by 1.6, 2.0 and 1.6 fold, respectively. There was no further significant increase in 7,8-NP levels after 48 hours of incubation compared to those after 24 hours of treatment (**Figure 3.17**).

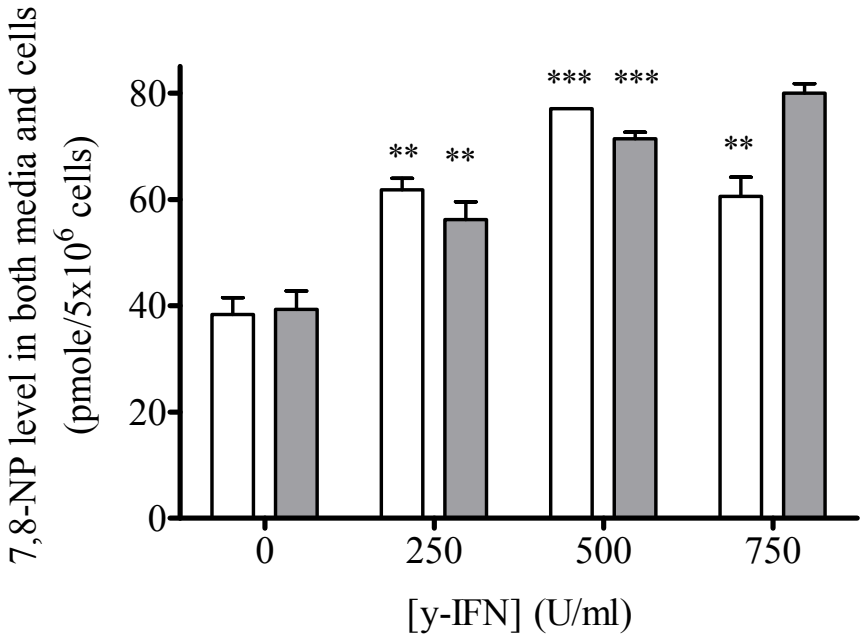

Figure 3.17 7,8-NP synthesis in IFN-γ activated HMDM cells.
HMDM cells (5×10^6 cells/ml) were treated with increasing IFN-γ concentrations in HMDM culture medium for 24 (white bars) or 48 hours (gray bars), followed by measuring and combining 7,8-NP levels in both cells and the respective media by HPLC analyses. Significance is indicated from the respective 0 U/ml γ-IFN data.

The same experimental setup was performed to examine the effect of IFN-γ treatment on HMDM cell viability (**Figure 3.18**). HMDM cells incubated with 250, 500 and 750 U/ml IFN-γ for 24 hours did not cause significant cell viability loss, although 750 U/ml IFN-γ caused the cell viability to vary greatly. HMDM cells incubated with 250, 500 and 750 U/ml IFN-γ for 48 hours showed cell viability loss of approximately 16, 18 and 54% of the control, respectively. Taken together, incubation with 500 U/ml IFN-γ for 24 hours showed maximum 7,8-NP synthesis in HMDM cells without affecting cell viability. This experimental condition was used for the later related experiments. The cell viability loss observed after IFN-γ treatment was possibly due to either IFN-γ or the 7,8-NP produced, which will be discussed in details in **section 3.3.6**.

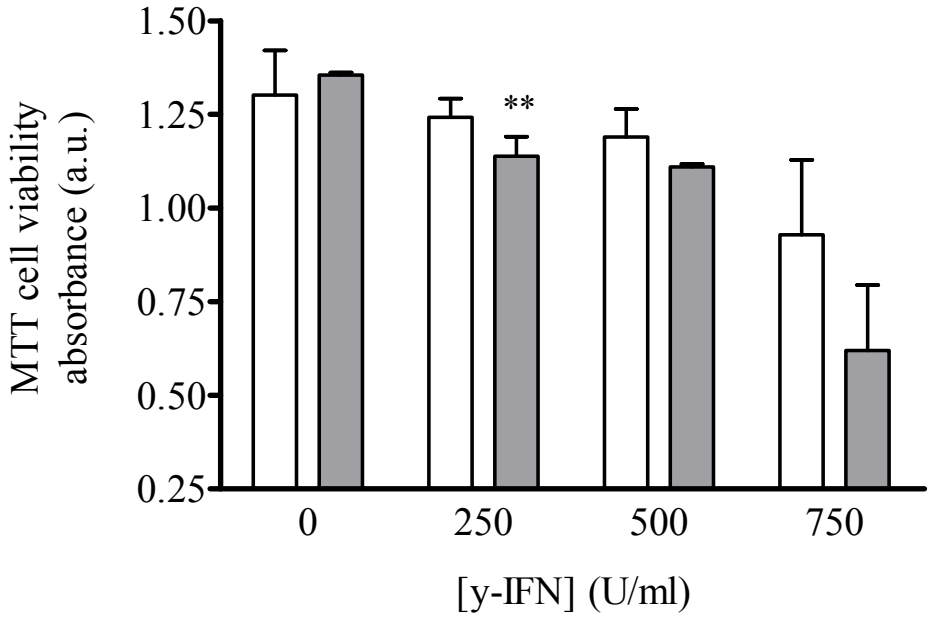

Figure 3.18 Effect of IFN-γ on HMDM cell viability.
HMDM cells (5×10^6 cells/ml) were treated with increasing IFN-γ concentrations in HMDM culture media for 24 (white bars) or 48 hours (gray bars), followed by cell viability determination with the MTT reduction assay. Significance is indicated from the respective 0 U/ml IFN-γ data.

7,8-NP added to the reaction medium significantly prevented HOCl-induced intracellular GSH and cell viability loss (**Figure 3.15**). 7,8-NP is produced *in vivo* by IFN-γ-stimulated macrophages (Gieseg *et al.*, 2007), which leads to the hypothesis that IFN-γ-induced 7,8-NP can also prevent HOCl-induced intracellular GSH and HMDM cell viability loss. To prove this hypothesis, HMDM cells were pre-incubated with or without 500 U/ml IFN-γ for 24 hours for 7,8-NP synthesis. These IFN-γ-treated cells were then exposed to increasing concentrations of HOCl and analysed for cell viability (**Figure 3.19**). The amount of 7,8-NP released into the culture media was added back to the reaction media during HOCl treatment. There was no significant cell viability loss below 150 μM HOCl in HMDM cells pre-treated either with or without IFN-γ ($p > 0.05$). At 150, 200, 300 and 400 μM HOCl, HMDM cells treated without IFN-γ showed approximately 6, 12, 61 and 73% cell viability loss, respectively, whereas HMDM cells treated with IFN-γ showed approximately 18, 15, 62 and 66% cell viability loss, respectively. The percentages of cell viability loss between the corresponding IFN-γ-treated and non-treated cells were not statistically different. Taken together, *de novo* 7,8-NP synthesis did not prevent HOCl-mediated cell viability loss in HMDM cells.

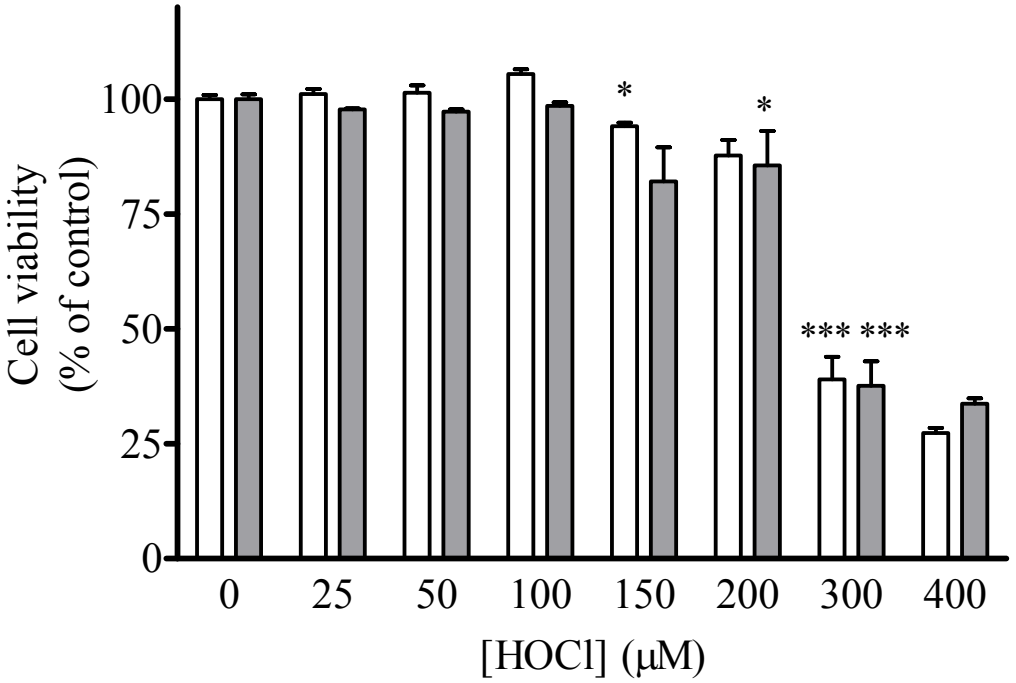

Figure 3.19 Effect of IFN-γ-induced 7,8-NP production in preventing HOCl-mediated HMDM cell viability loss.
HMDM cells (5×10^6 cells/ml) were treated with (gray bars) or without (open bars) 500 U/ml IFN-γ in HMDM culture media for 24 hours. The net 7,8-NP levels in media were measured by HPLC analysis (47.025 ± 28.846 nM). Subsequently, the IFN-γ-treated and non-treated cells were incubated in EBSS media, with 47.025 ± 28.846 nM 7,8-NP added back to the EBSS media of IFN-γ-treated cells. The cells were then exposed to increasing HOCl concentrations for 10 minutes and incubated in HMDM culture media for 1 hour. Cell viability was measured using the MTT reduction assay and presented as percentage of the respective 0 μM HOCl controls. Significance is indicated from the respective 0 μM HOCl controls.

The same experimental setup was carried out for examining the effect of IFN-γ-induced 7,8-NP in preventing HOCl-mediated intracellular GSH loss (**Figure 3.20**). The intracellular GSH levels of control cells (without HOCl treatment) treated with or without IFN-γ were measured 36.7 ± 1.4 or 46.7 ± 1.2 nmol/mg protein, respectively. A HOCl concentration of 50 μM did not cause statistically significant intracellular GSH losses in both HMDM cells with and without IFN-γ treatment. At 100, 150, 200, 250 and 300 μM HOCl, the GSH levels in IFN-γ-non-treated HMDM cells were decreased by 20, 40, 56, 76 and 85%, respectively, while the GSH levels in IFN-γ-treated HMDM cells were decreased by 22, 55, 77, 86 and 91%, respectively, compared to their controls. The GSH levels in IFN-γ-treated HMDM cells were significantly lower than those in the corresponding IFN-γ-non-treated cells either with or without HOCl treatment. The only exception was at 300

μM HOCl, where there was no difference in intracellular GSH levels between IFN-γ-treated and non-treated HMDM cells. Overall, IFN-γ treatment induced intracellular GSH loss and IFN-γ-induced 7,8-NP synthesis did not prevent HOCl-mediated intracellular GSH loss.

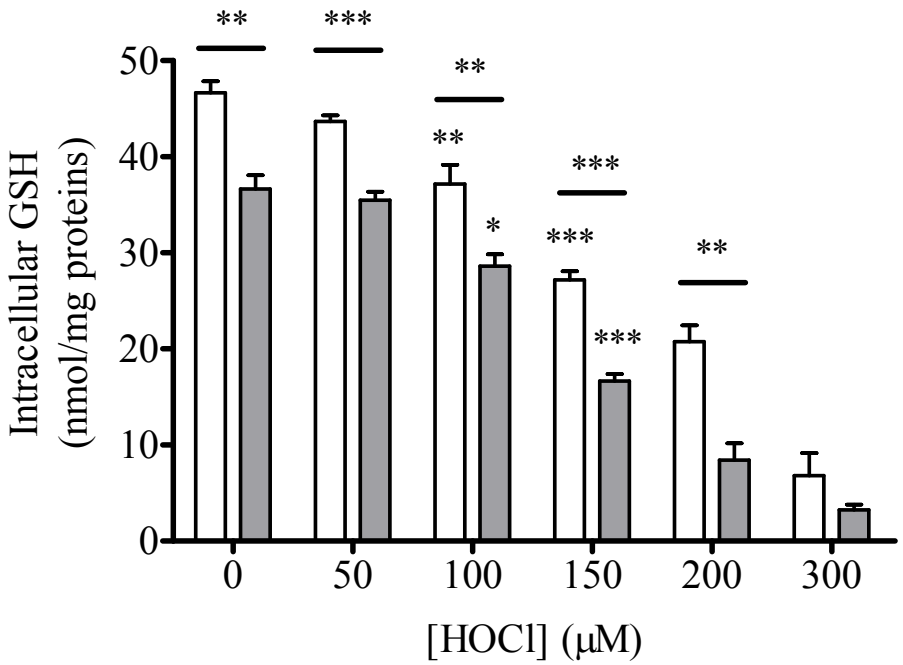

Figure 3.20 Effect of IFN-γ-induced 7,8-NP production in preventing HOCl-mediated intracellular GSH loss in HMDM cells.
HMDM cells (5×10^6 cells/ml) were treated with (gray bars) or without (open bars) 500 U/ml IFN-γ in HMDM culture media for 24 hours. The net 7,8-NP levels in media were measured by HPLC analysis (47.025 ± 28.846 nM). Subsequently, the IFN-γ-treated and non-treated cells were incubated in EBSS media, with 47.025 ± 28.846 nM 7,8-NP added back to the media of IFN-γ treated-cells. The cells were then exposed to increasing HOCl concentrations for 10 minutes and incubated in HMDM culture media for 1 hour. Intracellular GSH levels were then measured by HPLC analysis. Significance is indicated from the respective 0 μM HOCl controls. Significance between IFN-γ-treated and non-treated HMDM cells at each HOCl concentration are shown on top of the bars.

3.2.9 The effect of 7,8-NP, taken up by HMDM cells from culture media, on HMDM cell viability and in preventing loss of HOCl-mediated intracellular GSH and cell viability

7,8-NP produced by IFN-γ-treated HMDM cells could not prevent HOCl-induced intracellular GSH (**Figure 3.20**) and cell viability loss (**Figure 3.19**). This was possibly because the amount of 7,8-NP produced was too little compared to the intracellular GSH level (**section 3.3.6**). This section aims to study whether incubating HMDM cells with 7,8-NP would lead to 7,8-NP accumulating in HMDM cells to a level that is more comparable to intracellular GSH level, hence became more efficient in preventing HOCl-induced intracellular GSH and cell viability loss. This was carried out by pre-incubating HMDM cells with increasing concentrations of 7,8-NP in HMDM culture medium for 24 hours, followed by removal of the 7,8-NP-rich medium and measurement of the 7,8-NP levels accumulated in HMDM cells by HPLC analysis. The same experimental setup was also carried out for the examination of cell viability to study the effect of 7,8-NP accumulation in HMDM cells on the HMDM cell viability.

After 24 hours, the control cells without 7,8-NP treatment showed an intracellular 7,8-NP level of 3.4 ± 3.6 pmol/5×10^6 cells. Pre-incubation of cells with 100, 200 and 300 μM 7,8-NP had their intracellular 7,8-NP levels increased to 89.3 ± 0.3, 167.3 ± 1.4, 240.1 ± 6.8 pmol/5×10^6 cells, respectively (**Figure 3.21a**). Incubating HMDM cells with up to 300 μM 7,8-NP for 24 hours did not cause cell viability loss (**Figure 3.21b**). Taken together, incubating HMDM cells with extracellular 7,8-NP up to 300 μM for 24 hours caused intracellular 7,8-NP increase without affecting cell viability.

The next question was whether the intracellular 7,8-NP increase, resulting from incubation of HMDM cells with extracellular 7,8-NP (**Figure 3.21**), would prevent loss of HOCl-mediated cell viability and intracellular GSH. HMDM cells were incubated with 300 μM 7,8-NP for 24 hours, followed by removal of the 7,8-NP-rich medium and exposure to increasing HOCl concentrations. HMDM cell viability and intracellular GSH in cells were subsequently determined. At 100, 150 and 200 μM HOCl, the 7,8-NP-treated and the respective non-treated HMDM cells showed statistically the same loss of cell viability ($P > 0.05$) (**Figure 3.22**) and intracellular GSH ($P > 0.05$) (**Figure 3.23**). Taken together, the 7,8-NP accumulated in cells (resulting from pre-incubation of HMDM cells with 300 μM

7,8-NP in the medium for 24 hours) could not prevent the subsequent HOCl-mediated cell viability and intracellular GSH loss.

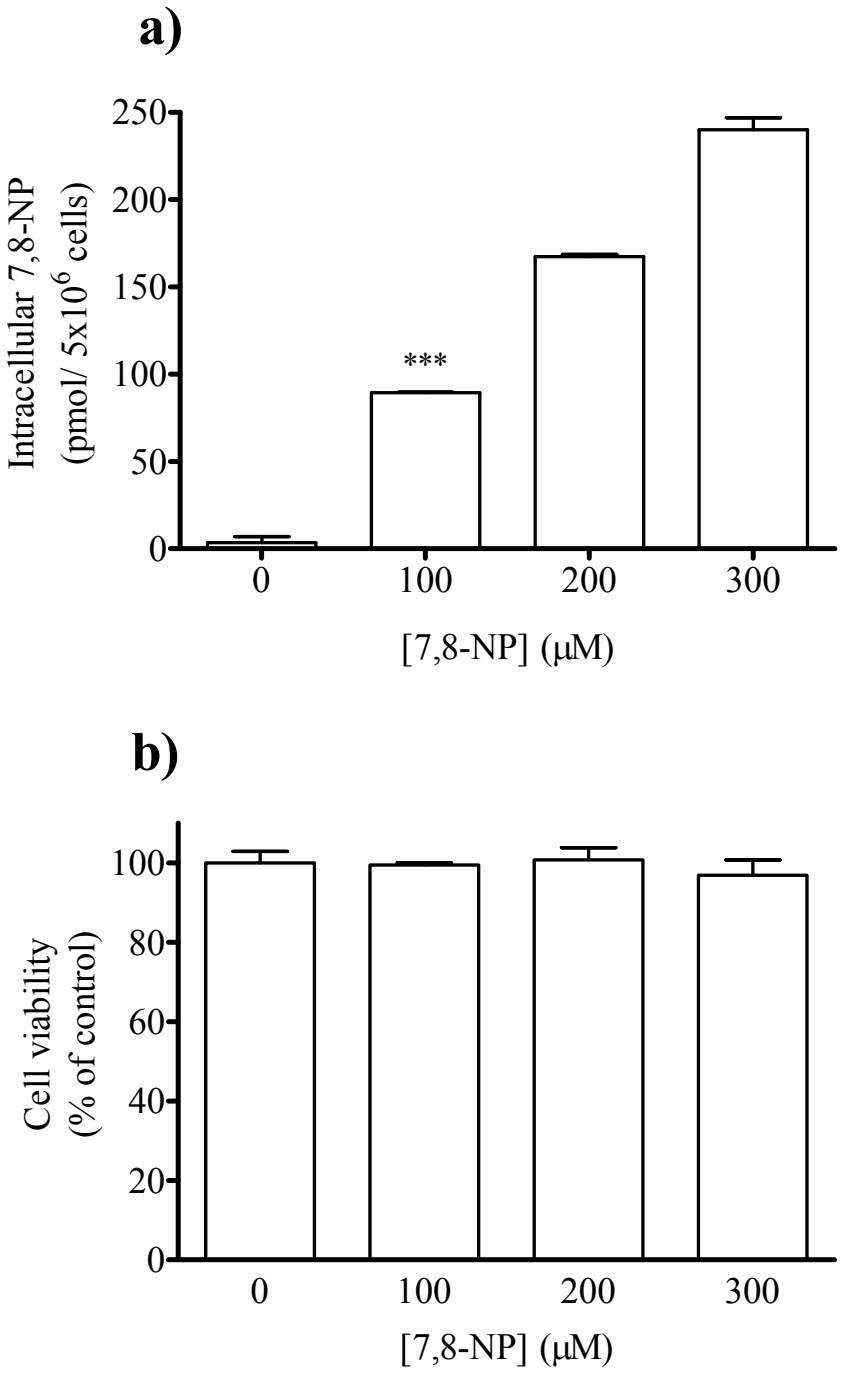

Figure 3.21 Uptake of 7,8-NP by HMDM cells from the medium supplemented with increasing concentrations of 7,8-NP and the effect on HMDM cell viability.
HMDM cells (5×10^6 cells/ml) were exposed to increasing 7,8-NP concentrations in HMDM culture media for 24 hours, followed by determination of **a)** 7,8-NP levels in cells by HPLC analyses and **b)** cell viability by the MTT reduction assay. Significance is indicated from the respective 0 μM 7,8-NP controls.

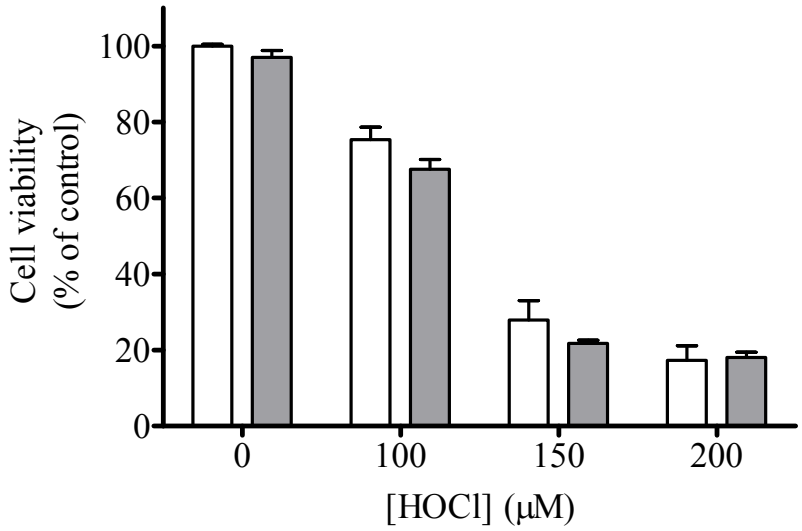

Figure 3.22 Intracellular 7,8-NP increase resulting from treatment of HMDM cells with extracellular 7,8-NP did not prevent HOCl-induced HMDM cell viability loss. HMDM cells (5×10^6 cells/ml) were incubated with (gray bars) or without (white bars) 300 μM 7,8-NP in HMDM culture media for 24 hours, followed by treatment with or without increasing HOCl concentrations in EBSS media. The cells were subsequently analysed for cell viability using the MTT reduction assay. Cell viability is presented as a percentage of the non-7,8-NP-treated and 0 μM HOCl control. There was no statistical difference in cell viability loss between 7,8-NP-treated and the respective non-treated HMDM cells ($P > 0.05$).

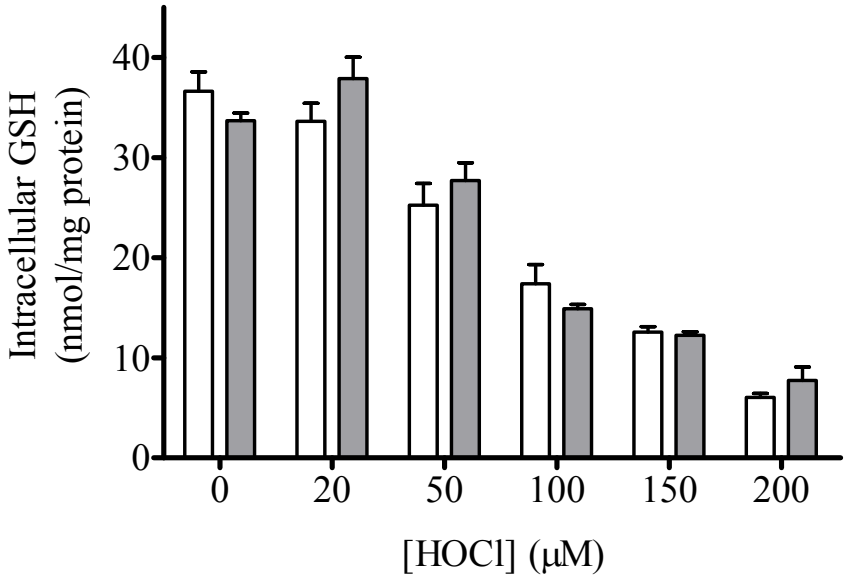

Figure 3.23 Intracellular 7,8-NP increase resulting from treatment of HMDM cells with extracellular 7,8-NP did not prevent HOCl-induced GSH loss in HMDM cells. HMDM cells (5×10^6 cells/ml) were incubated in the presence (gray bars) or absence (white bars) of 300 μM 7,8-NP in HMDM culture media for 24 hours, followed by treatment with or without increasing HOCl concentrations in EBSS media. The cells were subsequently analysed for intracellular GSH by HPLC analysis. There was no statistical difference in intracellular GSH loss between 7,8-NP-treated and the respective non-treated HMDM cells ($P > 0.05$).

3.3 Discussion

3.3.1 Effect of HOCl on HMDM cell viability and intracellular GSH

HOCl caused a concentration-dependent loss of HMDM cell viability above a critical HOCl concentration threshold (i.e. above 50 μM) (**Figure 3.2**). This is in agreement with a number of studies using different cell types, including endothelial cells (Vissers *et al*., 1999; Pullar *et al*., 1999), red blood cells (Vissers *et al.*, 1994), human skin fibroblasts cells (Vile *et al*., 2000), cultured cortical neurons (Yap *et al*., 2006) and THP-1 monocyte and J774 macrophage cells (Hawkins *et al*., 2001). Activated neutrophils have been demonstrated to produce 20-400 μM HOCl through the $MPO/H_2O_2/Cl^-$ system (Weiss *et al.*, 1982; Foote *et al.*, 1983). Hence, the HOCl concentrations used that caused HMDM cell viability loss were well within the physiological range of HOCl production.

Cell viability was measured by both MTT reduction assay (**Figure 3.2a**) and trypan blue exclusion assay (**Figure 3.2b**). The MTT reduction assay measures metabolic activity of cells; MTT compound is reduced by mitochondrial NADH dehydrogenases to formazan only in living, metabolically active cells and formazan production is directly proportional to cell number (Mosmann, 1983). Yet, stimulated cells can produce more formazan than resting cells, suggesting that the observed HMDM cell viability loss could be attributed to either an increased ratio of dead to viable cells or decreased metabolic activity in the viable cells. Cell viability measured by the trypan blue exclusion assay (monitors cell membrane integrity) agrees with that obtained by the MTT assay. This indicates the observed cell viability loss was indeed due to cell death. Irrespective of their different mechanisms for detecting cell death, these two assays provided strong corroboration of all viability results obtained.

The MTT reduction assay was chosen over the trypan blue assay as the general cell viability assay in this thesis, because it gives a quantitative result, which is more accurate than the more biased result obtained by the trypan blue assay due to the cell counting errors under inverted microscope. For the trypan blue assay, PI dye tend to enter HMDM cells and formed tiny blue spots rather than an obvious blue patch, which made it very hard to distinguish between dead and live HMDM cells. As a result, more HMDM cells than needed were possibly assigned as dead cells. This explains why the HOCl-induced cell viability loss measured by the trypan blue assay was slightly greater than that measured by the MTT reduction assay.

The loss of MTT reduction in HOCl-treated HMDM cells implicated mitochondria toxicity. In agreement with the current result, HOCl has been previously shown to cause mitochondria swelling in mitochondria isolated from rat liver, indicating that HOCl caused impairment of isolated mitochondrial function (Whiteman *et al.*, 2005). This HOCl-mediated mitochondria toxicity was unlikely a result of cell membrane lysis, since it was shown in **Chapter 4** that preventing MPT-mediated mitochondrial membrane potential loss inhibited HOCl-induced HMDM cell viability loss.

HMDM cells exposed to the same HOCl concentration for 10 to 60 minutes, followed by incubation in RPMI culture media for 20 hours, showed similar percentages of viability loss (**Figure 3.3**). This indicates that HOCl was completely consumed and caused rapid cell viability loss within 10 minutes. It was less likely that any HOCl remained for more than 10 minutes, since HOCl is a highly oxidising agent and rapidly react with a range of biomolecules (see **section 1.5.2**). HOCl (60 μM) was completely consumed by 0.2 x 10^6 human hepatoma cells within 20 minutes, indicating rapid consumption of HOCl when in contact with these cells (Whiteman *et al.*, 2005). The time course of HOCl-mediated cell viability loss showed that the cell viability decreased most significantly during the initial 10-minute HOCl treatment and did not decrease further after the initial treatment (**Figure 3.4**). Taken together, HOCl caused rapid (i.e. within 10 minutes), not gradual cell viability loss (i.e. over 24-hour period), irrespective of the concentrations applied.

The rapid metabolic energy loss (measured by MTT assay) and perturbation of cellular membranes (measured by trypan blue assay) implied that HOCl induced necrotic cell death in HMDM cells. This is consistent with the HOCl-induced morphological changes. HOCl concentrations at or less than 50 μM did not cause significant morphological changes, while concentrations above 100 μM caused the cells to enlarge significantly with the cell membranes deformed or ruptured (**Figure 3.5**). HOCl causes necrotic cell death in many other cell types (Vissers *et al*., 1994; Tatsumi and Fliss, 1994; Abernathy and Pacht, 1995; Vile *et al*., 2000; Slivka *et al*., 1980; Schraufstatter *et al.* 1990). Yet, it is also suggested that low HOCl doses induced apoptosis while high doses induced necrosis (Vissers *et al.*, 1999). The mechanism(s) of HOCl-induced HMDM cell death will be discussed in detail in **Chapters 4** and **5**.

It was found that HMDM cells treated with HOCl only showed significant cell viability loss after the intracellular GSH level was significantly decreased (**Figure 3.6**). This implies

that HOCl did not react with cell membranes first causing membrane integrity loss, but penetrated the plasma membrane to react with intracellular GSH rapidly, within 10 minutes. This agrees with Vissers and Winterbourn (1995), who suggested that HOCl penetrated the red cell membranes to oxidise GSH rapidly, within 2 minutes. It is possible that HOCl penetrates cell membranes, as HOCl is an uncharged free acid, which can pass through the hydrophobic lipid bilayer while undergoing minimum reaction with membrane components (Pullar *et al*., 2000).

The above results also imply that once GSH was no longer abundant enough in cells to effectively scavenge HOCl, the remaining HOCl then reacted with other biomolecules, causing metabolic energy and membrane integrity loss. This hypothesis is consistent with some previous studies, which showed significant HOCl-induced intracellular GSH loss before cell lysis or cell swelling were observed (Vissers and Winterbourn., 1995; Carr and Winterbourn, 1997). In contrast to this hypothesis, Schraufstatter *et al.* (1990) have argued that cell membrane in tumor cells was the prime target of HOCl and would provide a protective barrier for cytoplasmic components (Schraufsttater *et al.*, 1990). This difference from the current result suggests that this particular cell type allows more restricted access to HOCl than HMDM cells.

Interestingly, there were no statistically significant intracellular GSH loss at HOCl concentrations at or less than 50 μM (**Figures 3.6** and **3.10**). One possible explanation is that HOCl also reacted with some other biomolecules, which showed greater or similar reactivity with HOCl and/or abundance as GSH, either before or at the same time as intracellular GSH. As a result, the effect of HOCl at low concentrations on intracellular GSH was less profound. For example, GAPDH enzyme, which possesses thiol groups at its active site, showed decreased activity at the same rate as intracellular GSH loss in HOCl-treated HMDM cells (see **Chapter 4**). Moreover, though GSH shows extremely high reactivity with HOCl with a rate constant above 10^7 $M^{-1}s^{-1}$, ascorbate can also react rapidly with HOCl with a rate constant approximately 6×10^6 $M^{-1}s^{-1}$ (Folkes *et al.*, 1995). Amine groups are oxidized by HOCl at a rate about 100 times less than thiol groups and thioethers such as Met residues, but they would compete favourably for HOCl as they are generally present in considerable excess over sulfur compounds (Winterbourn, 1985).

3.3.2 Effect of intracellular GSH in preventing HOCl-induced cell viability loss

Intracellular GSH loss occurring before HMDM cell viability loss during HOCl exposure (see **Figure 3.6**) implies that intracellular GSH plays an important role in protecting HMDM cells from HOCl insult. The time course of GSH loss in HMDM cells treated with increasing HOCl concentrations showed that there was no GSH recovery when the initial GSH loss was 50% of the control GSH value or when the GSH concentration has decreased to approximately 30 nmol/mg protein (**Figure 3.14**). This result implies that the initial GSH loss in HMDM cells treated with 100 μM HOCl in **Figure 3.6** should not be recovered with time, because the initial GSH loss was approximately 50% of the control GSH value and the GSH concentration has decreased to less than 20 nmol/mg protein. The lack of GSH recovery was possibly due to HOCl inactivating the GSH synthesis and repair enzymes, depleting NADPH (required for glutathione reductase), ATP and cysteine (substrates required for GSH biosynthesis), and causing the irreversible formation of higher oxidation products (such as sulphonamide and thiolsulfonate) when the initial intracellular GSH concentration is relatively low (**Figure 3.1**). The above possibilities are discussed in further details in **section 3.3.4**.

The cell viability curve in **Figure 3.6** is different from that in **Figure 3.3**. This was possibly because the HMDM cell batches used in these two studies contained significantly different initial intracellular GSH level, which led to their different resistance towards HOCl insult. The correlation study (**Figure 3.13a**) has shown that the initial intracellular GSH level in a particular cell batch was significantly correlated with the HOCl concentration required to kill 50% cell population of that cell batch.

This hypothesis was further confirmed by the finding that HMDM cells depleted of approximately 90% of intracellular GSH (using DEM) showed significantly lower cell viability after HOCl treatment compared to HMDM cells with intact GSH (**Figure 3.10**). The result is similar to Gotoh *et al.* (1993), who demonstrated that GSH depletion renders oxLDL cytotoxic to both THP-1 cells and PMA-derived macrophage cells at a concentration well tolerated by cells with intact GSH. However, this theory does not apply to HMDM cells exposed to high HOCl concentrations. At 200 or 500 μM HOCl, the percentage of cell viability loss was the same between HMDM cells with or without intact intracellular GSH. This was possibly because intracellular GSH could not protect HMDM

cells from high concentrations of HOCl. High HOCl concentrations caused extremely rapid loss of intracellular GSH and the huge excess of HOCl reacted overwhelmingly with other intracellular components of HMDM cells within the 10-minute incubation.

The lower sensitivity of DEM-treated HMDM cells towards HOCl exposure was not caused by DEM reacting with cellular protein thiols. This was demonstrated by the finding that incubation of HMDM cells with up to 300 μM DEM did not affect protein thiol levels, while 100 μM DEM caused approximately 80% decrease in intracellular GSH (**Figure 3.8**). It was previously shown that incubation of rat brain slices with 10 mM DEM for 2 hours decreased protein thiol level by 13% of control (Bizzozero *et al*., 2006). This difference from the current result was possibly due to the much higher DEM concentration used by the investigators compared to the concentration used in this study.

Incubation with 100 μM DEM for 3 hours was the chosen experimental condition for depleting intracellular GSH, as this condition caused intracellular GSH to decrease by approximately 60-90% (**Figures 3.7-3.9**). Interestingly, cell viability was not affected by the absence of intracellular GSH (**Figure 3.7**). This agrees with a previous study, which demonstrated that monocytic THP-1 cells and phorbol-12-myristate-13-acetate (PMA)-derived macrophage cells depleted of intracellular GSH using L-buthionine-S-sulfoxomine (a selective inhibitor of γ-glutamyl cysteine synthase) showed no decrease in cell viability (Gotoh *et al*., 1993). The result from this study suggests that either other antioxidants were protecting the cells from oxidative stress in the absence of GSH or there was little or no oxidative stress within the incubation period.

DEM (100 μM) caused intracellular GSH to deplete by approximately 75% and 60% in **figures 3.8** and **3.9**, respectively. This percentage difference was due to the different initial GSH levels in the HMDM cell batches used. The initial intracellular GSH levels in **Figures 3.8** and **3.9** were measured 28 and 35 nmol/mg protein, respectively. However, the GSH levels in both HMDM cell batches decreased by approximately 21 nmol/mg protein after 100 μM DEM treatment.

Keeping in mind that intracellular GSH plays a crucial role in protecting HMDM cells from HOCl insult, the next question was how exactly intracellular GSH prevented HOCl-induced cell viability loss. The data in **Chapter 5** will show that HOCl-induced cytosolic Ca^{2+} increase was the major cause of necrotic cell death in HMDM cells. This cytosolic

Ca^{2+} increase was attributed to both Ca^{2+} influx from the media via Ca^{2+} channels on cell membranes and Ca^{2+} release from ER via Ca^{2+} channels on ER membranes (see **section 5.2**). Since these Ca^{2+} channels (on both cell and ER membranes) can be activated by HOCl interacting with the essential thiol groups within them (see **section 5.3**), it was possible that intracellular GSH scavenged HOCl from inside the cells, preventing HOCl from interacting with cell membrane Ca^{2+} channels (from cytoplasmic side) and ER Ca^{2+} channels. This could then prevent cytosolic Ca^{2+} increase and subsequently cell death.

3.3.3 Effect of intracellular GSH concentration in protecting HMDM cells from HOCl insult

HMDM cell preparations from different donors showed different sensitivity towards the same HOCl concentration (**Figure 3.11**). This varying level of resistance to HOCl in each cell preparation was not caused by differences in experimental conditions (**Figure 3.12**), nor by cell number differences in each cell batch (the cell number in each cell batch was relatively constant) (**Figure 3.13b**). The correlation study suggested that the level of resistance to HOCl in a cell preparation increased with their intracellular GSH level (**Figure 3.13a**). This is possibly due to the fact that elevated GSH levels generally increase antioxidant capacity and resistance to oxidative stress. The current result agrees with Rosenblat *et al.* (2007), who showed that intracellular GSH elevation by administering liposomal GSH to a mouse model of atherosclerosis diminished blood plasma and macrophage oxidative stress levels and macrophage cholesterol mass. Moreover, low intracellular GSH levels have been implicated in a number of diseases, such as Parkinson's disease, Alzheimer's disease, myocardial infarction, multiple sclerosis, and rheumatoid arthritis (Fadeel *et al*., 1999; Pastore *et al*., 2003). This is possibly attributed to low GSH levels increasing susceptibility of cells towards oxidative stress, resulting in damages that lead to onset and/or progression of the diseases (Ballatori *et al*., 2009).

Varying GSH levels in HMDM cells of different donors are possibly attributed to the varying expression levels and activity of GSH-related enzymes such as y-glutamylcysteine ligase, glutathione synthetase and glutathione reductase, and/or availability of ATP, NADPH and the substrate L-cysteine (Ballatori *et al*., 2009).

3.3.4 Intracellular GSH recovery/loss over time in response to HOCl insult

For intracellular GSH to be an effective antioxidant against HOCl, it should scavenge HOCl rapidly, and the oxidized GSH should be recycled back to the reduced form for maintaining intracellular redox homeostasis and preventing the next round of oxidative insult. This research showed that intracellular GSH was not recovered over time when the initial intracellular GSH concentration in HMDM cells was decreased by 50% upon 200 μM HOCl exposure (**Figure 3.14**).

One possibility for the lack of recovery at high HOCl concentrations is that the initial intracellular GSH was lost through the ruptured cell membranes. However, this was less likely as HOCl-induced cell viability loss was not significant when the intracellular GSH concentration was decreased by approximately 50% (**Figure 3.6**). Another possibility was that higher HOCl concentrations (above 200 μM HOCl) favoured the irreversible formation of sulfonamide and thiosulfonate (Pullar *et al*., 2001) (see also **Figure 3.1**), which could not be regenerated to the reduced state. Other possibilities are the generation of mixed disulfides with proteins (Carr and Winterbourn, 1997), inactivation of glutathione reductase at higher HOCl concentration (Vissers and Winterbourn, 1995) and depletion of NADPH by HOCl (required for glutathione reductase) (Auchere and Capeillere-Blandin, 1999). Inactivation of GSH re-synthesis could also prevent GSH recovery. Both ATP (see **Chapter 4**) and cysteine (Pattison and Davies, 2001) are essential substrates of GSH biosynthesis and can be rapidly oxidized by HOCl, hence possibly limiting GSH synthesis. HOCl was shown to induce activation of calpains in HMDM cells (see **Chapter 5**). Calpains are Ca^{2+}-dependent cysteine proteases that cleave a diverse range of cellular proteins (see **section 1.8** and **Chapter 5**). It is possible that those activated calpains damaged γ-glutamylcysteine synthetase and glutathione synthetase, hence inhibiting GSH re-synthesis and recovery. However, further investigation is required to prove this theory.

Pullar *et al.* (2001) have suggested that the irreversible products (sulfonamide and thiosulfonate) can be exported into the extracellular space via the cell's transport mechanism, which possibly explains why intracellular GSH was further lost after the initial loss in HMDM cells treated 200 μM HOCl. The progressive loss was also possibly due to further oxidative stress generated. HMDM cells have demonstrated generation of superoxide radicals after HOCl treatment (see **Chapter 4**). HOCl can also react with amine

groups to form chloramines. Cell permeable chloramines such as glycine-chloramine can oxidize GSH in Jurkat cells (Midwinter *et al.*, 2006). However, chloramines were only detected in red cells at HOCl concentrations above those required to oxidize all available thiols (Vissers and Winterbourn, 1995).

The data from the time course study also showed that intracellular GSH was recovered when the initial intracellular GSH loss was only 25% in HMDM cells after treatment with 100 μM HOCl (**Figure 3.14**). This was possibly because lower HOCl concentrations favoured the formation of GSSG, which could be recycled back to reduced GSH (Winterbourn and Brennan, 1997). However, GSH could also be recovered by GSH re-synthesis, which requires further investigation.

One hypothesis that can be made from the above time course data and the reaction of GSH with HOCl (Winterbourn and Brennan, 1997) is that intracellular GSH concentration may be one important determinant of whether GSH can recover after HOCl treatment and therefore a determinant of whether GSH in HMDM cells is a good antioxidant against HOCl. In other words, at a particular HOCl concentration, a cell preparation with higher GSH level may favour GSSG formation that can be regenerated to GSH in reduced state, while a cell preparation with lower GSH level may favour the formation of irreversible GSH products, thereby blocking regeneration of GSH.

The HMDM cell batch used for this time course study (**Figure 3.14**) contained a GSH level of approximately 60 nmol/mg protein. However, GSH level does vary between HMDM cell batches (5 x 10^6 cells/ml) in a range between 20-60 nmol/mg protein (**Figure 3.13a**). In comparison, 0.2 x 10^6 cells/ml human hepatoma cells (Whiteman *et al*., 2005) and human chondrocytes (Whiteman *et al*., 2007) contained a GSH level of 16 and 8 nmol/mg protein, respectively.

3.3.5 Effect of extracellular 7,8-NP in preventing HOCl-mediated HMDM cell damage

It has been hypothesized that 7,8-NP is synthesised by γ-IFN-stimulated macrophages to protect the cells against the oxidants encountered within an inflammatory site; including HOCl (Gieseg *et al*. 2007). HMDM cells were fully protected from 400 μM HOCl-induced

cell viability and intracellular GSH loss by addition of 7,8-NP to give a media concentration of 300 μM (**Figure 3.15**). This indicates that extracellular 7,8-NP scavenged HOCl efficiently to prevent HOCl from oxidizing intracellular GSH and causing cell death. This is in agreement with previous studies, which showed that 7,8-NP is an efficient scavenger of HOCl (Widner *et al.*, 2000) and protects monocytic U937 cells (Gieseg *et al.*, 2001a) and erythrocytes (Gieseg *et al.*, 2001b) from HOCl-induced cellular damage. The current result also suggests that in the presence of a highly reactive external substrate, GSH in HMDM cells was unable to compete effectively for HOCl. This agrees with Vissers and Winterbourn (1995), who showed that intracellular GSH in red cells was unable to compete for HOCl effectively in the presence of ascorbate in the extracellular medium.

7,8-NP, at a concentration of 300 μM, was sufficient to fully prevent cell viability and intracellular GSH loss in HMDM cells treated with 400 μM HOCl, indicating that every 3 molecules of 7,8-NP scavenged 4 molecules of HOCl. Yet, this result does not necessarily mean that 7,8-NP did not react with HOCl at 1:1 ratio. It was possible that while the majority of HOCl reacted with 7,8-NP, some HOCl molecules reacted with cell membrane components or entered the cells to react with intracellular components and the effect was too minor to damage the cells. HOCl can also react with neopterin (Widner *et al.*, 2000).

The effective concentrations of 7,8-NP added to cells in the above experiments appeared to be higher than the *in vivo* neopterin concentrations reported. Serum concentrations of neopterin usually range from 5 nM in healthy individuals to approximately 100 nM in severely ill patients (Fuchs *et al.*, 1994). Up to 2 μM neopterin has been reported in atherosclerotic plaques from carotid artery (Gieseg *et al.*, 2007). However, the 7,8-NP concentrations in the local environment of cells is likely to be higher than the above reported values. Also *in vivo* there is a continuous high level of neopterin and 7,8-NP release occurring in body fluids of patients due to continuous stimulation with γ-IFN. In contrast, the experiments reported here had 7,8-NP added as a single bolus, at time zero. Direct cell-to-cell contact may further facilitate the accumulation of even higher concentrations of 7,8-NP in the microenvironment of cells and its effects may be further augmented in concert with other inflammatory cytokines, which are induced upon activation of cells with IFN-γ such as interleukin-1 and TNF-α (Billiau and Dijkmans, 1990; Enzinger *et al.*, 2002b).

3.3.6 Effect of IFN-γ-stimulated production of 7,8-NP in preventing HOCl-mediated HMDM cell damage

HMDM cells pre-incubated with 500 U/ml of IFN-γ for 24 hours showed increased production of 7,8-NP, which was detected in both cells and extracellular media (**Figure 3.17**). This is consistent with the previous findings that 7,8-NP was synthesized in human macrophages upon induction by IFN-γ and was released into extracellular space (Wachter *et al*., 1989; Wachter *et al*., 1992). This particular IFN-γ concentration and incubation period was chosen because 7,8-NP synthesis was maximized at these conditions (**Figure 3.17**) without affecting the HMDM cell viability (**Figure 3.18**). The γ-IFN-non treated control cells showed approximately 40 pmole/5×10^6 cells of 7,8-NP. This is possibly because the HIHS used for pre-incubating the cells already contained the inflammatory factor γ-IFN, hence inducing some 7,8-NP synthesis.

IFN-γ-treated HMDM cells exposed to increasing concentrations of HOCl showed statistically similar cell viability loss as those of the respective non-IFN-γ-treated cells (**Figure 3.19**). This is not surprising, since the total 7,8-NP synthesized did not appear to be enough to scavenge HOCl. The net 7,8-NP released into media after γ-IFN treatment was only approximately 47 nM, whereas the intracellular 7,8-NP concentration was approximately 1.13 μM, calculated using the cell volume of human macrophage (2.48 μl per 10^6 macrophage cells) calculated by Dorian *et al*. (2001). In comparison, the intracellular GSH level prior to IFN-γ treatment was approximately 10.7 nmol/5×10^6 cells (**Figure 3.20**), equivalent to approximately 863 μM. The much higher concentration of intracellular GSH over that of the total 7,8-NP suggested that 7,8-NP would not compete efficiently for HOCl with intracellular GSH, assuming 7,8-NP and GSH have similar rate constants reacting with HOCl.

IFN-γ-treated HMDM cells that were treated with or without HOCl showed lower intracellular GSH levels than those of the respective IFN-γ-non-treated cells (**Figure 3.20**). This was possibly caused by IFN-γ treatment inducing ROS formation in HMDM cells, which led to a decrease or depletion of intracellular GSH and eventually cell death. Primary hepatocytes treated with 100 U/ml IFN-γ for 24 hours showed significant ROS generation (Watanabe *et al.*, 2003). This theory can also explain why high IFN-γ concentrations (750 U/ml) and a long period of IFN-γ incubation (48 hours) caused cell viability loss (**Figure 3.18**).

It was also possible that the 7,8-NP synthesized in human macrophages upon IFN-γ induction acted as a pro-oxidant by causing intracellular ROS generation and subsequently intracellular GSH loss, which eventually led to cell death. Antioxidants ranging form N-acetylcysteine (NAC) to pyrrolidine dithiocarbamate (PDTC), catalase and superoxide dismutase (SOD) have been demonstrated to significantly inhibit 7,8-NP-mediated apoptosis (Baier-Bitterlich *et al*., 1995; Baier-Bitterlich *et al*., 1996a; Hoffmann *et al*., 2003; Spottl *et al*., 2000), indicating that 7,8-NP induced apoptosis by mediating ROS generation. In addition, 7,8-NP at a high concentration (5 mM) superinduced TNF-α-mediated apoptosis in U937 cells (Baier-Bitterlich *et al*., 1995) and induced apoptosis in Jurkat T-lymphocytes via a Bcl-2-sensitive pathway (Enzinger *et al*., 2002a). Neopterin or 7,8-NP with concentrations as low as 10 μM also induced apoptosis and augmented TNF-α/IFN-γ-mediated apoptosis in rat alveolar epithelial cell line L2 cells (Schobersberger *et al*., 1996). However, the above studies did not mention whether 7,8-NP was taken up by cells and how much was taken up to induce ROS generation and apoptosis.

Incubation of HMDM cells with extracellular 7,8-NP (100-300 μM) increased intracellular 7,8-NP concentrations to much higher values (**Figure 3.21a**) than that in IFN-γ-treated HMDM cells (**Figure 3.17**), without affecting cell viability (**Figure 3.21b**) and intracellular GSH levels (**Figure 3.23**). These results indicated that the amount of 7,8-NP synthesized in macrophage cells upon induction by IFN-γ was not enough to have caused the observed cell viability and intracellular GSH loss after IFN-γ treatment.

3.3.7 The effect of 7,8-NP-treated HMDM cells in preventing HOCl-mediated intracellular GSH and cell viability loss

As mentioned above, the intracellular 7,8-NP concentration in HMDM cells incubated with extracellular 7,8-NP was significantly higher than that of IFN-γ-treated HMDM cells. For example, at 300 μM 7,8-NP, the intracellular 7,8-NP concentration was equivalent to approximately 19 μM (**Figure 3.21**). However, this higher concentration of intracellular 7,8-NP was still not enough to prevent HOCl-mediated intracellular GSH (**Figure 3.23**) and cell viability (**Figure 3.22**) loss. This was not surprising, as intracellular GSH concentration was approximately 36 nmol/mg protein (equivalent to approximately 580 μM), which was possibly too high to be out-competed by 7,8-NP.

3.4 Conclusion

HOCl caused a concentration-dependent loss of HMDM cell viability rapidly (within 10 minutes) above critical HOCl concentration thresholds, and the treatment caused no latent damaging effect on HMDM cells, regardless of HOCl concentrations. Rapid metabolic energy loss (measured by MTT reduction assay), cell membrane integrity loss (measured by trypan blue exclusion assay), cell membrane rupture, and cell swelling were observed. This implies that HOCl caused HMDM to undergo necrotic cell death.

Depletion of intracellular GSH rendered HMDM cells more sensitive to HOCl exposure, whereas HMDM cell preparations with higher intracellular GSH levels showed greater resistance to HOCl insult. These results indicate that intracellular GSH played an important role in protecting HMDM cells from HOCl insult. However, the time course of GSH loss in HMDM cells treated with increasing HOCl concentrations showed that intracellular GSH lost initially was not regenerated over time when the initial GSH loss was over 50% in HMDM cells, whereas the loss was regenerated when the initial loss was 25%. This suggests that intracellular GSH acted as an efficient antioxidant protecting HMDM cells from HOCl insult only at relatively low HOCl concentrations, since the parent thiols could be regenerated to prevent further rounds of oxidative insult.

Exposing HMDM cells to HOCl in the presence of 7,8-NP significantly reduced intracellular GSH and cell viability loss, indicating that 7,8-NP added extracellularly was an efficient scavenger of HOCl and out-competed intracellular GSH for HOCl. However, 7,8-NP synthesized by HMDM cells upon IFN-γ induction or 7,8-NP accumulated in HMDM cells after cell incubation with 7,8-NP added extracellularly, did not prevent HOCl-mediated intracellular GSH and cell viability loss. This may have resulted because the concentrations of 7,8-NP were too low to efficiently scavenge HOCl.

4. HOCL MEDIATED NECROTIC CELL DEATH IN HMDM CELLS

4.1 Introduction

The acellular areas (often called the necrotic core) of advanced plaques are rich in cell debris (Stary *et al*., 1995), which is suggested to result from the death of macrophages (Ball *et al*., 1995; Berberian *et al*., 1990). These findings imply that macrophages within plaques undergo cell lysis, contributing to advanced plaque formation. The macrophage cell death may be caused by the oxidant HOCl, since macrophages, MPO enzyme and 3-chlorotyrosine (Domigan *et al*., 1995; Kettle, 1996) were found colocalizing in atherosclerotic lesions (Daugherty *et al*., 1994; Malle *et al*., 2000; Sugiyama *et al*., 2001). Researchers have emphasized that MPO-H_2O_2-Cl^--generated HOCl oxidizes (lipo)proteins under *in vivo* conditions. The oxidized (lipo)proteins are then taken up by macrophages, resulting in cell death. However, it is also possible that HOCl exerts a toxic effect on macrophage cells leading to cell death.

The strong oxidizing nature of HOCl means that it can potentially damage host cells. Exposure of cells to HOCl results in the oxidation of a range of critical biomolecules, including plasma membrane lipids, proteins, DNA, and small molecules, including ascorbate, nucleotides, sulfhydryls, and thioethers (see **section 1.5.2**). HOCl has been shown to cause caspase-3-dependent apoptosis in human umbilical vein endothelial cells (HUVESs) (Vissers *et al*., 1999; Vissers *et al*., 2001) and HL-60 human leukemia cells (Wagner *et al*., 2000). HOCl also caused human mesenchymal progenitor cells (Whiteman *et al*., 2007) and murine neuronal cells (Yap *et al*., 2006) to undergo caspase-3-independent apoptosis. In addition, HOCl caused necrotic cell death in HeLa cells (Park *et al*., 2008), red blood cells (Vissers *et al*., 1994), endothelial cells (Tatsumi and Fliss, 1994), rat type II alveolar epithelial cells (Abernathy and Pacht, 1995), human skin fibroblast cells (Vile *et al*., 2000), human granulocytes (Slivka *et al*., 1980) and murine macrophage-like tumor cells (Schraufstatter *et al*., 1990).

Collapse of the mitochondrial membrane potential is an important event that occurs in mitochondria when a cell dies, whether it is a result of apoptosis or necrosis. Mitochondrial membrane potential loss may be induced via the opening of high-conductance membrane permeability transition (MPT) pores (see also **section 1.7.3**). Whiteman *et al*. (2005b) have

demonstrated MPT activation and mitochondrial membrane potential loss in HOCl-treated human hepatoma HepG2. The pore is a complex of the voltage-dependent anion channel (VDAC; permeable to molecules < 5000 Da) in the outer mitochondrial membrane (OMM), the adenine nucleotide translocase (ANT; involved in the exchange of ATP from matrix and ADP from cytosol) in the inner mitochondrial membrane (IMM), and the matrix isomerase cyclophilin-D (CyP-D) (Crompton, 1999). Under conditions such as oxidative stress and excessive calcium ion (Ca^{2+}) uptake by mitochondria, the MPT pores may form, allowing free passage of molecules (< 1500 Da) between the mitochondrial matrix and the cytosol (Chernyak *et al*., 1995; Kowaltowski *et al.*, 2001; see also **Chapter 5**). Consequently, depolarization and uncoupling of oxidative phosphorylation occur. Moreover, the entry of molecules into the mitochondrial matrix from the cytosol is accompanied by the entry of water, which results in mitochondrial matrix swelling. Eventually, the mitochondrial matrix will swell to an extent that the OMM ruptures (because the IMM contains cristae, which have greater surface area than the OMM) (Kim *et al*., 2003a; Kim *et al*., 2003b). The consequences of OMM rupture are the release of molecules such as cytochrome c from the mitochondrial intermembrane space (IMS) with the activation of caspases triggering apoptosis, or a drastic loss of ATP production followed by necrosis (Kim *et al*., 2003a; Kim *et al*., 2003b; Green and Kroemer, 2004; Crompton, 1999). Intracellular ATP level is suggested to determine whether cells undergo necrosis or apoptosis (Eguchi *et al.*, 1997).

The intracellular redox environment is critical in regulating MPT, as the oxidation of the ANT thiol groups results in conformational changes that appear to lead to MPT pore opening (Kowaltowski *et al*., 2001; Armstrong and Jones, 2002; see also **Chapter 5**). The intracellular redox environment is partly controlled by glutathione (GSH). The intracellular depletion of GSH creates an increasingly oxidized environment in the cytosol and mitochondria due to increased production of mitochondrial ROS by respiratory complex III (Armstrong and Jones, 2002). Since HOCl is known to deplete intracellular GSH (Pullar *et al*., 2000), and it was demonstrated in **Chapter 3** that significant intracellular GSH loss preceded HOCl-mediated HMDM cell death, HOCl may potentially create favourable oxidizing conditions for the activation of the MPT during HOCl-induced cytotoxicity to HMDM cells.

In this chapter, the mode of HMDM cell death (apoptosis or necrosis) mediated by HOCl was further investigated to confirm the observation from the previous chapter that HOCl-

treated HMDM cells underwent necrotic cell death. Caspase-3 activation (a hallmark of apoptosis) and the influx of propidium iodide (PI) were examined after HOCl treatment. Tyrosine loss was measured as an indication of HOCl damaged proteins. Since intracellular ATP levels appear to determine the cell death pathways, ATP level, mitochondrial membrane potential and GAPDH activity (an indicator of glycolysis efficiency) were examined. The occurrence of HOCl-mediated MPT activation and its role in mitochondrial membrane potential loss and HMDM cell death were also examined.

4.2 Results

4.2.1 Effect of HOCl on caspase-3 activation in HMDM cells

Caspase-3 activation is a hallmark of apoptosis (Reed, 2000). Caspase-3 activation in HMDM cells upon HOCl treatment was examined as an indicator of apoptosis. HMDM cells were treated with HOCl and examined for caspase-3 activation after 20 hours by measuring caspase-3 enzyme activity and Western blotting analysis. Upon activation, the inactive 32 kDa procaspase-3 (p32) is proteolyticly cleaved to release the active 17 and 20 kDa subunits (p17 and p20). The active caspase-3 subunits cleave the synthetic substrate Ac-DEVD-AMC to release the fluorescent AMC, which can be detected by the fluorometry and acts as an indicator of caspase-3 activation.

HMDM cells treated with increasing HOCl concentrations showed no statistically significant increases in free AMC levels compared to that of the HOCl-free control cells (**Figure 4.1a**), indicating that caspase-3 was not activated. The western blotting analysis showed no decreased intensity of pro-caspase-3 band with increasing HOCl concentration (**Figure 4.1b**). Faint 17 kDa bands appeared in the lanes representing 0, 50 and 100 μM HOCl samples. This suggests that the 17 kDa bands that appeared in the 50 and 100 μM HOCl lanes did not result from HOCl-induced pro-caspase-3 cleavage (**Figure 4.1b**). Actin staining confirmed that there was similar loading of protein samples in each well of the SDS-PAGE gel. Taken together, HOCl did not induce caspase-3 activation in HMDM cells at concentrations up to 300 μM.

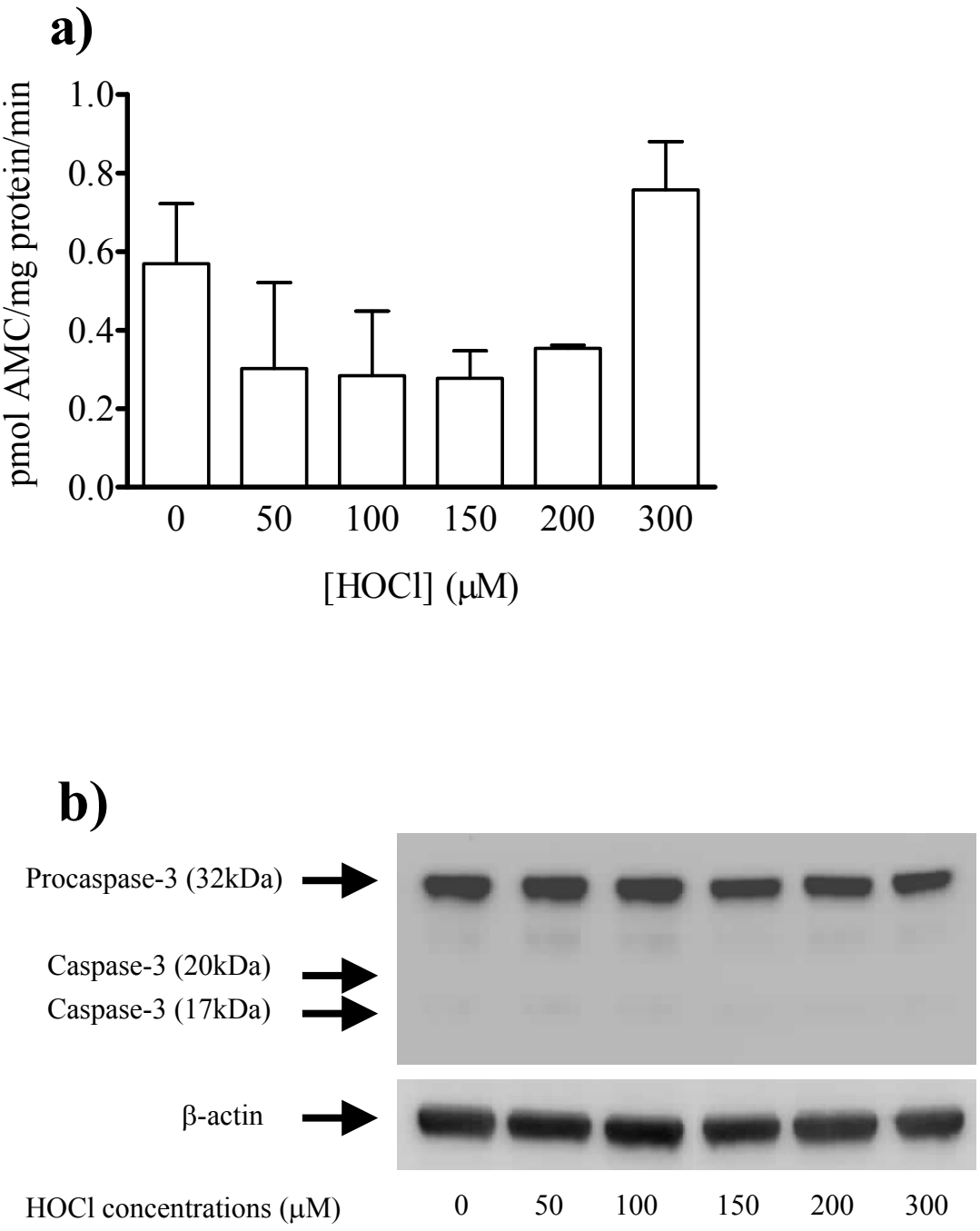

Figure 4.1 Caspase-3 enzyme is not activated in HMDMS after HOCl treatment.
HMDM cells (5×10^6 cells/ml) were treated with increasing HOCl concentrations for 10 minutes, followed by incubation in HMDM culture medium for 20 hours. Subsequently, **a)** caspase-3 enzyme activity and **b)** the presence of activated caspase-3 enzymes in HMDM cells were examined by fluorescence spectrophotometry and Western blotting, respectively. The Western blot photo was modified using Photoshop.

H_2O_2-treated T lymphocytes (Hampton and Orrenius, 1997), HOCl-treated human endothelial cells (Vissers *et al*., 1999), and HOCl-treated human fetal liver cells (Whiteman *et al*., 2005b) have shown caspase-3 activation 1-3 hours after treatment. To determine whether caspase-3 activation occurred at much earlier times, HMDM cells treated with HOCl were measured for caspase-3 activation at time intervals. An HOCl concentration of 150 μM was used, because it caused approximately 50% cell viability loss in this particular cell preparation 20 hours after HOCl treatment. The free AMC levels measured over time in HOCl-treated HMDM cells were statistically comparable to the control cells (**Figure 4.2a**). The variability in free AMC levels over time was possibly due to the low levels of AMC fluorescence, which were below the accurate detection limit of the fluorometer. Western blotting analysis showed decreased intensities of procaspase-3 band, but no active p17 and p20 caspase-3 subunits in HOCl-treated HMDM cells over time (**Figure 4.2b**). This will be further discussed in **section 4.3**. Overall, HOCl did not induce caspase-3 activation in HMDM cells at any time point.

Monocytic THP-1 cells treated with 6% ethanol showed a significant increase in free AMC after 5 hours, compared to the 0 hr and 5 hr non-treated controls (**Figure 4.3a**), implying the presence of active caspase-3 enzyme. Western blotting analysis also showed the active p17 subunits in 6% ethanol-treated THP-1 cells after 5 hours (**Figure 4.3b**), and the p17 band of the ethanol-treated sample was 1.5 times higher in intensity than that of the control (**Figure 4.3c**). These results suggest that 6% ethanol induced caspase-3 activation in monocytic THP-1 cells, and that no caspase-3 activation being detected in HOCl-treated HMDM cells was not due to the failure of the experimental systems for detecting caspase-3 activation.

4.2.2 HOCl induced rapid necrotic cell death in HMDM cells

HOCl induced rapid HMDM cell death, possibly via necrosis (**Chapter 3**). Whether HMDM cells undergo necrosis after HOCl treatment was further examined by incubating HOCl-treated HMDM cells with the fluorescent propidium iodide (PI) dye, which is used for detecting necrotic cells. The intact cell membranes of viable and apoptotic cells exclude PI, whereas disrupted membranes of necrotic cells are permeable to PI.

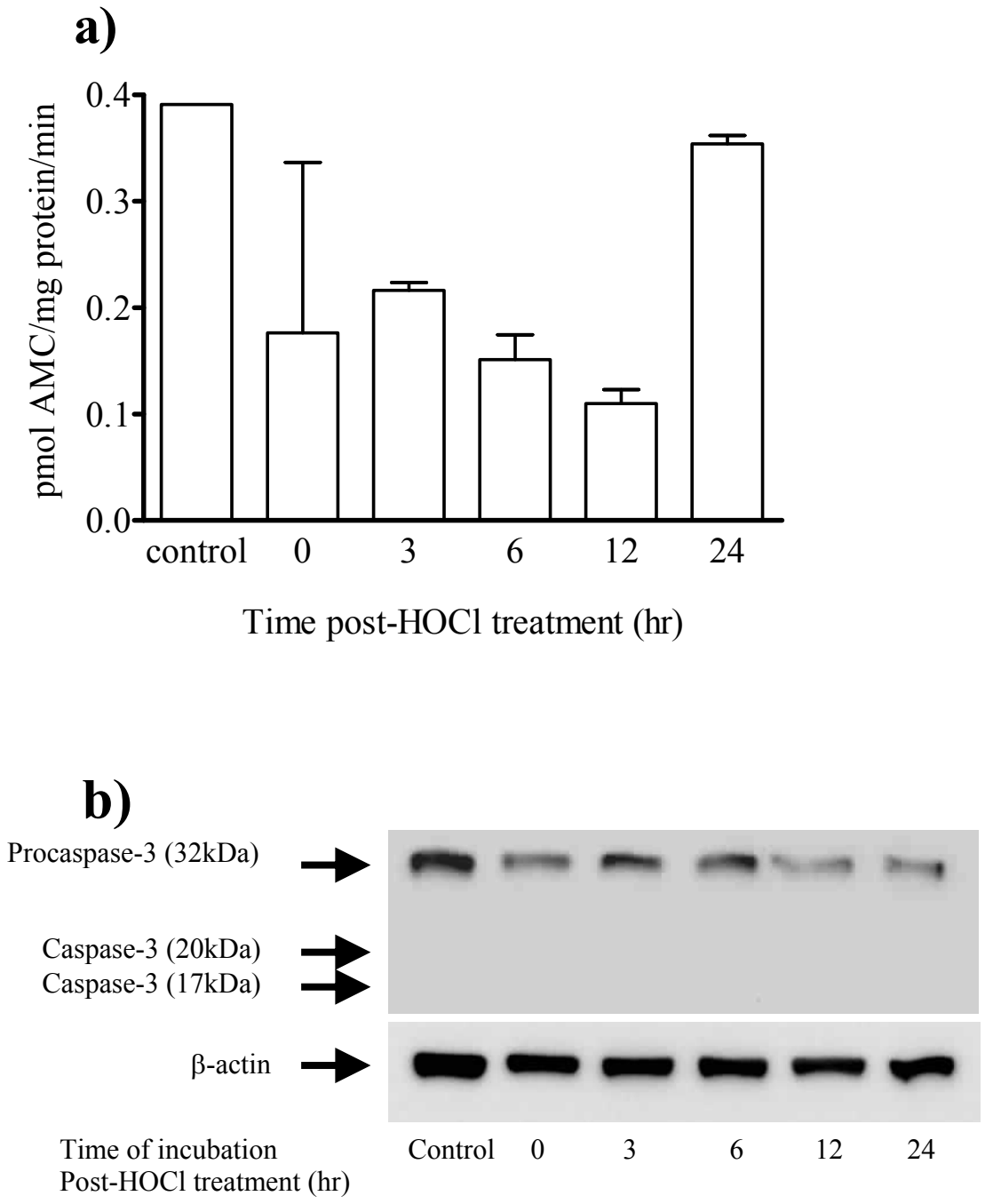

Figure 4.2 Time course of caspase-3 enzyme activation in HMDMs treated with HOCl. HMDMs (5×10^6 cells/ml) were treated with 150 μM HOCl for 10 minutes, followed by incubation in HMDM culture media. The cells were then collected at time intervals for determining **a)** caspase-3 enzyme activity and **b)** the presence of activated caspase-3 enzymes by fluorescence spectrophotometry and Western blotting, respectively. The Western blot photo was modified using Photoshop.

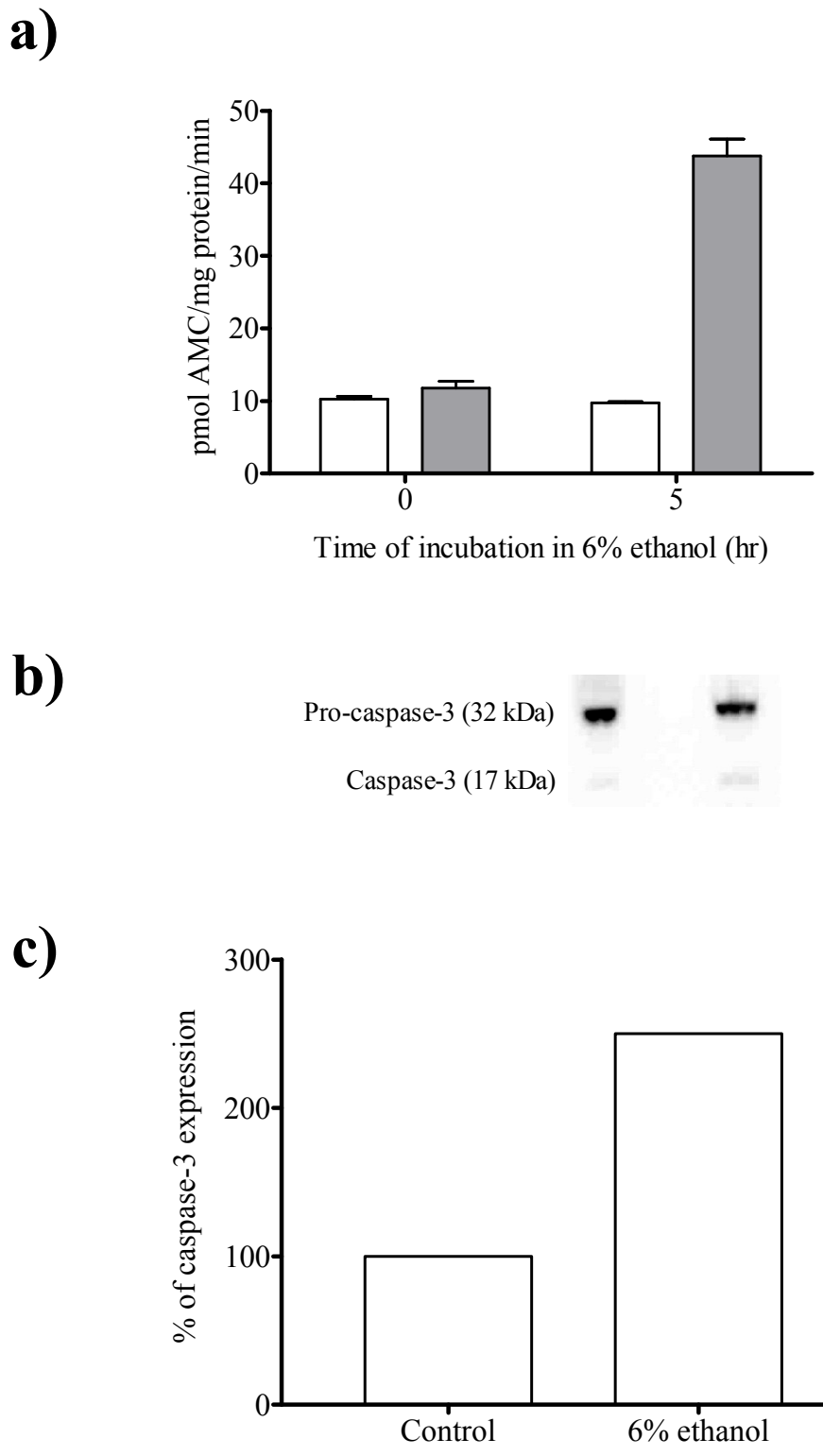

Figure 4.3 Caspase-3 enzyme is activated in THP-1 cells treated with 6% ethanol.
a) THP-1 cells (1×10^6 cells/ml) were treated in the absence (white bars) or presence (gray bars) of 6% ethanol in HMDM culture media at 37°C for 5 hours. The cells were subsequently analysed for caspase-3 enzyme activity at 0 hour and 5 hour post-treatment. **b)** THP-1 cells (1×10^6 cells/ml) were treated in the absence or presence of 6% ethanol in HMDM culture media at 37°C for 5 hours, followed by Western blotting analysis for the presence of activated caspase-3 enzymes. **c)** The intensity of the 17 kDa caspase-3 band in **b)** was quantified by the Image J software. The Western blot photo was modified using Photoshop.

HMDM cells were pre-incubated with PI and examined for fluorescence intensity straight after the 10-minute HOCl exposure (**Figure 4.4**). HOCl at 50 μM did not cause an increase in PI fluorescence intensity in HMDM cells compared to the control, and the differential interference contrast (DIC) image was comparable to that of the control. The fluorescence intensity in HMDM cells treated with HOCl concentrations above 50 μM increased with increasing HOCl concentrations, indicating that HOCl caused a concentration-dependent cell membrane disruption in HMDM cells above a particular HOCl concentration threshold. Apoptotic cells in the late stages can also undergo necrosis (termed secondary necrosis) and stain positive for PI. However, the rapid PI uptake in combination with the lack of caspase-3 activity in HOCl-treated HMDM cells (**figures 4.1 and 4.2**) provided enough evidence that HMDM cells underwent necrosis upon HOCl treatment. PI fluorescent staining was found to spread across the entire cytosol. Yet, it also appeared to accumulate at one spot inside the HOCl-treated HMDM cells. This will be discussed in **section 4.3**.

4.2.3 Effect of HOCl on cellular tyrosine residues

The damaging effect of HOCl on HMDM cell proteins was studied by examining HOCl-induced tyrosine loss in HMDM cells. Tyrosine residues were measured by their native fluorescence (λex/λem = 280 nm/320 nm) via reverse phase gradient HPLC following the acid hydrolysis of the protein into free amino acids (Gieseg *et al*., 1993) (**Figure 4.5**).

Control HMDM cells had a tyrosine concentration of 139.7 ± 3.2 nmol/mg protein. A HOCl concentration of 50 μM did not induce statistically significant loss of cell viability and cellular tyrosine residues. In contrast, HOCl concentrations above 50 μM caused concentration-dependent decrease in both cellular tyrosine residues and cell viability of HMDM cells, with 100 μM HOCl causing approximately 50% loss in both parameters (**Figure 4.6a**). The tyrosine residue loss correlated very strongly with cell viability loss (r^2 = 0.9925) (**Figure 4.6b**). This suggests that HOCl caused concentration-dependent protein damage once an HOCl concentration threshold was reached, and the tyrosine residue loss might be related to the cell viability loss.

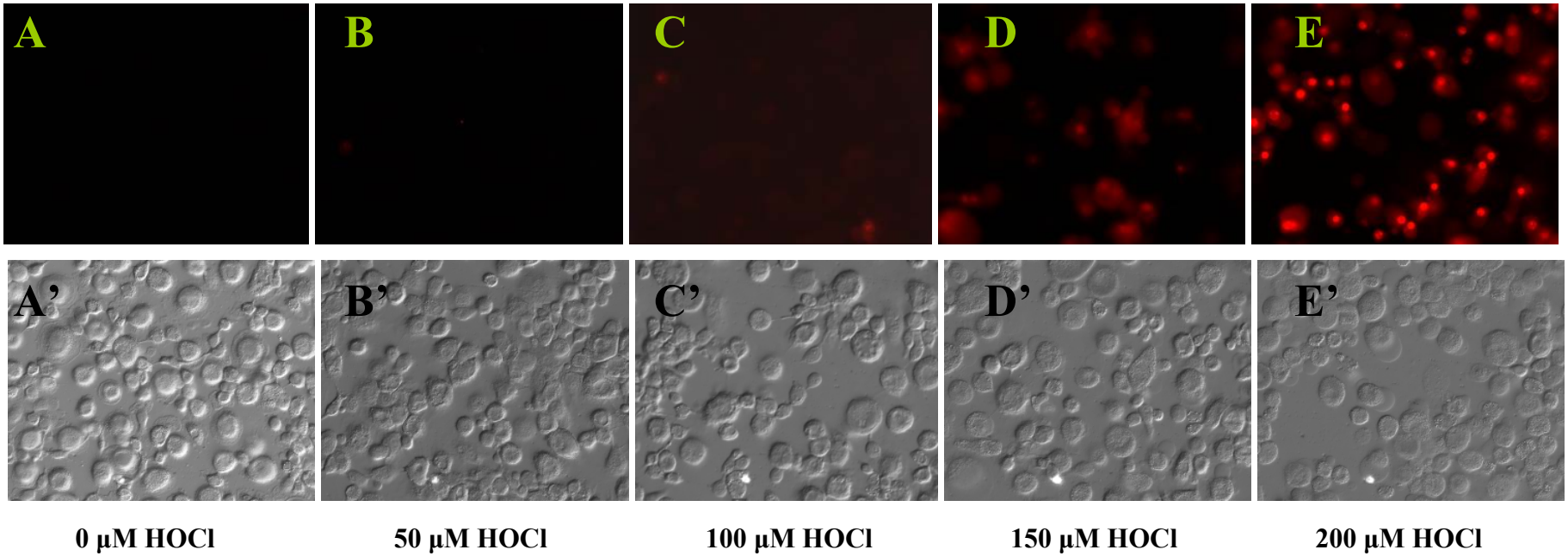

Figure 4.4 HMDM cells showed necrotic cell death with increasing HOCl concentrations.
HMDM cells were treated with 0, 50, 100, 150, and 200 µM HOCl for 10 minutes. Necrotic cells were identified by uptake of propidium iodide (PI) fluorescent dye by HMDMs and viewed under a fluorescence microscope with 40× magnification **(A to E)**. **A'**, **B'**, **C'**, **D'** and **E'** represent differential interference contrast (DIC) photos of **A**, **B**, **C**, **D** and **E**, respectively.

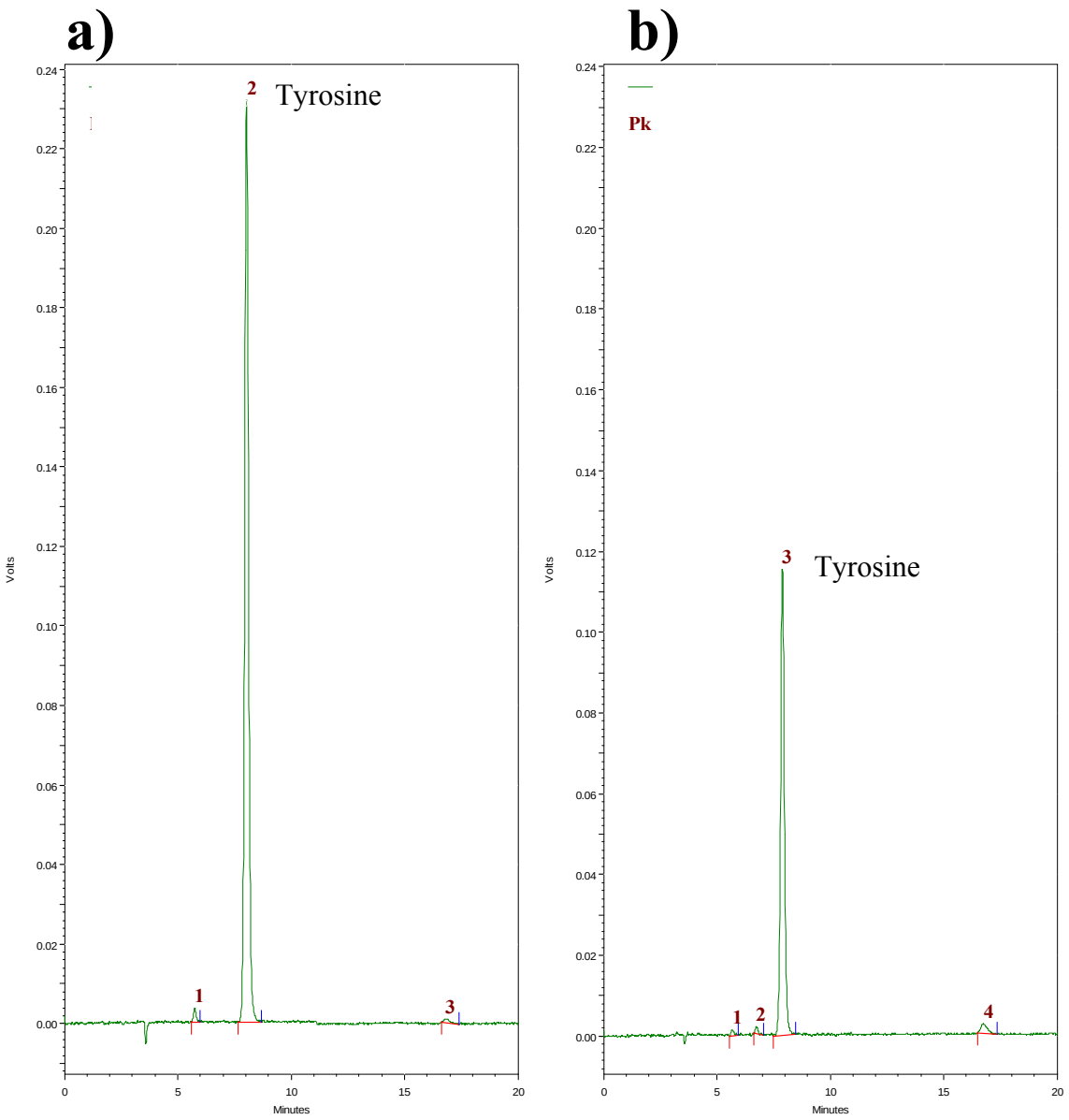

Peak #	Retention time	Area
1	5.747	30193
2	**8.033**	**2738315**
3	16.813	18056

Peak #	Retention time	Area
1	5.673	17278
2	6.727	16695
3	**7.893**	**1352118**
4	16.767	50775

Figure 4.5 HPLC tyrosine analysis of cellular protein hydrolysates from HMDM cells treated with or without HOCl.

HMDM cells were treated **a)** without or **b)** with 100 µM HOCl for 10 minutes, followed by incubation in HMDM culture media for 1 hour. The cells were subsequently processed for tyrosine measurement using the HPLC analysis (see **section 2.2.7.3**). Peak 2 of chromatogram **a)** and peak 3 of chromatogram **b)** represent the tyrosine traces in control HMDM cells and HOCl-treated HDMM cells, respectively.

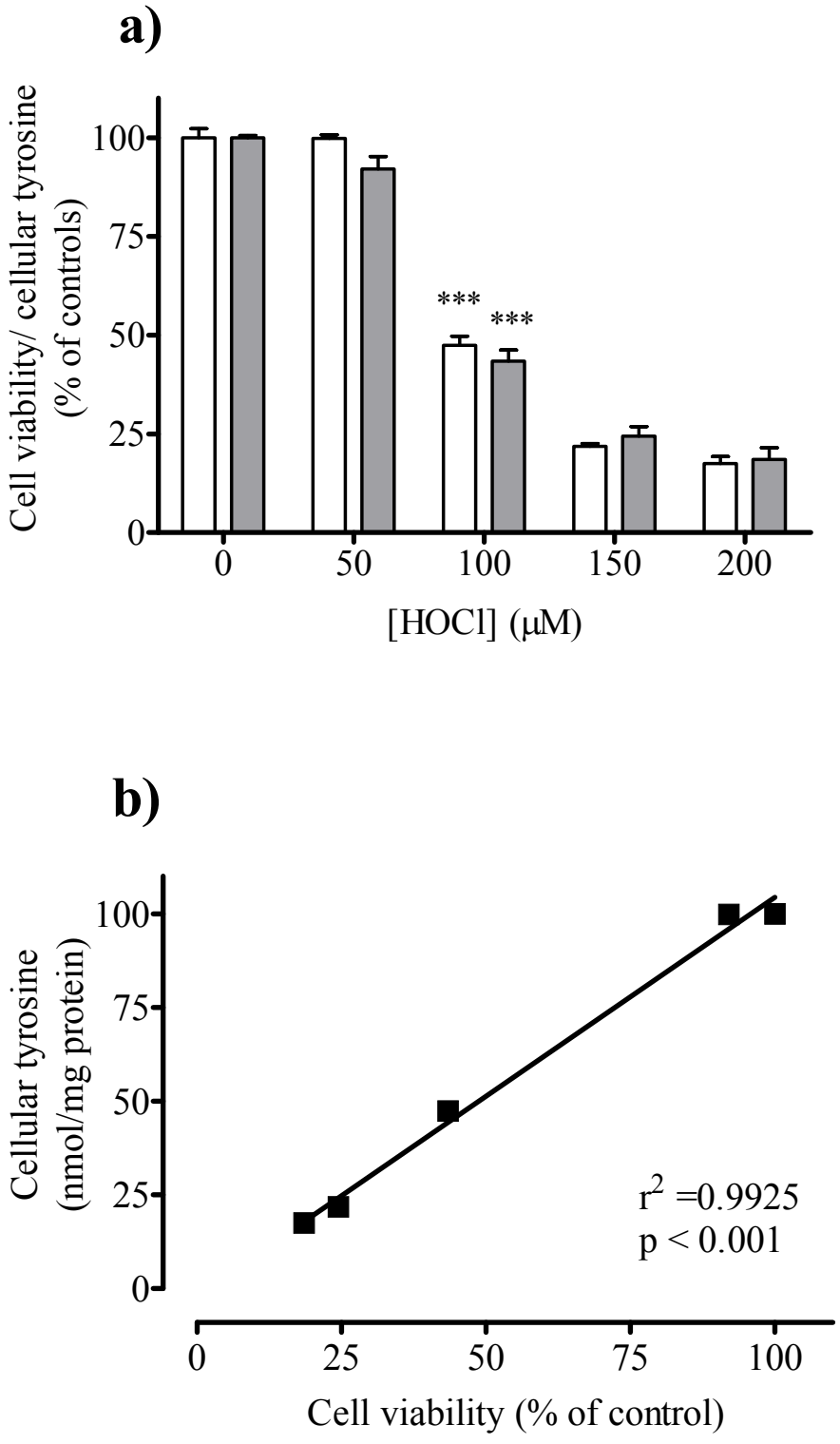

Figure 4.6 HOCl induced concurrent loss of tyrosine residues and HMDM cell viability.

HMDM cells (5×10^6 cells/ml) were treated with increasing HOCl concentrations for 10 minutes, followed by incubation in HMDM culture medium for 1 hour. **a)** The cells were then analysed for cell viability (white bars) and cellular tyrosine level (gray bars) using the MTT reduction assay and HPLC analysis, respectively. The data was expressed as a percentage of the respective 0 μM HOCl controls and significance is indicated from the respective 0 μM HOCl. **b)** A correlation analysis is included to illustrate the correlation between the tyrosine residue loss and cell viability loss.

4.2.4 Effect of HOCl on metabolic energies in HMDM cells

4.2.4.1 Effect of HOCl on GAPDH enzyme activity

Glyceraldehyde-3-phosphate dehydrogenase (GAPDH) is an essential enzyme in glycolysis, the pathway converting glucose to pyruvate and 2 ATP molecules. The effect of HOCl on HMDM metabolic energy was hence studied by examining the loss of GAPDH enzymatic activity in HMDM cells. HOCl at 50 μM reduced the GAPDH activity in HMDM cells from a control value of 23.6 ± 0.8 to 20.6 ± 2.5 μM/min/mg protein (13% decrease), though it was statistically insignificant. HOCl at 100, 150, 200, and 500 μM reduced the GAPDH activity in HMDM cells to 11.9 ± 1.9 (50% decrease), 3.7 ± 1.1 (84% decrease), 1.8 ± 0.8 (92% decrease), and 0.4 ± 0.1 (100% decrease) μM/min/mg protein, respectively (**Figure 4.7a**).

The GAPDH activity was measured concurrently with cell viability and intracellular GSH (see **Figure 3.6**). HOCl at 100 μM caused statistically insignificant cell viability loss, while 150 μM HOCl caused approximately 50% loss in cell viability. Moreover, GAPDH activity loss directly correlated with intracellular GSH loss (r^2 = 0.9298) (**Figure 4.7b**). Taken together, HOCl caused a concentration-dependent decrease in GAPDH activity at HOCl concentrations above 50 μM, which occurred concurrently with intracellular GSH loss but preceded the cell viability loss.

4.2.4.2 Effect of HOCl on intracellular ATP

The effect of HOCl on metabolic energy in HMDM cells was also studied by treating HMDM cells with HOCl and examining intracellular adenosine triphosphate (ATP) loss after 20 hours via HPLC analysis (see **section 2.2.7.4**). HOCl at 50 μM did not cause a statistically significant decrease in intracellular ATP concentration compared to the control (containing 31.2 ± 3.4 nmol/mg protein). In contrast, HOCl at 100, 150 and 200 μM reduced intracellular ATP concentrations by approximately 33, 52 and 82% of the control, respectively. Cell viability loss directly correlated with the ATP loss. HOCl at 50 μM did not cause statistically significant HMDM cell viability loss, while 100, 150 and 200 μM HOCl caused approximately 40, 75 and 86% cell viability loss, respectively (**Figure 4.8**). By using HMDM cells from the same cell preparation used in **Figure 4.8**, intracellular ATP depletion following the HOCl treatment was measured for the next 24 hours (**Figure 4.9**). This showed that the ATP loss only occurred during the HOCl treatment. There was no further loss, nor was there a significant recovery.

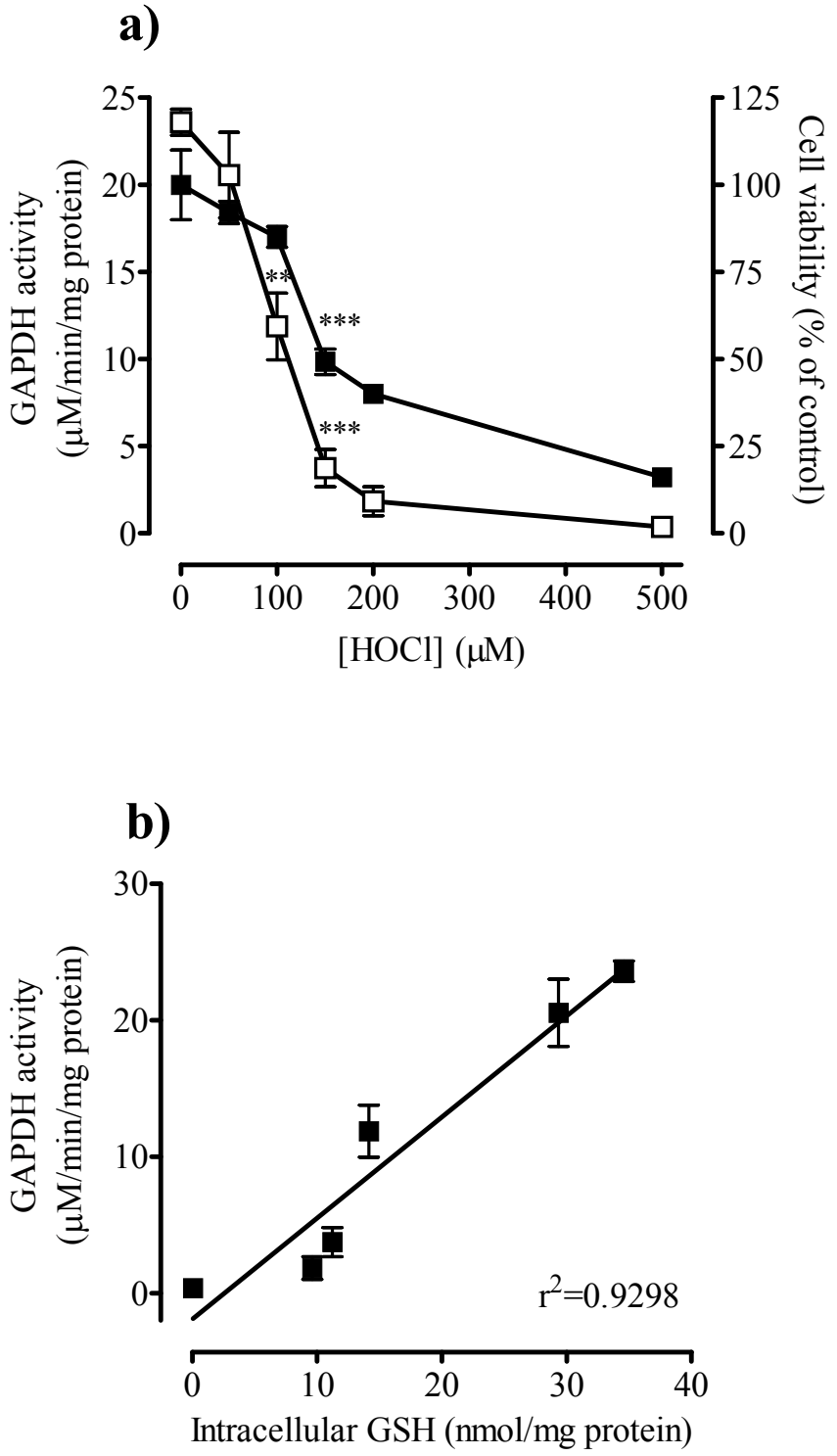

Figure 4.7 GAPDH activity loss in HOCl-treated HMDM cells occurred before cell viability loss and correlated directly with intracellular GSH loss.
HMDM cells (5×10^6 cells/ml) were treated with varying HOCl concentrations for 10 minutes, followed by incubation in HMDM culture medium for 1 hour. **a)** The cells were then analysed for cell viability (■) and GAPDH enzyme activity (□). Cell viability is presented as a percentage of the 0 μM HOCl control. Significance is indicated from the respective 0 μM HOCl controls. **b)** The GAPDH enzyme activity was compared with intracellular GSH after HOCl treatment using a trend line to illustrate the correlation.

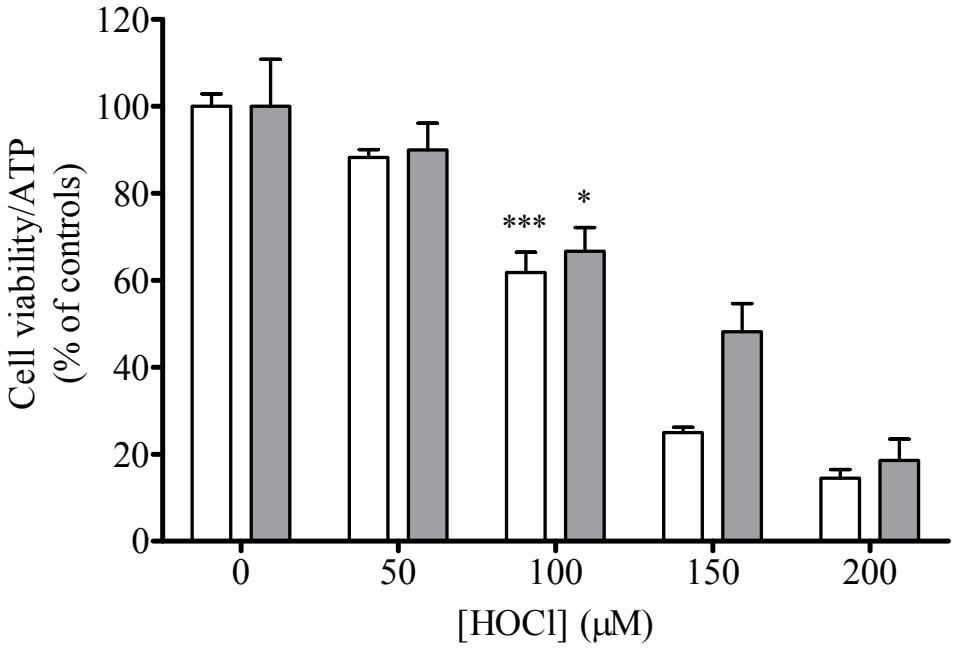

Figure 4.8 Effect of HOCl on intracellular ATP and cell viability.
HMDM cells (5×10^6 cells/ml) were treated with increasing HOCl concentrations for 10 minutes, followed by incubation in HMDM culture medium for 20 hours. The cells were subsequently analysed for cell viability (white bars) by the MTT assay, and intracellular ATP (grey bars) by the HPLC analysis. Each parameter is presented as a percentage of the respective 0 μM HOCl control. Significance is indicated from the respective 0 μM HOCl control.

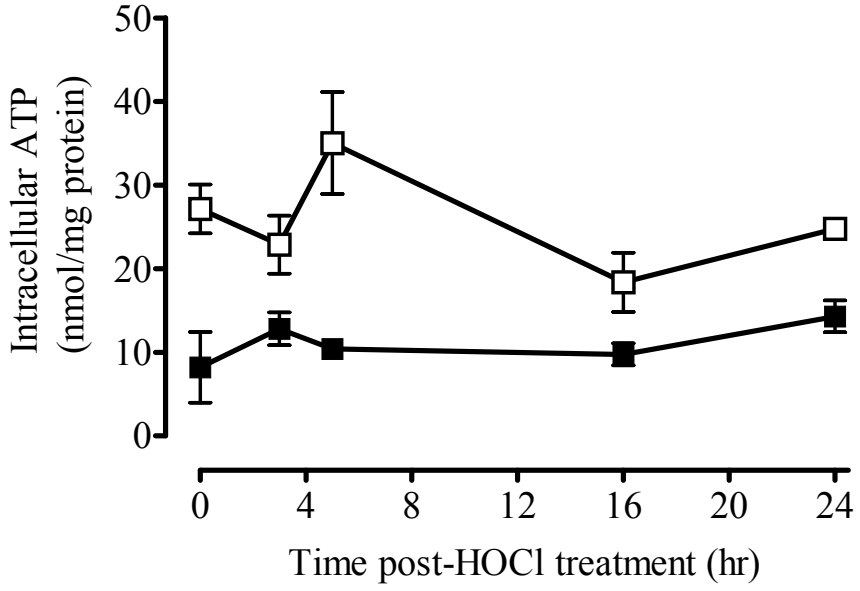

Figure 4.9 Time course of ATP loss in HMDM cells after HOCl treatment.
HMDM cells (5×10^6 cells/ml) were treated with (■) or without (□) 100 μM HOCl for 10 minutes, followed by incubation in HMDM culture medium. The cells were then removed at time intervals for the analyses of intracellular ATP by HPLC analyses. Significance is indicated from the respective 0 hr data.

4.2.4.3 Effect of HOCl on mitochondrial membrane potential

The loss of cell viability as measured by the MTT assay and ATP depletion in HOCl-treated HMDM cells suggested that HOCl may also induce mitochondrial dysfunction. To study the effect of HOCl on mitochondria, HOCl-treated HMDM cells were examined for mitochondrial membrane potential loss using a mitochondria-specific potentiometric probe, tetramethylrhodamine methyl ester (TMRM), with assessment of fluorescence intensities.

With increasing HOCl concentrations, there was a rapid decrease in mitochondrial membrane potential within 10 minutes, indicated by the fluorescence intensity decrease of the TMRM (**Figure 4.10a**). The concurrent analysis of HMDM cell viability loss showed that the fluorescence intensity decrease occurred before significant cell viability loss was observed (**Figure 4.10b**). This indicates that mitochondrial membrane potential loss may precede and contribute to HMDM necrotic cell death.

To investigate whether HOCl-induced loss of mitochondrial membrane potential was due to the opening of high-conductance membrane permeability transition pores (MPT), HMDM cells were incubated with cyclosporin A (CSA) together with TMRM before HOCl treatment. CSA is an inhibitor of the cyclophilin D protein of the MPT complex. This inhibitor improves loading of TMRM due to inhibition of the multi-drug resistance (MDR) pump (Bernardi *et al*., 1990). Therefore, all the samples (both controls and HOCl-treated) were treated identically with CSA to increase the fluorescence intensities. HOCl at 150 μM induced significant and rapid mitochondrial membrane potential loss by approximately 80%, while 5 and 10 μM CSA inhibited the mitochondrial membrane potential loss completely (not different from the control ($p > 0.05$)) (**Figure 4.11a** and **b**). This suggested that HOCl induced MPT pore opening in HMDM cells via CSA-sensitive site such as cyclophilin D, which then led to mitochondrial membrane potential loss.

Cell viability in HOCl-treated HMDM cells was also analysed in the presence or absence of CSA. HMDM cells exposed to 150 μM HOCl showed approximately 50% cell viability loss, whereas HMDM cells pre-incubated with 5 and 10 μM CSA before HOCl treatment completely prevented the cell viability loss (**Figure 4.12**). This suggests that HOCl-induced cell viability loss can be prevented by inhibiting opening of the MPT.

4.10a)

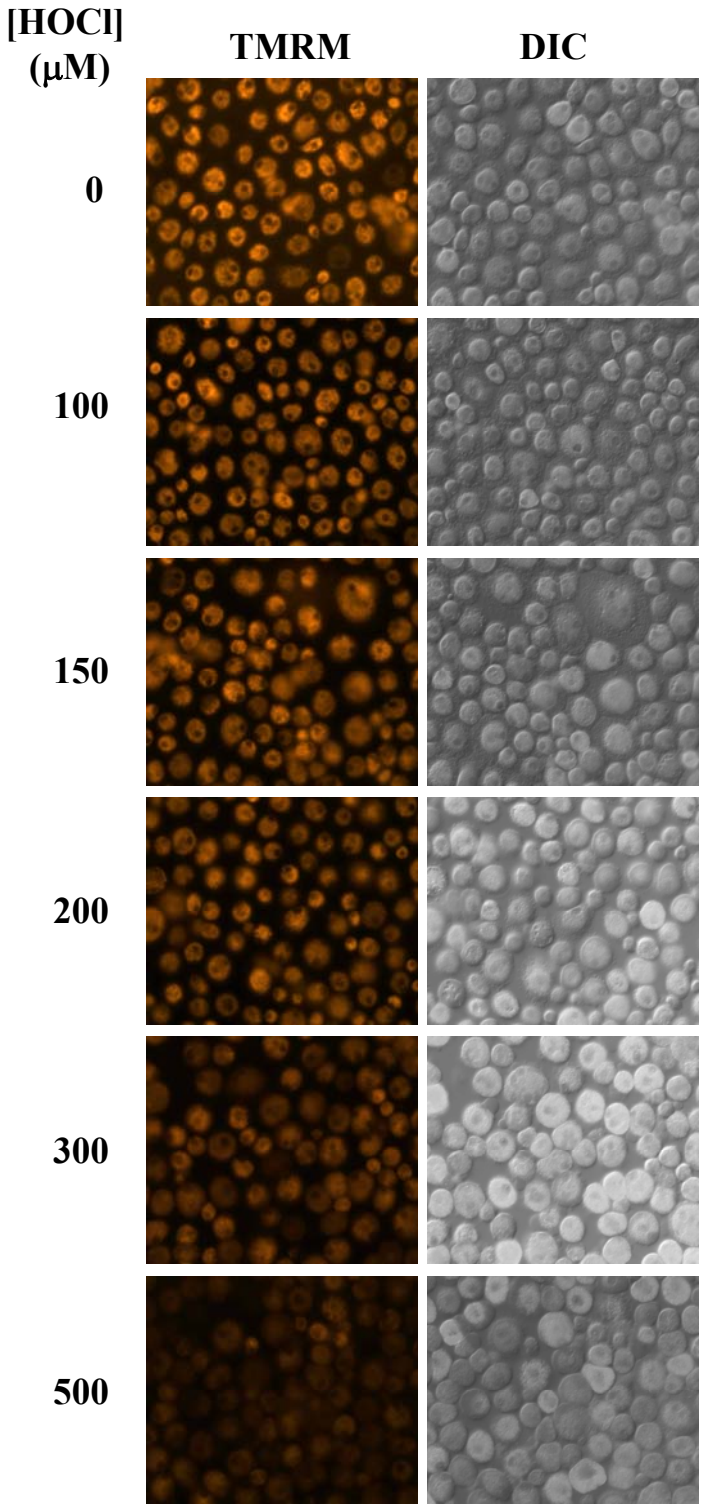

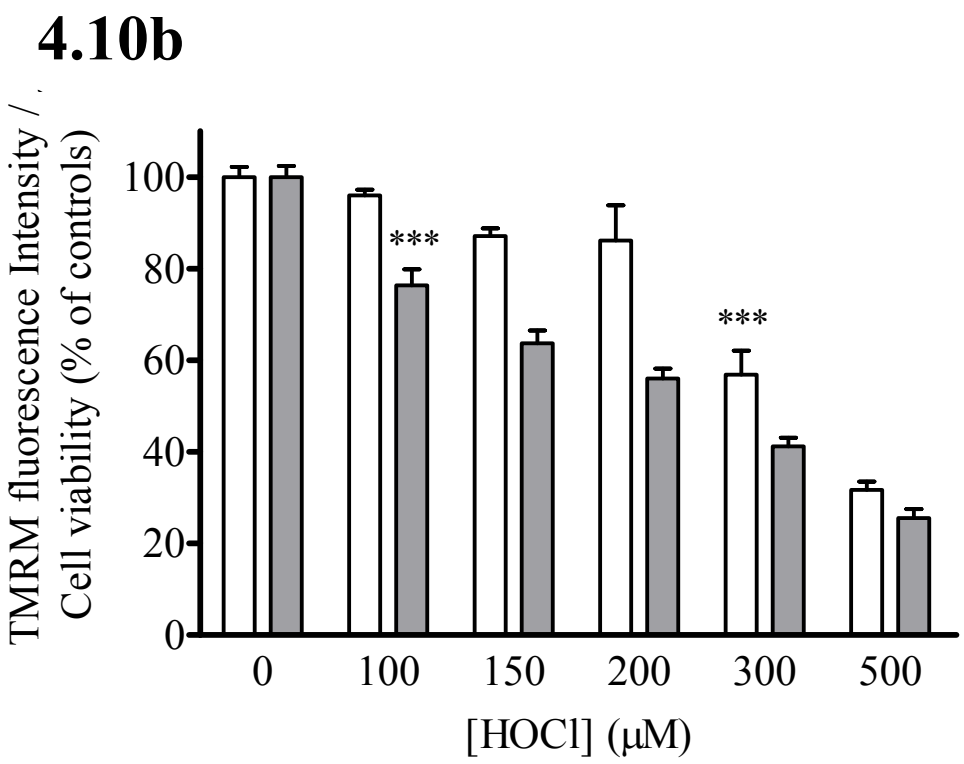

Figure 4.10 Effect of HOCl on HMDM mitochondrial membrane potential.
HMDM cells (5×10^6 cells/ml) on coverslips were pre-incubated with 100 nM of tetramethylrhodamine methyl ester (TMRM) for 30 minutes (see **section 2.2.12.4**). **a)** The cells were then treated with increasing HOCl concentrations for 10 minutes, followed by immediate examination under a fluorescence microscope (λex/λem = 548/574nm). DIC photos for each of the respective fluorescence photos are shown. **b)** Fluorescence intensities of the cells are converted to numerical values using Image J software. HMDM cells of the same cell preparation were also examined for cell viability by the MTT assay after the 10-minute HOCl treatment. Both data were presented as percentages of the respective 0 μM HOCl controls. Significance is indicated from the respective 0 μM HOCl control.

4.11a)

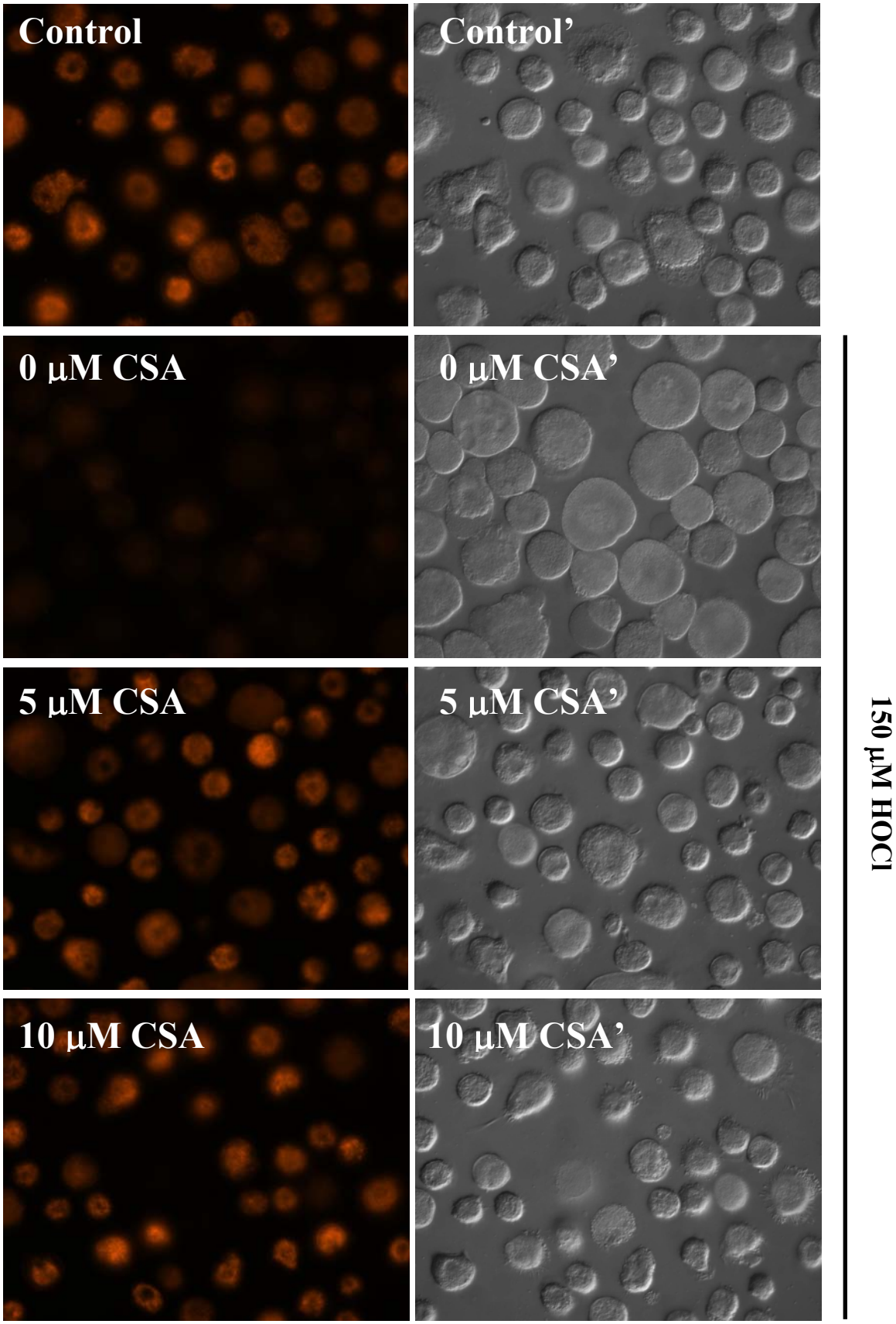
Control
Control'
0 µM CSA
0 µM CSA'
5 µM CSA
5 µM CSA'
10 µM CSA
10 µM CSA'
150 µM HOCl

4.11b)

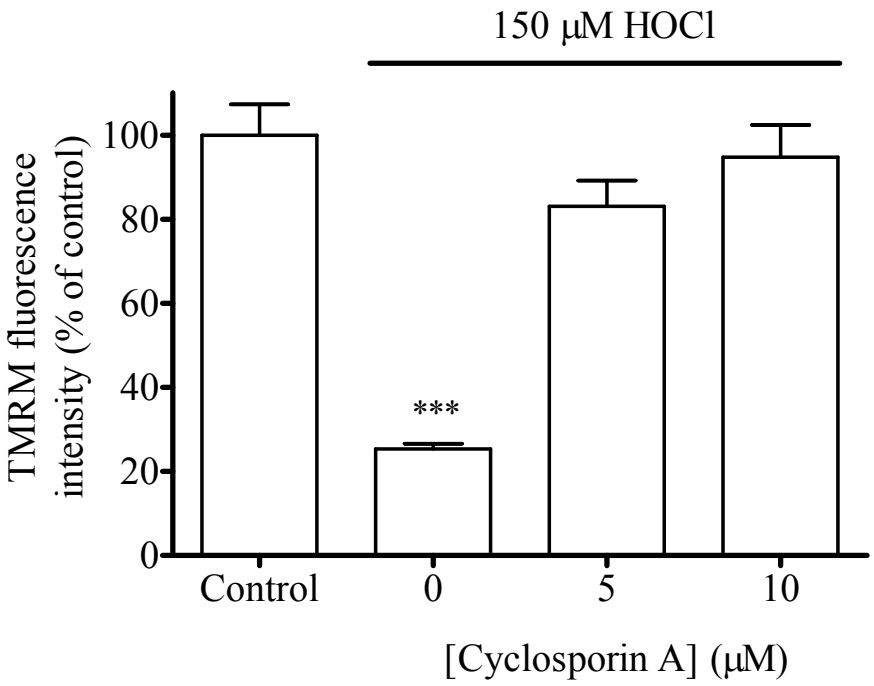

Figure 4.11 Mitochondrial membrane potential loss was inhibited in HMDM cells treated with 150 μM HOCl by cyclosporin A (CSA).
a) HMDM cells (5×10^6 cells/ml) on coverslips were pre-incubated with 100 nM TMRM in the presence of 0, 5 or 10 μM CSA for 30 minutes. The cells were then treated with 150 μM HOCl for 10 minutes. A control without CSA and HOCl treatments was also prepared. The cells were then examined under a fluorescence microscope (λex/λem = 548/574nm). The photos on the right hand side (labelled with ') represent the DIC photos of the respective fluorescence photos on the left hand side. **b)** Fluorescence intensities are converted to numerical values, which are presented as percentages of the control. Significance is indicated from the same control.

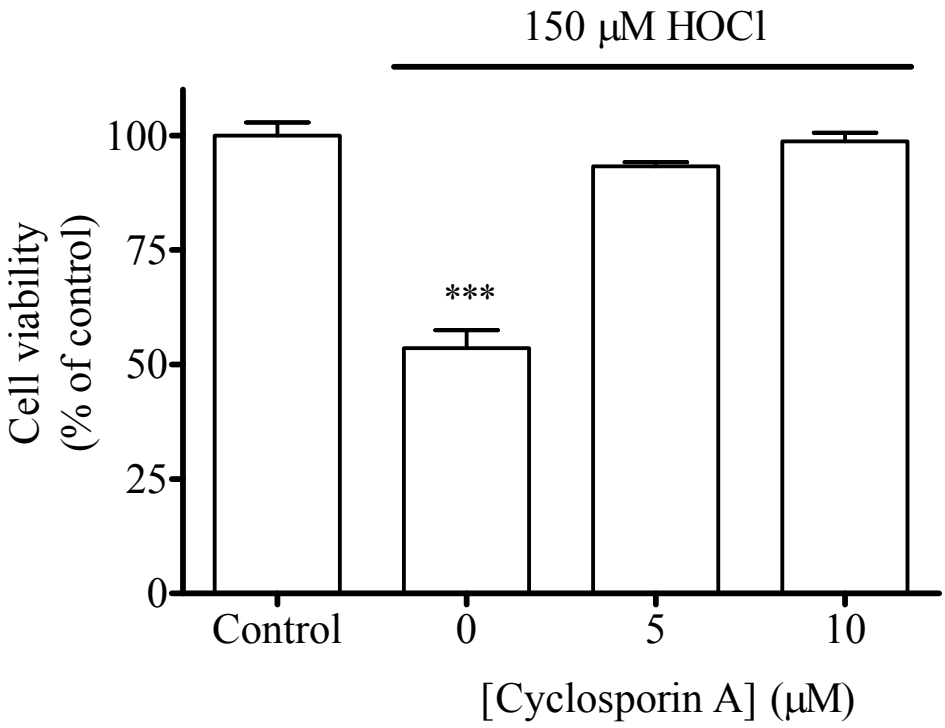

Figure 4.12 Cell viability loss was inhibited in HMDM cells treated with 150 μM HOCl by cyclosporin A (CSA).
HMDM cells (5×10^6 cells/ml) were pre-incubated with 0, 5 or 10 μM CSA for 30 minutes. The cells were then treated with 150 μM HOCl for 10 minutes. A control without CSA and HOCl treatments was also prepared. The cells were examined for cell viability after 6 hours using the MTT reduction assay. Cell viability is presented as a percentage of the control and significance is indicated from the same control.

4.2.5 Effect of HOCl on superoxide generation in HMDM cells

HOCl was shown to cause mitochondrial membrane potential loss in HMDM cells as mentioned before. Mitochondrial membrane potential loss may lead to ROS generation in cells, such as superoxide (Cai and Jones, 1998; Stridth *et al*., 1998; Gottlieb *et al.*, 2000). To study whether HOCl induces superoxide generation in HMDM cells, the cells were treated with 150 μM HOCl, followed by incubation with dihydroethidium (DHE) dye (see **section 2.2.14.1**) and examination of fluorescence intensities. The cells treated with HOCl showed increased fluorescence intensities compared to the control cells (**Figure 4.13**), indicating that HOCl induced superoxide generation.

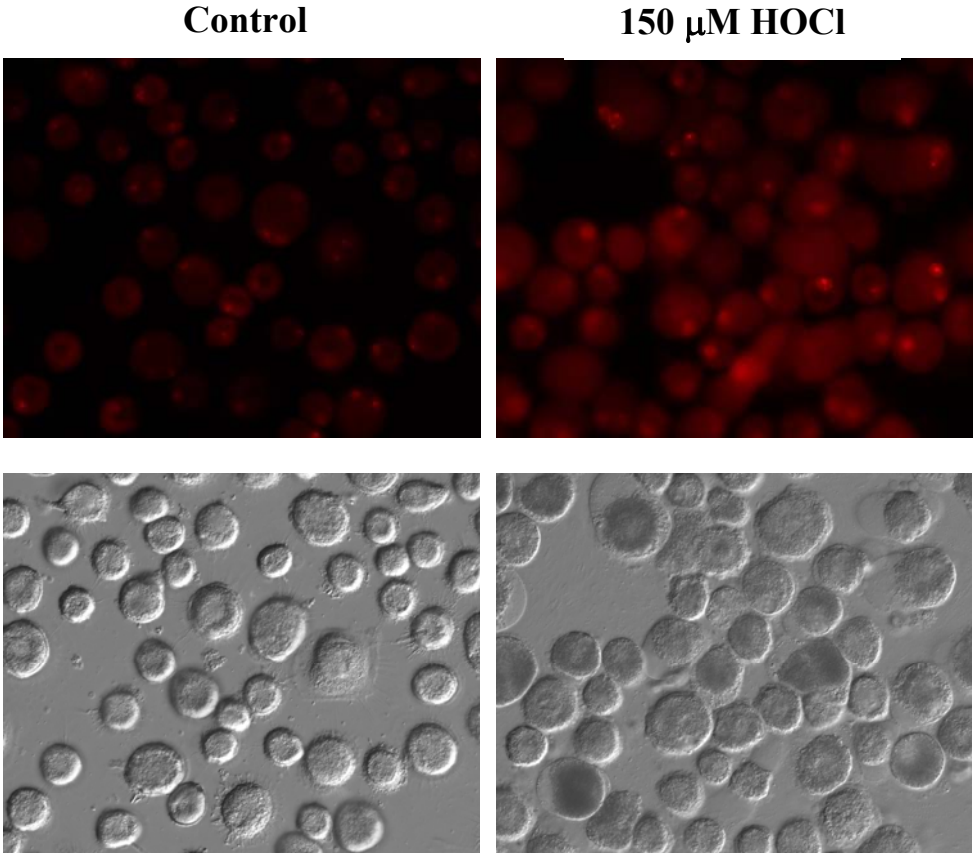

Figure 4.13 Effect of HOCl on superoxide production in HMDM cells.
HMDM cells (5×10^6 cells/ml) on coverslips were treated with (B) or without (A) 150 μM HOCl for 10 minutes, followed by incubation with 10 μM DHE for 20 minutes for the fluorescence probing of superoxide in HMDM cells. The cells were then viewed under a fluorescence microscope (λex/λem of 500-530nm/590-620nm). The photos at the bottom represent the DIC photos of the respective fluorescence photos at the top.

4.3 Discussion

4.3.1 Effect of HOCl on caspase-3 activation in HMDM cells

The results in **Chapter 3** showed that HOCl caused rapid necrotic cell death within 10 minutes of treatment, as determined by the loss of plasma membrane integrity (measured by trypan blue assay) and the rapid loss of metabolic energy (measured by MTT reduction assay). To further validate that HMDM cells underwent necrotic cell death upon HOCl treatment, caspase-3 activation in HOCl-induced HMDM cells was examined. Caspase-3 is an effector caspase involved in inducing a large number of apoptotic processes within the cells (Reed, 2000). Its activation would hence be a reliable indicator of caspase-mediated apoptosis in cells (see **section 1.7.1.2** for the mechanism of caspase-3 activation).

Enzyme activity and Western blotting analyses of caspase-3 showed that HOCl did not induce caspase-3 activation in HMDM cells at any of the concentrations tested and at any time post treatment (**Figures 4.1** and **4.2**). These results agree with some previous studies, which showed that oxLDL and HOCl did not activate caspase-3 in HMDM cells (Asmis and Begley, 2003) and neuronal cells (Yap *et al*., 2006), respectively. By using the same methodologies, caspase-3 activation was detected in monocytic THP-1 cells treated with 6% ethanol for 5 hours (**Figure 4.3**). This suggests that the lack of detection of caspase-3 activation in HOCl-treated HMDMs was not due to methodological errors.

HMDM cells treated with 150 μM HOCl showed decreases in procaspase-3 band intensities compared to the non-treated control (**Figure 4.2b**), although no caspase-3 activity was observed. This was possibly because HOCl caused procaspase-3 protein fragmentation. In **Chapter 5**, HOCl was shown to cause calpain activation and lysosomal destabilisation. Hence, it was possible that cathepsin proteases from ruptured lysosomes and calpains caused procaspase-3 cleavage and degradation. Indeed, calpains have been shown to cleave caspases and prevent them processing into active forms (Lankiewicz *et al.*, 2000; Bizat *et al*., 2003).

The lack of pro-caspase-3 activation or caspase-3 enzyme activity in HOCl-treated HMDM cells can be attributed to the possible inactivation of caspase-9. HMDM cell viability occurred only after intracellular GSH was significantly decreased (see **Figure 3.6**). It was highly likely that HOCl in the presence of insufficient amount of antioxidant GSH oxidised the critical cysteine thiol group at the active site of caspase-9, resulting in inactivation.

Loss of protein thiols was observed in endothelial cells exposed to HOCl (Pullar *et al*., 1999). Hampton and Orrenius (1997) have also suggested that H_2O_2 inhibited Fas-mediated caspase activity in Jurkat T lymphocytes, possibly via oxidative inactivation at the critical cysteine group. In addition, dithiocarbamate was shown to inactivate caspases at critical thiol-containing residues (Orrenius *et al.*, 1996).

HOCl can also indirectly inactivate caspase-9 by interacting with the components that form apoptosome and hence preventing its formation. Apoptosome (composed of Apaf-1, cytochrome c, and dATP or ATP) activates caspase-9, which in turn activates pro-caspase-3 (Kroemer and Martin, 2005). HOCl has been shown to oxidize cytochrome c at lysine residues (Chen *et al*., 2004). Post-translational modification of the lysine residue of yeast isocytochrome c results in a low affinity for Apaf-1 and consequently an inability to induce caspase activation (Kluck *et al.*, 2000). Hence oxidized cytochrome c possibly prevented the formation of apoptosome due to its lowered affinity for Apaf-1. Furthermore, ATP or dATP are required for caspase-3 activation (Liu *et al.*, 1996; Hampton *et al.*, 1998a). Since intracellular ATP concentration was rapidly decreased in HMDM cells within 10 minutes of HOCl treatment (**Figure 4.9**), there was possibly insufficient energy in HMDM cells to drive apoptosome formation and caspase-3 activation.

Finally, calpain enzymes can cleave several apoptosis regulatory proteins, including Apaf-1 (Reimertz *et al*., 2001). Furthermore, as mentioned above, calpain enzymes cleave caspases and therefore prevent them from being processed into the active forms. HOCl was shown to activate calpains in HMDM cells (see **Chapter 5**), indicating that calpains might have inhibited the activation of caspases.

Although the lack of caspase-3 activation in HOCl-treated HMDM cells suggests that HMDM cells undergo necrotic cell death upon HOCl treatment, apoptosis can still occur via a caspase-3-independent pathway (Kroemer and Martin, 2005). However, HOCl caused a rapid and concentration-dependent increase of propidium iodide (PI) in HMDM cells at concentrations above 50 μM (**Figure 4.4**). This was indicative of increased cell membrane disruption and hence necrosis above a particular HOCl concentration threshold. This result was in agreement with the results in **Chapter 3,** which demonstrated that HOCl caused HMDM cell swelling and cell membrane rupture (**Figure 3.5**).

Taken the above results together, HOCl caused HMDM cells to undergo rapid necrotic cell death once a concentration threshold was reached, below which no cell viability loss was observed. This agrees with Park *et al*. (2008), who demonstrated that HOCl caused HeLa cells to undergo necrosis at HOCl concentrations above 50 μM. In contrast to the current result, some studies have shown that a low dose of HOCl (less than 100 μM) triggered apoptosis in human endothelial cells and human fetal liver cells, while a higher dose induced necrosis (Vissers *et al*., 1999; Whiteman *et al*., 2005b; Sugiyama *et al.*, 2004). HMDM cells did not undergo apoptosis and lose cell viability at lower HOCl concentrations like the cell types mentioned above, possibly because of the difference in cell defense mechanisms and hence tolerance to HOCl. It is possible that at relatively low HOCl concentrations, the intracellular GSH level of HMDM cells was sufficient to scavenge all HOCl to prevent apoptosis and the reduced GSH was able to regenerate.

4.3.2 Effect of HOCl on general protein damage in HMDM cells

Tyrosine loss is an indicator of general protein damage. HOCl caused cellular tyrosine loss in a concentration-dependent manner once an HOCl concentration threshold was reached (**Figure 4.6a**), indicating that HOCl inflicted damage on the cellular proteins. The tyrosine loss strongly correlated with the cell viability loss in HMDM cells upon HOCl treatment (**Figure 4.6**). Cell viability in this research was measured by both MTT reduction assay (a measure of mitochondrial activity) and trypan blue assay (a measure of cell membrane integrity). Hence, it can be hypothesized that HOCl-mediated tyrosine residue loss and therefore general protein oxidation either led to or was caused by mitochondrial dysfunction and the loss of cell membrane integrity.

A tyrosine residue (called Y1176) was found to locate in the calpain cleavage site of spectrin, which is a component of the cell membrane skeleton (Nicolas *et al.*, 2002). Since HOCl has demonstrated to mediate calpain activation and calpains were previously demonstrated to cause cytoskeleton damage and hence plasma membrane deformation (see **Chapter 5**), one speculation was that calpains cleaved at site where tyrosine is located in spectrin and damaged it to a form that could not be identified by the HPLC analysis.

4.3.3 Effect of HOCl on metabolic energies in HMDM cells

HOCl caused a concentration-dependent decrease in glyceraldehyde 3-phosphate dehydrogenase (GAPDH) activity at HOCl concentrations above 50 μM, which occurred concurrently with intracellular GSH loss but preceded cell viability loss (**Figure 4.7**). GAPDH is an enzyme in glycolysis, which is responsible for converting glucose into pyruvate with a net production of 2 ATP and 2 NADH molecules. It catalyses the conversion of glyceraldehyde-3-phosphate to 1,3-bis-phosphoglycerate with the generation of 2 NADH (Mathews and van Holde, 1995). As a result of GAPDH activity loss in HMDM cells after HOCl treatment, the efficiency of the Krebs cycle and oxidative phosphorylation in mitochondria might reduce, resulting in decreased ATP production.

The loss of GAPDH activity could be partly attributed to the loss of NAD^+, a cofactor required for the activity of GAPDH, since Schraufstatter *et al.* (1990) showed that HOCl can react with NAD^+ within 10 minutes in murine macrophage-like cells. However, this was less likely the major cause of GAPDH inactivation in HOCl-treated HMDM cells, because GAPDH activity was measured in this research by supplementing the HOCl-treated cell samples with required substrates including NAD^+, after which GAPDH activity was still not recovered. A more likely explanation for GAPDH inactivation in HOCl-treated HMDM cells was that HOCl induced thiol oxidation at critical site. GAPDH contains an essential reduced cysteine (Cys149) at the active site (Pullar *et al*., 2000), and HOCl has been shown to oxidise GAPDH thiol groups with parallel loss of activity (Peskin and Winterbourn, 2006). The same study also showed that dithiothreitol (DTT) treatment reversed the HOCl-induced thiol oxidation and inactivation of GAPDH by at least 70%. This suggested that the most likely products of HOCl reacting with GAPDH thiol groups were disulfides and sulfenic acids. In addition, GAPDH in colon epithelial cells (Mckenzie *et al*., 1999), human endothelial cells (Pullar *et al*., 1999), and human mononuclear leukocyte (Smit and Anderson, 1992) were found susceptible to HOCl oxidation. GAPDH inactivation by thiol oxidation was also found in inflamed mucosa of patients with inflammatory bowel disease (Mckenzie *et al*., 1996).

The loss of GAPDH activity strongly correlated to the GSH loss in HMDM cells treated with increasing HOCl concentrations (**Figure 4.7b**). One possible speculation for this strong correlation was that GAPDH and GSH show similar abundance in HMDM cells and reactivity with HOCl. GAPDH thiol group is very susceptible to HOCl oxidation as mentioned above, implying that it is highly reactive with HOCl. Macrophages show a high

metabolic rate to provide fuels for their function regarding immune responses (Newsholme and Newsholme, 1989). Disruption of the respiratory chain induced by the uncoupler adriamycin and inhibition of ATP synthase by oligomycin promote macrophage lysis within 24 hours (Asmis and Begley, 2003). Based on these findings, GAPDH should be abundant in HMDM cells in order to maintain glycolysis and provide substrates for the Krebs cycle and electron transport chain at high rate. It has also been suggested that GAPDH and some other glycolytic enzymes are localized in erythrocyte membrane as an enzyme complex (Campanella *et al*., 2005). It is possible that as HOCl passed through membrane, it encountered GAPDH thiols first or at the same time as GSH, hence causing the same degree of loss as intracellukar GSH loss.

In this research, GAPDH activity loss in HMDM cells was measured only 1 hour after HOCl treatment, not at time intervals (**Figure 4.7**). Hence, it was unknown whether the GAPDH activity loss could be recovered over time. GAPDH recovery was unlikely to occur, as the ATP levels in HOCl-treated HMDM cells remained low over time (**Figure 4.9**). NO caused the thiols at the active site of GAPDH enzyme to form sulfenic acid, resulting in activity loss (Ishii *et al*., 1999). This suggests that the lack of GAPDH activity recovery could be due to HOCl oxidising the essential cysteine thiol group to a sulfenic acid or another high oxidation product(s) that could not be repaired (see also **section 3.3**).

Effect of HOCl on metabolic energies was further investigated by examining the ATP loss in HOCl-treated HMDM cells. HOCl caused a concentration-dependent decrease in ATP above 50 μM concentration, which was strongly correlated to the cell viability loss (**Figure 4.8**). The time course study showed that 100 μM HOCl-induced ATP depletion occurred within 10 minutes of the treatment and did not decrease further or recover over time (**Figure 4.9**). These results suggest that HOCl-mediated intracellular ATP loss in HMDM cells contributed to the resulting necrotic cell death, since rapid ATP loss is suggested to result in necrosis (Eguchi *et al.*, 1997).

The rapid decrease in intracellular ATP in HOCl-treated HMDM cells is in corroboration with Spragg *et al*. (1985), who showed 83% decrease in ATP level in murine macrophage like cells within the first few minutes of H_2O_2 treatment. In contrast to the current result, rat type II alveolar epithelial cells treated with HOCl showed an increase in ATP level in the first 30 minutes of treatment, followed by a decrease (Abernathy and Pacht, 1995). The same study also showed that HOCl only caused approximately 5% cell viability loss. The

differences between their result and the current result might be attributed to the different media used during HOCl treatment. Abernathy and Pacht (1995) used Dulbecco's modified eagle medium (DMEM) during HOCl treatment, whereas EBSS buffer was used in this research. DMEM contained amino acids and proteins, which could be oxidized by HOCl forming chloramines, which can also damage biomolecules (Pullar *et al*., 2000). For instance, taurine chloramines at 500 μM concentration caused approximately 15-20% ATP loss in erythrocytes within 1 hour (Thomas *et al*., 1985). This indicates that chloramines, not HOCl, might be the primary oxidant attacking ATP in rat type II alveolar epithelial cells in Abernathy and Pacht's experimental system.

The rapid ATP loss in HMDM cells upon HOCl treatment might be attributed to HOCl reacting directly with ATP (Prutz, 1996). In addition, the results in **Chapter 5** will show that HOCl-induced mitochondrial membrane potential loss was attributed to calcium ion (Ca^{2+}) accumulation in matrix, as a result of mitochondria taking up excess cytosolic Ca^{2+} via the Ca^{2+} uniporter in the inner mitochondrial membrane (IMM). This uniporter is gated/activated by ATP (Bianchi *et al.*, 2004). Therefore, the HOCl-induced Ca^{2+} uptake process might have consumed ATP, resulting in ATP loss. Intracellular ATP decrease could also be attributed to increased activity of the membrane associated cation ATPase pumps. Modest damage to lipid components of the cell membrane might allow augmented passive leak of Na^+, K^+, or Ca^{2+} across the membrane, stimulating ATPase activity, at the expense of ATP (Spragg *et al*., 1985). However, this was less likely to happen in HOCl-treated HMDM cells, because HOCl was shown to inactivate Na^+-K^+-ATPase (Kato *et al*., 1998) and Ca^{2+}-ATPase (Eley *et al*., 1991).

As mentioned above, intracellular ATP loss was not recovered in HMDM cells over time after the initial HOCl treatment. This could be due to HOCl causing mitochondrial membrane potential loss (**Figure 4.10**), suggesting dysfunction of electron transport chain (ETC) and therefore ATP synthesis. Succinate dehydrogenase enzymes in the Krebs cycle in mitochondria were also inactivated by HOCl. MTT reduction assay relies on the activity of cellular succinate dehydrogenase enzymes (see **section 2.2.5.1**). The cell viability loss (measured by MTT reduction assay) in HMDM cells upon HOCl treatment hence indicated that HOCl caused the activity loss of succinate dehydrogenase enzymes in HMDM cells. The consequent effect would be impairment of the Krebs cycle, dysfunction of the ETC, and hence decreased ATP generation. Furthermore, the generation of superoxide within 10 minutes of HOCl treatment (**Figure 4.13**) suggested dysfunction of complex III in the ETC.

HOCl was also found to inactivate GAPDH enzyme (**Figures 4.7**), which might have impaired glycolysis. ATPase-synthase enzyme complex catalyzing the phosphorylation of ADP in mitochondrial matrix could be inhibited in alveolar type II cells after H_2O_2 treatment, resulting in decreased ATP generation (LaCagnin *et al*., 1990). It was possible that HOCl could also inhibit this enzyme complex in HMDM cells. Glucose transport inhibition has been demonstrated in HOCl-treated murine macrophage-like tumor cells (Schraufstatter *et al*., 1990), which may also affect ATP generation. Accumulation of Ca^{2+} in mitochondrial matrix can induce cysteine protease calpain 10 that are present in the mitochondrial matrix, which can inhibit complex I of the ETC (Arrington *et al.*, 2006). It will be hypothesized in **Chapter 5** that mitochondrial calpains might be activated in HMDM cells upon HOCl treatment, indicating that they might have damaged complex I and prevent ATP generation.

4.3.4 Effect of HOCl on MPT activation and mitochondrial membrane potential in HMDM cells

ATP depletion in HOCl-treated HMDM cells suggests that HOCl might have caused damage to mitochondria, the major machinery for ATP generation in cells. In this research, HOCl was shown to cause mitochondrial membrane potential loss in HMDM cells in a concentration-dependent manner, and the loss occurred before significant cell viability was observed (**Figures 4.10**). This suggests that this mitochondrial membrane potential loss might contribute to the HMDM necrotic cell death.

The probe used in this thesis for detecting mitochondrial membrane potential was the methyl ester of tetramethylrhodamine (TMRM). A number of probes for mitochondrial membrane potential detection exist. Yet, none of them are perfect sensors as they all generate artifacts that can confound the interpretations of fluorescence emission in determining mitochondrial function. Such artifacts include toxicity, photobleaching, binding passively to mitochondria or other intracellular organelles, and activation of the MDR pump. Nonetheless, Bernardi *et al.* (1999) have suggested that the rhodamine group is the least problematic, in particular TMRM. Low nanomolar range of TMRM exclusively stains the mitochondria and it does not accumulate in cell membranes or interact with membrane proteins. Therefore, it is not retained by the mitochondria upon mitochondrial membrane potential loss.

It was unlikely that the detected mitochondrial membrane potential loss in HOCl-treated HMDM cells was an artifect, caused by HOCl directly reacting with TMRM. HMDM cells treated with HOCl in Ca^{2+}-free EBSS medium showed a TMRM fluorescence intensity that was comparable to that of the HOCl-non-treated cells, whereas HMDM cells treated with HOCl in Ca^{2+}-rich EBSS medium showed a significant decrease in TMRM fluorescence intensity (**Figure 5.12**). This result indicates that HOCl did not directly react with TMRM, because a direct reaction should lead to TMRM fluorescence intensity decrease in HOCl-treated HMDM cells in both the Ca^{2+}-free and Ca^{2+}-rich EBSS media.

The observed mitochondrial membrane potential loss in HMDM cells after HOCl treatment was prevented by cyclosporin A (CSA) with as low as 5 μM concentration (**Figure 4.11**). CSA is a potent immunosuppressant widely used to reduce rejection in transplantation surgery. It is also known to bind and block the peptidylprolyl isomerase activity of matrix CyP-D, which is required to form an ANT/CyP-D protein complex for MPT pore opening (Connern and Halestrap, 1992; Halestrap and Davidson, 1990; Woodfield *et al*., 1998; McStay *et al.*, 2002; Vieira *et al.*, 2000). MPT was significantly activated by mitochondria taking up excess Ca^{2+} from the cytosol (see **chapter 5**). Whiteman *et al*. (2004) have shown that CSA did not prevent MPT activation by preventing Ca^{2+} uptake by mitochondria. Taken together, the observed inhibitory effect of CSA confirmed the involvement of the MPT activation in mitochondrial membrane potential loss. This is in agreement with Park *et al*. (2008) and Whiteman *et al.* (2005b), who showed MPT-induced mitochondrial membrane potential loss in HOCl-treated HeLa cells and human hepatoma HepG2 cells, respectively.

CSA, at 5 μM concentration, prevented HOCl-induced cell viability loss completely (**Figure 4.12**). CSA at the same concentration also significantly prevented cell morpho-logical changes (i.e. cell swelling and cell membrane rupture) (**Figure 4.11** DIC photos). This suggests that HOCl-mediated MPT activation induced mitochondrial membrane potential loss, which resulted in HMDM necrotic cell death. This agrees with Asmis and Begley (2003), who showed that oxLDL-induced peroxyl radical generation caused mitochondrial membrane potential loss and subsequently necrotic cell death in macrophages. HOCl can inactivate Na^{+}-, K^{+}-, and Ca^{2+}-ATPase ion pumps (Eley *et al*., 1991; Kato *et al*., 1998), which are essential for maintaining plasma membrane potential. Inactivation of these ion pumps would directly promote macrophage lysis. In this research, blocking the L- and T-type calcium ion channels in HMDM cell membranes, inhibiting

calpain activation (see **Chapter 5**) and preventing MPT activation (in this chapter) prevented HOCl-induced HMDM cell viability loss. This suggests that HOCl caused necrotic cell death in HMDM cells via HOCl-induced cytosolic calcium ion accumulation, calpain activation and MPT activation (discussed in **Chapter 5**), not by directly damaging HMDM cell membrane and causing inactivation of Na^+-, K^+- and Ca^{2+}-ATPase ion pumps.

MPT activation has been suggested to be a common pathway leading to both apoptosis and necrosis (Kim *et al.*, 2003a). The MPT pore formation allows the solutes (< 1500 Da) to pass non-selectively between cytosol and matrix, leading to rapid depolarization, matrix swelling and eventually outer membrane rupture (Kim *et al*., 2003b). The consequences for the cell include either release of cytochrome c, activation of caspase cascades, and apoptosis or the drastic loss of ATP via disruption of the inner mitochondrial membrane (IMM) and necrotic cell death. However, it has also been suggested that a clear distinction between these two death pathways may not always be possible (Lemasters, 1999; Jacschke and Lemasters, 2003). In this thesis, HMDM cells treated with HOCl showed several necrotic features, including cell swelling, cell membrane disruption, caspase-3 inactivation, and rapid metabolic energy loss. It can be concluded that the predominant mode of HMDM cell death induced by HOCl was necrotic, rather than apoptotic.

HOCl induced superoxide generation in HMDM cells within 10 minutes of HOCl treatment (**Figure 4.13**). This radical was detected by the cell-permeable dihydroethidium fluorescent dye (DHE). This dye is oxidized by superoxide radicals to form ethidium, which then binds to DNA/RNA leading to enhancement of red fluorescence (Budd *et al*., 1997; Zhao *et al*., 2003). The red fluorescence was enhanced significantly in a localized area in HOCl-treated HMDM cells, possibly mitochondria, because mitochondria are the main source of superoxide radicals and DNA/RNA are present there to react with the resulting ethidium. The red fluorescence was also increased in cytosol of HMDM cells treated with HOCl. This implied that ethidium bound to mitochondrial DNA/RNA were leaked out of mitochondria, supporting the hypothesis of MPT activation and mitochondrial outer membrane rupture as mentioned earlier. The enhanced red fluorescence intensity in HOCl-treated HMDM cells was not caused by HOCl reacting directly with DHE, because HMDM cells were treated with DHE after HOCl treatment.

The results in this research have demonstrated that HOCl caused MPT pore opening in HMDM cells (**Figure 4.11**), which might have contributed to the superoxide generation.

The components of the ETC, such as cytochrome *c*, could be leaked out of mitochondria through the activated MPT pore. This loss of ETC components can lead to the escape of electrons from complex III, which can then reduce oxygen molecules and form superoxide radicals (Luetjens *et al*., 2000). In contrast, some studies suggest that mitochondria-mediated ROS generation, as a result of exposing cells to oxidative stress or apoptotic stimulus, can cause MPT activation (Kim *et al*., 2003b; Kowaltowski *et al*., 2001). Further studies are required to understand how exactly HOCl mediated superoxide generation in HMDM cells.

MPT is regulated by a number of factors. High membrane potential, Mg^{2+}, ADP, NAD(P)H, and low pH keep the pore in a closed conformation, while Ca^{2+}, Pi, $NAD(P)^{+}$, oxidizing agents, and high pH tend to open the pore (Hansson *et al*., 2003). This research will focus on the effect of Ca^{2+} and oxidizing agent (i.e. HOCl) on MPT activation, together with how MPT activation leads to necrotic cell death (**Chapter 5**).

4.4 Conclusion

HOCl caused HMDM cells to undergo necrotic cell death, demonstrated by the influx of propidium iodide dye (PI) into the cells, lack of caspase-3 activation, and intracellular ATP loss within 10 minutes of HOCl treatment. The initial intracellular ATP loss was not recovered over time after the treatment. This was possibly due to HOCl compromising the intracellular machinery for ATP production, since HOCl treatment also led to the loss of GAPDH activity and mitochondrial membrane potential in HMDM cells within 10 minutes of treatment.

CSA prevented HOCl-mediated loss of mitochondrial membrane potential and cell viability by inhibiting MPT pore formation. These results indicate that HOCl caused MPT-mediated mitochondrial membrane potential loss, which led to necrotic cell death. Superoxide generation was detected in HMDM cells upon HOCl treatment, which could be attributed to MPT activation and dysfunction of the electron transport chain. HOCl also caused cellular tyrosine loss, which correlated strongly with the HMDM cell viability loss. This indicates that this HOCl-induced tyrosine loss was in a cause-and-effect relationship with the MPT-mediated mitochondrial membrane potential loss and necrotic cell death.

5. THE ROLE OF CALCIUM IN HOCL-MEDIATED NECROTIC CELL DEATH IN HMDM CELLS

5.1 Introduction

Free calcium ions (Ca^{2+}) play a key role in signaling in eukaryotic cells. Transient increases in cytosolic free Ca^{2+} can regulate many physiological processes, including cell proliferation and neurotransmitter release (Halliwell and Gutteridge, 2007). Influx of Ca^{2+} into the cytosol also leads to mitochondrial accumulation of Ca^{2+}, activation of the Krebs cycle, and oxidative phosphorylation with the subsequent ATP production (Maack and O'Rourke, 2007; Brookes *et al*., 2004). Mitochondrial Ca^{2+} plays a role in allosteric activation of pyruvate dehydrogenase, isocitrate dehydrogenase, and α-ketoglutarate dehydrogenase (McCormack and Denton, 1993). It also plays a role in stimulation of the ATP synthase (complex V) (Das and Harris, 1990), α-glycerophosphate dehydrogenase (Wernette *et al*., 1981), and the adenine nucleotide translocase (ANT) (Mildaziene *et al*., 1995). Many other mitochondrial functions are also regulated by Ca^{2+}. For example, Ca^{2+} activation of *N*-acetylglutamine synthetase generates *N*-acetylglutamine, a potent allosteric activator of carbamoyl-phosphate synthetase, the rate-limiting enzyme in the urea cycle (Brookes *et al*., 2004). Ca^{2+}-sensitive protein kinase (PKC) isoforms and calmodulin have also been reported in mitochondria, although their precise targets within the organelle are less well understood (Fernandez *et al*., 1995; Ruben *et al*., 1980).

Most unstimulated cells tightly regulate free Ca^{2+} in the range of 100 to 200 nM in both the cytosol and the mitochondria, whereas the extracellular free Ca^{2+} concentration is approximately 2 mM. This concentration gradient is maintained by a number of cellular systems. For example, Ca^{2+} is bound to proteins such as calmodulins. Moreover, Ca^{2+} can be extruded out of cells or taken up by endoplasmic reticulum (ER) via ATP-dependent Ca^{2+} pumps in the plasma or ER membrane, respectively. Ca^{2+} can also be transported out of cells (against its concentration gradient) with the entry of Na^{+} (down its concentration gradient) through Na^{+}/Ca^{2+} exchange transporters across the plasma membrane. The Na^{+} is then exported out of cells by the ATP-dependent sodium pump. In addition, to a lesser extent, mitochondria can take up excess cytosolic Ca^{2+} (Halliwell and Gutteridge, 2007). Ca^{2+} can diffuse through the outer mitochondrial membrane (OMM) into the inter-

membrane space via the voltage-dependent anion channel (VDAC), which is a large conductance channel permeable to ions and small proteins (< 5000 Da) (see **Chapter 4**). Ca^{2+} can then be transported into the matrix by the Ca^{2+} uniporter (i.e. a transport across the membrane driven only by the electrochemical gradient, with no immediate exchange or co-transport of other ions) located in the inner mitochondrial membrane (IMM) (Kirichok *et al*., 2004). The rate of Ca^{2+} uptake was shown to be significant only above a threshold of 200-300 nM Ca^{2+}. This uniporter appears to be gated by local adenine nucleotide concentrations (ATP > ADP > AMP) at a site located at the outer surface of the IMM (Bianchi *et al*., 2004).

With physiological stimulation, free Ca^{2+} in both cytosol and mitochondria can rapidly and transiently increase by 10 to 20-fold as occurs on a beat to beat basis in cardiac myocytes due to mitochondrial Ca^{2+} uptake (Trollinger *et al.*, 2000). Hormonal and other stimuli activate phospholipase C enzyme, which cleaves a phospholipid phosphatidylinositol 4,5-bisphosphate (PIP2) into diacyl glycerol (DAG) and inositol 1,4,5-triphosphate (IP_3). DAG remains bound to the membrane, whereas IP_3 is released into the cytosol and then bind to IP_3 receptors, in particular Ca^{2+} channels in the ER (Lemasters *et al*., 2009). This causes the release of Ca^{2+} from ER into cytosol. Membrane depolarization of cardiac cells also causes Ca^{2+} entry through voltage-gated Ca^{2+} channels (Bers, 2002; Fabiato, 1985a; Fabiato, 1985b). During the action potential (a transient alteration of the membrane potential across a membrane in an excitable cell such as a neuron or myocyte), the voltage-gated Na^{+}-channels are activated. The inward Na^{+}-current induces a rapid depolarization of the cell membrane, facilitating voltage-dependent opening of L-type Ca^{2+}-channels. In certain cell types (such as monocytes, neutrophils, lymphocytes and certain neurons), ROS such as H_2O_2 open the NAD^{+}-dependent TRPM2 cation channels in the plasma membrane and let Ca^{2+} in. These channels are non-selective, also transporting Na^{+} and K^{+}, thus depolarizing the membrane and letting even more Ca^{2+} in by opening voltage-gated channels (Halliwell and Gutteridge, 2007). The Ca^{2+} influx triggers the opening of the ryanodine receptor (RyR2 subtype) of sarcoplasmic reticulum (SR) or ER, inducing the release of even greater amount of Ca^{2+}, a process termed Ca^{2+}-induced Ca^{2+}-release. The Ca^{2+} released from RyRs floods the space between the SR and the cell membrane (junctional cleft), a gap of typically ~10 nm and covering a volume with a radius of ~200 nm. Computational modeling predicted a temporarily and spatially limited increase of the Ca^{2+} concentration in the range from ~10 μM to ~7 mM within the first couple of milliseconds after opening of the RyR2 (Bers, 2002; Peskoff and Langer, 1998; Shannon *et*

al., 2004). However, this high junctional calcium concentration decays rapidly by diffusion into the submembrane space (such as mitochondria) and then further into the bulk cytosol, where it peaks later and at much lower concentrations than in the cleft (at ~1.5 μM in the submembrane space and ~0.5 μM in the bulk cytosol (Shannon *et al.*, 2004; Weber *et al.*, 2002).

Dysregulation of Ca^{2+} homeostasis has long been implicated to play an important role in cell injury. Pathological Ca^{2+} overload and calcification are frequent features of tissue ischemia and infarction. Previous studies in hepatocytes showed that removal of extracellular Ca^{2+} protects against various hepatotoxicants, suggesting that influx of extracellular Ca^{2+} is responsible for irreversible cell injury (Lemasters *et al.*, 2009). Moreover, a range of cell types showed increased cytosolic Ca^{2+} level after ROS or toxin treatment, leading to either caspase-3-dependent or -independent apoptosis (Yap *et al.*, 2006; Ding *et al.*, 2002; Escargueil-Blanc *et al.*, 1994; Vindis *et al.*, 2005; Mishra *et al.*, 2006) or necrosis (Escargueil-Blanc *et al.*, 1994; Hurne *et al.*, 2002; Aguilar *et al.*, 1996).

An abnormal rise in free calcium can result in ROS formation (such as superoxide). Stimulation of the Krebs cycle and oxidative phosphorylation by Ca^{2+} would enhance ROS output by making the whole mitochondrion work faster and consume more O_2, resulting in more respiratory chain electron leakage. Mitochondrial ROS generation correlates well with metabolic rate (Perez-Campo *et al.*, 1998; Sohal and Allen, 1985). Ca^{2+} stimulation of nitric oxide synthase (NOS) (Alderton *et al.*, 2001) generates nitric monoxide ($NO^{\cdot}$), which inhibits complex IV (Cleeter *et al.*, 1994), and this would enhance ROS generation from the Q cycle on IMM (Alexander *et al.*, 2000), in conjunction with high mitochondrial Ca^{2+} concentration, can inhibit mitochondrial complex I (Jekabsone *et al.*, 2003). It is not yet known whether this event would lead to ROS generation (Brookes *et al.*, 2004). Ca^{2+} can enhance cytochrome *c* dislocation from the inner mitochondrial membrane (IMM), either by competing for cardiolipin binding sites or by inducing the mitochondrial permeability transition (MPT) pore opening (see below). This results in an effective block of the respiratory chain at complex III, which would cause ROS generation (Ott *et al.*, 2002; Grijalba *et al.*, 1999).

An abnormal rise in free Ca^{2+} can also lead to activation of phospholipase A_2 that cleaves membrane phospholipids and leads to disruption of membrane organization, activation of Ca^{2+}-dependent endonucleases in the nucleus causing DNA fragmentation, and activation

of transglutaminases catalysing the cross-linking of proteins to produce insoluble aggregates (Halliwell and Gutteridge, 2007; Kowaltowski *et al.*, 2001). Furthermore, excessive rise in extracellular Ca^{2+} (above 5 μM) often results in membrane blebbing, possibly as a result of calpain activation (a class of non-lysosomal cysteine proteases). There are two ubiquitous forms, μ-calpain and m-calpain that are activated by micromolar and millimolar concentrations of Ca^{2+} *in vitro* (Saido *et al.*, 1994b; Huang and Wang, 2001). They can cleave spectrin (an actin-binding protein that control the polymerization and reorganization of actin), or α-actinin and talin (cytoskeletal proteins that connect actin filaments with the plasma membrane), eliminating the plasma membrane anchorage to the cytoskeleton and allowing it to bleb out (Miyoshi *et al*., 1996; Weber *et al*., 2005; Halliwell and Gutteridge, 2007). Oxidation of thiol groups on cytoskeletal proteins by ROS and loss of intracellular ATP (required for maintenance of cytoskeletal integrity) also facilitate blebbing. If blebbing proceeds to such an extent that bleb rupture occurs without immediate resealing, the cell loses its ion gradients and is effectively dead. Its contents are released into the surrounding area, thus necrotic cell death occurs (Halliwell and Gutteridge, 2007). Calpain activation in neuronal cells in response to HOCl also mediated lysosomal rupture with the resultant release of cathepsins and caspase- 3-independent apoptosis, indicating calpain activation and the subsequent cathepsin release could induce apoptosis. Cathepsins are synthesized as inactive precursors and undergo proteolytic activation in the optimal acidic pH. They are localized mainly to the lysosomes (B, D, H, L, S, C and K subtypes) but also to the nucleus (B and L) and cytosol (B and E). These proteases may cause degradation of certain cellular constituents (Yap *et al*., 2006). Calpains were also implicated in inducing Bid (a proaopoptotic BH3-only member of the Bcl-2 family) cleavage to form active truncated Bid (tBid), which in turn promotes the release of cytochrome c from mitochondria, leading to caspase-3 activation and apoptosis (Vindis *et al*., 2005).

Excessive cytosolic Ca^{2+} can also be taken up by mitochondria to trigger the MPT pore opening (Bianchi *et al*., 2004; Richter, 1993; Crompton *et al*., 2002; Whiteman *et al*., 2004), which then leads to either apoptotic or necrotic cell death (see **section 4.1**). In addition, cathepsin D caused MPT activation in alveolar macrophage cells exposed to silica (Thibodeau *et al*., 2003). Oxidative stress and calpains also appear to play a role in MPT activation, which will be discussed in detail in **section 5.3**.

The results present in **Chapter 4** showed that HOCl-induced MPT activation in HMDM cells lead to necrotic cell death. But how exactly MPT activation was initiated by HOCl and how it led to HMDM necrotic cell death was unknown. This chapter aims to examine whether HOCl caused cytosolic Ca^{2+} level to increase in HMDM cells, and the association of this increase with necrotic cell death in relation to MPT activation, calpain activation and lysosomal destabilization.

5.2 Results

5.2.1 Effect of HOCl on intracellular calcium ion influx

Free Ca^{2+} concentrations in resting cells are maintained between 100 and 200 nM in cytosol and mitochondria; abnormal increases can lead to both apoptotic and necrotic cell death (see **section 5.1**). The effect of HOCl on cytosolic Ca^{2+} level increase in HMDM cells was therefore studied. HMDM cells were probed with the cell-permeable fluorescent indicator, fluo-3-acetoxymethyl (AM) ester, for the detection of free cytosolic Ca^{2+}. The cells were then exposed to a range of HOCl concentrations in EBSS buffer with or without Ca^{2+}, followed by examination of their fluorescence intensities (**Figure 5.1a**). The fluorescence intensities were also converted to numerical values (**Figure 5.1b**).

HOCl in EBSS buffer without Ca^{2+} caused cytosolic fluorescence intensity to increase by approximately 28% at 100 μM concentration compared to the control. There was no further statistically significant ($P > 0.05$) increases in fluorescence intensity above 100 μM HOCl (**Figure 5.1a** and **b**). HOCl in EBSS buffer with Ca^{2+} (referred to as Ca^{2+}-enriched EBSS in this thesis) at 100, 150 and 200 μM caused cytosolic fluorescence intensity to increase by 25%, 60%, and 69%, respectively, compared to the control. The results suggest that HOCl induced an increase in cytosolic free Ca^{2+}, which was released mainly from intracellular stores at or below 100 μM HOCl, while Ca^{2+} in the extracellular medium also contributed to the cytosolic Ca^{2+} increase above 100 μM HOCl. Cell swelling and cell membrane disruption were observed in cells treated with HOCl above 100 μM concentration in Ca^{2+}-enriched EBSS (as shown in the DIC images); these morphological changes were less obvious in cells treated with the same HOCl concentrations in Ca^{2+}-free EBSS buffer (**Figure 5.1a**). These results indicate that the increase in cytosolic Ca^{2+} needed to reach a certain intracellular concentration before cell swelling and cell membrane rupture were significant.

5.1a)

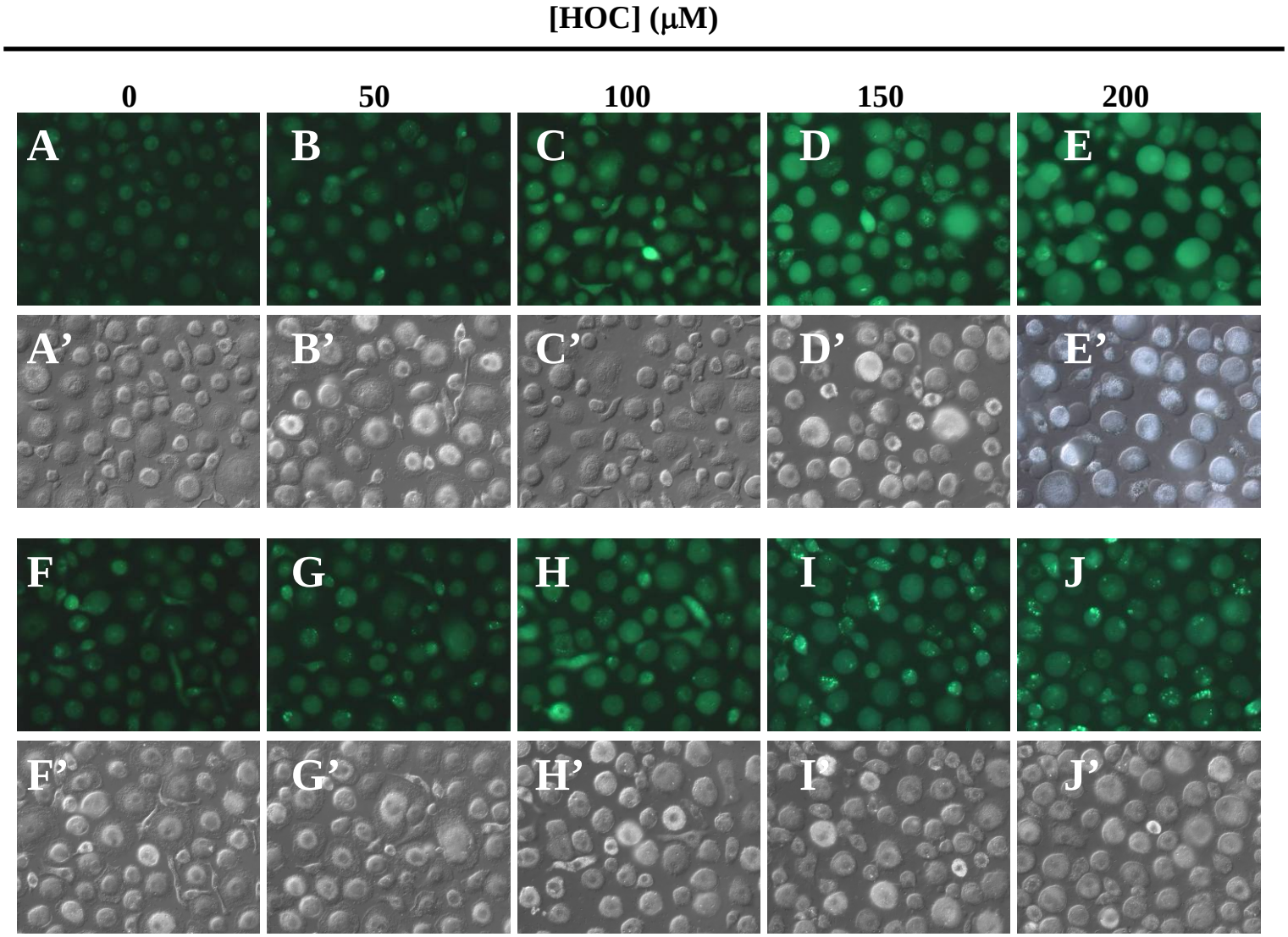

5.1b)

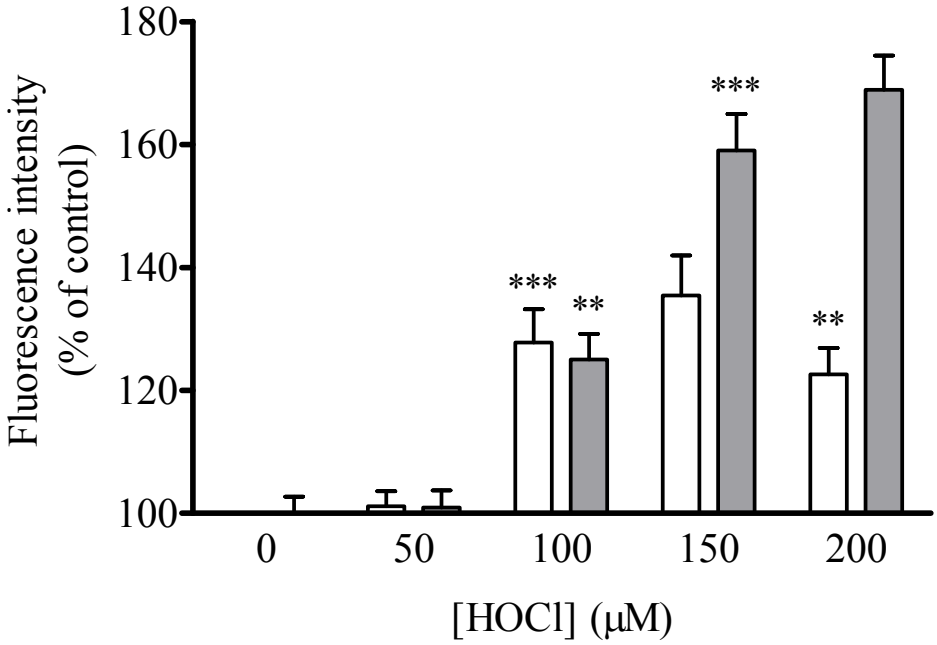

Figure 5.1 HOCl induced an increase in cytosolic Ca^{2+} in HMDM cells.
HMDM cells (5×10^6 cells/ml) on coverslips were pre-incubated with 10 μM of Fluo-3-AM ester for 40 minutes, followed by treatment with increasing HOCl concentrations in EBSS buffer in the presence (A to E) or absence (F to J) of 0.68 mM $CaCl_2$ for 10 minutes. **a)** The cells were subsequently viewed under a fluorescence microscope (λex/λem = 488/530nm). A' to J' represent the DIC photos of A to J, respectively. **b)** Fluorescence intensities of the cells in the presence (gray bars) or absence (white bars) of Ca^{2+} are converted to numerical values. Each data is presented as a percentage of the 0 μM (with Ca^{2+}) control. Significance is indicated from the respective 0 μM controls.

Calcium ionophore A23187 is a lipid soluble molecule that is highly selective for Ca^{2+} and greatly increases the ability of Ca^{2+} to cross cell membranes. It was used here as a positive control to confirm that the detected green fluorescence resulted from Ca^{2+} reacting with fluo-3 dye, not from HOCl reacting with the dye. The fluorescence intensities (**Figure 5.2a**) and the numerical values converted from the fluorescence intensities (**Figure 5.2b**) showed that HMDM cells exposed to 3, 5 and 7 μM A23187 caused the cytosolic fluorescence intensities to increase by 26%, 53%, and 58% compared to the control, respectively. Cell swelling and cell membrane disruption were observed in HMDM cells treated with A23187 at concentrations above 5 μM, suggesting that an increase in cytosolic Ca^{2+} level resulted in cell swelling and cell membrane disruption. These results imply that the morphological changes in HOCl-treated HMDM cells (**Figure 5.1**) were attributed to the cytosolic Ca^{2+} increase, not to HOCl causing general damage on cell membranes.

5.2a)

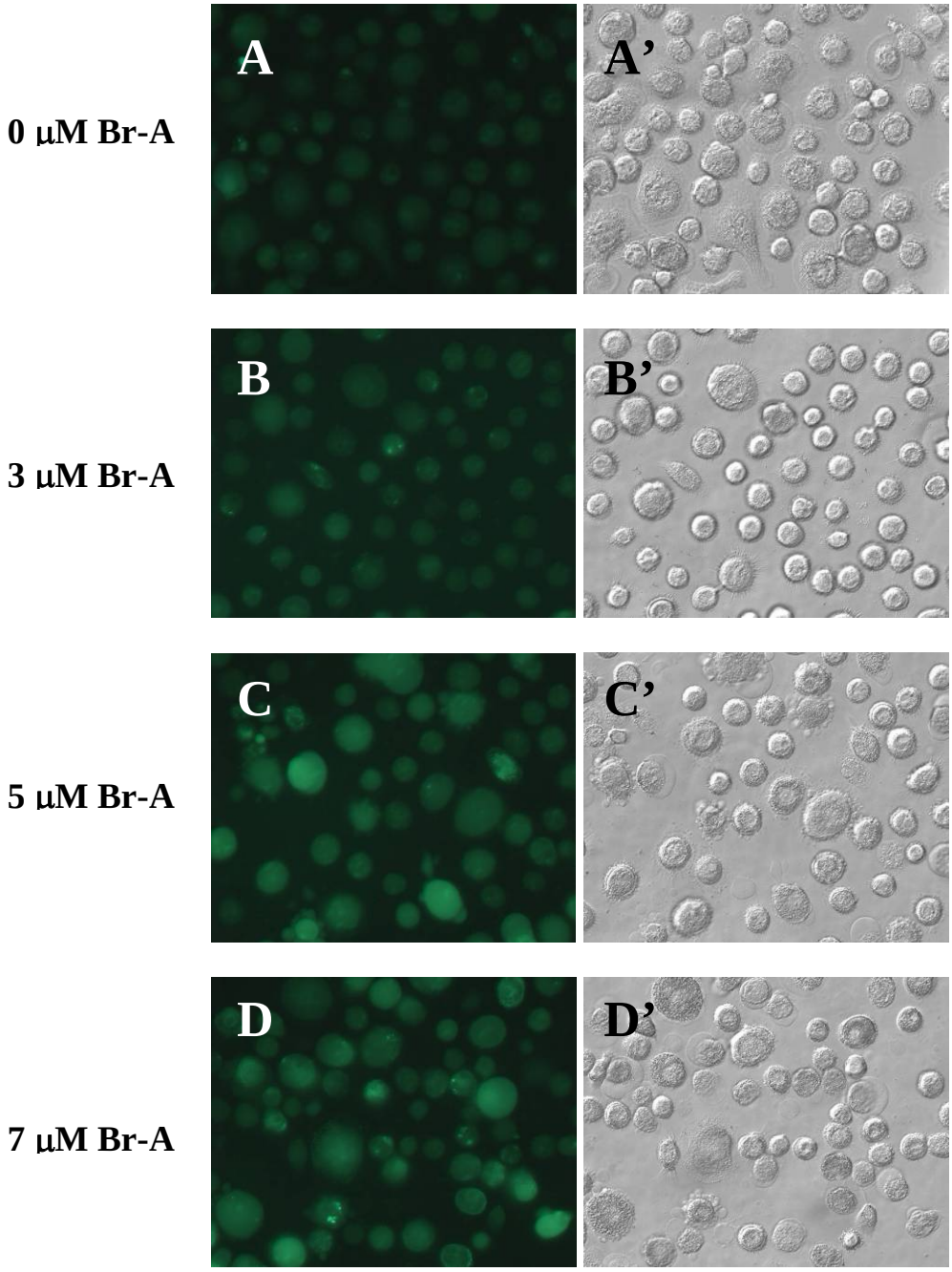

5.2b)

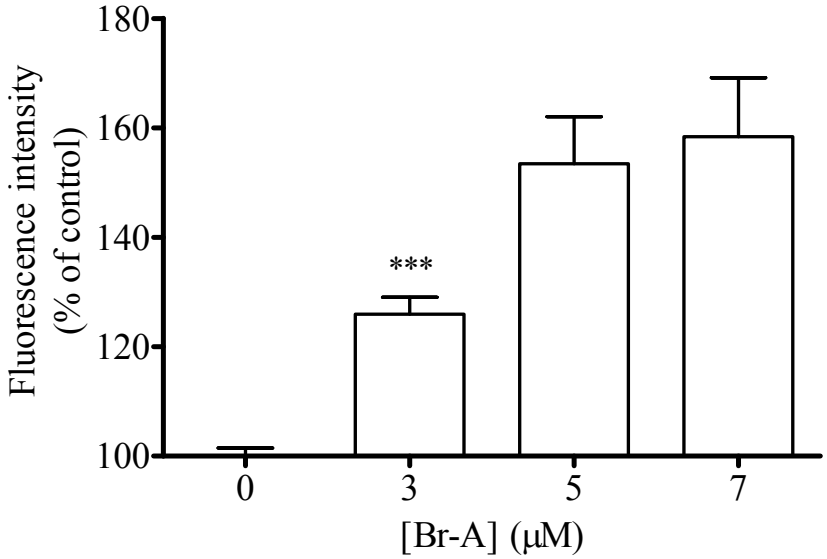

Figure 5.2 Ca^{2+} ionophore A23187 induced an increase in cytosolic Ca^{2+} in HMDM cells.
HMDM cells (5×10^6 cells/ml) on coverslips were pre-incubated with 10 μM of Fluo-3-AM ester for 40 minutes. The cells were then treated with or without increasing concentrations of calcium ionophore A23187 in EBSS buffer containing 0.68 mM Ca^{2+} (referred to as Ca^{2+}-enriched EBSS) for 5 minutes (A to D), followed by viewing under a fluorescence microscope (λex/λem = 488/530nm). A' to D' represent the DIC photos of A to D, respectively. **b)** Numerical values for the fluorescence intensities are presented as percentage of the control and significance is indicated from the same control.

5.2.2 Effect of HOCl-induced cytosolic Ca^{2+} increase on HMDM cell death

To examine the effect of HOCl-induced cytosolic Ca^{2+} increase on HMDM cell viability loss, HMDM cells were exposed to HOCl in EBSS buffer with or without Ca^{2+} for 10 minutes and analysed for cell viability over time. HOCl at 100 and 200 μM concentrations in EBSS buffer with Ca^{2+} caused HMDM cell viability to decrease initially by approximately 50% and 80%, respectively (**Figure 5.3**). In contrast, HOCl at 100 and 200 μM concentrations in EBSS buffer without Ca^{2+} caused cell viability to decrease initially by approximately 12% and 60%, respectively. These results suggest that the initial HOCl-induced HMDM cell viability loss was mainly caused by the increase in cytosolic Ca^{2+} contributed from both intracellular and extracellular stores. However, when HOCl concentration was too high (i.e. 200 μM), the oxidant reacted with cells overwhelmingly and even Ca^{2+} exclusion from extracellular medium could not restore cell viability.

After the 10-minute treatment, the HOCl reaction media (at both 100 and 200 μM) were replaced with RPMI culture media. HOCl treatment in Ca^{2+}-enriched EBSS did not cause further significant decreases in cell viability over time, while HOCl treatment in Ca^{2+}-free EBSS caused significant decreases within 6 hours (especially at 100 μM), which then plateaued after 6 hours and were comparable to those of HOCl-treated HMDM cells in Ca^{2+}-containing EBSS (**Figure 5.3**). This observation could be attributed to the replacement of HOCl reaction medium (without Ca^{2+}) with RPMI culture medium (containing Ca^{2+}) after the initial HOCl treatment, which led to extracellular Ca^{2+} influx and hence cell viability loss. This theory was supported by the observation that HMDM cells incubated with HOCl in Ca^{2+}-free EBSS for 6 hours, without replacing the reaction medium with HMDM culture medium, showed minor loss of cell viability (**Figure 5.6**). For the future experiments, the HOCl reaction medium was not replaced with HMDM culture medium after 10-minute treatment in order to prevent the possible Ca^{2+} influx from the HMDM culture medium. The cells were just incubated with the reaction medium for 6 hours before analyses.

To further confirm that the cytosolic Ca^{2+} increase was indeed able to cause rapid HMDM cell viability loss, HMDM cells were exposed to Ca^{2+} ionophore A23187 (0-7 μM) for 5 minutes and cell viability was analysed (**Figure 5.4**). A23187 at 3 μM did not cause any cell viability loss at 0 and 20 hr post-treatment. At 0 hr post-treatment, 5 and 7 μM A23187 caused approximately 40% and 76% cell viability loss, respectively, and there was no further significant cell viability loss occurring at 20 hr post treatment. The results suggest that the cytosolic Ca^{2+} increase induced by A23187 treatment did cause a rapid loss of cell viability. No cell viability loss was observed at 3 μM A23187 indicates that cytosolic Ca^{2+} needed to reach a certain intracellular concentration before cell viability was lost.

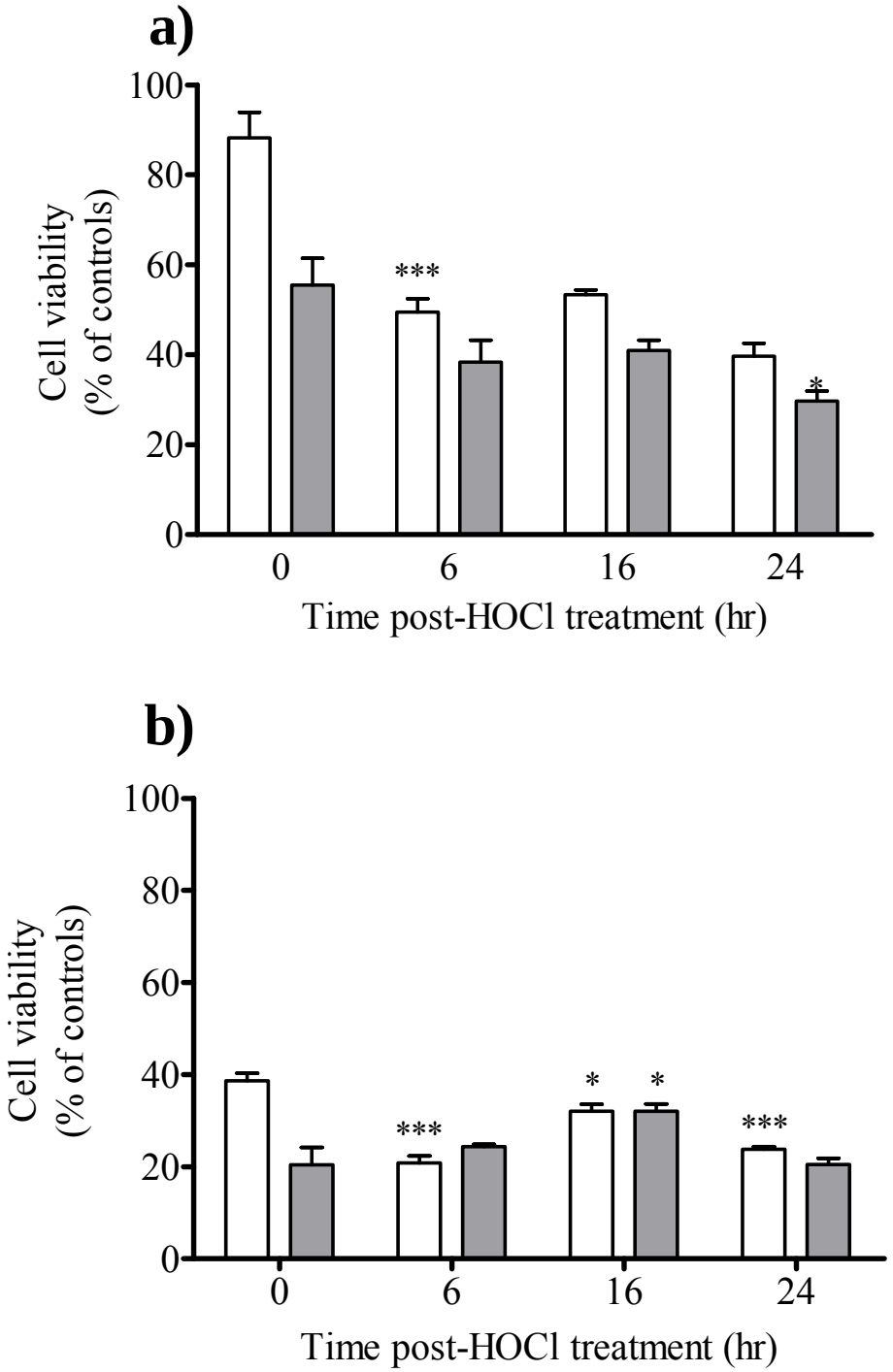

Figure 5.3 Contribution of HOCl-induced cytosolic Ca^{2+} increase to cell viability loss. HMDM cells (5×10^6 cells/ml) were treated with **a)** 100 or **b)** 200 μM HOCl in Ca^{2+}-free EBSS (white bars) or Ca^{2+}-enriched EBSS (gray bars) for 10 minutes, followed by incubation in HMDM culture medium. The cells were then analysed at time intervals for cell viability using the MTT reduction assay. Cell viability is presented as a percentage of the respective 0 μM HOCl controls and significance is indicated from the respective 0 hr data.

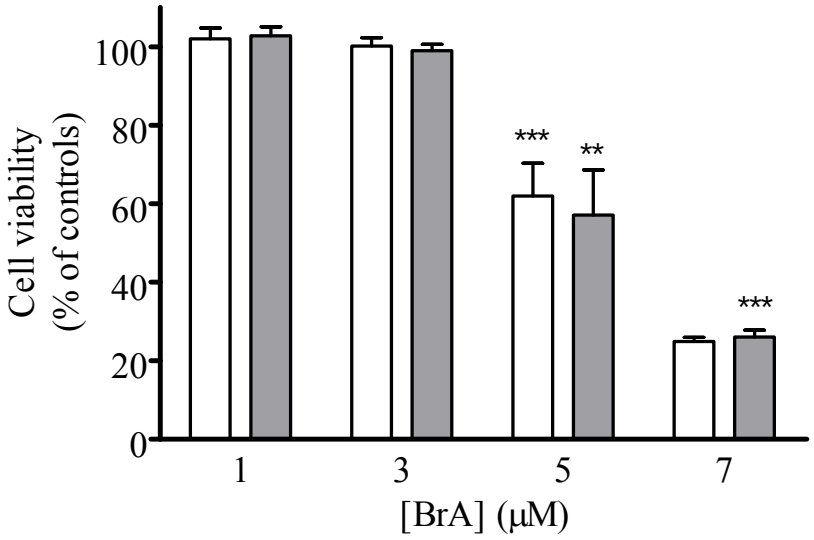

Figure 5.4 A23187-induced cytosolic Ca^{2+} increase caused HMDM cell viability loss. HMDM cells (5×10^6 cells/ml) were treated with or without increasing concentrations of A23187 in Ca^{2+}-enriched EBSS for 5 minutes, followed by incubation in HMDM culture medium. The cells were then analysed for cell viability at 0 hr (white bars) and 24 hr (gray bars) post-treatment using the MTT reduction assay. Cell viability is presented as a percentage of the respective 0 μM HOCl controls and significance is indicated from the respective 0 μM HOCl data.

To further evaluate the sources of Ca^{2+} for cytosolic Ca^{2+} increase and cell injury, HMDM cells were incubated with the Ca^{2+} chelator EGTA and various Ca^{2+} channel blockers before HOCl treatment, followed by immediate fluorescence microscopy analysis (**Figure 5.5**) and cell viability analysis after 6 hours (**Figure 5.6**). The preliminary results showed that incubation of HMDM cells with EBSS in the presence or absence of Ca^{2+}, and with EBSS in the presence of Ca^{2+} and various Ca^{2+} channel blockers and EGTA for 6 hours did not affect the cell viability. The extracellular Ca^{2+} pool is derived from the culture medium, whereas ER is the principal intracellular Ca^{2+} pool. Upon ER stress, Ca^{2+} from the ER pool is released via two types of receptor/channels: the ryanodine receptor (RyR) and the IP_3 receptor (IPR).

Treatment with 150 μM HOCl in the presence of extracellular Ca^{2+} caused the cytosolic fluorescence intensity to increase by approximately 8.6 times and the cell viability to decrease by 74% compared to their respective controls. HOCl treatment in the absence of extracellular Ca^{2+} (by using Ca^{2+}-free EBSS and by chelating Ca^{2+} with EGTA) caused cytosolic Ca^{2+} to increase only by approximately 2.9 and 1.7 times compared to the control, respectively, and cell viability loss was prevented significantly. Nifedipine and verapamil

(both are L-type Ca^{2+} channel inhibitors blocking Ca^{2+} entry into cells), and flunarizine (T-type Ca^{2+} channel inhibitor) in the presence of extracellular Ca^{2+} only induced cytosolic Ca^{2+} to increase by approximately 4.06, 3.07, and 2.07 times compared to the control, respectively, while cell viability losses were prevented significantly. Dantrolene (a selective blocker of RyR) in the presence of extracellular Ca^{2+} only induced cytosolic Ca^{2+} to increase by approximately 1.79 times, and surprisingly, it prevented cell viability loss completely. This will be discussed further later.

Taken together, both blocking extracellular Ca^{2+} influx and intracellular Ca^{2+} release from the ER could prevent cytosolic Ca^{2+} increase and cell viability loss significantly. This suggests that cytosolic Ca^{2+} increase did play an important role in mediating HOCl-induced HMDM cell viability loss.

5.5a)

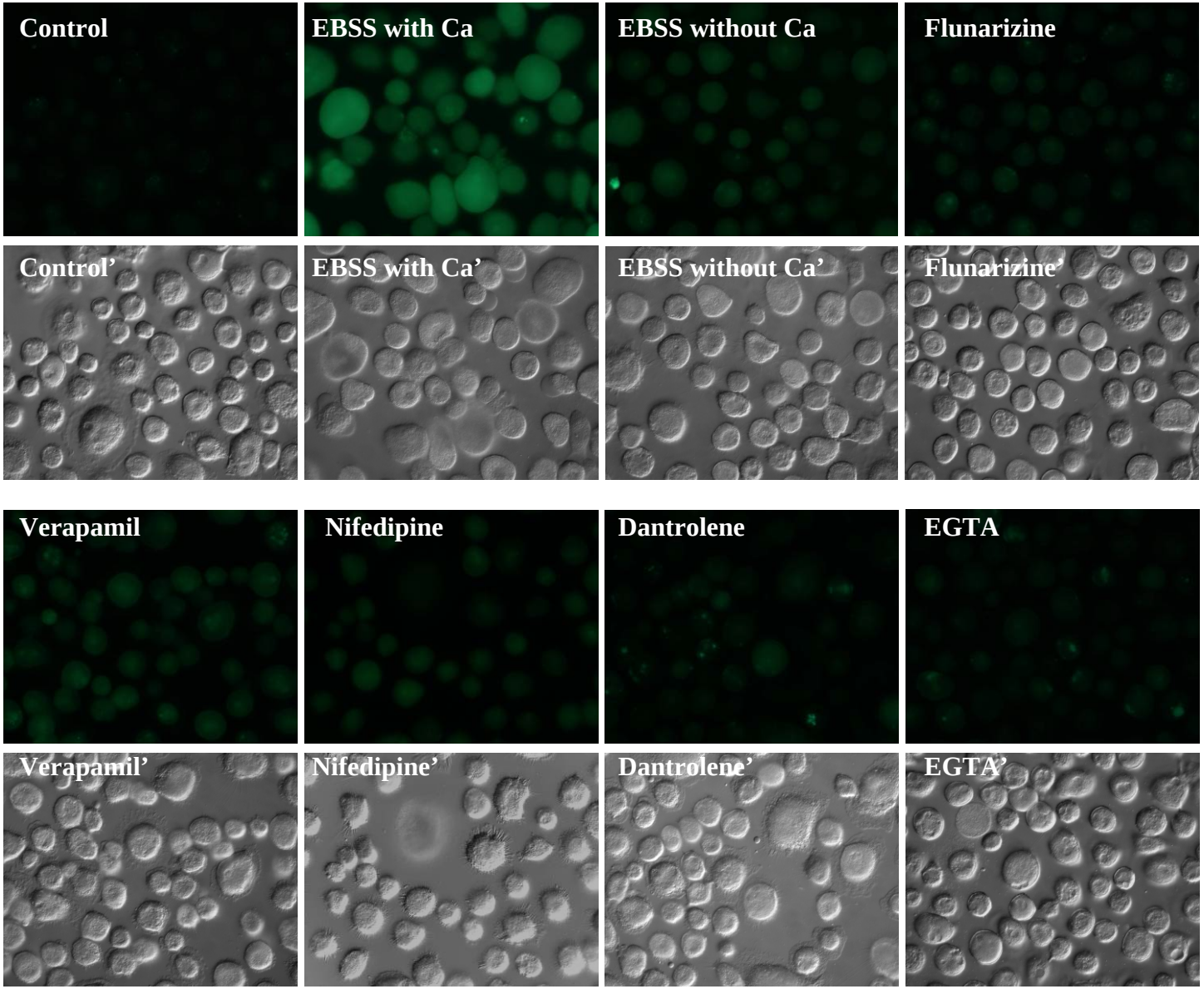
Control
EBSS with Ca
EBSS without Ca
Flunarizine
Control'
EBSS with Ca'
EBSS without Ca'
Flunarizine'
Verapamil
Nifedipine
Dantrolene
EGTA
Verapamil'
Nifedipine'
Dantrolene'
EGTA'

5.5b)

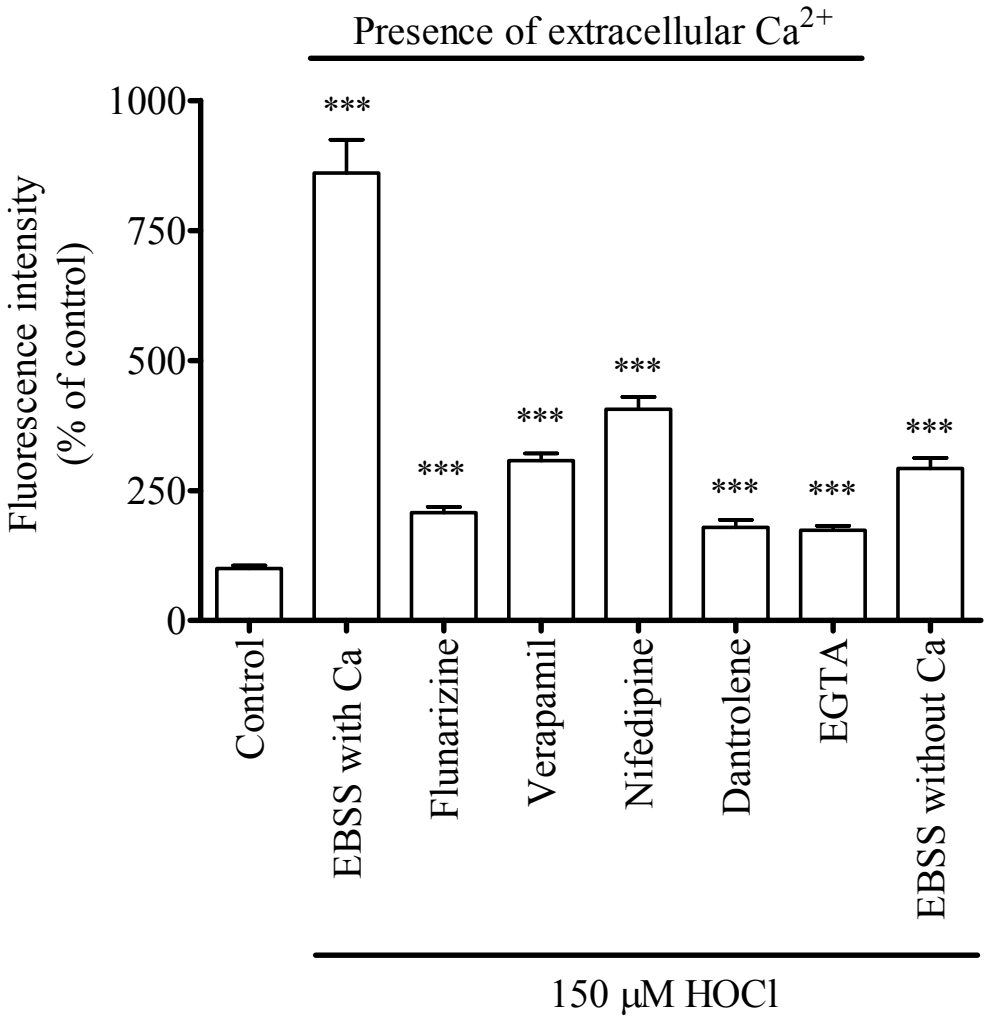

Figure 5.5 Ca^{2+} channel blockers or chelator significantly prevented HOCl-induced cytosolic Ca^{2+} increase.

a) HMDM cells (5×10^6 cells/ml) on coverslips were pre-incubated with control medium (HMDM culture medium), Ca^{2+}-enriched EBSS or Ca^{2+}-free EBSS, 50 μM flunarizine, 50 μM verapamil, 50 μM nifedipine, 10 μM dantrolene and 1 mM EGTA for 40 minutes, followed by the addition of 150 μM HOCl. Cell treatment with EGTA and the Ca^{2+} channel blockers were carried out in Ca^{2+}-enriched EBSS. After 10 minutes of HOCl treatment, cytosolic Ca^{2+} increase was detected using 10 μM of Fluo-3-AM ester and a fluorescence microscope (λex/λem = 488/530nm). The photos labelled with ' represent the DIC photos of the respective fluorescence photos. **b)** Fluorescence intensities are converted to numerical values. Each data is presented as a percentage of the 0 μM HOCl control. Significance is indicated from the respective 0 μM HOCl controls.

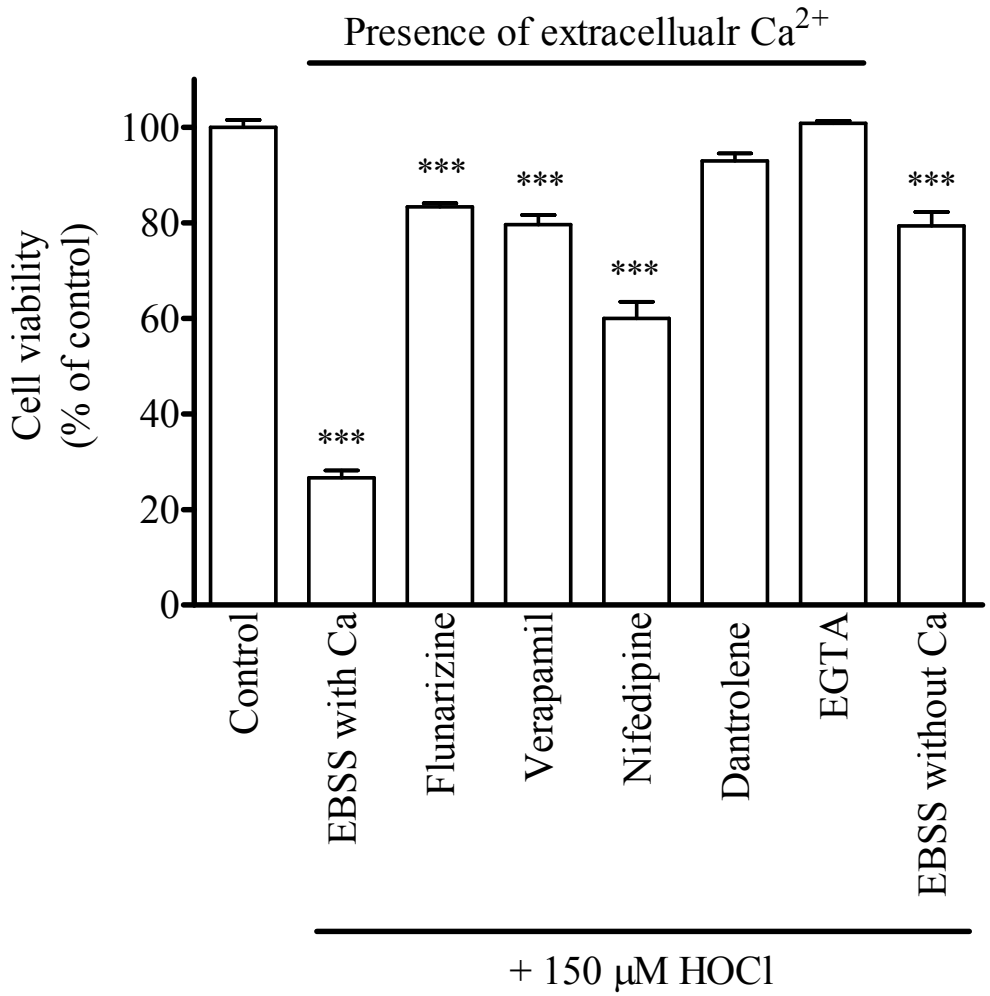

Figure 5.6 Blocking HOCl-induced cytosolic Ca^{2+} increase prevented HMDM cell viability loss significantly.

HMDM cells (5×10^6 cells/ml) were pre-incubated with control medium (HMDM culture medium), Ca^{2+}-enriched EBSS or Ca^{2+}-free EBSS, flunarizine (50 μM), verapamil (50 μM), nifedipine (10 μM), dantrolene (10 μM), and EGTA (1 mM) for 40 minutes, followed by the addition of 150 μM HOCl. Cell treatment with EGTA and the Ca^{2+} channel blockers were carried out in Ca^{2+}-enriched EBSS. After 6 hours, the cells were analysed for cell viability using the MTT reduction assay. Cell viability is presented as a percentage of the 0 μM HOCl control (in HMDM culture medium) and significance is indicated from the same 0 hr control.

5.2.3 HOCl-induced cytosolic Ca^{2+} influx caused HMDM lysosomal destabilization

The changes in lysosomal membrane stability were examined using the lysosomotropic fluorescence probe, acridine orange (AO), which freely enters living cells and accumulates in the acidic compartiments. AO emits a red fluorescence, under UV excitation, only if it has been protonated. Less concentrated AO in cytosol emits a diffuse green fluorescence. This property can be exploited to reveal impairments of the lysosomal proton gradient (Zdolsek *et al.*, 1990). HMDM cells treated with 150 μM HOCl for 10 minutes immediately showed a significant reduction of red fluorescence intensity and increase in green fluorescence intensity (**Figure 5.7**), implicating AO relocation and therefore disrupted acidic properties of lysosomes. No further significant AO relocation was observed after 6 hours, suggesting that this HOCl-induced lysosomal destabilization occurred rapidly within first 10 minutes of HOCl treatment.

HOCl-induced calpain enzyme activation has been found to rupture lysosomes, and stabilization of lysosomes rescued cells from HOCl-induced neurotoxicity (Yap *et al.*, 2006). To study whether this was the case in HOCl-treated HMDM cells, HMDM cells were treated with HOCl in the presence of calpain inhibitors, calpeptin and SJA6017 (0-20 μM). Lysosomal stability and cell viability were subsequently examined. Both calpeptin (**Figure 5.8**) and SJA6017 (**Figure 5.9**) could completely prevent AO relocation and cell viability loss (**Figure 5.10**) at concentrations as low as 10 μM.

AO also binds to DNA and RNA (Walle and Wong, 1989). To confirm that AO relocation was indeed associated with lysosomal destabilization, HMDM cells were treated with guanabenz and idazoxan to stabilize lysosomes prior to HOCl treatment, followed by examining AO distribution. Guanabenz and idazoxan are imidazoline drugs that have been previously used as lysosomal stabilizers (Choi *et al.*, 2002; Yap *et al.*, 2006). Whereas 150 μM HOCl caused significant AO relocation (indicated by the decreased red fluorescence compared to the control), 10 μM guanabenz and idazoxan prevented this HOCl-induced AO relocation significantly (indicated by the similar red fluorescence compared to the control) (**Figure 5.11**). This suggests that AO relocation was indeed associated with lysosomal destabilization, and calpain activation preceded the provoked lysosomal rupture in HOCl-treated cells.

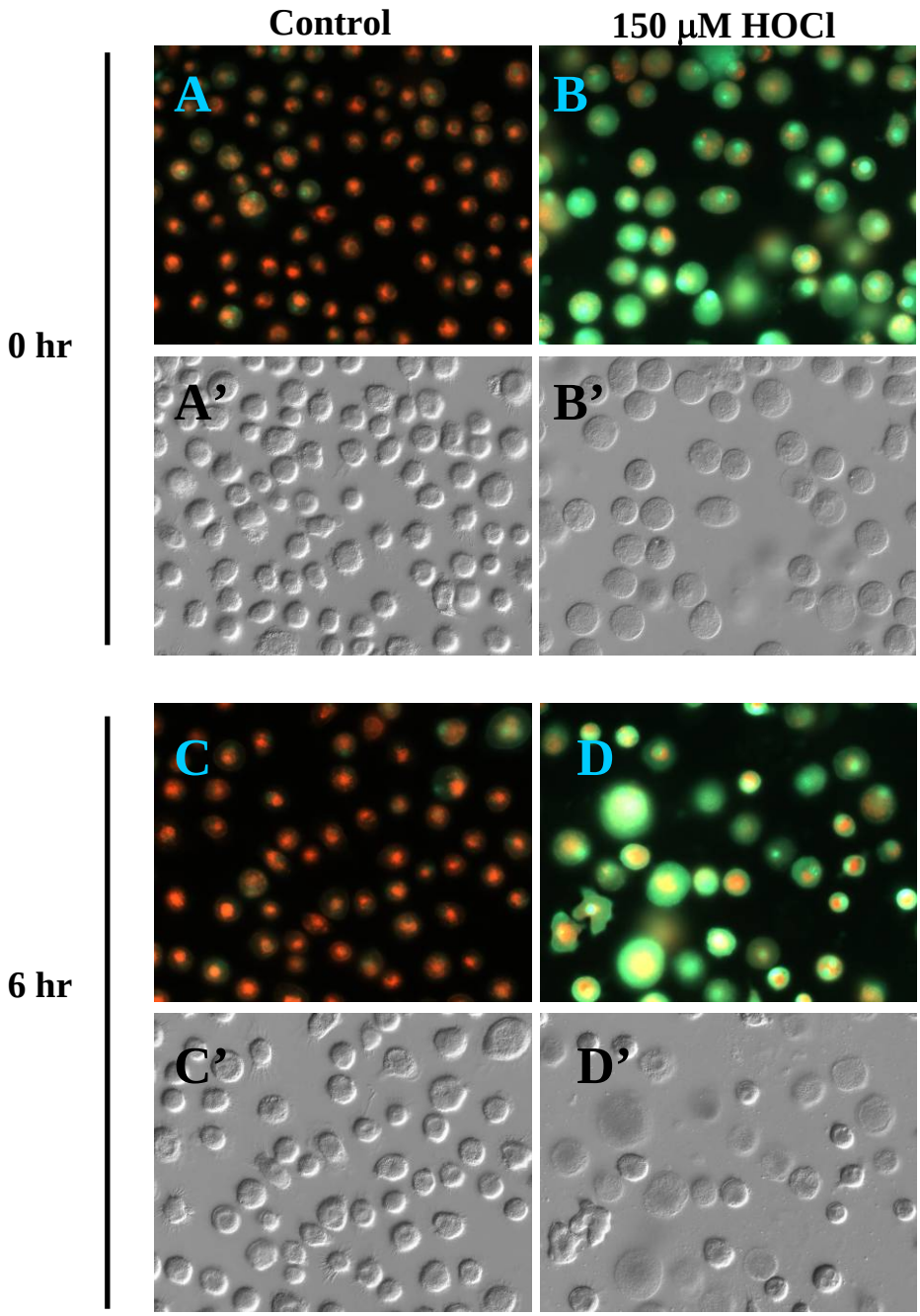

Figure 5.7 HOCl induced lysosomal destabilisation in HMDM cells.
HMDM cells (5×10^6 cells/ml) on coverslips were treated with (**B** and **D**) or without (**A** and **C**) 150 μM HOCl in Ca^{2+}-enriched EBSS for 10 minutes, followed by incubation in HMDM culture medium. The cells were then probed with 10 μg/ml acridine orange (AO) for 20 minutes at 0 and 6 hr post-HOCl treatment. Lysosomal integrity was examined under a fluorescence microscope (λex 487 nm). A', B', and C' represent the DIC photos of A, B, and C, respectively.

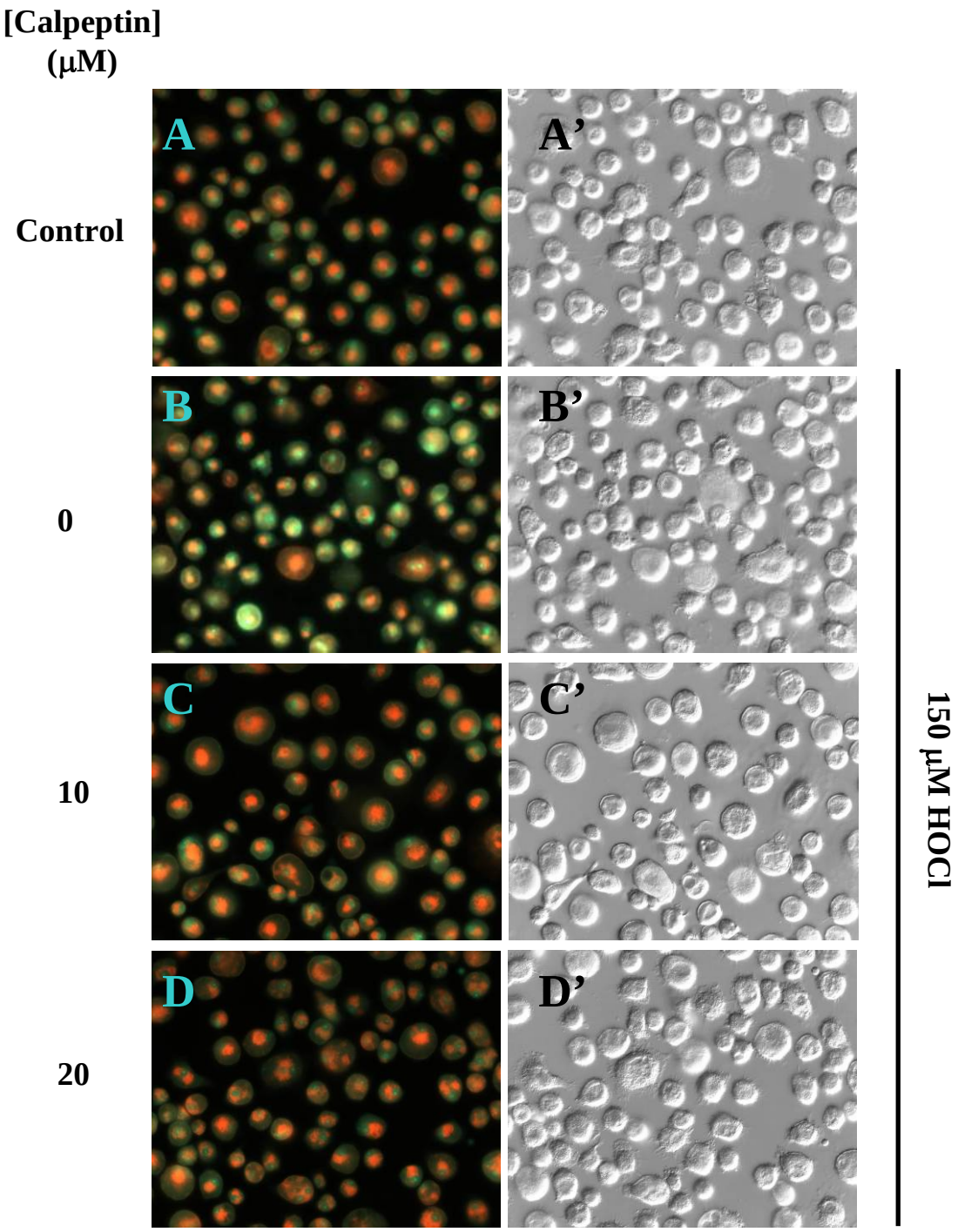

Figure 5.8 Inhibition of calpain enzyme activity using calpeptin prevented HOCl-induced lysosomal destabilisation.
HMDM cells (5×10^6 cells/ml) on coverslips were pre-incubated with 0 (**A** and **B**), 10 (**C**), or 20 (**D**) μM of a calplain inhibitor calpeptin in Ca^{2+}-enriched EBSS for 1 hour, followed by treatment with (**B** to **D**) or without (**A**) 150 μM HOCl. After 6 hours, the cells were analysed for lysosomal integrity (**A** to **D**) by probing the cells with 10μg/ml AO for 20 minutes and viewing the cells under a fluorescence microscope (λex 487 nm). A', B', C' and D' represent the DIC photos of A, B, C and D, respectively.

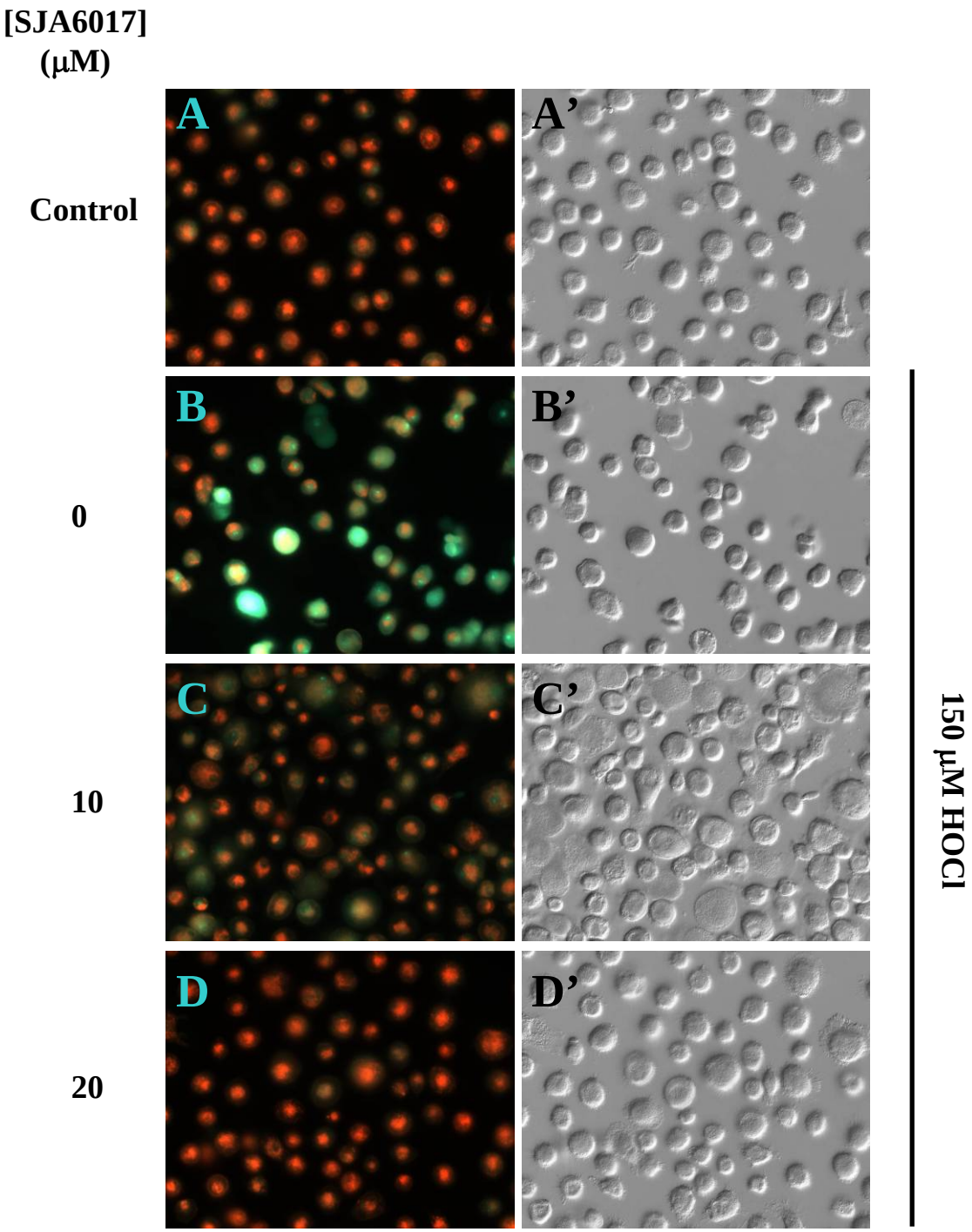

Figure 5.9 Inhibition of calpain enzyme activity using SJA6017 prevented HOCl-induced lysosomal destabilisation.
HMDM cells (5×10^6 cells/ml) on coverslips were pre-incubated with 0 (**A** and **B**), 10 (**C**), or 20 (**D**) μM of a calplain inhibitor SJA6017 in Ca^{2+}-enriched EBSS for 1 hour, followed by treatment with (**B** to **D**) or without (**A**) 150 μM HOCl. After 6 hours, the cells were analysed for lysosomal integrity (**A** to **D**) by probing the cells with 10μg/ml AO for 20 minutes and viewing the cells under a fluorescence microscope (λex 487 nm). A', B', C' and D' represent the DIC photos of A, B, C and D, respectively.

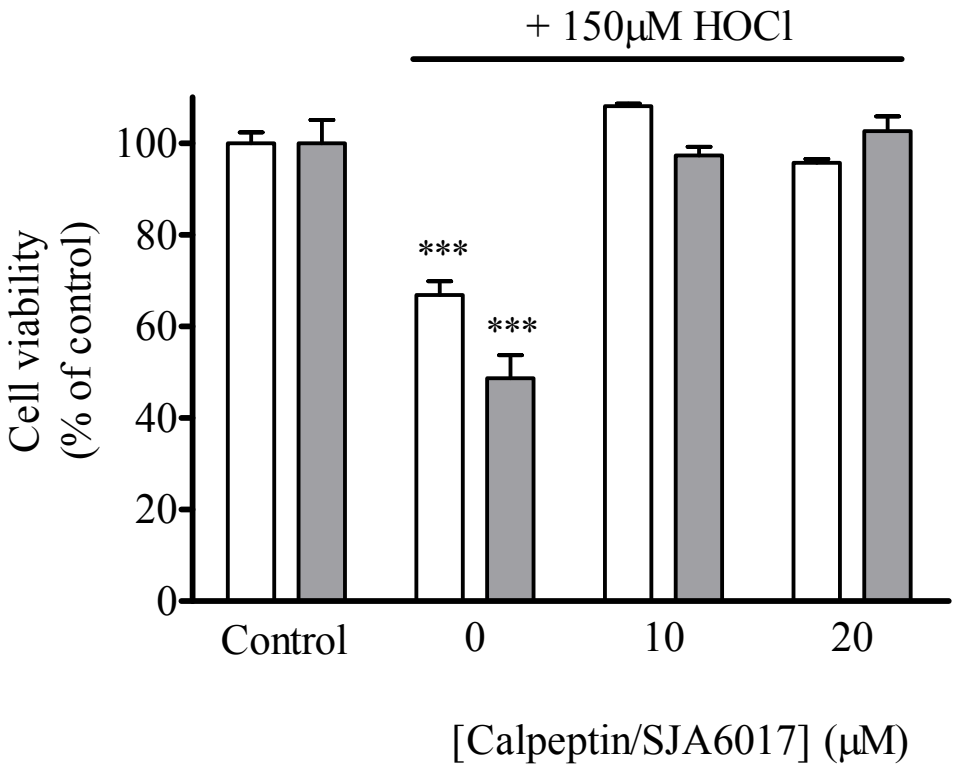

Figure 5.10 Inhibition of calpain enzyme activity prevented HOCl-induced HMDM cell viability loss.
HMDM cells (5×10^6 cells/ml) in 12-well plates were pre-incubated with 0, 10, or 20 μM of the calplain inhibitors calpeptin (white bars) and SJA6017 (gray bars) in Ca^{2+}-enriched EBSS for 1 hour, followed by treatment with or without 150 μM HOCl. After 6 hours, the cells were analysed for cell viability using the MTT reduction assay. Cell viability is presented as a percentage of the respective 0 μM HOCl controls and significance is indicated from the same respective controls.

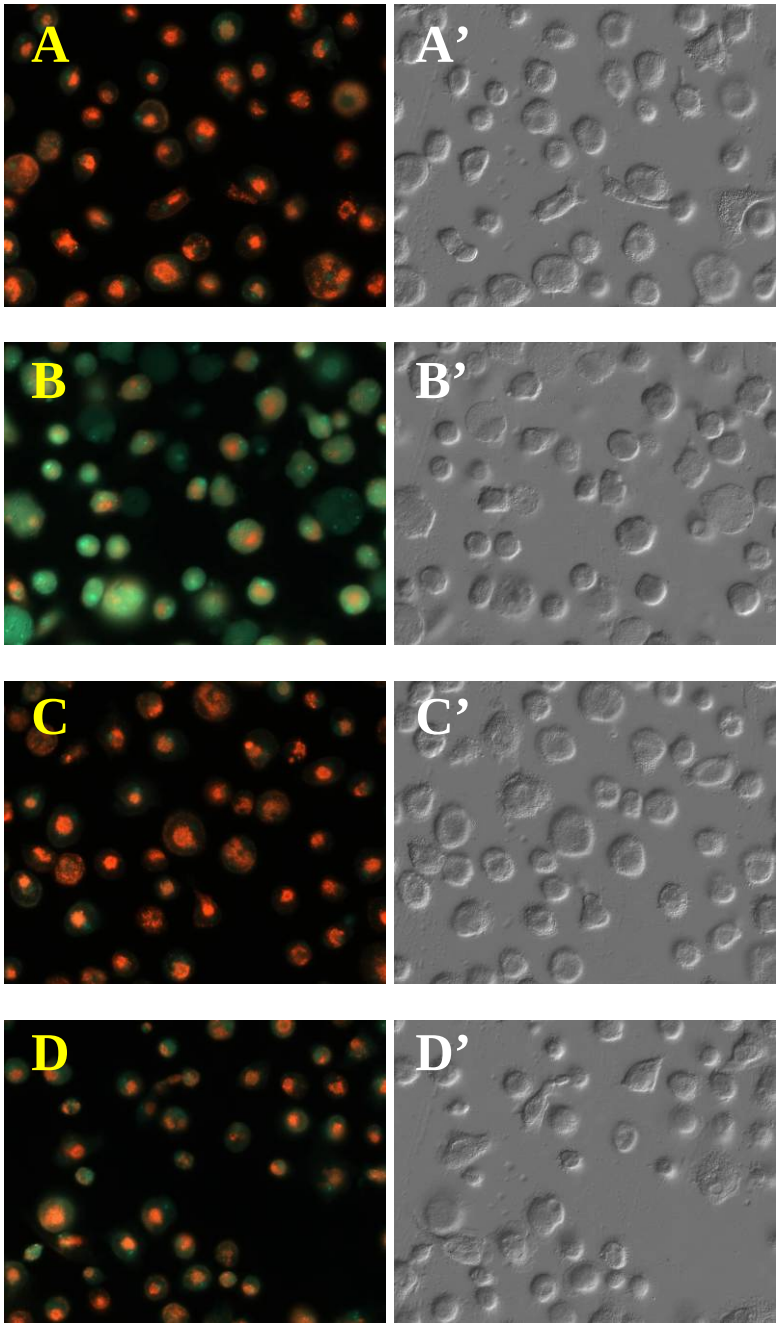

Figure 5.11 Guanabenz and idazoxan prevented HOCl-induced lysosomal destabilization.
HMDM cells (5×10^6 cells/ml) on coverslips were pre-incubated with 0 (**A** and **B**), 10 μM guanabenz (**C**), or 10 μM idazoxan (**D**) in Ca^{2+}-enriched EBSS for 1 hour, followed by treatment with (**B** to **D**) or without (**A**) 150 μM HOCl. After 6 hours, the cells were analysed for lysosomal integrity by probing the cells with 10 μg/ml of AO for 20 minutes and viewing the cells under a fluorescence microscope (λex 487 nm). A', B', C' and D' represent the DIC photos of A, B, C and D, respectively.

5.2.4 Effect of HOCl-induced cytosolic Ca^{2+} increase on mitochondrial membrane potential loss

HOCl has been shown to cause mitochondrial membrane potential loss (**Figure 4.11**). To investigate whether HOCl-induced cytosolic Ca^{2+} increase resulted in mitochondrial membrane potential loss, HMDM cells were treated with HOCl in Ca^{2+}-free EBSS (i.e. in the absence of extracellular Ca^{2+}) or in Ca^{2+}-free EBSS in the presence of dantrolene (i.e. in the absence of both extracellular and cytosolic Ca^{2+}). Mitochondrial membrane potential was then analysed by fluorescence microscopy (**Figure 5.12a**). The fluorescence intensity was converted to numerical values (**Figure 5.12b**). HOCl at 150 μM concentration caused significant loss of mitochondrial membrane potential, indicated by the decreased fluorescence intensity compared to that of the control. Removing extracellular or both extracellular and cytosolic Ca^{2+} during HOCl treatment completely prevented mitochondrial membrane potential loss.

To confirm that it was the cytosolic Ca^{2+} increase that led to mitochondrial membrane potential loss, HMDM cells were treated with Ca^{2+} ionophore A23187 (0-5 μM) and examined for mitochondrial membrane potential (**Figure 5.13**). HMDM cells treated with 5 μM A23187 showed mitochondrial membrane potential loss within 5 minutes, indicating that A23187-induced extracellular Ca^{2+} influx caused mitochondrial membrane potential loss in HMDM cells. Taken together, HOCl-induced cytosolic Ca^{2+} increase was responsible for the mitochondrial membrane potential loss in HMDM cells.

The next question was whether mitochondrial membrane potential loss and the subsequent cell viability loss in HOCl-treated HMDM cells resulted from mitochondria taking up the excess cytosolic Ca^{2+}. The mitochondrial uniporter in HMDM cells for taking up cytosolic Ca^{2+} was blocked using ruthenium red (Kirichok *et al*., 2004) prior to HOCl treatment, followed by mitochondrial membrane potential (**Figure 5.14**) and cell viability (**Figure 5.15**) analyses. HMDM cells treated with HOCl alone showed decreases in mitochondrial membrane potential and cell viability by approximately 80 and 53% compared to the controls, respectively. Ruthenium red at 10 and 50 μM prevented mitochondrial membrane potential loss by approximately 40 and 60%, respectively, and prevented cell viability losses by approximately 9 and 34%, respectively. The results suggest that blocking Ca^{2+} uptake by mitochondria significantly prevented the mitochondrial membrane potential loss and the subsequent cell viability loss in HOCl-treated HMDM cells.

5.12a)

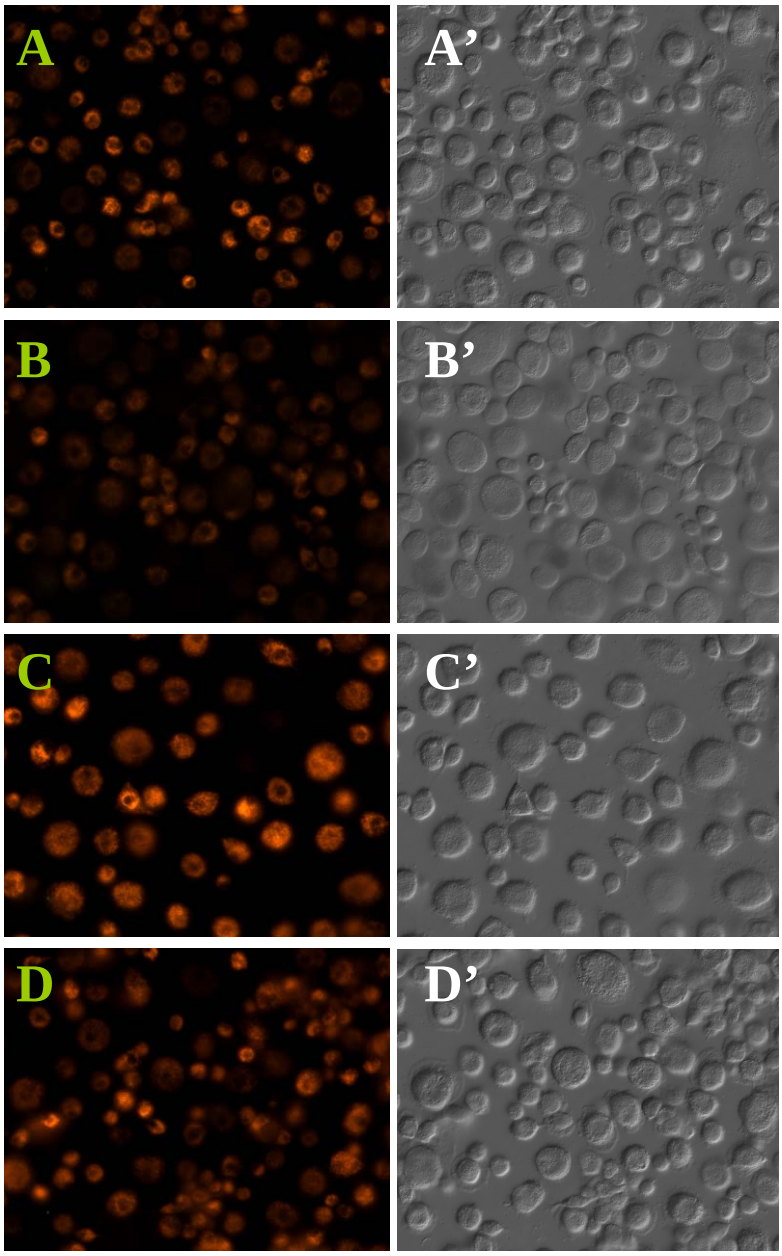

5.12b)

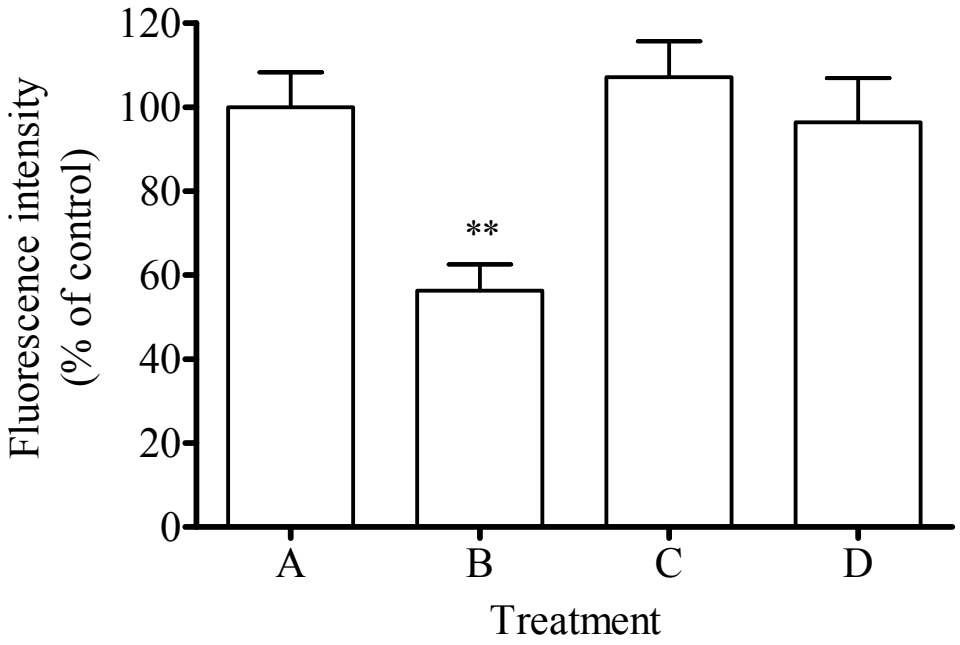

Figure 5.12 Preventing cytosolic Ca^{2+} increase inhibited mitochondrial membrane potential loss in HOCl-treated HMDM cells.
a) HMDM cells (5×10^6 cells/ml) on coverslips were pre-incubated with 100 nM of TMRM in the presence (**D**) or absence (**A** to **C**) of 10 μM dantrolene for 30 minutes. The cells were then treated with Ca^{2+}-enriched EBSS (**A**), 150 μM HOCl in Ca^{2+}-enriched EBSS (**B**), 150 μM HOCl in Ca^{2+}-free EBSS (**C**), and 150 μM HOCl in Ca^{2+}-free EBSS containing 10 μM dantrolene (**D**) for 10 minutes. Subsequently, mitochondrial membrane potential of the cells was detected by viewing under a fluorescence microscope (λex/λem = 548/574nm). A', B', C' and D' represent the DIC photos of A, B, C and D, respectively. **b)** The numerical values of the fluorescence intensities are presented as percentage of the 0 μM HOCl control **(A)**. Significance is indicated from the 0 μM HOCl control.

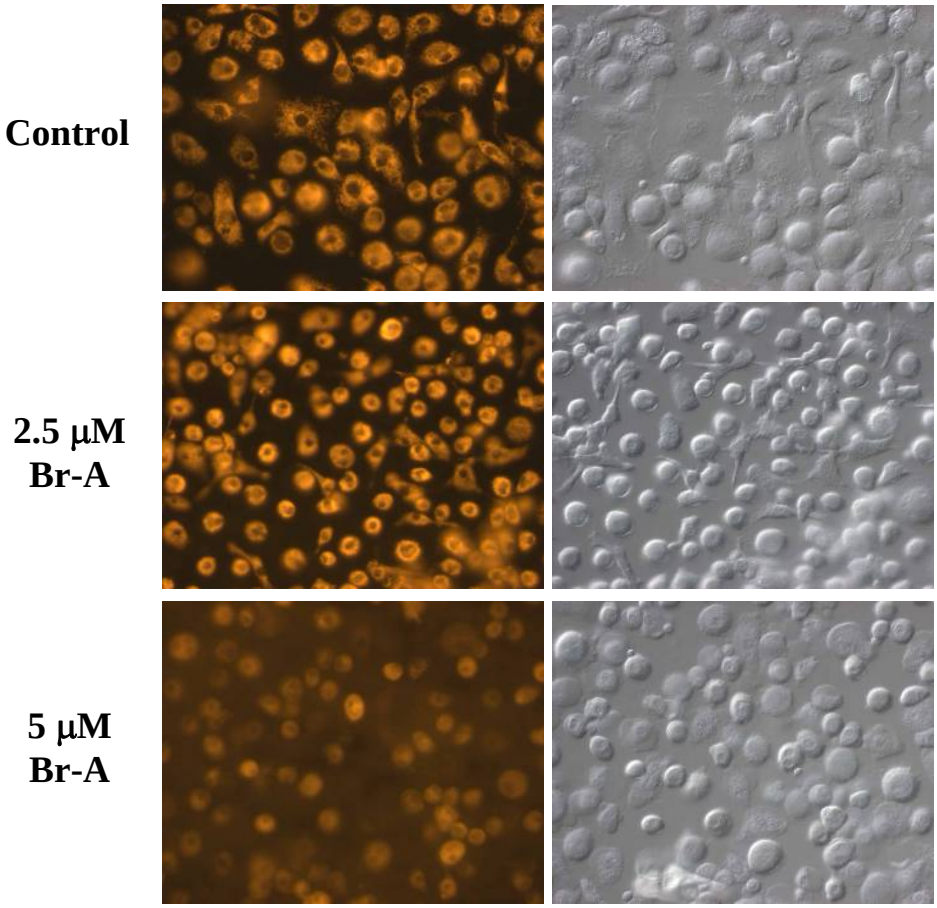

Figure 5.13 A23187-induced cytosolic Ca^{2+} increase caused mitochondrial membrane potential loss in HMDM cells.
HMDM cells (5×10^6 cells/ml) on coverslips were pre-incubated with 100 nM TMRM for 30 minutes, followed by treatment with or without 2.5 or 5 μM Ca^{2+} ionophore A23187 in Ca^{2+}-enriched EBSS buffer for 5 minutes. The cells were subsequently viewed under a fluorescence microscope with 40× magnification (λex/λem = 548/574nm).

5.14a)

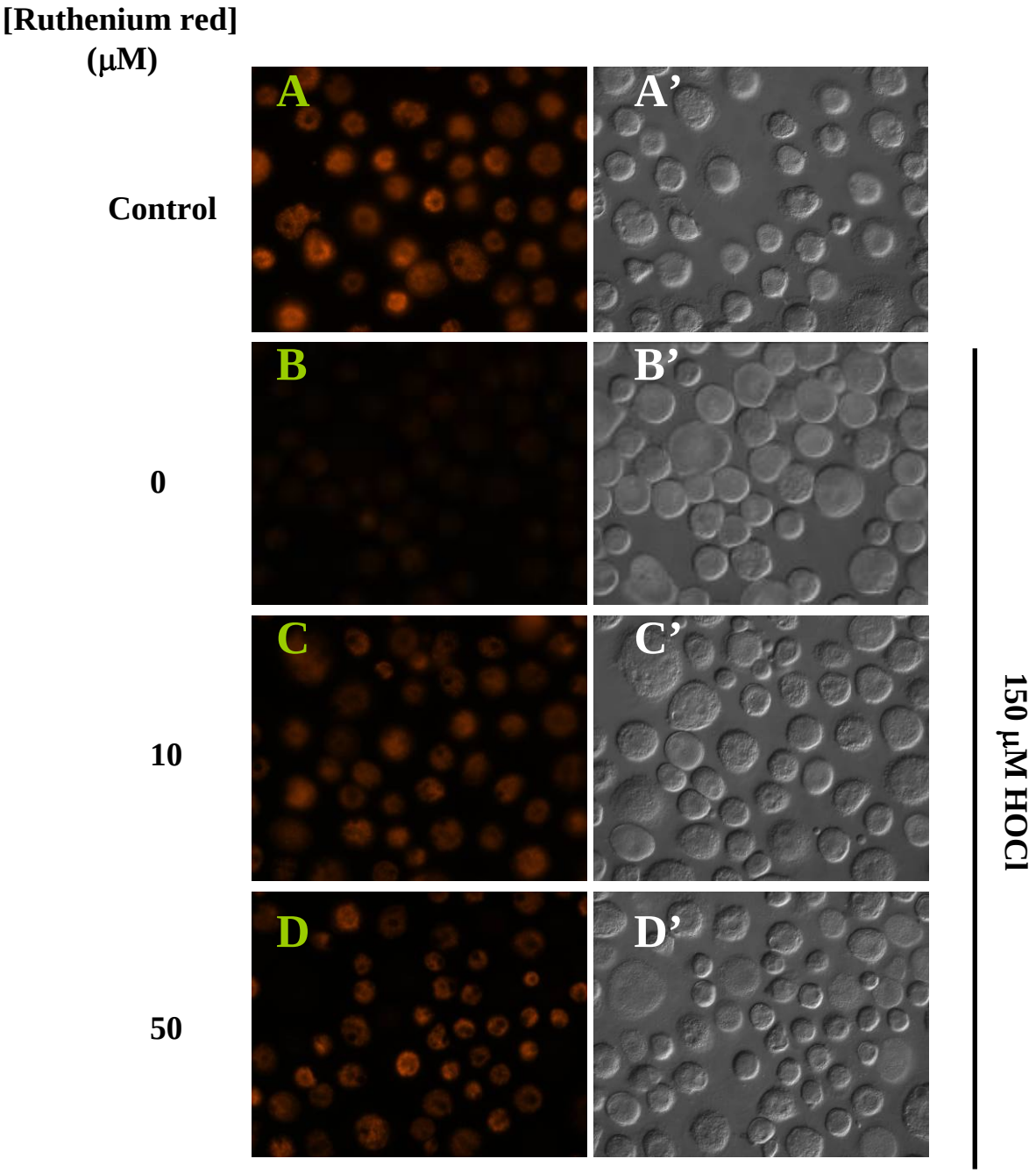

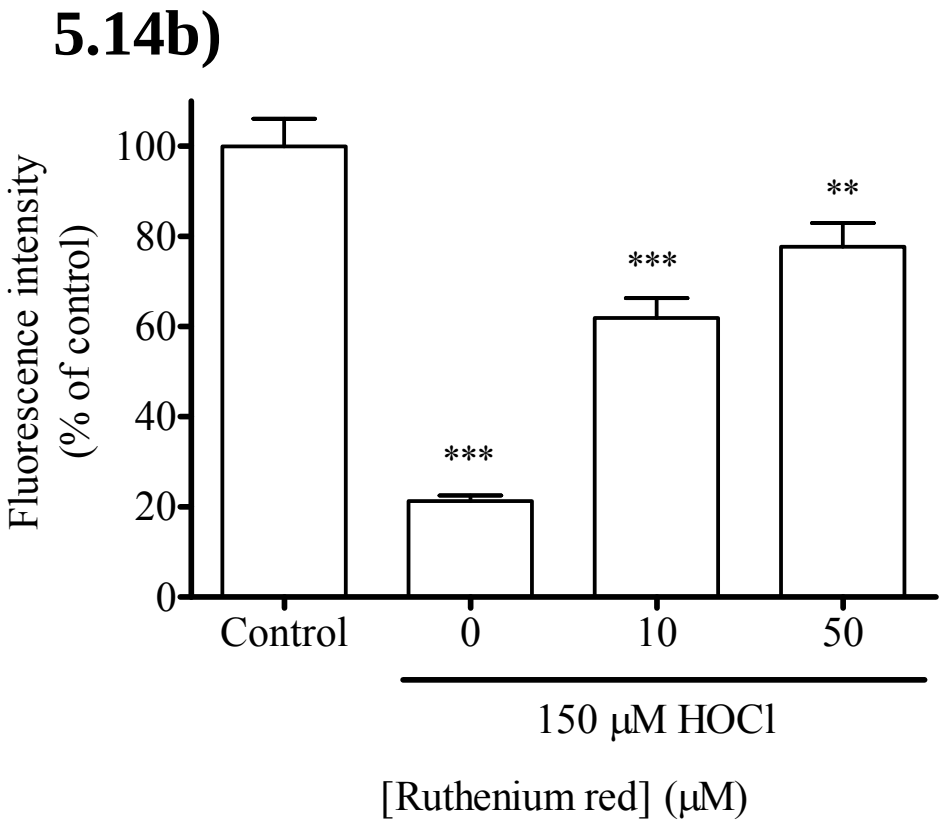

Figure 5.14 Effect of preventing Ca^{2+} uptake by mitochondria using ruthenium red on HOCl-induced HMDM mitochondrial membrane potential loss.
a) HMDM cells (5×10^6 cells/ml) on coverslips were pre-incubated with 100 nM of TMRM in the presence (**C** and **D**) or absence (**A** and **B**) of 10 μM or 50 μM ruthenium red for 30 minutes. The cells were then treated with Ca^{2+}-rich EBSS (**A**), 150 μM HOCl in Ca^{2+}-enriched EBSS (**B**), and 150 μM HOCl in Ca^{2+}-enriched EBSS containing 10 μM (**C**) or 50 μM (**D**) ruthenium red for 10 minutes. Mitochondrial membrane potential was examined under a fluorescence microscope. A', B', C' and D' represent the DIC photos of A, B, C and D, respectively. **b)** Fluorescence intensities are converted to numerical values and each data point is presented as a percentage of the control (white bar) **(A)**. Significance is indicated from the same control.

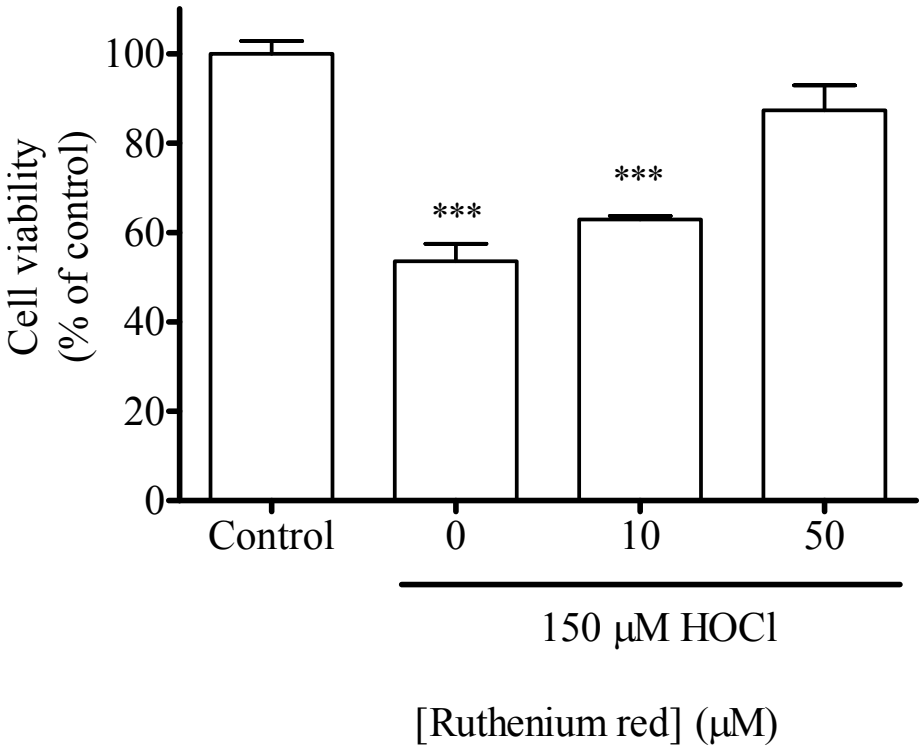

Figure 5.15 Effect of preventing Ca^{2+} uptake by mitochondria using ruthenium red on HOCl-induced HMDM cell viability loss.
HMDMs (5×10^6 cells/ml) were pre-incubated with or without 10 μM or 50 μM ruthenium red in Ca^{2+}-enriched EBSS for 30 minutes. The cells were then treated with Ca^{2+}-enriched EBSS control medium, 150 μM HOCl in Ca^{2+}-rich EBSS, and 150 μM HOCl in Ca^{2+}-enriched EBSS containing 10 μM or 50 μM ruthenium red. Cell viability was measured after 6 hours using the MTT reduction assay. Cell viability is presented as a percentage of the 0 μM HOCl control and significance is indicated from the same control.

The effect of HOCl-induced calpain activation in HMDM cells on mitochondrial membrane potential was examined. HMDM cells treated with 150 μM HOCl alone showed significant mitochondrial membrane potential loss, indicated by the decreased fluorescence intensity. Ten μM calpeptin completely prevented the mitochondrial membrane potential loss in HMDM cells treated with 150 μM HOCl, as indicated by the comparable fluorescence intensity to the control (**Figure 5.16a** and **b**). The result suggests that calpain activation in HMDM cells after HOCl treatment played an important role in causing mitochondrial membrane potential loss.

5.16a)

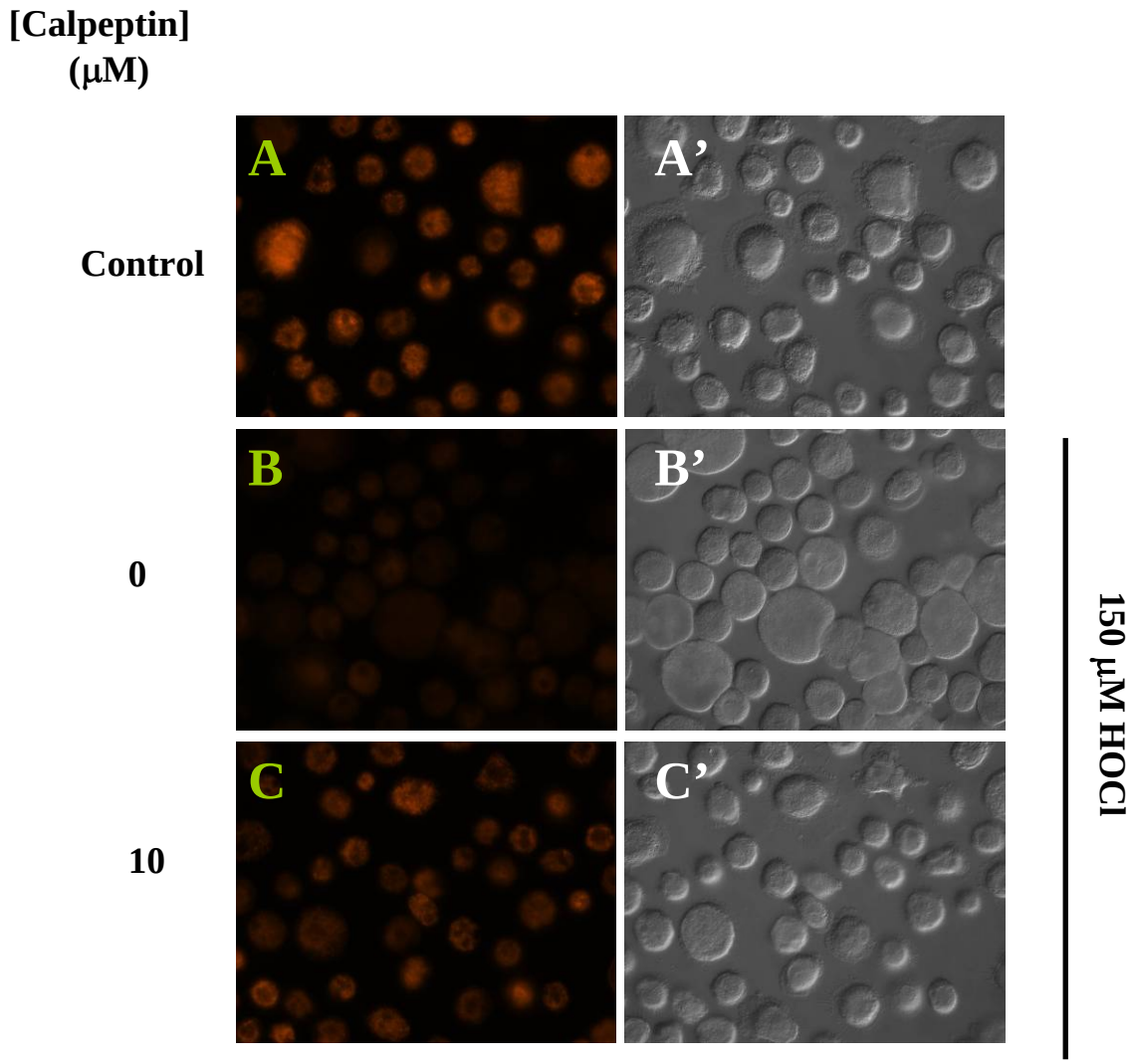

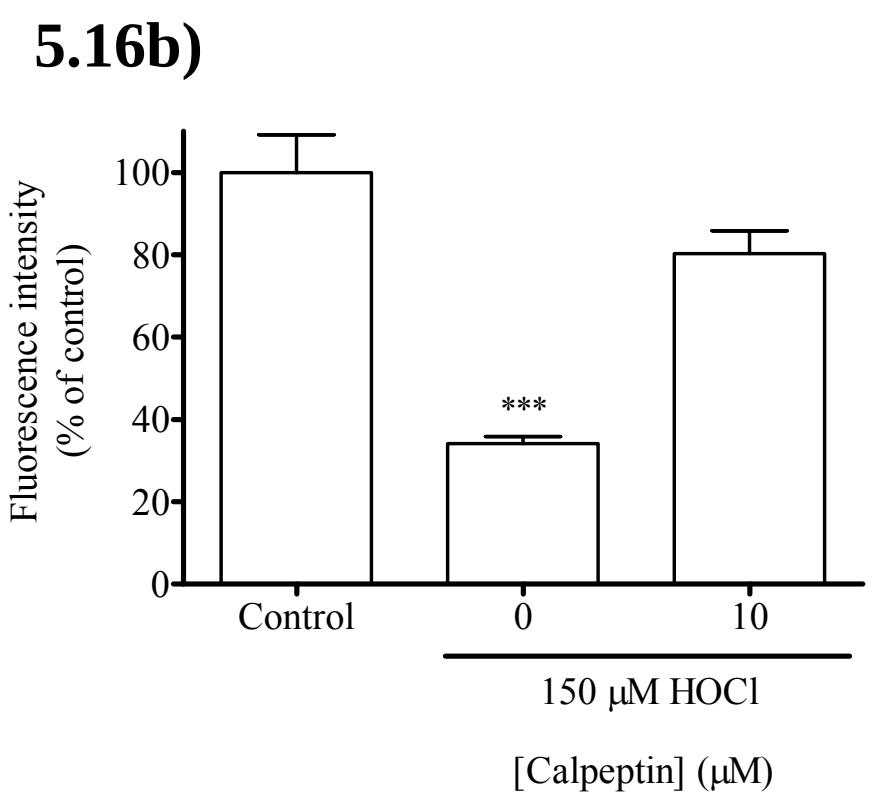

Figure 5.16 Effect of preventing calpain activation in HMDMs using calpeptin on HOCl-induced mitochondrial membrane potential loss.
a) HMDMs (5×10^6 cells/ml) on coverslips were pre-incubated with 100 nM of TMRM in the presence (**C**) or absence (**A** and **B**) of 10 μM calpeptin for 30 minutes. The cells were then treated with Ca^{2+}-enriched EBSS control medium (**A**), 150 μM HOCl in Ca^{2+}-enriched EBSS (**B**), or 150 μM HOCl in Ca^{2+}-enriched EBSS containing 10 μM calpeptin (**C**) for 10 minutes. Mitochondrial membrane potential was subsequently examined under a fluorescence microscope. A', B' and C' represent the DIC photos of A, B and C, respectively. **b)** Fluorescence intensities are converted to numerical values. Each data point is presented as a percentage of the control **(A)** and significance is indicated from the same control.

Since calpain activation is important in mediating mitochondrial membrane potential loss (**Figure 5.16**) and lysosomal destabilization (**Figures 5.8** and **5.9**), it was possible that calpains caused mitochondrial membrane potential loss that resulted in lysosomal destabilization. To investigate this possibility, HMDM cells were treated with 150 μM HOCl in the presence of 10 μM cyclosporin A (CSA) to block MPT activation, followed by lysosomal stability analysis using AO. While HOCl-treated HMDM cells in the absence of CSA showed significant lysosomal destabilization (indicated by the decreased intensity of red fluorescence), HOCl-treated cells in the presence of CSA prevented lysosomal destabilization (**Figure 5.17**). This indicates that MPT activation and mitochondrial membrane potential loss resulted in lysosomal destabilization; calpain enzymes might be mediating these events. This will be further discussed in **section 5.3**.

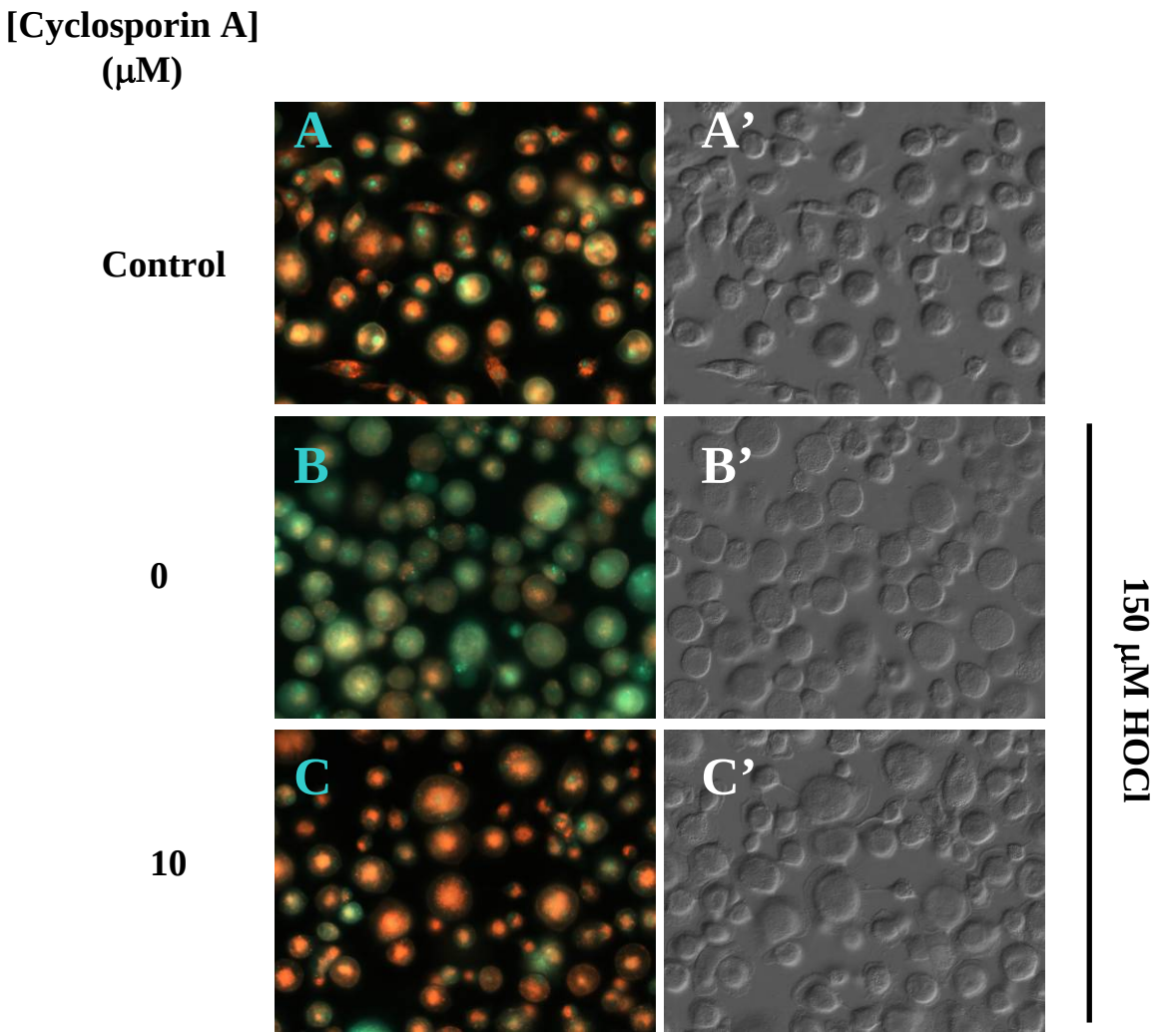

Figure 5.17 Effect of preventing MPT by CSA on lysosomal destabilization in HOCl-treated HMDM cells.
HMDM cells (5×10^6 cells/ml) on coverslips were pre-incubated in the presence (**C**) or absence (**A** and **B**) of 10 μM CSA in Ca^{2+}-enriched EBSS for 30 minutes, followed by treatment with (**B** and **C**) or without (**A**) 150 μM HOCl. After 6 hours, the cells were analysed for lysosomal integrity by probing the cells with 10 μg/ml of AO for 20 minutes and viewing the cells under a fluorescence microscope (λex 487 nm). A', B' and C' represent the DIC photos of A, B and C, respectively.

5.3 Discussion

The possible mechanism(s) of HOCl-mediated necrotic cell death in HMDM cells in relation to cytosolic Ca^{2+} increase, calpain activation, lysosomal destabilization and MPT activation is summarized below (**Figure 5.18**), which will be discussed in the following sections.

5.3.1 Effect of HOCl on cytosolic Ca^{2+} increase and the subsequent effect on cell viability

HOCl induced cytosolic free Ca^{2+} to increase significantly in a concentration-dependent manner above 50 μM HOCl (**Figure 5.1a**). The source of this Ca^{2+} increase was mainly from intracellular stores when the HOCl concentrations were 100 μM or less. Above 100 μM HOCl, the extracellular Ca^{2+} also contributed to the rise in cytosolic Ca^{2+} (**Figure 5.1**). This result agrees with a number of other studies that used different types of cells treated with different oxidants (including HOCl) or toxins, which showed cytosolic Ca^{2+} increases (Yap *et al.*, 2006; Mishra *et al*. 2006, Vindis *et al*. 2004; Aguilar *et al*., 1996; Weber *et al*., 2005; Escargueil-Blanc *et al*., 1994; Hurne *et al*., 2002). The cytosolic Ca^{2+} increase occurred rapidly within 10 minutes of HOCl treatment, corroborating with the almost immediate cytosolic Ca^{2+} increase observed in neuronal cells treated with HOCl (Yap *et al*., 2006). Cell swelling and cell membrane disruption was more evident at HOCl concentrations above 100 μM in Ca^{2+}-enriched EBSS buffer (**Figures 5.1a**). This indicates that cytosolic Ca^{2+} needed to reach a certain level to cause the observed morphological changes, and that level could only be reached when both intracellular and extracellular sources of Ca^{2+} were contributing to the cytosolic Ca^{2+} pool.

The Ca^{2+} ionophore A23187 caused a concentration-dependent increase in cytosolic Ca^{2+} level, cell swelling and cell membrane disruption (**Figures 5.2**), and the percentages of fluorescence intensity increases after treatment with 3-7 μM A23187 (26-58% of the control) were within the similar range as those after 100-200 HOCl treatment (25-69% of the control). This indicates that the observed increase in fluorescence intensity in HOCl-treated HMDM cells was possibly due to the cytosolic Ca^{2+} reacting with the Fluo-3-AM ester dye, not HOCl reacting with the dye. Moreover, since cytosolic Ca^{2+} increase after A23187 treatment also resulted in cell swelling and cell membrane disruption, this implies

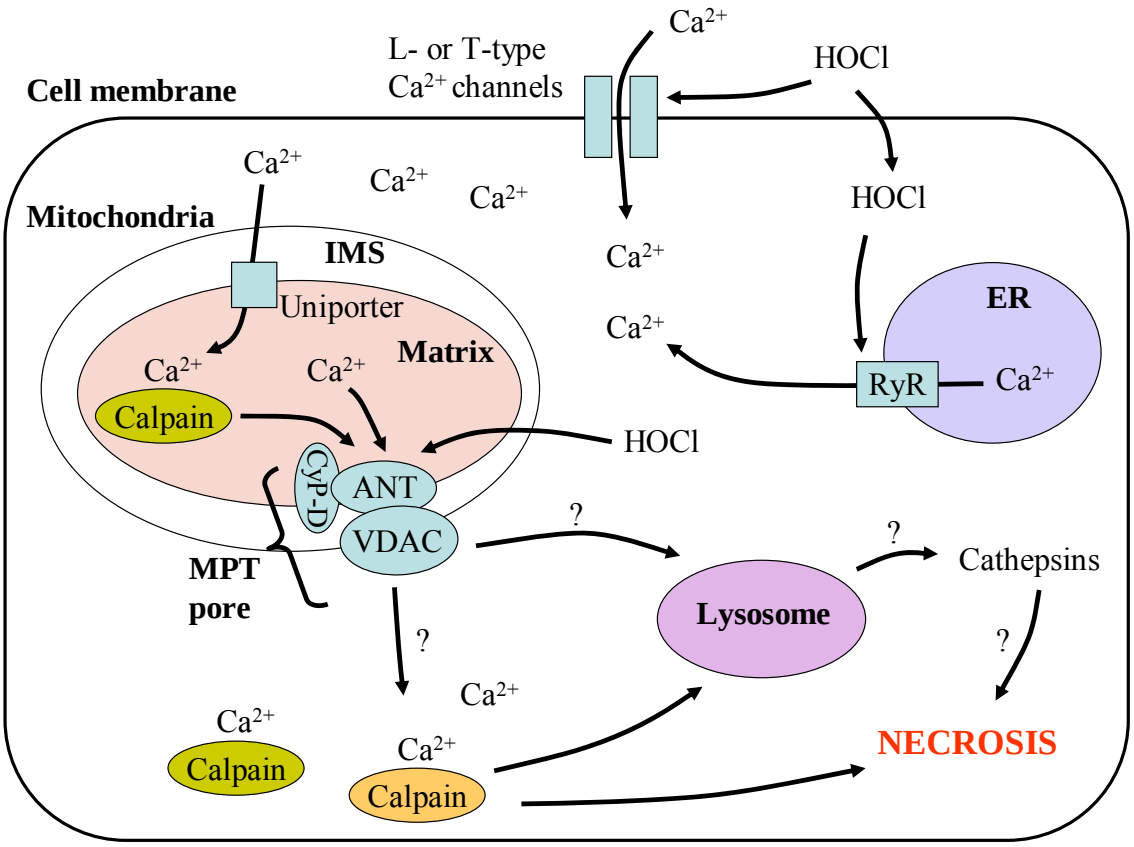

Figure 5.18 Proposed mechanism of HOCl-mediated cytotoxicity to HMDM cells. HOCl activates the voltage-dependent L- and T-type calcium ion (Ca^{2+}) channels on cell membrane resulting in Ca^{2+} influx. HOCl also passes through cell membrane to activate ryanodine receptors (RyRs) on endoplasmic reticulum (ER) membrane releasing Ca^{2+} from ER into cytosol. Both events lead to cytosolic Ca^{2+} increase. The excess Ca^{2+} in cytosol can be taken up into the mitochondrial matrix via Ca^{2+} uniporter on the inner mitochondrial membrane (IMM). Ca^{2+} accumulation in mitochondrial matrix possibly activates matrix calpains, causing transformation of adenine nucleotide translocase (ANT) that favours mitochondrial permeability transition (MPT) pore opening. Ca^{2+} and HOCl may also work together to induce ANT transformation and activate MPT. MPT activation results in mitochondrial membrane potential loss, which may lead to the outer mitochondrial membrane (OMM) rupture. The rupture will release apoptotic factors, Ca^{2+}, possibly the activated mitochondrial matrix calpains (green) and other unknown factors. The released Ca^{2+} may activate more calpains in cytosol (orange). Together with the matrix calpains, they may lead to necrotic cell death possibly by degrading cytoskeletal proteins, leading to cell membrane blebbing and rupture. Calpains can also destabilize lysosomes, resulting in the release of cathepsin proteases that may degrade cellular components. There may also be some unknown factors released by mitochondria that may trigger cytosolic calpain activation or lysosomal destabilization. The arrows with "?" indicates that either the pathways are a hypothesis or are not investigated in this research.

that the morphological changes in HMDM cells after HOCl treatment were possibly caused by cytosolic Ca^{2+} increase, not due to HOCl damaging cell membranes directly.

The studies with Ca^{2+} channel blockers and Ca^{2+} chelator showed that extracellular Ca^{2+} entered HMDM cells upon HOCl treatment mainly through the L- and T-type Ca^{2+} ion channels in HMDM plasma membrane, while intracellular Ca^{2+} was mainly released from ER through the RyR receptors in the ER membrane (**Figures 5.5**). These results agreed with Yap *et al*. (2006), who demonstrated activation of L-type Ca^{2+} ion channels in plasma membranes and dantrolene-sensitive Ca^{2+} ion channels in ER membranes in neuronal cells upon HOCl treatment. However, the cytosolic Ca^{2+} increase was never completely prevented using any of the Ca^{2+} channel blockers or Ca^{2+} chelator, suggesting that cytosolic Ca^{2+} accumulation might also occur through other pathway(s). HOCl was previously found to inactivate Na^{+}-Ca^{2+}-ATPase (Eley *et al*., 1991) and Na^{+}-K^{+}-ATPase (Kato *et al*., 1998). Na^{+}-Ca^{2+}-ATPase functions by expelling one Ca^{2+} from cytosol into extracellular space with one Na^{+} entering the cell down its gradient, whereas Na^{+}-K^{+}-ATPase expels excess Na^{+} from cytosol to extracellular medium to create a Na^{+} gradient across the cell membrane. The inactivation of Na^{+}-K^{+}-ATPase would then disturb the Na^{+} gradient across the plasma membrane and affect the Na^{+}-Ca^{2+}-ATPase. Inactivation of both enzymes would therefore result in Ca^{2+} accumulation in the cytosol.

The opening of Ca^{2+}-channels in the plasma membrane can occur via plasma membrane depolarization. Plasma membrane depolarization in cardiocytes caused by voltage-gated Na^{+}-channels activation resulted in inward Na^{+}-current, which facilitates L-type Ca^{2+}-channels on the plasma membrane (Maack and O'Rourke, 2007). The activity of voltage-gated Na^{+}-channels and plasma membrane potentials in HMDM cells after HOCl treatment should be examined in the future to validate this hypothesis. It is also possible that HOCl activated the L-type Ca^{2+} channels by interacting with the essential thiols within the protein complex. This is supported by the fact that the thiol oxidizing agent 5,5'-Dithio-bis(2-nitrobenzoic acid) (DTNB) up-regulated L-type Ca^{2+} channels at the extracellular face of the cell membrane (Campbell *et al.*, 1996). The same study hypothesized that an allosteric thiol-containing "redox switch" is present on the L-type Ca^{2+} channel subunit complex. Contradictory to this hypothesis, cumene hydroperoxides and H_2O_2 were shown to decrease Ca^{2+} current through the L-type Ca^{2+} channels (Gill *et al.*, 1995; Goldhaber *et al*., 1989). This discrepancy might be due to different oxidants exerting different effects on the L-type Ca^{2+} channels, resulting in different regulation mechanisms. HOCl (10-40 μM)

was also found to decrease Ca^{2+} current through the L-type Ca^{2+} channels in ventricular cardiomyocytes (Hammerschmidt and Wahn, 1998). However, the researchers did not address whether the amount of HOCl used caused the onset of apoptosis. Non-lethal HOCl concentrations of HOCl have been reported to cause growth arrest (Vissers *et al*., 1999) and enhance cell survival (Midwinter *et al*., 2001). Moreover, carbon monoxide protects cardiomyogenic cells against ischemic death through L-type calcium channel inhibition (Uemura *et al.*, 2005). Therefore, it is possible that low HOCl concentrations inhibited L-type calcium channels as a protective mechanism.

Ca^{2+} release from ER can be caused by Ca^{2+} influx from extracellular medium triggering the opening of the ryanodine receptor (RyR2 subtype) in the ER membrane, inducing the release of Ca^{2+} from the ER (a process called Ca^{2+}-induced Ca^{2+}-release) (Maack and O'Rourke, 2007). This was less likely the scenario in HOCl-treated HMDM cells, as incubation of HMDM cells with HOCl in the absence of Ca^{2+} in extracellular medium (i.e. no Ca^{2+} influx to trigger the RyR2 channel opening) still showed cytosolic Ca^{2+} increase (**Figure 5.1**). More likely, HOCl interacted with the essential thiols within the RyR protein, leading to RyR activity. Favero *et al*. (2003) have shown that HOCl activated RyR protein on skeletal muscle SR and induced Ca^{2+} release by targeting the critical thiol groups for RyR protein function. Similarly, Sun *et al*. (2001) demonstrated that oxidation of up to 10 thiol groups does not modify RyR activity, while oxidation of an additional 10–15 thiol groups reversibly stimulates RyR activity. Thiol oxidizing agents and ROS (such as superoxide radicals and hydroxyl radicals) could also activate RyR receptors (Eager and Dulhunty, 1998; Marengo *et al.*, 1998; Zima *et al*., 2004; Anzai *et al.*, 1998).

The cytosolic Ca^{2+} increase from intracellular sources (i.e. HMDM cells treated with HOCl in the absence of extracellular Ca^{2+}) plateaued at 100 μM HOCl (**Figure 5.1**). Similar result was also observed in a previous study, which showed that the amount of Ca^{2+} released from SR plateaued above 400 μM HOCl (Favero *et al.,* 2003). The same study suggested that higher HOCl concentrations (above 100 μM) activated the RyR receptor initially, followed by inhibition. This could also be the case in HMDM cells treated with HOCl above 100 μM, resulting in the cytosolic Ca^{2+} level plateauing.

5.3.2 Effect of HOCl-induced cytosolic Ca^{2+} increase on cell viability

The question then becomes, is the observed cytosolic Ca^{2+} increase responsible for the HOCl- mediated necrotic cell death. HOCl treatment in the presence of the Ca^{2+} chelating agent EGTA prevented HMDM cell viability loss completely (**figure 5.6**). This suggests that HOCl-induced cytosolic Ca^{2+} rise was responsible for the cell viability loss. To further support this conclusion, HOCl treatment with Ca^{2+} influx inhibited (by using Ca^{2+}-free EBSS buffer or L- and T-type Ca^{2+} channel blockers) also prevented HMDM cell viability loss (**Figures 5.6** and **5.3**). However, the inhibition was not complete, indicating that Ca^{2+} was released from intracellular sources (such as ER) into cytosol resulting in cell death, and/or HOCl caused cell death via other pathways. Surprisingly, HOCl treatment with Ca^{2+} release from ER blocked (by using RyR blocker dantrolene) completely prevented cell viability loss (**Figure 5.6**). This agrees with Yap *et al*. (2006), who showed complete prevention of Ca^{2+}-mediated cell viability loss using dantrolene. Although dantrolene is generally known as a blocker of RyR receptor on ER/SR so blocking the release of Ca^{2+}, it is possible that it has other unknown functions that prevent Ca^{2+} influx. Even though HOCl-induced cytosolic Ca^{2+} increase appeared to play an important role in HMDM necrotic cell death, HOCl at higher concentration (200 μM) reacted non-specifically with cellular components contributing to HMDM necrotic cell death (**Figure 5.3**).

A23187-treated HMDM cells in the presence of extracellular Ca^{2+} displayed cell swelling and cell membrane rupture (**Figure 5.2**) and concentration-dependent cell viability loss (above 3 μM) with no latent cell death observed (**Figure 5.4**). The similarities between HOCl- and A23187-mediated HMDM cell deaths further implicate that HOCl-induced cytosolic Ca^{2+} increase causes a rapid necrotic cell death. A23187 at 7 μM concentration did not cause any further cytosolic Ca^{2+} increase (**Figure 5.2**), while cell viability was decreased further (**Figure 5.4**). This was possibly due to a limitation to the maximum fluorescence intensity that can be detected by the fluorescence microscopy. Furthermore, although 10 μM Fluo-3 was applied to the cells, the actual amount of Fluo-3 that moved into cells and the actual level of cytosolic Ca^{2+} increase were unknown. It is possible that the cytosolic Ca^{2+} concentration has reached the upper limit of the actual Fluo-3 concentration in the cytosol.

5.3.3 Effect of HOCl-mediated cytosolic Ca^{2+} increase on calpain activation and lysosomal destabilization

Alteration of Ca^{2+} homeostasis can lead to the activation of calpains, which are a class of Ca^{2+}-dependent cysteine proteases. μ-Calpain and m-calpain (the two ubiquitous forms) are activated by micromolar and millimolar concentrations of Ca^{2+} *in vitro*, respectively (Saido *et al*., 1994b). The next question is, therefore, whether HOCl-induced cytosolic Ca^{2+} increase leads to calpain activation in HMDM cells.

Lysosomal stability was examined in this research as an indicator of calpain activation, as activated calpains were shown to mediate lysosomal disruption (Yamashima, 2004). HOCl caused rapid lysosomal destabilization in HMDM cells within 10 minutes (no further destabilization was observed over time) (**Figure 5.7**), which was prevented significantly using the calpain inhibitors calpeptin and SJA6017 (inhibit both μ- and m-calpains) (**Figures 5.8** and **5.9**). Although SJA6017 inhibits both μ- and m-calpains, it preferentially inhibited m-calpains (Fukiage *et al.*, 1997). This implies that both μ- and m-calpains were activated in HOCl-treated HMDM cells. Furthermore, stabilizing lysosomes with guanabenz or idazoxan (Choi *et al.*, 2002; Cheung *et al*., 2007; Yap *et al*., 2006) prior to HOCl treatment prevented lysosomal destabilization (**Figure 5.11**). Taken together, these results indicate that HOCl mediated calpain activation, which preceded and induced lysosomal destabilization. This is in agreement with Yap *et al*. (2006), who also demonstrated lysosomal destabilization downstream of HOCl-mediated calpain activation in neuronal cells.

How exactly activated calpains cause lysosomal destabilization and how guanabenz and idazoxan stabilize lysosomes is not yet fully understood. Activated calpains have been found in disrupted lysosomal membranes in hippocampal neurons of primates after acute ischemia (Yamashima, 2004). This observation led to the hypothesis that calpains compromise the integrity of lysosomal membranes, causing leakage of their acidic contents into the cytoplasm. Alternatively, both lysosomal stabilizers guanabenz and idazoxan share the preferential affinity for the imidazoline-2 receptors, bind to α2-adrenergic receptors, and block N-methyl-d-aspartate (NMDA)-receptor channels (Cheung *et al.*, 2007). It was, therefore, proposed in this research that calpains cleaved the receptors that guanabenz and idazoxan acted on, resulting in lysosomal destabilization.

HOCl treatment in the presence of calpeptin or SJA6017 also prevented HOCl-mediated HMDM cell viability loss completely (**Figure 5.10**), indicating that HOCl-mediated calpain activation consequently led to necrotic cell death in HMDM cells. Calpain activation may lead to necrotic cell death via a number of pathways. As mentioned above, HOCl-mediated calpain activation induced lysosomal destabilization in HMDM cells (**Figures 5.8, 5.9** and **5.11**). This destabilization might have resulted in HMDM cell viability loss by releasing the hydrolytic enzymes, such as cathepsins, which digest the cell's own cytoplasm and cause cell death. For example, the activity of cathepsin L and its cytosolic expression are increased in β-amyloid (Aβ)-mediated neuronal apoptosis (Boland and Campbell, 2004). Elevated levels of lysosomal cathepsin D are also observed in the early stages of Alzheimer's disease (AD) and co-localize with intraneuronal tangles. In addition, cathepsin S is up-regulated in AD brain, and cathepsin S contributes to the generation of Aβ in the lysosomal compartment (Munger *et al.*, 1995). Yap *et al*. (2006) have shown that the release of cathepsins D and L from lysosomes appeared to be important in causing HOCl-induced neurotoxicity as their inhibitors fully prevented the onset of apoptosis. However, HOCl caused cleavage of cathepsin G (Shao *et al.*, 2005), suggesting that HOCl can also have a direct effect on other cathepsin proteases. Furthermore, 0.4 μmol/L cathepsin G induced injury to human umbilical vein endothelial cell (HUVEC) shape and F-actin cytoskeleton within 15 minutes, yet cell viability loss did not occur even after 6 hours (Iacoviello *et al*., 1995). This latent cell death did not fit the rapid HOCl-induced cell death observed in HMDM cells. Hence, whether cathepsins were released after lysosomal destabilization and whether they were responsible for HOCl-mediated necrotic cell death requires further investigation.

The activated calpains could also contribute to HOCl-mediated necrotic cell death by themselves. Calpains have been found to proteolytically cleave cytoskeletal proteins in hippocampal neurons (Lee *et al*., 1991) and gerbil forebrain (Yokota *et al*., 2003) within minutes of ischemia, and in rat hepatocytes after exposure to tert-butyl hydroperoxide (Miyoshi *et al*., 1996). Degrading of cytoskeletal proteins can result in necrotic cell death by promoting bleb formation and rupture (Saido *et al*., 1994b). It is very likely that HOCl-mediated cytosolic Ca^{2+} increase activates calpains, which in turn degrade cytoskeletal proteins proteolytically, resulting in bleb formation, cell membrane rupture and necrotic cell death. Since HOCl-mediated necrotic cell death in HMDM cells occurred rapidly within 10 minutes, this series of events had to occur within 10 minutes. The rapidness of calpains damaging cytoskeletal proteins (as mentioned above), the significant Ca^{2+} rise

occurring within seconds of HOCl treatment in neuronal cells (Yap *et al*., 2006), and the activation of calpains occurring within 1 minute of Ca^{2+} treatment (Saido *et al*., 1994a) suggest that this series of events could occur within 10 minutes. However, the cytoskeletal protein damage had to be extensive to cause necrotic cell death in such a short period of time. This area requires further investigation.

It is interesting to see that calpains were activated in HOCl-mediated cytotoxicity to HMDM cells. Since calpains require a reduced cysteine residue at the active site to maintain proteolytic activity, cells exposed to oxidative stress should not favour calpain activation. For instance, neurons from rats exposed to hypoglycaemia, which caused a more oxidised intracellular redox state, showed little activated calpains despite of abundant presence of Ca^{2+} (Ferrand-Drake *et al.*, 2003). The same neurons exposed to hypoglycemia followed by a recovery period (i.e. the cellular redox state was normalized) showed significant calpain activation. In addition, Ca^{2+} ionophore ionomycin-mediated calpain activation in human neuroblastoma cells was decreased in the presence of oxidative stress induced by the addition of either doxorubicin or 2-mercaptopyridine *N*-oxide (Guttmann and Johnson, 1998). With these findings in mind, the intracellular redox status was more oxidised in HMDM cells treated with HOCl, which should not have favoured calpain activation even in the presence of excess cytosolic Ca^{2+}. The activation of calpain enzymes observed in HOCl-treated HMDM cells seems to suggest that HOCl might have shown selectivity towards thiol groups in HMDM cells.

5.3.4 Effect of HOCl-mediated cytosolic Ca^{2+} increase on mitochondria

The results in **Chapter 4** showed that HOCl treatment caused MPT-mediated mitochondrial membrane potential loss in HMDM cells. In this chapter, HOCl treatment in the presence of ruthenium red (to prevent Ca^{2+} influx into the mitochondrial matrix by blocking Ca^{2+} uniporter in the IMM) significantly prevented mitochondrial membrane potential loss in HMDM cells (**Figure 5.14**). This suggests that mitochondria taking up Ca^{2+} and Ca^{2+} accumulation in mitochondrial matrix were essential for the observed MPT activation. The conclusion is in agreement with Whiteman *et al*. (2004), who showed that $ONOO^-$-mediated mobilization of Ca^{2+} from the cytosol to the mitochondria led to MPT activation in human articular chondrocytes. Ruthenium red did not prevent increases in cytosolic Ca^{2+} (Whiteman *et al.*, 2004; Trollinger *et al*., 2000), therefore its effect in

preventing mitochondrial membrane potential loss was purely by acting on the Ca^{2+} uniporter.

Mitochondrial membrane potential loss was prevented in HMDM cells treated with HOCl in the absence of extracellular Ca^{2+} or both extracellular and intracellular Ca^{2+} (**Figure 5.12**). This indicates that cytosolic Ca^{2+} rise resulting from the intracellular source alone was not enough to induce MPT-activated mitochondrial membrane potential loss. This is not surprising, as Bianchi *et al*. (2004) have shown that the rate of Ca^{2+} uptake by mitochondria was significant only above a threshold of 200-300 nM Ca^{2+}.

Many mechanisms have been hypothesized to explain how mitochondrial Ca^{2+} leads to MPT activation. One hypothesis suggests that cardiolipin molecules (an important component of inner mitochondrial membrane) were bound in unusually high amounts to the ANT for the normal ANT translocation activity. The negative charges of the cardiolipin headgroups bind to the positive charges, particularly on lysine residues, located in the ANT primarily on the matrix side (Bogner *et al*., 1986). At high concentrations, Ca^{2+} binds to the two phosphate headgroups of cardiolipin and thus releases the positive charges at the ANT interface. The positive charges repulse each other and convert ANT into a large unselective channel, which is a key component in the MTP (Brustovetsky and Klingenberg, 1996).

It is also hypothesized that the sensitivity of MPT pore to Ca^{2+} can be increased by an "inducing agent" such as an oxidizing agent (it is referred to as **the oxidation hypothesis** in this thesis). MPT was demonstrated to be fully inhibited in the complete absence of ROS even in the presence of excess amount of Ca^{2+} (Kowaltowski *et al.*, 2001). However, the mechanisms are not yet fully elucidated. One possible mechanism involves oxidation of thiols on the pore complex in cooperation with Ca^{2+} (Petronilli *et al*., 1994; Costantini *et al*., 1996). Oxidation or cross-linking of critical dithiol(s) in membrane proteins increase its sensitivity to Ca^{2+} that regulates the MPT pore opening (Chernyak *et al*., 1995). Similarly, McStay *et al.* (2002) demonstrated that the oxidation of the ANT molecules caused cross-linking of Cys160 and Cys257, which stabilizes the c conformation of the ANT (a conformation that favours interaction with VDAC), enhances CyP-D binding to the ANT and antagonizes the ADP binding. These effects together greatly sensitize the MPT pore to Ca^{2+}. The alternative mechanism is that Ca^{2+} binds to the matrix side of the IMM and promotes extensive alterations to the conformation of membrane proteins that

change the locations of the thiol groups, which render them more readily oxidized. This leads to cross-linking of membrane protein thiol groups and irreversible MPT formation (Kowaltowski *et al*. 1997).

Mitochondrial Ca^{2+} may also induce MPT pore opening via activation of mitochondrial calpains (it is referred to as **the matrix calpain hypothesis** in this thesis). Investigators have reported calpain-like activities in isolated mitochondria (Aguilar *et al*., 1996; Tavares and Duque-Magalhaes, 1991). Active calpain 10 has been demonstrated in the outer membrane, intermembrane space, and mostly matrix fractions of isolated mitochondria (Arrington *et al*. 2006). The same study also showed that mitochondrial matrix calpain 10 triggered MPT and also damaged two proteins of complex I, NDUFV2 and ND6. Aguilar *et al*. (1996) suggested that mitochondrial calpains activate MPT by cleaving proteins to generate positively charged peptide fragments that may allosterically modulate pore opening by binding at a site that normally binds cations.

It is possible that mitochondrial Ca^{2+} accumulation in HOCl-treated HMDM cells caused all of the above mentioned mechanisms to occur and activate MPT. The oxidation hypothesis is possible because HOCl could have served as the oxidizing agent needed for the MPT activation. Yet, A23157-induced cytosolic Ca^{2+} increase also caused mitochondrial membrane potential loss rapidly even in the absence of HOCl (**Figure 5.13**). It is possible that mitochondrial Ca^{2+} accumulation led to ROS generation in mitochondria, which served as the oxidizing agent needed for MPT activation. In addition, Grijalba *et al.* (1999) have shown that Ca^{2+} alters the lipid organization of the IMM by interacting with the anionic head of cardiolipin molecules. These alterations in membrane organization may affect respiratory chain function, including coenzyme Q mobility, and favor mono-electronic oxygen reduction (i.e. superoxide radical generation) at intermediate steps of the respiratory chain. The same study also showed that this event occurred within 5 minutes of Ca^{2+} treatment to inverted bovine heart submitochondrial particles. The detection of superoxide radicals in HMDM cells immediately after the 10-minute treatment (**Figure 4.13**) supported the mitochondrial Ca^{2+}-mediated ROS generation theory.

The matrix calpain hypothesis is even more plausible than the oxidative hypothesis to explain mitochondrial Ca^{2+}-mediated MPT activation in HOCl-treated HMDM cells. HOCl treatment in the presence of calpeptin prevented mitochondrial membrane potential loss in HMDM cells significantly (**Figure 5.16**), implicating a role of calpains in MPT activation.

Since calpeptin can also prevent mitochondrial matrix calpain-10 activity (Giguere and Schnellmann, 2008; Giguere *et al*., 2008), it was highly possible that mitochondrial Ca^{2+} caused matrix calpain activation that subsequently induced MPT activation. Moreover, matrix calpain-mediated MPT activation in isolated mitochondria was shown to occur in less than 1 minute after Ca^{2+} treatment in isolated mitochondria (Aguilar *et al*., 1996). This implies that this event may occur within the time frame (i.e. within 10 minutes) of MPT-mediated mitochondrial membrane potential loss in HOCl-treated HMDM cells.

It is less possible that cytosolic calpains, rather than mitochondrial calpains, caused MPT activation in HOCl-treated HMDM cells. HOCl treatment in the presence of CSA (i.e. preventing MPT activation) prevented lysosomal destabilization in HMDM cells (**Figure 5.17**). If cytosolic calpains were activated upstream of MPT activation, those calpains could have destabilized lysosomes in cytosol before or at the same time as the MPT activation, and CSA treatment should have not been able to prevent lysosome destabilization completely. This theory agrees with Ding *et al*. (2002), who showed that CSA prevented toxin-induced calpain activation and suggested that calpain activation may be a post-mitochondrial event (Ding *et al*., 2002). Hence, calpeptin and SJA6017 prevented cell viability loss and lysosomal destabilization (**Figures 5.8-5.10**) could be due to these calpain inhibitors preventing mitochondrial calpain activation. The inhibition of mitochondrial calpain activation then prevented MPT activation, cytosolic calpain activation and lysosomal destabilization. However, there is currently no documentation on whether SJA6017 can prevent mitochondrial calpains. Further studies are required for validation of the above hypothesis; the time line of mitochondrial and cytosolic calpain activation, and MPT activation.

The above hypothesis leads to the questions why cytosolic calpains were not activated before MPT activation and how do MPT activation and the subsequent mitochondrial membrane potential loss lead to cytosolic calpain activation. One possibility is that the cytosolic volume diluted the increased Ca^{2+} concentration in HOCl-treated HMDM cells, preventing the cytosolic Ca^{2+} concentration reaching the required level for cytosolic calpain activation. One future direction is to measure cytosolic Ca^{2+} concentration in HMDM cells upon HOCl treatment to see whether it reaches the level required for cytosolic calpain activation. The excess Ca^{2+} may then diffuse into IMS of mitochondria via VDAC, and taken up into the mitochondrial matrix via the Ca^{2+} uniporter (Maack and O'Rourke, 2007). Since mitochondrial volume is supposed to be less than the cytosolic

volume, Ca^{2+} concentrations in matrix or IMS should be able to reach high concentrations easily in comparison to Ca^{2+} concentrations in the cytosol. Hence, mitochondrial calpains may be more easily activated than cytosolic calpains. The activated mitochondrial calpains then cause MPT activation, mitochondrial membrane potential loss, matrix swelling, and mitochondrial outer membrane rupture. This series of events may result in the release of Ca^{2+} and other unknown factors from the mitochondria into the cytosol, which can activate cytosolic calpains. Activated mitochondrial calpains may also be released into the cytosol. Consequently, necrotic cell death ensues.

The presence of ruthenium red during HOCl treatment also prevented cell viability loss in HMDM cells (**Figure 5.15**). As mentioned in **Chapter 4**, blocking MPT activation (by using CSA) prevented HOCl-induced cell viability loss. Together these results imply that mitochondrial Ca^{2+}-mediated MPT activation resulted in HOCl-mediated necrotic cell death in HMDM cells. However, ruthenium red did not prevent cell viability loss completely, suggesting other mechanisms might also be at work inducing MPT activation. Since calpains are also found in intermembrane space of mitochondria (Tavares and Duque-Magalhaes, 1991), it is possible Ca^{2+} diffused to the intermembrane space via VDAC and activated calpains there, which somehow triggered MPT. Moreover, MPT might have been activated via Ca^{2+} binding to an extramitochondrial site. Mitochondrial membrane permeabilization induced by phenylarsine oxide is inhibited by EGTA, but not by ruthenium red. This result suggests that phenylarsine oxide leads to MPT through a mechanism independent of matrix Ca^{2+}, but dependent on Ca^{2+} binding to an extramitochondrial site (Kowaltowski *et al.*, 1997).

5.4 Conclusion

In **Chapters 3** and **4**, it was shown how HOCl-treated HMDM cells underwent rapid MPT-mediated mitochondrial membrane potential loss, resulting in necrosis. In this chapter, it was demonstrated that HOCl-mediated cytosolic free calcium ion (Ca^{2+}) increase in HMDM cells was responsible for this necrotic cell death. ER and extracellular media were the major Ca^{2+} sources contributing to the HOCl-mediated cytosolic Ca^{2+} increase when HOCl concentrations applied were above 100 μM, whereas ER was the only major source when HOCl concentrations were 100 μM or below. Inhibitors of the RyR proteins in ER membrane (dantrolene), the L-type (nifedipine and verapamil) and T-type (flunarizine) Ca^{2+} ion channels inhibited HOCl-mediated cytosolic Ca^{2+} rise significantly. This suggests

that Ca^{2+} in ER was released into the cytosol via the RyR proteins, while Ca^{2+} in media entered HMDM cells via the voltage-dependent L- and T-type Ca^{2+} ion channels.

HOCl caused calpain activation within the 10-minute treatment, possibly mediated by the HOCl-induced cytosolic Ca^{2+} increase. This calpain activation was implicated in the HOCl-mediated necrotic cell death in HMDM cells, since calpain inhibitors as low as 10 μM (calpeptin and SJA6017) completely inhibited HOCl-induced cell viability loss. Lysosomal destabilization was also observed in HMDM cells within 10 minutes of HOCl treatment; and was prevented by calpain inhibitors and lysosomal stabilizers (guanabenz and idazoxan). This suggests that lysosomal destabilization was mediated by calpains. The cathepsins released from destabilized lysosomes and activated calpains would lead to degradation of cellular components, especially cytoskeletal proteins, causing membrane rupture and hence necrotic cell death.

It was shown in this chapter that the excess cytosolic Ca^{2+} in HOCl-treated HMDM cells, after reaching a critical level, was taken up by mitochondria into the matrix via the Ca^{2+} uniporter in IMM (inhibited by ruthenium red), resulting in MPT-mediated mitochondrial membrane potential loss and subsequently necrotic cell death. Calpeptin was found to prevent HOCl-mediated mitochondrial membrane potential loss in HMDM cells. The results indicate that HOCl-mediated Ca^{2+} accumulation in matrix resulted in mitochondrial calpain activation, which in turn activated MPT. MPT activation possibly occurred upstream of lysosomal destabilization, as blocking MPT activation prevented lysosomal destabilization completely. The proposed mechanism of HOCl killing HMDM cells is described in **Figure 5.18**.

6. GENERAL DISCUSSION AND CONCLUSIONS

The major findings of this research is HOCl causes HMDM cells to undergo rapid necrotic cell death, which is caused by rapid HOCl-mediated accumulation of cytosolic calcium ion (Ca^{2+}). The cytosolic Ca^{2+} increase results in MPT activation, calpain activation, lysosomal destabilization and ultimately necrotic cell death. Intracellular GSH plays an important role in preventing this HOCl-mediated necrotic cell death. 7,8-NP prevents HOCl-induced cell death and intracellular GSH loss. However, the amount of 7,8-NP synthesized by HMDM cells upon IFN-γ treatment is insufficient to prevent the HOCl-induced loss of intracellular GSH and HMDM cell viability. The chronological order of the HOCl-induced events described above leading to HMDM necrotic cell death is hypothesized and summarised in **Figure 6.1**.

6.1 HOCl induced rapid necrotic cell death in HMDM cells

HOCl caused a concentration-dependent cell viability loss in HMDM cells above a critical HOCl concentration. There was no further significant cell viability loss after the 10-minute treatment, indicating that HOCl caused no latent damaging effect on HMDM cells. Incubating HMDM cells with HOCl for 30 or 60 minutes showed similar level of cell viability loss compared to the corresponding loss after 10-minute treatment. This indicates that the main reactions of HOCl affecting cell viability occurred within the first 10 minutes. The rapid uptake of PI dye by HMDM cells, loss of regulation of intracellular ion homeostasis (see below for HOCl-induced cytosolic Ca^{2+} increase), loss of intracellular ATP, and cell morphological changes (i.e. cell swelling, cell membrane blebbing and rupture) after HOCl exposure were all features of necrosis (Halliwell and Gutteridge, 2007). These results indicated that HMDM cells underwent necrotic cell death in response to HOCl.

There was no caspase-3 activation in HMDM cells upon HOCl treatment, further supporting that HOCl-treated HMDM cells underwent necrotic cell death. Although cells can also undergo caspase-3-independent apoptosis (Whiteman *et al.*, 2007; Yap *et al.*, 2006; Kroemer and Martin, 2005), it was not the case in HOCl-treated HMDM cells, since those cells have shown features of necrosis as mentioned above. The lack of pro-caspase-3 activation or caspase-3 enzyme activity in HOCl-treated HMDM cells can be attributed to

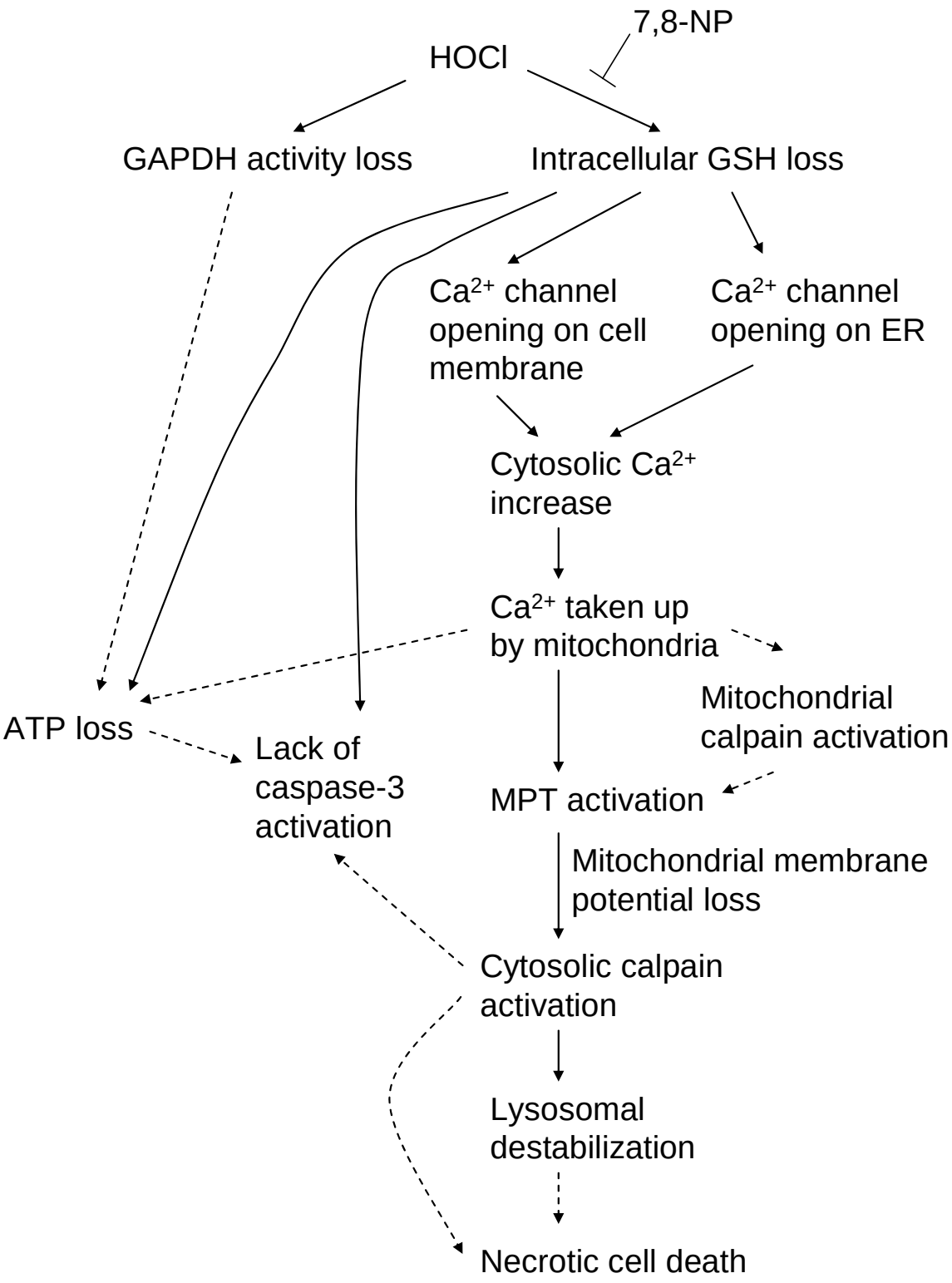

Figure 6.1 Proposed time line of HOCl-induced events leading to necrotic cell death in HMDM cells.
The solid arrows represent the findings in this research, and the dotted arrows represent hypotheses.

the possible inactivation of caspase-9. Caspases require the critical cysteine thiol group at their active site in the reduced state for activity. Since HMDM cell viability only started to decrease once intracellular GSH was significantly lost, the lack of intracellular GSH might have rendered the critical thiol group of caspase-9 susceptible to oxidation by the remaining HOCl and therefore to inactivation. In addition, calpain enzymes can cleave several apoptosis regulatory proteins, including Apaf-1 (Reimertz *et al*., 2001), as well as caspases to prevent their processing into active forms (Lankiewicz *et al*., 2000; Bizat *et al*., 2003). In this research, HOCl was shown to cause calpain activation in HMDM cells (see **section 6.3**), indicating that this scenario is possible. Moreover, activation of pro-caspase-3 requires ATP or dATP (Liu *et al.*, 1996; Hampton *et al.*, 1998) for apoptosome formation, which activates caspase-9 that in turn activates pro-caspase-3 (Kroemer and Martin, 2005). This research has demonstrated rapid and drastic loss of ATP in HMDM cells upon HOCl treatment (see below), indicating that intracellular ATP was possibly not sufficient for caspase-3 activation.

The current finding showed that ATP in HMDM cells was rapidly and significantly lost after 10 minutes of HOCl treatment. Intracellular ATP level is an important determinant factor of cells undergoing apoptosis or necrosis (Kim *et al*., 2003a; Green and Kroemer, 2004; Crompton, 1999; Kim *et al.*, 2003b). Treatment of a human T-cell line with the Ca^{2+} ionophore induces apoptosis under ATP-supplying conditions, but induces necrotic cell death under ATP-depleting conditions (Eguchi *et al*., 1997). Based on these findings, the current data implied that HMDM cells underwent necrotic cell death. This ATP loss might have also contributed to cell membrane integrity loss observed in HOCl-treated HMDM cells. Falls in ATP is suggested to facilitate blebbing and eventually cell membrane rupture, as ATP is required for maintenance of cytoskeletal integrity (Halliwell and Gutteridge, 2007). GSH loss might have preceded ATP loss in HMDM cells, as intracellular GSH loss preceded cell viability loss (see **section 6.2**), and intracellular ATP loss was directly correlated to cell viability loss.

The rapid intracellular ATP loss might be caused by HOCl reacting directly with ATP (Prutz, 1996). HOCl was also found to induce mitochondrial membrane potential loss in HMDM cells by mitochondria taking up excess cytosolic Ca^{2+} via the Ca^{2+} uniporter at the IMM (see **section 6.3**). This uniporter is gated/activated by ATP (Bianchi *et al.*, 2004). Hence, the Ca^{2+} uptake by mitochondria might have consumed ATP, resulting in ATP loss.

The lack of intracellular ATP recovery in HMDM cells over time after the initial HOCl treatment was possibly due to the impaired glycolytic pathway, as HOCl was shown in this research to inactivate GAPDH enzyme (see below). Another possibility was the breakdown of the electron transport chain (ETC), which was supported by the finding of superoxide radical generation in HMDM cells within 10 minutes of HOCl treatment. Luetjens *et al*. (2000) showed that the ETC components, such as cytochrome c, can escape the ETC through the opened MPT pores (MPT activation was observed in this research; see **section 6.3**). This loss of ETC components can lead to escape of electrons from complex III, which can then reduce oxygen molecules and form superoxide radicals. In this research, Ca^{2+} was found to be taken up by mitochondria, which might also have caused superoxide radical generation. It was previously found that Ca^{2+} alters the lipid organization of the inner mitochondrial membrane (IMM) by interacting with the anionic head of cardiolipin molecules (an important component of IMM). These alterations in membrane organization may affect respiratory chain function, including coenzyme Q mobility, and favour mono-electronic oxygen reduction (i.e. superoxide radical generation) (Grijalba *et al.*, 1999). In addition, Ca^{2+} accumulation in mitochondria may activate mitochondrial calpains, which can damage the two proteins of complex I, NDUFV2 and ND6, resulting in the ETC dysfunction (Arrington *et al*. 2006).

In this research, GAPDH enzyme activity decreased in HMDM cells with increasing HOCl concentrations at the same rate as intracellular GSH loss, suggesting that GAPDH enzyme and GSH show similar reactivity towards HOCl and abundance in HMDM cells. GAPDH contains an essential reduced cysteine (Cys149) at the active site (Pullar *et al*., 2000), which is susceptible to HOCl oxidation that results in its inactivation (Peskin and Winterbourn, 2006). GAPDH oxidation by HOCl was also observed in colon epithelial crypt cells (Mckenzie *et al*., 1999), human endothelial cells (Pullar *et al.*, 1999), human mononuclear leukocyte (Smit and Anderson, 1992) and in inflamed mucosa of patients with inflammatory bowel disease (Mckenzie *et al*., 1996). These findings imply high reactivity of GAPDH towards HOCl. GAPDH enzyme should also be as abundant as GSH in HMDM cells in order to compete for HOCl with GSH. Macrophages show a high metabolic rate for providing fuels for their function in an immune response (Newsholme and Newsholme, 1989). Hence, theoretically, GAPDH should be abundant in HMDM cells in order to keep glycolysis going and provide substrates for the Krebs cycle and ETC at high rate. Furthermore, it has been suggested that GAPDH along with some other glycolytic enzymes are also localized in erythrocyte membrane as an enzyme complex

(Campanella *et al*., 2005). Hence it is possible that HOCl passed through membrane and encountered GAPDH thiols first or at the same time as GSH, causing similar rate of loss.

HOCl also caused rapid tyrosine residue loss, indicating damages on cellular proteins. The loss could be caused by direct interaction between HOCl and tyrosine residues, forming products such as 3-chlorotyrosine, which was detected in a number of inflammatory tissues (Winterbourn, 2002; Domigan *et al*., 1995; Kettle, 1996; Hazen and Heinecke, 1997). The current research did not examine formation of 3-chlorotyrosine in HOCl-treated HMDM cells, which should be considered as an important future direction for proving the afore-mentioned theory. In addition, a tyrosine residue (called Y1176) was located in the calpain cleavage site of spectrin, which are components of the cell membrane skeleton (Nicolas *et al*., 2002). Since HOCl has been shown in this research to cause calpain activation and it has been hypothesized that this calpain activation might result in cytoskeleton damage and hence plasma membrane deformation (see **Chapter 5**), one speculation was that activated calpains cleaved at the site where tyrosine is located in spectrin and damaged it to a form that could not be identified by HPLC analysis.

6.2 The protective effect of intracellular GSH and 7,8-NP on HOCl-mediated HMDM cell damage

Glutathione (GSH) acts as an important intracellular antioxidant in HMDM cells against HOCl insult. This research shows that cell viability decreased significantly only after intracellular GSH level was significantly decreased in HMDM cells upon HOCl treatment. Furthermore, HMDM cells depleted of intracellular GSH were more susceptible to HOCl compared to HMDM cells with intact GSH.

The intracellular GSH level is an important factor in determining whether GSH is an efficient antioxidant against HOCl. HMDM cell batches prepared from different donors showed different sensitivity towards the same concentration of HOCl, attributed greatly to their varying intracellular GSH levels. This agrees with other authors (Ballatori *et al*., 2009; Fadeel *et al*., 1999; Pastore *et al*., 2003), who suggested that low intracellular GSH levels increase susceptibility of cells towards oxidative stress, resulting in damage that lead to onset and/or progression of a number of diseases. In addition, increasing intracellular GSH concentrations by administering liposomal GSH to a mouse model of atherosclerosis reduced macrophage oxidative stress levels and cholesterol mass (Rosenblat *et al*., 2007).

The effectiveness of GSH in preventing HOCl insult also depends on whether the parent thiols can be regenerated (Pullar *et al*., 2000), and therefore prevent further rounds of HOCl insult. In this research, intracellular GSH was recovered over time when the initial GSH loss in HMDM cells was 25% after exposure to 100 μM HOCl. This suggested that intracellular GSH would act as an effective antioxidant against HOCl at relatively low HOCl concentrations. This was possible because GSH reacted with HOCl at lower concentration to form GSSG, which could be regenerated to the reduced state (Winterbourn and Brennan, 1997). In contrast, intracellular GSH was not recovered over time when the initial loss was 50% in HMDM cells after exposure to 200 μM HOCl. This was possible because intracellular GSH reacted with higher concentrations of HOCl all the way to form irreversible products including sulfonamide and thiosulfonate (Winterbourn and Brennan, 1997; Pullar *et al*., 2001). HOCl was shown in this research to cause calpain activation. Whether this calpain activation caused degradation of the GSH re-synthesis system or GSH reductase at higher HOCl concentrations, hence preventing GSH recovery, requires further study.

This research demonstrated that 300 μM 7,8-NP in the extracellular medium was able to fully prevent cell viability and intracellular GSH loss in HMDM cells caused by treatment with 400 μM HOCl. This agrees with a previous study that extracellular 7,8-NP protects monocytic U937 cells from HOCl-induced cellular damage (Gieseg *et al.*, 2001a). This data also suggest that in the presence of a highly reactive external substrate, intracellular GSH was unable to compete effectively for HOCl. This agrees with Vissers *et al.* (1995), who showed that intracellular GSH in red cells was unable to compete for HOCl effectively in the presence of ascorbate in the extracellular medium.

The concentration of 7,8-NP is important in determining whether it can effectively prevent HOCl insult. 7,8-NP is synthesized *in vivo* and released from human macrophages upon induction by IFN-γ (Wachter *et al.*, 1989; Wachter *et al.*, 1992). This is consistent with the current finding that 7,8-NP was found both in and out of HMDM cells after incubation with 500 U/ml IFN-γ for 24 hours. After IFN-γ induction, the 7,8-NP level was only approximately 47 nM in the medium and 1 μM in the HMDM cells, based on the human macrophage cell volume (2.48 μl/million cells) calculated by Dorian *et al*. (2001). This amount of 7,8-NP production was not sufficient to prevent HOCl-induced intracellular GSH and cell viability loss. Comparatively, the GSH concentration in HMDM cells measured concurrently as the intracellular 7,8-NP was approximately 863 μM. This

suggests that intracellular GSH would out-compete 7,8-NP for HOCl, assuming that both GSH and 7,8-NP have similar rate constants when reacting with HOCl.

Intracellular GSH level was found to decrease after treatment with 500 U/ml IFN-γ, while 750 U/ml IFN-γ caused cell viability loss. These were possibly caused by IFN-γ increasing production of reactive nitrogen and oxygen species in macrophages (Hansson *et al*., 2006), hence oxidizing intracellular GSH and resulting in cell death. Incubation of U937 cell line (Baier-Bitterlich *et al*., 1995), Jurkat T-lymphocytes (Enzinger *et al*., 2002a), PC12 cells (Enzinger *et al*., 2002b) and rat alveolar epithelial cell line (Schobersberger *et al*., 1996) with high concentrations of 7,8-NP induced apoptosis. In contrast, the current finding showed that HMDM cells treated with extracellular 7,8-NP (up to 300 μM) increased intracellular 7,8-NP concentration to a much higher value (approximately 19 μM) than that in IFN-γ-treated HMDM cells without affecting cell viability and intracellular GSH levels.

The intracellular 7,8-NP concentration measured (approximately 19 μM) after HMDM cell incubation with 7,8-NP was still insufficient to prevent HOCl-mediated intracellular GSH and cell viability loss in HMDM cells. The current findings suggest that IFN-γ-induced 7,8-NP synthesis was not enough to prevent HOCl-mediated HMDM cell damage.

6.3 The role of Ca^{2+} in HOCl-mediated necrotic cell death in HMDM cells

HOCl induced cytosolic Ca^{2+} increase rapidly within 10 minutes of treatment. This agrees with Yap *et al.* (2006), who showed almost immediate cytosolic Ca^{2+} increase in neuronal cells upon HOCl treatment. The source of cytosolic Ca^{2+} increase in HMDM cells was mainly from intracellular store at or below 100 μM HOCl, and from both intracellular store and extracellular medium above 100 μM HOCl. This cytosolic Ca^{2+} increase contributed greatly to the HOCl-induced cell viability loss, as HMDM cells treated with the Ca^{2+} chelator EGTA and various Ca^{2+} channel blockers (dantrolene, nifedipine, verapamil and flunarizine) significantly prevented HOCl-induced cell viability loss.

In this research, Ca^{2+} from extracellular medium entered HMDM cells mainly through the L- and T-type Ca^{2+} channels on the cell membranes, as blocking both Ca^{2+} channels greatly prevented HOCl-induced Ca^{2+} influx. The intracellular Ca^{2+} was mainly released into the

cytosol from ER via the RyR2 channels, as blocking the RyR2 protein on ER significantly inhibited cytosolic Ca^{2+} increase in HOCl-treated HMDM cells. HOCl possibly reacted with the essential thiol groups within the Ca^{2+} channels to induce their opening. Oxidation of thiol groups of L-type Ca^{2+} channels using the thiol oxidizing agent (DTNB) up-regulated L-type Ca^{2+}-channels (Campbell *et al.*, 1996). The thiol oxidizing agents and ROS (superoxide and hydroxyl radicals) were also found to activate RyR receptors (Eager and Dulhunty, 1998; Marengo *et al.*, 1998; Zima *et al*., 2004; Anzai *et al.*, 1998).

Micromolar and millimolar concentrations of Ca^{2+} were known to activate μ- and m-calpains, respectively (Saido *et al*., 1994b). By using both μ- and m-calpain inhibitors, HOCl-induced HMDM cell viability loss was found to be completely prevented. This indicated that HOCl induced calpain activation, which led to necrotic cell death in HMDM cells. HOCl-induced calpain activation was also found to destabilise lysosomes. The cathepsin proteases released from destabilised lysosomes was important in causing HOCl-induced neurotoxicity (Yap *et al*., 2006). Furthermore, cathepsin G induced injury to human umbilical vein endothelial cells and F-actin cytoskeleton within 15 minutes (Iacoviello *et al*., 1995). However, whether cathepsins were released after lysosomal destabilization in HOCl-treated HMDM cells and whether they were in active state causing HOCl-mediated necrotic cell death requires further investigation.

The activated calpains could also contribute to HOCl-mediated necrotic cell death by themselves. Calpains have been found to proteolytically cleave cytoskeletal proteins in hippocampal neurons (Lee *et al*., 1991) and gerbil forebrain (Yokota *et al*., 2003) within minutes of ischemia, and in rat hepatocytes after exposure to tert-butyl hydroperoxide (Miyoshi *et al*., 1996). This degradation of cytoskeletal proteins can result in necrotic cell death by promoting bleb formation and cell rupture (Saido *et al*., 1994b). Moreover, calpain activation was rapid, with both μ- and m-calpains activated by Ca^{2+} within 1 minute (Saido *et al*., 1994a). HOCl-induced cytosolic Ca^{2+} rise was also found to occur within seconds in neuronal cells (Yap *et al.*, 2006). The rapidness of HOCl-induced cytosolic Ca^{2+} rise and Ca^{2+}-mediated calpain activation agrees with the rapid (i.e. within 10 minutes) necrotic cell death in HMDM cells treated with HOCl. Hence, it was very likely that HOCl-mediated cytosolic Ca^{2+} increase activated calpains, which in turn proteolytically degraded cytoskeletal proteins. This then resulted in bleb, formation, cell membrane rupture and necrotic cell death.

This cytosolic Ca^{2+} increase also caused mitochondrial Ca^{2+} accumulation and MPT activation, as preventing Ca^{2+} influx into mitochondria (by blocking the IMM Ca^{2+} uniporter) (Kirichok *et al*., 2004) significantly prevented MPT-mediated mitochondrial membrane potential and cell viability loss in HOCl-treated HMDM cells. This agrees with previous studies, which showed that excessive cytosolic Ca^{2+} can be taken up by mitochondria to trigger the MPT pore opening (Bianchi *et al*., 2004; Richter, 1993; Crompton *et al*., 2002; Whiteman *et al*., 2004). HOCl also caused rapid MPT-mediated mitochondrial membrane potential loss within 10 minutes, leading to necrotic cell death in HMDM cells, as blocking MPT activation with CSA prevented both mitochondrial membrane potential and cell viability losses in HOCl-treated HMDM cells.

HOCl was also found to cause rapid MPT-mediated mitochondrial membrane potential loss within 10 minutes, as blocking MPT pore formation using CSA prevented mitochondrial membrane potential loss. This agrees with previous findings, which showed MPT-induced mitochondrial membrane potential loss in HOCl-treated HeLa cells and human hepatoma HepG2 cells (Park *et al*., 2008; Whiteman *et al.*, 2005b). MPT activation in HOCl-treated HMDM cells was found in this research to be induced by mitochondria taking up excess Ca^{2+} in cytosol via the Ca^{2+} uniporter, which was located in the IMM (Kirichok *et al*., 2004). This agrees with Whiteman *et al*. (2004), who showed that $ONOO^-$ mediated mobilization of cytosolic Ca^{2+}, sequestration of Ca^{2+} into the mitochondria, and subsequently MPT activation within 10 minutes of treatment. MPT can also be triggered by cathepsins in silica-mediated cytotoxicity in alveolar macrophage cells (Thibodeau *et al*., 2003). MPT activation in HOCl-treated HMDM cells was less likely to be triggered by cathepsins, since blocking MPT activation using CSA prevented lysosomal destabilisation. This suggested that lysosomal destabilisation was downstream of MPT activation.

Blocking MPT activation was found to prevent cell viability loss in HOCl-treated HMDM cells. To make the matter more complicated, preventing calpain activation was also found to inhibit MPT activation and cell viability loss. This indicates that MPT activation and calpain activation were in a cause and effect relationship. Cytosolic calpain activation possibly did not occur upstream of MPT activation, because if that was the case, blocking MPT activation would have no effect on preventing lysosomal destabilisation, as the activated cytosolic calpains could still destabilise lysosomes.

Previous studies have demonstrated calpain-like activities in isolated mitochondria (Aguilar *et al*., 1996; Tavares and Duque-Magalhaes, 1991). Furthermore, calpain 10 and its activity have been identified in the outer mitochondrial membrane (OMM), intermembrane mitochondrial space (IMS) and mitochondrial matrix fractions of isolated mitochondria (Arrington *et al*., 2006). The same study also showed that Ca^{2+}-activated mitochondrial matrix calpain 10 caused MPT activation. In addition, Aguilar *et al.* (1996) have shown that Ca^{2+}-induced MPT occurred less than 1 minute after Ca^{2+} treatment in isolated mitochondria, which could be inhibited by CSA or the protease inhibitor. These findings indicate that mitochondrial calpain activation can cause MPT pore formation. Based on these findings, it was possible to speculate that the calpain inhibitor (calpeptin) used in this research prevented mitochondrial calpain activation as well, hence explaining why calpain inactivation could prevent HOCl-mediated MPT activation in HMDM cells. This theory was possible, because calpeptin has been shown to inhibit the mitochondrial matrix calpain 10 (Giguere and Schnellmann, 2008; Giguere *et al*., 2008). There was no documentation on whether the other calpain inhibitor used (SJA6017) could also prevent mitochondrial matrix calpain activation. This theory also suggests that mitochondrial calpain activation occurred upstream of MPT activation in HOCl-treated HMDM cells.

It was interesting to theorize that HOCl-mediated cytosolic Ca^{2+} increase did not activate cytosolic calpains first. But it was not surprising, considering that μ- and m-calpains require μM and mM concentrations of Ca^{2+} for activation, respectively (Halliwell and Gutteridge, 2007). Since cytosolic volume should be much greater than mitochondrial volume, Ca^{2+} possibly did not reach the expected concentration in cytosol for calpain activation, whereas Ca^{2+} concentration reached the required value for calpain activation more easily in the relatively smaller volume of mitochondria.

It requires further investigation to understand how exactly MPT activation led to cytosolic calpain activation in HOCl-treated HMDM cells. Ding *et al.* (2002) showed that MPT inactivation prevented toxin-induced cytosolic calpain activation, and suggested that cytosolic calpain activation might be a result of Ca^{2+} release from mitochondria after MPT activation. It was also possible that some other unknown factors were released from mitochondria after MPT activation to activate cytosolic calpains.

7. FUTURE DIRECTIONS

The lack of caspase-3 activation in HOCl-treated HMDM cells (**Figures 4.1** and **4.2**) might be caused by the inactivation of the upstream initiator caspases, such as caspase-9. One future direction will be to measure the activity of various upstream initiator caspases in HOCl-treated HMDM cells in order to see whether HOCl drives necrosis while blocking the apoptotic pathways in HMDM cells.

Calpain activation in HOCl-treated HMDM cells was found to cause lysosomal destabilisation (**Figures 5.8** and **5.9**). One consequence of lysosomal destabilisation is the release of cathepsin proteases, which can degrade intracellular components of the cells. It would be interesting to measure the activity of cathepsins in HMDM cells after HOCl treatment and examine their association with HOCl-induced viability loss.

One of the hypotheses proposed in this thesis was that mitochondrial calpains are activated in response to Ca^{2+} influx into mitochondria. To test this hypothesis, calpain activity in mitochondria should be examined in HMDM cells after HOCl treatment. The presence of activated calpains in atherosclerotic plaques, and whether they are colocalized with dead macrophages and HOCl-modified proteins in plaques should also be examined. This is to confirm whether the proposed calpain-mediated macrophage cell death in response to HOCl is likely to happen in real situations.

REFERENCES

Abernathy, F. and Pacht, E. R. (1995). Alteration of adenosine triphosphate and other nucleotides after sublethal oxidant injury to rat type II alveolar epithelial cells. *Am J Med Sci* **309**: 140-5.

Adam, W., Kurz, A. and Saha-Moller, C. R. (2000). Peroxidase-catalyzed oxidative damage of DNA and 2'-deoxyguanosine by model compounds of lipid hydroperoxides: involvement of peroxyl radicals. *Chem Res Toxicol* **13**(12): 1199-207.

Aguilar, H. I., Botla, R., Arora, A. S., Bronk, S. F. and Gores, G. J. (1996). Induction of the mitochondrial permeability transition by protease activity in rats: a mechanism of hepatocyte necrosis. *Gastroenterology* **110**(2): 558-66.

Akerboom, T. P., Bilzer, M. and Sies, H. (1982). The relationship of biliary glutathione disulfide efflux and intracellular glutathione disulfide content in perfused rat liver. *J Biol Chem* **257**(8): 4248-52.

Albrich, J. M., Gilbaugh, J. H. r., Callahan, K. B. and Hurst, J. K. (1986). Effects of the putative neutrophil-generated toxin, hypochlorous acid, on membrane permeability and transport systems of Escherichia coli. *J Clin Invest* **78**(1): 177-84.

Albrich, J. M. and Hurst, J. K. (1982). Oxidative inactivation of Escherichia coli by hypochlorous acid. Rates and differentiation of respiratory from other reaction sites. *FEBS Lett* **144**(1): 157-61.

Albrich, J. M., McCarthy, C. A. and Hurst, J. K. (1981). Biological reactivity of hypochlorous acid: implications for microbicidal mechanisms of leukocyte myeloperoxidase. *Proc Natl Acad Sci U S A* **78**(1): 210-4.

Alderton, W. K., Cooper, C. E. and Knowles, R. G. (2001). Nitric oxide synthases: structure, function and inhibition. *Biochem J* **357**(Pt 3): 593-615.

Alexander, C., Votruba, M., Pesch, U. E., Thiselton, D. L., Mayer, S., Moore, A., Rodriguez, M., Kellner, U., Leo-Kottler, B., Auburger, G., Bhattacharya, S. S. and Wissinger, B. (2000). OPA1, encoding a dynamin-related GTPase, is mutated in autosomal dominant optic atrophy linked to chromosome 3q28. *Nat Genet* **26**(2): 211-5.

Amit, Z. (2008). A model of complex plaque formation: 7,8-Dihydroneopterin protects human monocyte-derived macrophages from oxidised low density lipoprotein-induced death. *PhD thesis*.

Ando, Y. and Steiner, M. (1973). Sulfhydryl and disulfide groups of platelet membranes. I. Determination of sulfhydryl groups. *Biochim Biophys Acta* **311**: 26-37.

Anzai, K., Ogawa, K., Kuniyasu, A., Ozawa, T., Yamamoto, H. and Nakayama, H. (1998). Effects of hydroxyl radical and sulfhydryl reagents on the open probability of the purified cardiac ryanodine receptor channel incorporated into planar lipid bilayers. *Biochem Biophys Res Commun* **249**(3): 938-42.

Armstrong, J. S. and Jones, D. P. (2002). Glutathione depletion enforces the mitochondrial permeability transition and causes cell death in Bcl-2 overexpressing HL60 cells. *FASEB J* **16**(10): 1263-5.

Arrington, D. D., Van Vleet, T. R. and Schnellmann, R. G. (2006). Calpain 10: a mitochondrial calpain and its role in calcium-induced mitochondrial dysfunction. *Am J Physiol Cell Physiol* **291**(6): C1159-71.

Ashkenazi, A. (2002). Targeting death and decoy receptors of the tumour-necrosis factor superfamily. *Nat Rev Cancer* **2**: 420-30.

Asmis, R. and Begley, J. G. (2003). Oxidized LDL promotes peroxide-mediated mitochondrial dysfunction and cell death in human macrophages: a caspase-3-independent pathway. *Circ Res* **92**(1): e20-9.

Auchère, F. and Capeillère-Blandin, C. (1999). NADPH as a co-substrate for studies of the chlorinating activity of myeloperoxidase. *Biochem J* **343**(Pt 3): 603-13.

Baier-Bitterlich, G., Baier, G., Fuchs, D., Bock, G., Hausen, A., Utermann, G., Pavelka, M. and Wachter, H. (1996a). Role of 7,8-dihydroneopterin in T-cell apoptosis and HTLV-1 transcription *in vitro*. *Oncogene* **13**: 2281-2285.

Baier-Bitterlich, G., Fuchs, D., Murr, C., Reibnegger, G., Werner-Felmayer, G., Sgonc, R., Bock, G., Dierich, M. P. and Wachter, H. (1995). Effect of neopterin and 7,8-dihydroneopterin on tumor necrosis factor-alpha induced programmed cell death. *FEBS Lett* **364**(2): 234-8.

Baier-Bitterlich, G., Fuchs, D. and Wachter, H. (1996b). 7,8-Dihydroneopterin upregulates interferon-gamma promoter in T cells. *Immunobiology* **196**(4): 350-5.

Baier-Bitterlich, G., Fuchs, D. and Wachter, H. (1997a). Chronic immune stimulation, oxidative stress, and apoptosis in HIV infection. *Biochem Pharmacol* **53**(6): 755-63.

Baier-Bitterlich, G., Fuchs, D., Zangerle, R., Baeuerle, P. A., Werner, E. R., Fresser, F., Uberall, F. and Wachter, H. (1997b). Trans-activation of the HIV type 1 promoter by 7,8-dihydroneopterin in vitro. *AIDS Res and Human Retrovir* **13**(2): 173-8

Baird, S. K., Hampton, M. B. and Gieseg, S. P. (2004). Oxidized LDL triggers phosphatidylserine exposure in human monocyte cell lines by both caspase-dependent and -independent mechanisms. *FEBS Lett* **578**(1-2): 169-74.

Baird, S. K., Reid, L., Hampton, M. B. and Gieseg, S. P. (2005). OxLDL induced cell death is inhibited by the macrophage synthesised pterin, 7,8-dihydroneopterin, in U937 cells but not THP-1 cells. *Biochim Biophys Acta* **1745**(3): 361-9.

Baldus, S., Eiserich, J. P., Brennan, M. L., Jackson, R. M., Alexander, C. B. and Freeman, B. A. (2002). Spatial mapping of pulmonary and vascular nitrotyrosine reveals the pivotal role of myeloperoxidase as a catalyst for tyrosine nitration in inflammatory diseases. *Free Radic Biol Med* **33**(7): 1010.

Balendiran, G. K., Dabur, R. and Fraser, D. (2004). The role of glutathione in cancer. *Cell Biochem Funct* **22**(6): 343-52.

Ball, R. Y., Stowers, E. C., Burton, J. H., Cary, N. R., Skepper, J. N. and Mitchinson, M. J. (1995). Evidence that the death of macrophage foam cells contributes to the lipid core of atheroma. *Atherosclerosis* **114**(1): 45-54.

Ballatori, N., Krance, S. M., Notenboom, S., Shi, S., Tieu, K. and Hammond, C. L. (2009). Glutathione dysregulation and the etiology and progression of human diseases. *Biol Chem* **390**(3): 191-214.

Balogh, A., Mittermayr, M., Schlager, A., Balogh, D., Schobersberger, W., Fuchs, D. and Margreiter, J. (2005). Mechanism of neopterin-induced myocardial dysfunction in the isolated perfused rat heart. *Biochim Biophys Acta* **1724**(1-2): 17-22.

Barak, M. and Gruener, N. (1991). Neopterin augmentation of tumor necrosis factor production. *Immunol Lett* **30**(1): 101-6.

Berberian, P. A., Myers, W., Tytell, M., Challa, V. and Bond, M. G. (1990). Immunohistochemical localization of heat shock protein-70 in normal-appearing and atherosclerotic specimens of human arteries. *Am J Pathol* **136**(1): 71-80.

Barrette, W. C. J., Albrich, J. M. and Hurst, J. K. (1987). Hypochlorous acid-promoted loss of metabolic energy in Escherichia coli. *Infect Immun* **55**(10): 2518-25.

Barrette, W. C. j., Hannum, D. M., Wheeler, W. D. and Hurst, J. K. (1989). General mechanism for the bacterial toxicity of hypochlorous acid: abolition of ATP production. *Biochemistry* **28**(23): 9172-8.

Bernardi, P., Colonna, R., Costantini, P., Eriksson, O., Fontaine, E., Ichas, F., Massari, S., Nicolli, A., Petronilli, V. and Scorrano, L. (1998). The mitochondrial permeability transition. *Biofactors* **8**(3-4): 273-81.

Bernardi, P., Scorrano, L., Colonna, R., Petronilli, V. and Di Lisa, F. (1999). Mitochondria and cell death. Mechanistic aspects and methodological issues. *Eur J Biochem* **264**(3): 687-701.

Bers, D. M. (2002). Cardiac excitation-contraction coupling. *Nature* **415**(6868): 198-205.

Bi, X., Chang, V., Molnar, E., McIlhinney, R. A. and Baudry, M. (1996). The C-terminal domain of glutamate receptor subunit 1 is a target for calpain-mediated proteolysis. *Neuroscience* **73**(4): 903-6.

Bianchi, K., Rimessi, A., Prandini, A., Szabadkai, G. and Rizzuto, R. (2004). Calcium and mitochondria: mechanisms and functions of a troubled relationship. *Biochim Biophys Acta* **1742**(1-3): 119-31.

Billiau, A. and Dijkmans, R. (1990). Interferon-gamma: mechanism of action and therapeutic potential. *Biochem Pharmacol* **40**(7): 1433-9.

Bizat, N., Hermel, J. M., Humbert, S., Jacquard, C., Créminon, C., Escartin, C., Saudou, F., Krajewski, S., Hantraye, P. and Brouillet, E. (2003). In vivo calpain/caspase cross-talk during 3-nitropropionic acid-induced striatal degeneration: implication of a calpain-mediated cleavage of active caspase-3. *J Biol Chem* **278**(44): 43245-53.

Bizzozero, O. A., Ziegler, J. L., De Jesus, G. and Bolognani, F. (2006). Acute depletion of reduced glutathione causes extensive carbonylation of rat brain proteins. *J Neurosci Res* **83**(4): 656-67.

Blackburn, W. D. J., Minghetti, P. P., Schrohenloher, R. E. and Chatham, W. W. (1995). Activation of human neutrophils by surface-associated IgA is associated with the release of activated collagenase. *Clin Immunol Immunopathol* **76**(3 Pt 1): 241-7.

Blomgren, K., Zhu, C., Wang, X., Karlsson, J. O., Leverin, A. L., Bahr, B. A., Mallard, C. and Hagberg, H. (2001). Synergistic activation of caspase-3 by m-calpain after neonatal hypoxia-ischemia: a mechanism of "pathological apoptosis"? *J Biol Chem* **276**(13): 10191-8.

Boggs, S. E., McCormick, T. S. and Lapetina, E. G. (1998). Glutathione levels determine apoptosis in macrophages. *Biochem Biophys Res Commun.* **247**(**2**): 229-33.

Bogner, W., Aquila, H. and Klingenberg, M. (1986). The transmembrane arrangement of the ADP/ATP carrier as elucidated by the lysine reagent pyridoxal 5-phosphate. *Eur J Biochem* **161**(3): 611-20.

Boland, B. and Campbell, V. (2004). Abeta-mediated activation of the apoptotic cascade in cultured cortical neurones: a role for cathepsin-L. *Neurobiol Aging* **25**(1): 83-91.

Boyne, A. F. and Ellman, G. L. (1972). A methodology for analysis of tissue sulfhydryl components. *Anal Biochem* **46**: 639-653.

Brookes, P. S., Yoon, Y., Robotham, J. L., Anders, M. W. and Sheu, S. S. (2004). Calcium, ATP, and ROS: a mitochondrial love-hate triangle. *Am J Physiol Cell Physiol* **C817-33**(287): 4.

Brown, N. and Crawford, C. (1993). Structural modifications associated with the change in Ca2+ sensitivity on activation of m-calpain. *FEBS Lett* **322**(1): 65-8.

Brown, D. L., Hibbs, M. S., Kearney, M., Loushin, C. and Isner, J. M. (1995). Identification of 92-kD gelatinase in human coronary atherosclerotic lesions. Association of active enzyme synthesis with unstable angina. *Circulation* **91**(8): 2125-31.

Bruce, D., Fu, S., Armstrong, S. and Dean, R. T. (1999). Human apo-lipoprotein B from normal plasma contains oxidised peptides. *Int J Biochem Cell Biol* **31**(12): 1409-20.

Brustovetsky, N. and Klingenberg, M. (1996). Mitochondrial ADP/ATP carrier can be reversibly converted into a large channel by Ca2+. *Biochemistry* **35**(26): 8483-8.

Budd, S. L., Castilho, R. F. and Nicholls, D. G. (1997). Mitochondrial membrane potential and hydroethidine-monitored superoxide generation in cultured cerebellar granule cells. *FEBS Lett* **415**(1): 21-4.

Cai, H. and Harrison, D. G. (2000). Endothelial dysfunction in cardiovascular diseases: the role of oxidant stress. *Circ Res* **87**(10): 840-4.

Cai, J. and Jones, D. P. (1998). Superoxide in apoptosis. Mitochondrial generation triggered by cytochrome c loss. *J Biol Chem* **273**(19): 1401-4.

Campanella, M. E., Chu, H. and Low, P. S. (2005). Assembly and regulation of a glycolytic enzyme complex on the human erythrocyte membrane. *Proc Natl Acad Sci U S A* **102**(7): 2402-7.

Campbell, D. L., Stamler, J. S. and Strauss, H. C. (1996). Redox modulation of L-type calcium channels in ferret ventricular myocytes. Dual mechanism regulation by nitric oxide and S-nitrosothiols. *J Gen Physiol* **108**(4): 277-93.

Carpenter, K. L., Dennis, I. F., Challis, I. R., Osborn, D. P., Macphee, C. H., Leake, D. S., Arends, M. J. and Mitchinson, M. J. (2001). Inhibition of lipoprotein-associated phospholipase A2 diminishes the death-inducing effects of oxidised LDL on human monocyte-macrophages. *FEBS Lett* **505**(3): 357-63.

Carmody, R. J. and Cotter, T. G. (2001). Signalling apoptosis: a radical approach. *Redox Rep* **6**(2): 77-90.

Carr, A. C., van den Berg, J. J. and Winterbourn, C. C. (1996). Chlorination of cholesterol in cell membranes by hypochlorous acid. *Arch Biochem Biophys* **332**(1): 63-9.

Carr, A. C. and Winterbourn, C. C. (1997). Oxidation of neutrophil glutathione and protein thiols by myeloperoxidase-derived hypochlorous acid. *Biochem J* **327 (Pt 1)**: 275-81.

Chandra, J. and Orennius, S. (2002). Mitochondria, oxygen metabolism and the regulation of cell death. *International Congress Series* **1233**: 259-72.

Chatham, W. W., Turkiewicz, A. and Blackburn, W. D. J. (1994). Determinants of neutrophil HOCl generation: ligand-dependent responses and the role of surface adhesion. *J Leukoc Biol* **56**(5): 654-60.

Chen, Y. R., Chen, C. L., Liu, X., Li, H., Zweier, J. L. and Mason, R. P. (2004). Involvement of protein radical, protein aggregation, and effects on NO metabolism in the hypochlorite-mediated oxidation of mitochondrial cytochrome c. *Free Radic Biol Med* **37**(10): 1591-603.

Chen, M., He, H., Zhan, S., Krajewski, S., Reed, J. C. and Gottlieb, R. A. (2001). Bid is cleaved by calpain to an active fragment in vitro and during myocardial ischemia/reperfusion. *J Biol Chem* **276**(33): 30724-8.

Chernyak, B. V., Dedov, V. N. and Chernyak, V. Y. (1995). Ca(2+)-triggered membrane permeability transition in deenergized mitochondria from rat liver. *FEBS Lett* **365**(1): 75-8.

Cheung, N. S., Peng, Z. F., Chen, M. J., Moore, P. K. and Whiteman, M. (2007). Hydrogen sulfide induced neuronal death occurs via glutamate receptor and is associated with calpain activation and lysosomal rupture in mouse primary cortical neurons. *Neuropharmacology* **53**(4): 505-14.

Choi, S. H., Choi, D. H., Lee, J. J., Park, M. S. and Chun, B. G. (2002). Imidazoline drugs stabilize lysosomes and inhibit oxidative cytotoxicity in astrocytes. *Free Radic Biol Med* **32**(5): 394-405.

Chua, B. T., Guo, K. and Li, P. (2000). Direct cleavage by the calcium-activated protease calpain can lead to inactivation of caspases. *J Biol Chem* **275**(7): 5131-5.

Cilenti, L., Kyriazis, G. A., Soundarapandian, M. M., Stratico, V., Yerkes, A., Park, K. M., Sheridan, A. M., Alnemri, E. S., Bonventre, J. V. and Zervos, A. S. (2005). Omi/HtrA2 protease mediates cisplatin-induced cell death in renal cells. *Am J Physiol Renal Physiol* **288**(2): F371-9.

Cleeter, M. W., Cooper, J. M., Darley-Usmar, V. M., Moncada, S. and Schapira, A. H. (1994). Reversible inhibition of cytochrome c oxidase, the terminal enzyme of the mitochondrial respiratory chain, by nitric oxide. Implications for neurodegenerative diseases. *FEBS Lett* **345**(1): 50-4.

Cole, K. E., Strick, C. A., Paradis, T. J., Ogborne, K. T., Loetscher, M., Gladue, R. P., Lin, W., Boyd, J. G., Moser, B., Wood, D. E., Sahagan, B. G. and Neote, K. (1998). Interferon-inducible T cell alpha chemoattractant (I-TAC): a novel non-ELR CXC chemokine with potent activity on activated T cells through selective high affinity binding to CXCR3. *J Exp Med* **187**(12): 2009-21.

Coolican, S. A. and Hathaway, D. R. (1984). Effect of L-alpha-phosphatidylinositol on a vascular smooth muscle Ca2+-dependent protease. Reduction of the Ca2+ requirement for autolysis. *J Biol Chem* **259**(19): 11627-30.

Connern, C. P. and Halestrap, A. P. (1992). Purification and N-terminal sequencing of peptidyl-prolyl cis-trans-isomerase from rat liver mitochondrial matrix reveals the existence of a distinct mitochondrial cyclophilin. *Biochem J* **284**(Pt 2): 381-5.

Cory, S. and Adams, J. M. (2005). Killing cancer cells by flipping the Bcl-2/Bax switch. *Cancer Cell* **8**(1): 5-6.

Costantini, P., Chernyak, B. V., Petronilli, V. and Bernardi, P. (1996). Modulation of the mitochondrial permeability transition pore by pyridine nucleotides and dithiol oxidation at two separate sites. *J Biol Chem* **271**(12): 6746-51.

Cotgreave, I. A. and Moldéus, P. (1986). Methodologies for the application of monobromobimane to the simultaneous analysis of soluble and protein thiol components of biological systems. *J Biochem Biophys Methods* **13**(4-5): 231-49.

Cregan, S. P., Fortin, A., MacLaurin, J. G., Callaghan, S. M., Cecconi, F., Yu, S. W., Dawson, T. M., Dawson, V. L., Park, D. S., Kroemer, G. and Slack, R. S. (2002). Apoptosis-inducing factor is involved in the regulation of caspase-independent neuronal cell death. *J Cell Biol* **158**(3): 507-17.

Croall, D. E. and DeMartino, G. N. (1991). Calcium-activated neutral protease (calpain) system: structure, function, and regulation. *Physiol Rev* **71**(3): 813-47.

Cromheeke, K. M., Kockx, M. M., De Meyer, G. R., Bosmans, J. M., Bult, H., Beelaerts, W. J., Vrints, C. J. and Herman, A. G. (1999). Inducible nitric oxide synthase colocalizes with signs of lipid oxidation/peroxidation in human atherosclerotic plaques. *Cardiovascular Research* **43**(3): 744-754.

Crompton, M. (1999). The mitochondrial permeability transition pore and its role in cell death. *Biochem J* **341**(Pt 2): 233-49.

Crompton, M., Barksby, E., Johnson, N. and Capano, M. (2002). Mitochondrial intermembrane junctional complexes and their involvement in cell death. *Biochimie* **84**(2-3): 143-52.

Cross, J. V. and Templeton, D. J. (2004). Thiol oxidation of cell signaling proteins: Controlling an apoptotic equilibrium. *J Cell Biochem* **93**(1): 104-11.

Dalle-Donne, I., Rossi, R., Giustarini, D., Colombo, R. and Milzani, A. (2007). S-glutathionylation in protein redox regulation. *Free Radic Biol Med* **43**(6): 883-98.

Das, A. M. and Harris, D. A. (1990). Control of mitochondrial ATP synthase in heart cells: inactive to active transitions caused by beating or positive inotropic agents. *Cardiovasc Res* **24**(5): 411-7.

Daugherty, A., Dunn, J. L., Rateri, D. L. and Heinecke, J. W. (1994). Myeloperoxidase, a catalyst for lipoprotein oxidation, is expressed in human atherosclerotic lesions. *J Clin Invest* **94**(1): 437-44.

Daumer, K. M., Khan, A. U. and Steinbeck, M. J. (2000). Chlorination of pyridinium compounds. Possible role of hypochlorite, N-chloramines, and chlorine in the oxidation of pyridinoline cross-links of articular cartilage collagen type II during acute inflammation. *J Biol Chem* **275**(44): 34681-92.

Davies, M. J., Richardson, P. D., Woolf, N., Katz, D. R. and Mann, J. (1993). Risk of thrombosis in human atherosclerotic plaques: role of extracellular lipid, macrophage, and smooth muscle cell content. *Br Heart J* **69**(5): 377-81.

Ding, W. X., Shen, H. M. and Ong, C. N. (2002). Calpain activation after mitochondrial permeability transition in microcystin-induced cell death in rat hepatocytes. *Biochem Biophys Res Commun* **291**(2): 321-31.

Domigan, N. M., Charlton, T. S., Duncan, M. W., Winterbourn, C. C. and Kettle, A. J. (1995). Chlorination of tyrosyl residues in peptides by myeloperoxidase and human neutrophils. *J Biol Chem* **270**(28): 16542-8.

Dorian, M., Grellet, J. and Saux, M. C. (2001). Uptake of quinolones by in-vitro human monocyte derived macrophages. *J Pharm Pharmacol* **53**(5): 735-41.

Duggan, S., Rait, C., Gebicki, J. M. and Gieseg, S. P. (2001). Inhibition of protein oxidation by the macrophage-synthesised antioxidant 7,8-dihydroneopterin. *Redox Rep* **6**(3): 188-90.

Duggan, S., Rait, C., Platt, A. and Gieseg, S. (2002). Protein and thiol oxidation in cells exposed to peroxyl radicals is inhibited by the macrophage synthesised pterin 7,8-dihydroneopterin. *Biochim Biophys Acta* **1591**(1-3): 139-145.

Duke, R. C., Ojcius, D. M. and Young, J. D. (1996). Cell suicide in health and disease. *Sci Am* **275**(6): 80-7.

Eager, K. R. and Dulhunty, A. F. (1998). Activation of the cardiac ryanodine receptor by sulfhydryl oxidation is modified by Mg2+ and ATP. *J Membr Biol* **163**(1): 9-18.

Eguchi, Y., Shimizu, S. and Tsujimoto, Y. (1997). Intracellular ATP levels determine cell death fate by apoptosis or necrosis. *Cancer Res* **57**(10): 1835-40.

Eiserich, J. P., Baldus, S., Brennan, M. L., Ma, W., Zhang, C., Tousson, A., Castro, L., Lusis, A. J., Nauseef, W. M., White, C. R. and Freeman, B. A. (2002). Myeloperoxidase, a leukocyte-derived vascular NO oxidase. *Science* **296**(5577): 2391-4.

El-Benna, J., Dang, P. M., Gougerot-Pocidalo, M. A. and Elbim, C. (2005). Phagocyte NADPH oxidase: a multicomponent enzyme essential for host defenses. *Arch Immunol Ther Exp (Warsz)* **53**(3): 199-206.

Eley, D. W., Eley, J. M., Korecky, B. and Fliss, H. (1991). Impairment of cardiac contractility and sarcoplasmic reticulum Ca2+ ATPase activity by hypochlorous acid: reversal by dithiothreitol. *Can J Physiol Pharmacol* **69**(11): 1677-85.

Enzinger, C., Wirleitner, B., Bock, G., Baier-Bitterlich, G. and Fuchs, D. (2001). Influence of cytokines tumor necrosis factor-alpha and interferon-gamma on signaling cascades associated with apoptosis in rat PC12 cells. *Neurosci Lett* **316**(3): 157-60.

Enzinger, C., Wirleitner, B., Lutz, C., Bock, G., Tomaselli, B., Baier, G., Fuchs, D. and Baier-Bitterlich, G. (2002a). 7,8-Dihydroneopterin induces apoptosis of Jurkat T-lymphocytes via a Bcl-2-sensitive pathway. *Eur J Cell Biol* **81**(4): 197-202.

Enzinger, C., Wirleitner, B., Spottl, N., Bock, G., Fuchs, D. and Baier-Bitterlich, G. (2002b). Reduced pteridine derivatives induce apoptosis in PC12 cells. *Neurochem Int* **41**(1): 71-8.

Escargueil-Blanc, I., Salvayre, R. and Nègre-Salvayre, A. (1994). Necrosis and apoptosis induced by oxidized low density lipoproteins occur through two calcium-dependent pathways in lymphoblastoid cells. *FASEB J* **8**(13): 1075-80.

Fabiato, A. (1985a). Simulated calcium current can both cause calcium loading in and trigger calcium release from the sarcoplasmic reticulum of a skinned canine cardiac Purkinje cell. *J Gen Physiol* **85**(2): 291-320.

Fabiato, A. (1985b). Time and calcium dependence of activation and inactivation of calcium-induced release of calcium from the sarcoplasmic reticulum of a skinned canine cardiac Purkinje cell. *J Gen Physiol* **85**(2): 247-89.

Fadeel, B., Orrenius, S. and Zhivotovsky, B. (1999). Apoptosis in human disease: a new skin for the old ceremony? *Biochem Biophys Res Commun* **266**(3): 699-717.

Favero, T. G., Webb, J., Papiez, M., Fisher, E., Trippichio, R. J., Broide, M. and Abramson, J. J. (2003). Hypochlorous acid modifies calcium release channel function from skeletal muscle sarcoplasmic reticulum. *J Appl Physiol* **94**(4): 1387-94.

Fernández, E., Cuenca, N., García, M. and De Juan, J. (1995). Two types of mitochondria are evidenced by protein kinase C immunoreactivity in the Müller cells of the carp retina. *Neurosci Lett* **183**(3): 202-5.

Ferrand-Drake, M., Zhu, C., Gidö, G., Hansen, A. J., Karlsson, J. O., Bahr, B. A., Zamzami, N., Kroemer, G., Chan, P. H., Wieloch, T. and Blomgren, K. (2003). Cyclosporin A prevents calpain activation despite increased intracellular calcium concentrations, as well as translocation of apoptosis-inducing factor, cytochrome c and caspase-3 activation in neurons exposed to transient hypoglycemia. *J Neurochem* **85**(6): 1431-42.

Firth, C.A. (2006). 7,8-Dihydroneopterin-mediated protection of low density lipoprotein, but not human macrophages, from oxidative stress. *PhD thesis*.

Flavall, E.A. (2008). Localisation of antioxidants and oxidative markers within the atherosclerotic plaque. *Master thesis*.

Fliss, H. and Ménard, M. (1991). Hypochlorous acid-induced mobilization of zinc from metalloproteins. *Arch Biochem Biophys* **287**(1): 175-9.

Folcik, V. A., Aamir, R. and Cathcart, M. K. (1997). Cytokine modulation of LDL oxidation by activated human monocytes. *Arterioscler Thromb Vasc Biol* **17**(10): 1954-61.

Folkes, L. K., Candeias, L. P. and Wardman, P. (1995). Kinetics and mechanisms of hypochlorous acid reactions. *Arch Biochem Biophys* **323**(1): 120-6.

Foote, C. S., Goyne, T. E. and Lehrer, R. I. (1983). Assessment of chlorination by human neutrophils. *Nature* **301**(5902): 715-6.

Forman, H. J. and Torres, M. (2001). Signaling by the respiratory burst in macrophages. *IUBMB Life* **51**(6): 365-71.

Fu, S., Wang, H., Davies, M. and Dean, R. (2000). Reactions of hypochlorous acid with tyrosine and peptidyl-tyrosyl residues give dichlorinated and aldehydic products in addition to 3-chlorotyrosine. *J Biol Chem* **275**(15): 10851-8.

Fuchs, D., Stahl-Hennig, C., Gruber, A., Murr, C., Hunsmann, G. and Wachter, H. (1994). Neopterin--its clinical use in urinalysis. *Kidney Int Suppl* **47**: S8-11.

Fukiage, C., Azuma, M., Nakamura, Y., Tamada, Y., Nakamura, M. and Shearer, T. R. (1997). SJA6017, a newly synthesized peptide aldehyde inhibitor of calpain: amelioration of cataract in cultured rat lenses. *Biochim Biophys Acta* **1361**(3): 304-12.

Galis, Z. S., Sukhova, G. K., Lark, M. W. and Libby, P. (1994). Increased expression of matrix metalloproteinases and matrix degrading activity in vulnerable regions of human atherosclerotic plaques. *J Clin Invest* **94**(6): 2493-503.

Garner, B., Baoutina, A., Dean, R. T. and Jessup, W. (1997). Regulation of serum-induced lipid accumulation in human monocyte-derived macrophages by interferon-gamma. Correlations with apolipoprotein E production, lipoprotein lipase activity and LDL receptor-related protein expression. *Atherosclerosis* **128**(1): 47-58.

Gaut, J. P., Yeh, G. C., Tran, H. D., Byun, J., Henderson, J. P., Richter, G. M., Brennan, M. L., Lusis, A. J., Belaaouaj, A., Hotchkiss, R. S. and Heinecke, J. W. (2001). Neutrophils employ the myeloperoxidase system to generate antimicrobial brominating and chlorinating oxidants during sepsis. *Proc Natl Acad Sci USA* **98**(21): 11961-6.

Gazda, M. and Margerum, D. W. (1994). Reactions of monochloramine with Br2, Br3−, HOBr, and OBr−: formation of bromochloramines. *Inorg. Chem* **33**: 118-123.

Geng, Y. J. and Hansson, G. K. (1992). Interferon-gamma inhibits scavenger receptor expression and foam cell formation in human monocyte-derived macrophages. *J Clin Invest* **89**(4): 1322-30.

Ghezzi, P. and Di Simplicio, P. (2007). Glutathionylation pathways in drug response. *Curr Opin Pharmacol* **7**(4): 398-403.

Gieseg, S. P. and Cato, S. (2003). Inhibition of THP-1 cell-mediated low-density lipoprotein oxidation by the macrophage-synthesised pterin, 7,8-dihydroneopterin. *Redox Report* **8**(2): 113-119.

Gieseg, S. P., Crone, E. M., Flavall, E. A. and Amit, Z. (2007). Potential to inhibit growth of atherosclerotic plaque development through modulation of macrophage neopterin/7,8-dihydroneopterin synthesis. *Br J Pharmacol*: 1-9.

Gieseg, S. P., Pearson, J. and Firth, C. A. (2003). Protein hydroperoxides are a major product of low density lipoprotein oxidation during copper, peroxyl radical and macrophage-mediated oxidation. *Free Radic Res* **37**(9): 983-91.

Gieseg, S. P., Reibnegger, G., Wachter, H. and Esterbauer, H. (1995). 7,8 Dihydroneopterin inhibits low density lipoprotein oxidation in vitro. Evidence that this macrophage secreted pteridine is an anti-oxidant. *Free Radic Res* **23**(2): 123-36.

Gieseg, S. P., Simpson, J. A., Charlton, T. S., Duncan, M. W. and Dean, R. T. (1993). Protein-bound 3,4-dihydroxyphenylalanine is a major reductant formed during hydroxyl radical damage to proteins. *Biochemistry* **32**(18): 4780-6.

Gieseg, S. P., Whybrow, J., Glubb, D. and Rait, C. (2001a). Protection of U937 cells from free radical damage by the macrophage synthesized antioxidant 7,8-dihydroneopterin. *Free Radic Res* **35**(3): 311-8.

Gieseg, S. P., Maghzal, G. and Glubb, D. (2001b). Protection of erythrocytes by the macrophage synthesized antioxidant 7,8 dihydroneopterin. *Free Radic Res* **34**(2): 123-36.

Giguere, C. J., Covington, M. D. and Schnellmann, R. G. (2008). Mitochondrial calpain 10 activity and expression in the kidney of multiple species. *Biochem Biophys Res Commun* **366**(1): 258-62.

Giguere, C. J. and Schnellmann, R. G. (2008). Limitations of SLLVY-AMC in calpain and proteasome measurements. *Biochem Biophys Res Commun* **371**(3): 578-81.

Gill, J. S., McKenna, W. J. and Camm, A. J. (1995). Free radicals irreversibly decrease Ca2+ currents in isolated guinea-pig ventricular myocytes. *Eur J Pharmacol* **292**(3-4): 337-40.

Glass, C. K. and Witztum, J. L. (2001). Atherosclerosis. the road ahead. *Cell* **104**(4): 503-16.

Goldhaber, J. I., Ji, S., Lamp, S. T. and Weiss, J. N. (1989). Effects of exogenous free radicals on electromechanical function and metabolism in isolated rabbit and guinea pig ventricle. Implications for ischemia and reperfusion injury. *J Clin Invest.* **83**(6): 1800-9.

Goldstein, I. M., Roos, D., Kaplan, H. B. and Weissmann, G. (1975). Complement and immunoglobulins stimulate superoxide production by human leukocytes independently of phagocytosis. *J Clin Invest* **56**(5): 1155-63.

Guttmann, R. P. and Johnson, G. V. (1998). Oxidative stress inhibits calpain activity in situ. *J Biol Chem.* **273**(21): 13331-8.

Goll, D. E., Thompson, V. F., Li, H., Wei, W. and Cong, J. (2003). The calpain system. *Physiol Rev* **83**(3): 731-801.

Gotoh, N., Graham, A., Nikl, E. and Darley-Usmar, V. M. (1993). Inhibition of glutathione synthesis increases the toxicity of oxidized low-density lipoprotein to human monocytes and macrophages. *Biochem J* **296**(Pt 1): 151-4.

Gottlieb, E., Vander Heiden, M. G. and Thompson, C. B. (2000). Bcl-xL Prevents the Initial Decrease in Mitochondrial Membrane Potential and Subsequent Reactive Oxygen Species Production during Tumor Necrosis Factor Alpha-Induced Apoptosis *Molecular and Cellular Biology* **20**(15): 5680-89.

Green, D. R. and Kroemer, G. (2004). The pathophysiology of mitochondrial cell death. *Science* **305**(5684): 626-9.

Green, P. S., Mendez, A. J., Jacob, J. S., Crowley, J. R., Growdon, W., Hyman, B. T. and Heinecke, J. W. (2004). Neuronal expression of myeloperoxidase is increased in Alzheimer's disease. *J Neurochem* **90**(3): 724-33.

Gregoriou, M., Willis, A. C., Pearson, M. A. and Crawford, C. (1994). The calpain cleavage sites in the epidermal growth factor receptor kinase domain. *Eur J Biochem* **223**(2): 455-64.

Grewal, T., Priceputu, E., Davignon, J. and Bernier, L. (2001). Identification of a gamma-interferon-responsive element in the promoter of the human macrophage scavenger receptor A gene. *Arterioscler Thromb Vasc Biol* **21**(5): 825-31.

Grijalba, M. T., Vercesi, A. E. and Schreier, S. (1999). Ca2+-induced increased lipid packing and domain formation in submitochondrial particles. A possible early step in the mechanism of Ca2+-stimulated generation of reactive oxygen species by the respiratory chain. *Biochemistry* **38**(40): 13279-87.

Grösch, S., Fritz, G. and Kaina, B. (1998). Apurinic endonuclease (Ref-1) is induced in mammalian cells by oxidative stress and involved in clastogenic adaptation. *Cancer Res* **58**(19): 4410-6.

Grutter, M. G. (2000). Caspases: key players in programmed cell death. *Curr Opin Struct Biol* **10**(6): 649-55.

Gupta, S., Pablo, A. M., Jiang, X., Wang, N., Tall, A. R. and Schindler, C. (1997). IFN-gamma potentiates atherosclerosis in ApoE knock-out mice. *J Clin Invest* **99**(11): 2752-61.

Gurfinkel, E. P., Scirica, B. M., Bozovich, G., Macchia, A., Manos, E. and Mautner, B. (1999). Serum neopterin levels and the angiographic extent of coronary arterial narrowing in unstable angina pectoris and in non-Q-wave acute myocardial infarction. *Am J Cardiol* **83**(4): 515-8.

Halestrap, A. P. and Davidson, A. M. (1990). Inhibition of Ca2(+)-induced large-amplitude swelling of liver and heart mitochondria by cyclosporin is probably caused by the inhibitor binding to mitochondrial-matrix peptidyl-prolyl cis-trans isomerase and preventing it interacting with the adenine nucleotide translocase. *Biochem J* **268**(1): 153-60.

Halliwell, B., Gutteridge, J. M. and Aruoma, O. I. (1987). The deoxyribose method: a simple "test-tube" assay for determination of rate constants for reactions of hydroxyl radicals. *Anal Biochem* **165**(1): 215-9.

Halliwell, B. and Gutteridge, J. M. C. (2007). Free Radicals in Biology and Medicine. Oxford Oxford Univeristy Press.

Hammerschmidt, S. and Wahn, H. (1998). The effect of the oxidant hypochlorous acid on the L-type calcium current in isolated ventricular cardiomyocytes. *J Mol Cell Cardiol* **30**(9): 1855-67.

Hampton, M. B., Kettle, A. J. and Winterbourn, C. C. (1998b). Inside the neutrophil phagosome: oxidants, myeloperoxidase, and bacterial killing. *Blood* **92**(9): 3007-17.

Hampton, M. B., Morgan, P. E. and Davies, M. J. (2002). Inactivation of cellular caspases by peptide-derived tryptophan and tyrosine peroxides. *FEBS Lett* **527**(1-3): 289-92.

Hampton, M. B. and Orennius, S. (1997). Dual regulation of caspase activity by hydrogen peroxide: implications for apoptosis. *FEBS Letters* **414**: 552-6.

Hampton, M. B., Zhivotovsky, B., Slater, A. F., Burgess, D. H. and Orrenius, S. (1998a). Importance of the redox state of cytochrome c during caspase activation in cytosolic extracts. *Biochem J* **329**(Pt 1): 95-9.

Handelman, G. J., Nightingale, Z. D., Dolnikowski, G. G. and Blumberg, J. B. (1998). Formation of carbonyls during attack on insulin by submolar amounts of hypochlorite. *Anal Biochem* **258**(2): 339-48.

Hansson, G. K., Holm, J. and Jonasson, L. (1989a). Detection of activated T lymphocytes in the human atherosclerotic plaque. *Am J Pathol* **135**(1): 169-75.

Hansson, M. J., Persson, T., Friberg, H., Keep, M. F., Rees, A., Wieloch, T. and Elmér, E. (2003). Powerful cyclosporin inhibition of calcium-induced permeability transition in brain mitochondria. *Brain Res* **960**(1-2): 99-111.

Hansson, G. K., Robertson, A. K. and Söderberg-Nauclér, C. (2006). Inflammation and atherosclerosis. *Annu Rev Pathol* **1**: 297-329.

Harris, M. H. and Thompson, C. B. (2000). The role of the Bcl-2 family in the regulation of outer mitochondrial membrane permeability. *Cell Death Differ* **7**(12): 1182-91.

Harrison, J. E. and Schultz, J. (1976). Studies on the chlorinating activity of myeloperoxidase. *J Biol Chem* **251**(5): J Biol Chem. 1976 Mar 10;251(5):1371-4.

Haunstetter, A. and Izumo, S. (1998). Apoptosis: basic mechanisms and implications for cardiovascular disease. *Circ Res* **82**(11): 1111-29.

Haveman, J. W., Muller Kobold, A. C., Tervaert, J. W., van den Berg, A. P., Tulleken, J. E., Kallenberg, C. G. and The, T. H. (1999). The central role of monocytes in the pathogenesis of sepsis: consequences for immunomonitoring and treatment. *Neth J Med* **55**(3): 132-41.

Hawkins, C. L. and Davies, M. J. (1999). Hypochlorite-induced oxidation of proteins in plasma: formation of chloramines and nitrogen-centred radicals and their role in protein fragmentation. *Biochem J* **340**(Pt 2): 539-48.

Hawkins, C. L. and Davies, M. J. (2001). Hypochlorite-induced damage to nucleosides: formation of chloramines and nitrogen-centered radicals. *Chem Res Toxicol* **14**(8): 1071-81.

Hazell, L. J., Arnold, L., Flowers, D., Waeg, G., Malle, E. and Stocker, R. (1996). Presence of hypochlorite-modified proteins in human atherosclerotic lesions. *J Clin Invest* **97**(6): 1535-44.

Hazell, L. J., Davies, M. J. and Stocker, R. (1999). Secondary radicals derived from chloramines of apolipoprotein B-100 contribute to HOCl-induced lipid peroxidation of low-density lipoproteins. *Biochem J* **339 (Pt 3)**: 489-95.

Hazell, L. J. and Stocker, R. (1993). Oxidation of low-density lipoprotein with hypochlorite causes transformation of the lipoprotein into a high-uptake form for macrophages. *Biochem J* **290 (Pt 1)**: 165-72.

Hazell, L. J., van den Berg, J. J. and Stocker, R. (1994). Oxidation of low-density lipoprotein by hypochlorite causes aggregation that is mediated by modification of lysine residues rather than lipid oxidation. *Biochem J* **302**(Pt 1): 297-304.

Hazen, S. L., d'Avignon, A., Anderson, M. M., Hsu, F. F. and Heinecke, J. W. (1998a). Human neutrophils employ the myeloperoxidase-hydrogen peroxide-chloride system to oxidize alpha-amino acids to a family of reactive aldehydes. Mechanistic studies identifying labile intermediates along the reaction pathway. *J Biol Chem* **273**(9): 4997-5005.

Hazen, S. L. and Heinecke, J. W. (1997). 3-Chlorotyrosine, a specific marker of myeloperoxidase-catalyzed oxidation, is markedly elevated in low density lipoprotein isolated from human atherosclerotic intima. *J. Clin Invest* **99**: 2075-2081.

Hazen, S. L., Hsu, F. F., Mueller, D. M., Crowley, J. R. and Heinecke, J. W. (1996b). Human neutrophils employ chlorine gas as an oxidant during phagocytosis. *J Clin Invest* **98**(6): 1283-9.

Heales, S. J., Blair, J. A., Meinschad, C. and Ziegler, I. (1988). Inhibition of monocyte luminol-dependent chemiluminescence by tetrahydrobiopterin, and the free radical oxidation of tetrahydrobiopterin, dihydrobiopterin and dihydroneopterin. *Cell Biochem Funct* **6**(3): 191-5.

Heinecke, J. W., Li, W., Francis, G. A. and Goldstein, J. A. (1993). Tyrosyl radical generated by myeloperoxidase catalyzes the oxidative cross-linking of proteins. *J. Clin. Invest* **91**(6): 2866-72.

Hell, J. W., Westenbroek, R. E., Breeze, L. J., Wang, K. K., Chavkin, C. and Catterall, W. A. (1996). N-methyl-D-aspartate receptor-induced proteolytic conversion of postsynaptic class C L-type calcium channels in hippocampal neurons. *Proc Natl Acad Sci U S A* **93**(8): 3362-7.

Herpfer, I., Greilberger, J., Ledinski, G., Widner, B., Fuchs, D. and Jurgens, G. (2002). Neopterin and 7,8-dihydroneopterin interfere with low density lipoprotein oxidation mediated by peroxynitrite and/or copper. *Free Radic Res* **36**(5): 509-20.

Hirrlinger, J., König, J. and Dringen, R. (2002a). Expression of mRNAs of multidrug resistance proteins (Mrps) in cultured rat astrocytes, oligodendrocytes, microglial cells and neurones. *J Neurochem* **82**(3): 716-9.

Hirrlinger, J., Schulz, J. B. and Dringen, R. (2002b). Glutathione release from cultured brain cells: multidrug resistance protein 1 mediates the release of GSH from rat astroglial cells. *J Neurosci Res* **69**(3): 318-26.

Hockenbery, D. M., Oltvai, Z. N., Yin, X. M., Milliman, C. L. and Korsmeyer, S. J. (1993). Bcl-2 functions in an antioxidant pathway to prevent apoptosis. *Cell* **75**(2): 241-51.

Hoffmann, G., Frede, S., Kenn, S., Smolny, M., Wachter, H., Fuchs, D., Grote, J., Rieder, J. and Schobersberger, W. (1998). Neopterin-induced tumor necrosis factor-alpha synthesis in vascular smooth muscle cells in vitro. *Int Arch Allergy Immunol* **116**(3): 240-5.

Hoffmann, G., Rieder, J., Smolny, M., Seibel, M., Wirleitner, B., Fuchs, D. and Schobersberger, W. (1999). Neopterin-induced expression of intercellular adhesion molecule-1 (ICAM-1) in type II-like alveolar epithelial cells. *Clin Exp Immunol* **118**(3): 435-40.

Hoffmann, G., Schobersberger, W., Frede, S., Pelzer, L., Fandrey, J., Wachter, H., Fuchs, D. and Grote, J. (1996). Neopterin activates transcription factor nuclear factor-kappa B in vascular smooth muscle cells. *FEBS Lett* **391**(1-2): 181-4.

Hoffmann, G., Wirleitner, B. and Fuchs, D. (2003). Potential role of immune system activation-associated production of neopterin derivatives in humans. *Inflamm Res.* **52**(8): 313-21.

Horejsi, R., Estelberger, W., Mlekusch, W., Moller, R., Ottl, K., Vrecko, K. and Reibnegger, G. (1996). Effects of pteridines on chloramine-T-induced growth

inhibition in E. coli strains: correlations with molecular structure. *Free Radic Biol Med* **21**(2): 133-8.

Hsieh , C. C., Yen, M. H., Yen , C. H. and Lau, Y. T. (2001). Oxidized low density lipoprotein induces apoptosis via generation of reactive oxygen species in vascular smooth muscle cells. *Cardio Res* **49**(1): 135-45.

Huang, Y. and Wang, K. K. (2001). The calpain family and human disease. *Trends Mol Med* **7**(8): 355-62.

Humphreys, J. M., Davies, B., Hart, C. A. and Edwards, S. W. (1989). Role of myeloperoxidase in the killing of Staphylococcus aureus by human neutrophils: studies with the myeloperoxidase inhibitor salicylhydroxamic acid. *J Gen Microbiol* **135**(5): 1187-93.

Hurne, A. M., Chai, C. L., Moerman, K. and Waring, P. (2002). Influx of calcium through a redox-sensitive plasma membrane channel in thymocytes causes early necrotic cell death induced by the epipolythiodioxopiperazine toxins. *J Biol Chem* **277**(35): 31631-8.

Iacoviello, L., Kolpakov, V., Salvatore, L., Amore, C., Pintucci, G., de Gaetano, G. and Donati, M. B. (1995). Human endothelial cell damage by neutrophil-derived cathepsin G. Role of cytoskeleton rearrangement and matrix-bound plasminogen activator inhibitor-1. *Arterioscler Thromb Vasc Biol* **15**(11): 2037-46.

Inserte, J., Garcia-Dorado, D., Ruiz-Meana, M., Agulló, L., Pina, P. and Soler-Soler, J. (2004). Ischemic preconditioning attenuates calpain-mediated degradation of structural proteins through a protein kinase A-dependent mechanism. *Cardiovasc Res* **64**(1): 105-14.

Ishii, T., Sunami, O., Nakajima, H., Nishio, H., Takeuchi, T. and Hata, F. (1999). Critical role of sulfenic acid formation of thiols in the inactivation of glyceraldehyde-3-phosphate dehydrogenase by nitric oxide. *Biochem Pharmacol* **58**(1): 133-43.

Jaeschke, H. and Lemasters, J. J. (2003). Apoptosis versus oncotic necrosis in hepatic ischemia/reperfusion injury. *Gastroenterology* **125**(4): 1246-57.

Jekabsone, A., Ivanoviene, L., Brown, G. C. and Borutaite, V. (2003). Nitric oxide and calcium together inactivate mitochondrial complex I and induce cytochrome c release. *J Mol Cell Cardiol* **35**(7): 803-9.

Jessup, W. and Kritharides, L. (2000). Metabolism of oxidized LDL by macrophages. *Curr Opin Lipidol* **11**(5): 473-81.

Jessup, W., Kritharides, L. and Stocker, R. (2004). Lipid oxidation in atherogenesis: an overview. *Biochem Soc Trans* **32**(1): 134-138.

Jonasson, L., Hansson, G. K., Bondjers, G., Noe, L. and Etienne, J. (1990). Interferon-gamma inhibits lipoprotein lipase in human monocyte-derived macrophages. *Biochim Biophys Acta* **1053**(1): 43-8.

Kalkan, A., Ozden, M. and Akbulut, H. (2005). Serum neopterin levels in patients with chronic hepatitis B. *Jpn J Infect Dis* **58**(2): 107-9.

Kao, J. P., Harootunian, A. T. and Tsien, R. Y. (1989). Photochemically generated cytosolic calcium pulses and their detection by fluo-3. *J Biol Chem* **264**(14): 8179-84.

Kato, Y., Kitamoto, N., Kawai, Y. and Osawa, T. (2001). The hydrogen peroxide/copper ion system, but not other metal-catalyzed oxidation systems, produces protein-bound dityrosine. *Free Radic Biol Med* **31**(5): 624-32.

Kato, K., Shao, Q., Elimban, V., Lukas, A. and Dhalla, N. S. (1998). Mechanism of depression in cardiac sarcolemmal Na+-K+-ATPase by hypochlorous acid. *Am J Physiol* **275**(3 Pt 1): C826-31.

Kettle, A. J. (1996). Neutrophils convert tyrosyl residues in albumin to chlorotyrosine. *FEBS Lett* **379**(1): 103-6.

Kim, J. S., He, L. and Lemasters, J. J. (2003a). Mitochondrial permeability transition: a common pathway to necrosis and apoptosis. *Biochem Biophys Res Commun* **304**(3): 463-70.

Kim, J. S., He, L., Qian, T. and Lemasters, J. J. (2003b). Role of the mitochondrial permeability transition in apoptotic and necrotic death after ischemia/reperfusion injury to hepatocytes. *Curr Mol Med* **3**(6): 527-35.

Kirichok, Y., Krapivinsky, G. and Clapham, D. E. (2004). The mitochondrial calcium uniporter is a highly selective ion channel. *Nature* **427**(6972): 360-4.

Kirsch, D. G., Doseff, A., Chau, B. N., Lim, D.-S., de Souza-Pinto, N. C., Hansford, R., Kastan, M. B., Lazebnik, Y. A. and Hardwick, J. M. (1999). Caspase-3-dependent cleavage of Bcl-2 promotes release of cytochrome c. *J Biol Chem* **274**(30): 21155-61.

Kishimoto, A., Mikawa, K., Hashimoto, K., Yasuda, I., Tanaka, S., Tominaga, M., Kuroda, T. and Nishizuka, Y. (1989). Limited proteolysis of protein kinase C subspecies by calcium-dependent neutral protease (calpain). *J Biol Chem* **264**(7): 4088-92.

Kitahara, M., Eyre, H. J., Simonian, Y., Atkin, C. L. and Hasstedt, S. J. (1981). Hereditary myeloperoxidase deficiency. *Blood* **57**(5): 888-93.

Klebanoff, S. J. (1970). Myeloperoxidase: contribution to the microbicidal activity of intact leukocytes. *Science* **169**(950): 1095-7.

Klebanoff, S. J. (2005). Myeloperoxidase: friend and foe. *J Leukoc Biol* **77**(5): 598-625.

Klebanoff, S. J., Kinsella, M. G. and Wight, T. N. (1993). Degradation of endothelial cell matrix heparan sulfate proteoglycan by elastase and the myeloperoxidase-H2O2-chloride system. *Am J Pathol* **143**(3): 907-17.

Klein, R. L., Ascencao, J. L., Mironova, M., Huang, Y. and Lopes-Virella, M. F. (2001). Effect of inflammatory cytokines on the metabolism of low-density lipoproteins by human vascular endothelial cells. *Metabolism* **50**(1): 99-106.

Kluck, R. M., Ellerby, L. M., Ellerby, H. M., Naiem, S., Yaffe, M. P., Margoliash, E., Bredesen, D., Mauk, A. G., Sherman, F. and Newmeyer, D. D. (2000). Determinants of cytochrome c pro-apoptotic activity. The role of lysine 72 trimethylation. *J Biol Chem* **275**(21): 16127-33.

Kluck, R. M., Esposti, M. D., Perkins, G., Renken, C., Kuwana, T., Bossy-Wetzel, E., Goldberg, M., Allen, T., Barber, M. J., Green, D. R. and Newmeyer, D. D. (1999). The pro-apoptotic proteins, Bid and Bax, cause a limited permeabilization of the mitochondrial outer membrane that is enhanced by cytosol. *J Cell Biol* **147**(4): 809-22.

Kojima, S., Nomura, T., Icho, T., Kajiwara, Y., Kitabatake, K. and Kubota, K. (1993). Inhibitory effect of neopterin on NADPH-dependent superoxide-generating oxidase of rat peritoneal macrophages. *FEBS Lett* **329**(1-2): 125-8.

Kolodgie, F. D., Gold, H. K., Burke, A. P., Fowler, D. R., Kruth, H. S., Weber, D. K., Farb, A., Guerrero, L. J., Hayase, M., Kutys, R., Narula, J., Finn, A. V. and Virmani, R. (2003). Intraplaque hemorrhage and progression of coronary atheroma. *N Engl J Med* **349**(24): 2316-25.

Kosaka, S., Takahashi, S., Masamura, K., Kanehara, H., Sakai, J., Tohda, G., Okada, E., Oida, K., Iwasaki, T., Hattori, H., Kodama, T., Yamamoto, T. and Miyamori, I. (2001). Evidence of macrophage foam cell formation by very low-density lipoprotein receptor: interferon-gamma inhibition of very low-density lipoprotein receptor expression and foam cell formation in macrophages. *Circulation* **103**(8): 1142-7.

Kowaltowski, A. J., Castilho, R. F. and Vercesi, A. E. (2001). Mitochondrial permeability transition and oxidative stress. *FEBS Lett* **495**(1-2): 12-5.

Kowaltowski, A. J., Vercesi, A. E. and Castilho, R. F. (1997). Mitochondrial membrane protein thiol reactivity with N-ethylmaleimide or mersalyl is modified by Ca2+: correlation with mitochondrial permeability transition *Biochim Biophys Acta* **1318**(3): 395-402.

Kowaltowski, A. J., Vercesi, A. E. and Fiskum, G. (2000). Bcl-2 prevents mitochondrial permeability transition and cytochrome c release via maintenance of reduced pyridine nucleotides. *Cell Death Differ* **7**(10): 903-10.

Kroemer, G. (1998). The mitochondrion as an integrator/coordinator of cell death pathways. *Cell Death Differ* **5**(6): 547.

Kroemer, G. and Martin, S. J. (2005). Caspase-independent cell death. *Nat Med* **11**(7): 725-30.

LaCagnin, L. B., Bowman, L., Ma, J. Y. and Miles, P. R. (1990). Metabolic changes in alveolar type II cells after exposure to hydrogen peroxide. *Am J Physiol* **259**(2 Pt 1): L57-65.

LaMarre, J., Wolf, B. B., Kittler, E. L., Quesenberry, P. J. and Gonias, S. L. (1993). Regulation of macrophage alpha 2-macroglobulin receptor/low density lipoprotein receptor-related protein by lipopolysaccharide and interferon-gamma. *J Clin Invest* **91**(3): 1219-24.

Lankiewicz, S., Marc Luetjens, C., Truc Bui, N., Krohn, A. J., Poppe, M., Cole, G. M., Saido, T. C. and Prehn, J. H. (2000). Activation of calpain I converts excitotoxic neuron death into a caspase-independent cell death. *J Biol Chem* **275**(22): 17064-71.

Lee, K. S., Frank, S., Vanderklish, P., Arai, A. and Lynch, G. (1991). Inhibition of proteolysis protects hippocampal neurons from ischemia. *Proc Natl Acad Sci U S A* **88**(16): 7233-7.

Lee, R. T. and Libby, P. (1997). The Unstable Atheroma. *Arteriosclerosis, Thrombosis, and Vascular Biology* **17**: 1859-1867.

Lemasters, J. J. (1999). V. Necrapoptosis and the mitochondrial permeability transition: shared pathways to necrosis and apoptosis. *Am J Physiol* **276**(1 Pt 1): G1-6.

Leeuwenburgh, C., Rasmussen, J. E., Hsu, F. F., Mueller, D. M., Pennathur, S. and Heinecke, J. W. (1997). Mass spectrometric quantification of markers for protein oxidation by tyrosyl radical, copper, and hydroxyl radical in low density lipoprotein isolated from human atherosclerotic plaques. *J Biol Chem* **272**(6): 3520-6.

Lehrer, R. I. and Cline, M. J. (1969). Leukocyte myeloperoxidase deficiency and disseminated candidiasis: the role of myeloperoxidase in resistance to Candida infection. *J Clin Invest* **48**(8): 1478-88.

Lelli, J. L., Jr., Becks, L. L., Dabrowska, M. I. and Hinshaw, D. B. (1998). ATP converts necrosis to apoptosis in oxidant-injured endothelial cells. *Free Radic Biol Med* **25**(6): 694-702.

Lemasters, J. J. (1999). V. Necrapoptosis and the mitochondrial permeability transition: shared pathways to necrosis and apoptosis. *Am J Physiol* **276**(1 Pt 1): G1-6.

Lemasters, J. J., Theruvath, T. P., Zhong, Z. and Nieminen, A. L. (2009). Mitochondrial calcium and the permeability transition in cell death." *Biochim Biophys Acta.* .

Leon, M. L. and Zuckerman, S. H. (2005). Gamma interferon: a central mediator in atherosclerosis. *Inflamm Res* **54**(10): 395-411.

Libby, P. (1995). Molecular bases of the acute coronary syndromes. *Circulation* **91**(11): 2844-50.

Libby, P. and Hansson, G. K. (1991). Involvement of the immune system in human atherogenesis: current knowledge and unanswered questions. *Lab Invest* **64**(1): 5-15.

Liu, X., Kim, C., Yang, J., Jemmerson, R. and Wang, X. (1996). Induction of apoptotic program in cell-free extracts: Requirement for dATP and cytochrome c. *Cell* **86**(1): 147-57.

Liu, X. and Schnellmann, R. G. (2003). Calpain mediates progressive plasma membrane permeability and proteolysis of cytoskeleton-associated paxillin, talin, and vinculin during renal cell death. *J Pharmacol Exp Ther* **304**(1): 63-70.

Loew, L. M., Carrington, W., Tuft, R. A. and Fay, F. S. (1994). Physiological cytosolic Ca2+ transients evoke concurrent mitochondrial depolarizations. *Proc Natl Acad Sci U S A* **91**(26): 12579-83.

Luetjens, C. M., Bui, N. T., Sengpiel, B., Münstermann, G., Poppe, M., Krohn, A. J., Bauerbach, E., Krieglstein, J. and Prehn, J. H. (2000). Delayed mitochondrial dysfunction in excitotoxic neuron death: cytochrome c release and a secondary increase in superoxide production. *J Neurosci* **20**(15): 5715-23.

Luo, X., Budihardjo, I., Zou, H., Slaughter, C. and Wang, X. (1998). Bid, a Bcl2 interacting protein, mediates cytochrome c release from mitochondria in response to activation of cell surface death receptors. *Cell* **94**(4): 481-90.

Lusis, A. J. (2000). Atherosclerosis. *Nature* **407**(6801): 233-41.

Ly, J. D., Grubb, D. R. and Lawen, A. (2003). The mitochondrial membrane potential (deltapsi(m)) in apoptosis; an update. *Apoptosis* **8**(2): 115-28.

Maack, C. and O'Rourke, B. (2007). Excitation-contraction coupling and mitochondrial energetics. *Basic Res Cardiol* **102**(5): 369-92.

Malle, E., Waeg, G., Schreiber, R., Gröne, E. F., Sattler, W. and Gröne, H. J. (2000). Immunohistochemical evidence for the myeloperoxidase/H2O2/halide system in

human atherosclerotic lesions: colocalization of myeloperoxidase and hypochlorite-modified proteins. *Eur J Biochem* **267**(14): 4495-503.

Mannella, C. A. (1992). The 'ins' and 'outs' of mitochondrial membrane channels. *Trends Biochem Sci* **17**(8): 315-20.

Marengo, J. J., Hidalgo, C. and Bull, R. (1998). Sulfhydryl oxidation modifies the calcium dependence of ryanodine-sensitive calcium channels of excitable cells. *Biophys J* **74**(3): 1263-77.

Mathews, C. K. and Van Holde, K. E. (1990). Biochemistry. Redwood City, The Benjamin/Cummings Publishing Company, Inc.

Matsuyama, S. and Reed, J. C. (2000). Mitochondria-dependent apoptosis and cellular pH regulation. *Cell Death Differ* **7**(12): 1155-65.

Mazumder, B., Mukhopadhyay, C. K., Prok, A., Cathcart, M. K. and Fox, P. L. (1997). Induction of ceruloplasmin synthesis by IFN-gamma in human monocytic cells. *J Immunol* **159**(4): 1938-44.

McCormack, J. G. and Denton, R. M. (1993). Mitochondrial Ca2+ transport and the role of intramitochondrial Ca2+ in the regulation of energy metabolism. *Dev Neurosci* **15**(3-5): 165-73.

McKenna, S. M. and Davies, K. J. (1988). The inhibition of bacterial growth by hypochlorous acid. Possible role in the bactericidal activity of phagocytes. *Biochem J* **254**(3): 685-92.

McKenzie, S. J., Baker, M. S., Buffinton, G. D. and Doe, W. F. (1996). Evidence of oxidant-induced injury to epithelial cells during inflammatory bowel disease. *J Clin Invest* **98**(1): 136-41.

McKenzie, S. M., Doe, W. F. and Buffinton, G. D. (1999). 5-aminosalicylic acid prevents oxidant mediated damage of glyceraldehyde-3-phosphate dehydrogenase in colon epithelial cells. *Gut* **44**(2): 180-5.

McStay, G. P., Clarke, S. J. and Halestrap, A. P. (2002). Role of critical thiol groups on the matrix surface of the adenine nucleotide translocase in the mechanism of the mitochondrial permeability transition pore. *Biochem J* **367**(Pt 2): 541-8.

Meister, A. (1988). Glutathione metabolism and its selective modification. *J Biol Chem* **263**(33): 17205-8.

Midwinter, R. G., Cheah, F. C., Moskovitz, J., Vissers, M. C. and Winterbourn, C. C. (2006). IkappaB is a sensitive target for oxidation by cell-permeable chloramines: inhibition of NF-kappaB activity by glycine chloramine through methionine oxidation. *Biochem J* **396**(1): 71-8.

Midwinter, R. G., Peskin, A. V., Vissers, M. C. and Winterbourn, C. C. (2004). Extracellular oxidation by taurine chloramine activates ERK via the epidermal growth factor receptor. *J Biol Chem* **279**(31): 32205-11.

Midwinter, R. G., Vissers, M. C. and Winterbourn, C. C. (2001). Hypochlorous acid stimulation of the mitogen-activated protein kinase pathway enhances cell survival. *Arch Biochem Biophys* **394**(1): 13-20.

Mieyal, J. J., Gallogly, M. M., Qanungo, S., Sabens, E. A. and Shelton, M. D. (2008). Molecular mechanisms and clinical implications of reversible protein S-glutathionylation. *Antioxid Redox Signal* **10**(11): 1941-88.

Mildaziene, V., Baniene, R., Nauciene, Z., Bakker, B. M., Brown, G. C., Westerhoff, H. V. and Kholodenko, B. N. (1995). Calcium indirectly increases the control exerted by the adenine nucleotide translocator over 2-oxoglutarate oxidation in rat heart mitochondria. *Arch Biochem Biophys* **324**(1): 130-4.

Minta, A., Kao, J. P. and Tsien, R. Y. (1989). Fluorescent indicators for cytosolic calcium based on rhodamine and fluorescein chromophores. *J Biol Chem* **264**(14): 8171-8.

Mirkovic, N., Voehringer, D. W., Story, M. D., McConkey, D. J., McDonnell, T. J. and Meyn, R. E. (1997). Resistance to radiation-induced apoptosis in Bcl-2-expressing cells is reversed by depleting cellular thiols. *Oncogene* **15**: 1461-70.

Mishra, D. P., Pal, R. and Shaha, C. (2006). Changes in cytosolic Ca2+ levels regulate Bcl-xS and Bcl-xL expression in spermatogenic cells during apoptotic death. *J Biol Chem* **281**(4): 2133-43.

Miyoshi, H., Umeshita, K., Sakon, M., Imajoh-Ohmi, S., Fujitani, K., Gotoh, M., Oiki, E., Kambayashi, J. and Monden, M. (1996). Calpain activation in plasma membrane bleb formation during tert-butyl hydroperoxide-induced rat hepatocyte injury. *Gastroenterology* **110**(6): 1897-904.

Moldeus, P., Hogberg, J. and Orrenius, S. (1978). Isolation and use of liver cells. *Methods Enzymol* **52**: 60-71.

Morris, J. C. (1966). The Acid Ionization Constant of HOCl from 5 to 35°. *J. Phys. Chem* **70**(12): 3798-805.

Mosmann, T. (1983). Rapid colorimetric assay for cellular growth and survival: application to proliferation and cytotoxicity assays. *J Immunol Methods* **65**(1-2): 55-63.

Muguruma, M., Nishimuta, S., Tomisaka, Y., Ito, T. and Matsumura, S. (1995). Organization of the functional domains in membrane cytoskeletal protein talin. *J Biochem* **117**(5): 1036-42.

Munger, J. S., Haass, C., Lemere, C. A., Shi, G. P., Wong, W. S., Teplow, D. B., Selkoe, D. J. and Chapman, H. A. (1995). Lysosomal processing of amyloid precursor protein to A beta peptides: a distinct role for cathepsin S. *Biochem J* **311**(Pt 1): 299-305.

Murr, C., Baier-Bitterlich, G., Fuchs, D., Werner, E. R., Esterbauer, H., Pfleiderer, W. and Wachter, H. (1996). Effects of neopterin-derivatives on H2O2-induced luminol chemiluminescence: mechanistic aspects. *Free Radic Biol Med* **21**(4): 449-56.

Murr, C., Fuchs, D., Gössler, W., Hausen, A., Reibnegger, G., Werner, E. R., Werner-Felmayer, G., Esterbauer, H. and Wachter, H. (1994). Enhancement of hydrogen peroxide-induced luminol-dependent chemiluminescence by neopterin depends on the presence of iron chelator complexes. *FEBS Lett* **338**(2): 223-6.

Nagra, R. M., Becher, B., Tourtellotte, W. W., Antel, J. P., Gold, D., Paladino, T., Smith, R. A., Nelson, J. R. and Reynolds, W. F. (1997). Immunohistochemical and genetic evidence of myeloperoxidase involvement in multiple sclerosis. *J Neuroimmunol* **78**(1-2): 97-107.

Nakagawa, T., Nozaki, S., Nishida, M., Yakub, J. M., Tomiyama, Y., Nakata, A., Matsumoto, K., Funahashi, T., Kameda-Takemura, K., Kurata, Y., Yamashita, S. and Matsuzawa, Y. (1998). Oxidized LDL increases and interferon-gamma decreases expression of CD36 in human monocyte-derived macrophages. *Arterioscler Thromb Vasc Biol* **18**(8): 1350-7.

Nathan, C. F. (1986). Peroxide and pteridine: a hypothesis on the regulation of macrophage antimicrobial activity by interferon gamma. *Interferon* **7**: 125-43.

Nathan, C. F. (1987). Secretory products of macrophages. *J Clin Invest* **79**(2): 319-26.

Newsholme, P. and Newsholme, E. A. (1989). Rates of utilization of glucose, glutamine and oleate and formation of end-products by mouse peritoneal macrophages in culture. *Biochem J* **261**(1): 211-8.

Nicolas, G., Fournier, C. M., Galand, C., Malbert-Colas, L., Bournier, O., Kroviarski, Y., Bourgeois, M., Camonis, J. H., Dhermy, D., Grandchamp, B. and Lecomte, M. C. (2002). Tyrosine phosphorylation regulates alpha II spectrin cleavage by calpain. *Mol Cell Biol* **22**(10): 3527-36.

Nicholson, D. W., Ali, A., Thornberry, N. A., Vaillancourt, J. P., Ding, C. K., Gallant, M., Gareau, Y., Griffin, P. R., Labelle, M., Lazebnik, Y. A., Munday, N. A., Raju, S. M., Smulson, M. E., Yamin, T.-T., Yu, V. L. and Miller, D. K. (1995). Identification and inhibition of the ICE/CED-3 protease necessary for mammalian apoptosis. *Nature* **376**(6535): 37-43.

Njålsson, R. and Norgren, S. (2005). Physiological and pathological aspects of GSH metabolism. *Acta Paediatr* **94**(2): 132-7.

Oettl, K., Dikalov, S., Freisleben, H. J., Mlekusch, W. and Reibnegger, G. (1997). Spin trapping study of antioxidant properties of neopterin and 7,8-dihydroneopterin. *Biochem Biophys Res Commun* **234**(3): 774-8.

Oettl, K., Greilberger, J., Dikalov, S. and Reibnegger, G. (2004). Interference of 7,8-dihydroneopterin with peroxynitrite-mediated reactions. *Biochem Biophys Res Commun* **321**(2): 379-85.

Oettl, K. and Reibnegger, G. (1999). Pteridines as inhibitors of xanthine oxidase: structural requirements. *Biochim Biophys Acta* **1430**(2): 387-95.

Oettl, K. and Reibnegger, G. (2002). Pteridine derivatives as modulators of oxidative stress. *Curr Drug Metab* **3**(2): 203-9.

Oettl, K., Wirleitner, B., Baier-Bitterlich, G., Grammer, T., Fuchs, D. and Reibnegger, G. (1999). Formation of oxygen radicals in solutions of 7,8-dihydroneopterin. *Biochem Biophys Res Commun* **264**(1): 262-7.

Orrenius, S., Nobel, C. S., van den Dobbelsteen, D. J., Burkitt, M. J. and Slater, A. F. (1996). Dithiocarbamates and the redox regulation of cell death. *Biochem Soc Trans* **24**(4): 1032-8.

Ott, M., Robertson, J. D., Gogvadze, V., Zhivotovsky, B. and Orrenius, S. (2002). Cytochrome c release from mitochondria proceeds by a two-step process. *Proc Natl Acad Sci U S A* **99**(3): 1259-63.

Panousis, C. G. and Zuckerman, S. H. (2000). Regulation of cholesterol distribution in macrophage-derived foam cells by interferon-gamma. *J Lipid Res* **41**(1): 75-83.

Park, S. Y., Shin, S. W., Lee, S. M. and Park, J. W. (2008). Hypochlorous acid-induced modulation of cellular redox status in HeLa cells. *Arch Pharm Res* **31**(7): 905-10.

Pariat, M., Carillo, S., Molinari, M., Salvat, C., Debüssche, L., Bracco, L., Milner, J. and Piechaczyk, M. (1997). Proteolysis by calpains: a possible contribution to degradation of p53. *Mol Cell Biol* **17**(5): 2806-15.

Pastore, A., Federici, G., Bertini, E. and Piemonte, F. (2003). Analysis of glutathione: implication in redox and detoxification. *Clin Chim Acta* **333**(1): 19-39.

Patrick, L. and Uzick, M. (2001). Cardiovascular disease: C-reactive protein and the inflammatory disease paradigm: HMG-CoA reductase inhibitors, alpha-tocopherol, red yeast rice, and olive oil polyphenols. A review of the literature. *Altern Med Rev* **6**(3): 248-71.

Pattison, D. I. and Davies, M. J. (2001). Absolute rate constants for the reaction of hypochlorous acid with protein side chains and peptide bonds. *Chem Res Toxicol* **14**(10): 1453-64.

Pattison, D. I., Dean, R. T. and Davies, M. J. (2002). Oxidation of DNA, proteins and lipids by DOPA, protein-bound DOPA, and related catechol(amine)s. *Toxicology* **177**(1): 23-37.

Peppin, G. J. and Weiss, S. J. (1986). Activation of the endogenous metalloproteinase, gelatinase, by triggered human neutrophils. *Proc Natl Acad Sci U S A* **83**(12): 4322-6.

Perez-Campo, R., López-Torres, M., Cadenas, S., Rojas, C. and Barja, G. (1998). The rate of free radical production as a determinant of the rate of aging: evidence from the comparative approach. *J Comp Physiol B* **168**(3): 149-58.

Peskin, A. V. and Winterbourn, C. C. (2006). Taurine chloramine is more selective than hypochlorous acid at targeting critical cysteines and inactivating creatine kinase and glyceraldehyde-3-phosphate dehydrogenase. *Free Radic Biol Med* **40**(1): 45-53.

Peskoff, A. and Langer, G. A. (1998). Calcium concentration and movement in the ventricular cardiac cell during an excitation-contraction cycle. *Biophys J* **74**(1): 153-74.

Petronilli, V., Costantini, P., Scorrano, L., Colonna, R., Passamonti, S. and Bernardi, P. (1994). The voltage sensor of the mitochondrial permeability transition pore is tuned by the oxidation-reduction state of vicinal thiols. Increase of the gating potential by oxidants and its reversal by reducing agents. *J Biol Chem* **269**(24): 16638-42.

Podrez, E. A., Abu-Soud, H. M. and Hazen, S. L. (2000). Myeloperoxidase-generated oxidants and atherosclerosis. *Free Radical Biology and Medicine* **28**(12): 1717-1725.

Prutz, W. A. (1996). Hypochlorous acid interactions with thiols, nucleotides, DNA, and other biological substrates. *Arch Biochem Biophys* **332**(1): 110-20.

Pullar, J. M., Vissers, M. C. and Winterbourn, C. C. (2000). Living with a killer: the effects of hypochlorous acid on mammalian cells. *IUBMB Life* **50**(4-5): 259-266.

Pullar, J. M., Vissers, M. C. and Winterbourn, C. C. (2001). Glutathione oxidation by hypochlorous acid in endothelial cells produces glutathione sulfonamide as a major product but not glutathione disulfide. *J Biol Chem* **276**(25): 22120-5.

Pullar, J. M., Winterbourn, C. C. and Vissers, M. C. (1999). Loss of GSH and thiol enzymes in endothelial cells exposed to sublethal concentrations of hypochlorous acid. *Am J Physiol* **277**(4 Pt 2): H1505-12.

Qiao, J. H., Tripathi, J., Mishra, N. K., Cai, Y., Tripathi, S., Wang, X. P., Imes, S., Fishbein, M. C., Clinton, S. K., Libby, P., Lusis, A. J. and Rajavashisth, T. B. (1997). Role of macrophage colony-stimulating factor in atherosclerosis: studies of osteopetrotic mice. *Am J Pathol* **150**(5): 1687-99.

Razumovitch, J. A., Fuchs, D., Semenkova, G. N. and Cherenkevich, S. N. (2004). Influence of neopterin on generation of reactive species by myeloperoxidase in human neutrophils. *Biochim Biophys Acta* **1672**(1): 46-50.

Reed, J. C. (1997). Bcl-2 family proteins: regulators of apoptosis and chemoresistance in hematologic malignancies. *Semin Hematol* **34**(4 Suppl 5): 9-19.

Reed, J. C. (1998). Bcl-2 family proteins. *Oncogene* **17**(25): 3225-36.

Reed, J. C. (2000). Mechanisms of apoptosis. *Am J Pathol* **157**(5): 1415-30.

Reimertz, C., Kögel, D., Lankiewicz, S., Poppe, M. and Prehn, J. H. (2001). Ca(2+)-induced inhibition of apoptosis in human SH-SY5Y neuroblastoma cells: degradation of apoptotic protease activating factor-1 (APAF-1). *J Neurochem* **78**(6): 1256-66.

Reiss, A. B., Patel, C. A., Rahman, M. M., Chan, E. S., Hasneen, K., Montesinos, M. C., Trachman, J. D. and Cronstein, B. N. (2004). Interferon-gamma impedes reverse cholesterol transport and promotes foam cell transformation in THP-1 human monocytes/macrophages. *Med Sci Monit* **10**(11): BR420-5.

Richter, C. (1993). Pro-oxidants and mitochondrial Ca2+: their relationship to apoptosis and oncogenesis. *FEBS Lett* **325**(1-2): 104-7.

Ringger, N. C., O'Steen, B. E., Brabham, J. G., Silver, X., Pineda, J., Wang, K. K., Hayes, R. L. and Papa, L. (2004). A novel marker for traumatic brain injury: CSF alphaII-spectrin breakdown product levels. *J Neurotrauma* **21**(10): 1443-56.

Rippin, J. J. (1992). Analysis of fully oxidised neopterin in serum by high-performance liquid chromatography. *Clin Chem* **38**(9): 1722-4.

Ristoff, E. and Larsson, A. (2007). Inborn errors in the metabolism of glutathione. *Orphanet J Rare Dis* **2**(16).

Rosen, H. and Klebanoff, S. J. (1985). Oxidation of microbial iron-sulfur centers by the myeloperoxidase-H2O2-halide antimicrobial system. *Infect Immun* **47**(3): 613-8.

Rosenblat, M., Volkova, N., Coleman, R. and Aviram, M. (2007). Anti-oxidant and anti-atherogenic properties of liposomal glutathione: studies in vitro, and in the atherosclerotic apolipoprotein E-deficient mice. *Atherosclerosis* **195**(2): e61-8.

Ross, R. (1993). The pathogenesis of atherosclerosis: a perspective for the 1990s. *Nature* **362**(6423): 801-9.

Ross, R. (1999). Atherosclerosis--an inflammatory disease. *N Engl J Med* **340**(2): 115-26.

Ruben, L., Goodman, D. B. and Rasmussen, H. (1980). Identification of calmodulin in mitochondria from rat liver: a possible role in regulation of the oligomycin sensitive ATPase. *Ann N Y Acad Sci* **356**: 427-8.

Rudzite, V., Jurika, E., Fuchs, D., Kalnins, U., Erglis, A. and Trusinskis, K. (2003). Serum concentration of C-reactive protein, neopterin and phospholipids in patients with different grade of coronary heart disease. *Pteridines* **14**(4): 133-7.

Russell, C., Scaduto, J. and Lee, W. G. (1999). Measurement of Mitochondrial Membrane Potential Using Fluorescent Rhodamine Derivatives. *Biophysical Journal* **76**(1): 469-477.

Saido, T. C., Nagao, S. S., M., Tsukaguchi, M., Yoshizawa, T., Sorimachi, H., Ito, H., Tsuchiya, T., Kawashima, S. and Suzuki, K. (1994a). Distinct kinetics of subunit autolysis in mammalian m-calpain activation *FEBS Lett* **346**(2-3): 263-7.

Saido, T. C., Shibata, M., Takenawa, T., Murofushi, H. and Suzuki, K. (1992). Positive regulation of mu-calpain action by polyphosphoinositides. *J Biol Chem* **267**(34): 24585-90.

Saido, T. C., Sorimachi, H. and Suzuki, K. (1994b). Calpain: new perspectives in molecular diversity and physiological-pathological involvement. *FASEB J* **8**(11): 814-22.

Saito, K., Elce, J. S., Hamos, J. E. and Nixon, R. A. (1993). Widespread activation of calcium-activated neutral proteinase (calpain) in the brain in Alzheimer disease: a potential molecular basis for neuronal degeneration. *Proc Natl Acad Sci U S A* **90**(7): 2628-32.

Salunga, T. L., Cui, Z. G., Shimoda, S., Zheng, H. C., Nomoto, K., Kondo, T., Takano, Y., Selmi, C., Alpini, G., Gershwin, M. E. and Tsuneyama, K. (2007). Oxidative stress-induced apoptosis of bile duct cells in primary biliary cirrhosis. *J Autoimmun* **29**(2-3): 78-86.

Sandoval, M., Zhang, X. J., Liu, X., Mannick, E. E., Clark, D. A. and Miller, M. J. (1997). Peroxynitrite-induced apoptosis in T84 and RAW 264.7 cells: attenuation by L-ascorbic acid. *Free Radic Biol Med* **22**(3): 489-95.

Sato, Y., Kamo, S., Takahashi, T. and Suzuki, Y. (1995). Mechanism of free radical-induced hemolysis of human erythrocytes: hemolysis by water-soluble radical initiator. *Biochemistry* **34**(28): 8940-9.

Sato, K. and Kawashima, S. (2001). Calpain function in the modulation of signal transduction molecules. *Biol Chem* **382**(5): 743-51.

Schafer, F. Q. and Buettner, G. R. (2001). Redox environment of the cell as viewed through the redox state of the glutathione disulfide/glutathione couple. *Free Radic Biol Med* **30**(11): 1191-212.

Schobersberger, W., Hoffmann, G., Grote, J., Wachter, H. and Fuchs, D. (1995). Induction of inducible nitric oxide synthase expression by neopterin in vascular smooth muscle cells. *FEBS Lett* **377**(3): 461-4.

Schobersberger, W., Hoffmann, G., Hobisch-Hagen, P., Bock, G., Volkl, H., Baier-Bitterlich, G., Wirleitner, B., Wachter, H. and Fuchs, D. (1996). Neopterin and 7,8-dihydroneopterin induce apoptosis in the rat alveolar epithelial cell line L2. *FEBS Lett* **397**(2-3): 263-8.

Schraufstatter, I. U., Browne, K., Harris, A., Hyslop, P. A., Jackson, J. H., Quehenberger, O. and Cochrane, C. G. (1990). Mechanisms of Hypochlorite Injury of Target Cells. *J Clin Invest* **85**(2): 554-562.

Schroder, K., Hertzog, P. J., Ravasi, T. and Hume, D. A. (2004). Interferon-gamma: an overview of signals, mechanisms and functions. *J Leukoc Biol* **75**(2): 163-89.

Schroecksnadel, K., Murr, C., Winkler, C., Wirleitner, B., Fuith, L. C. and Fuchs, D. (2004). Neopterin to monitor clinical pathologies involving interferon-γ production. *Pteridines* **15**(3): 75-90.

Schumacher, M., Eber, B., Tatzber, F., Kaufmann, P., Esterbauer, H. and Klein, W. (1992). Neopterin levels in patients with coronary artery disease. *Atherosclerosis* **94**(1): 87-8.

Schumacher, M., Halwachs, G., Tatzber, F., Fruhwald, F. M., Zweiker, R., Watzinger, N., Eber, B., Wilders-Truschnig, M., Esterbauer, H. and Klein, W. (1997). Increased neopterin in patients with chronic and acute coronary syndromes. *J Am Coll Cardiol* **30**(3): 703-7.

Shabani, F., McNeil, J. and Tippett, L. (1998). The oxidative inactivation of tissue inhibitor of metalloproteinase-1 (TIMP-1) by hypochlorous acid (HOCI) is suppressed by anti-rheumatic drugs. *Free Radic Res* **28**(2): 115-23.

Shannon, T. R., Wang, F., Puglisi, J., Weber, C. and Bers, D. M. (2004). A mathematical treatment of integrated Ca dynamics within the ventricular myocyte. *Biophys J* **87**(5): 3351-71.

Shao, B., Belaaouaj, A., Verlinde, C. L., Fu, X. and Heinecke, J. W. (2005). Methionine sulfoxide and proteolytic cleavage contribute to the inactivation of cathepsin G by hypochlorous acid: an oxidative mechanism for regulation of serine proteinases by myeloperoxidase. *J Biol Chem* **280**(32): 29311-21.

Shao, B., Oda, M. N., Bergt, C., Fu, X., Green, P. S., Brot, N., Oram, J. F. and Heinecke, J. W. (2006). Myeloperoxidase impairs ABCA1-dependent cholesterol efflux through methionine oxidation and site-specific tyrosine chlorination of apolipoprotein A-I. *J Biol Chem* **281**(14): 9001-4.

Shi, Y., Melnikov, V. Y., Schrier, R. W. and Edelstein, C. L. (2000). Downregulation of the calpain inhibitor protein calpastatin by caspases during renal ischemia-reperfusion. *Am J Physiol Renal Physiol* **279**(3): F509-17.

Shen, R. S. (1994). Inhibition of luminol-enhanced chemiluminescence by reduced pterins. *Arch Biochem Biophys* **310**(1): 60-3.

Skepper, J. N., Karydis, I., Garnett, M. R., Hegyi, L., Hardwick, S. J., Warley, A., Mitchinson, M. J. and Cary, N. R. B. (1999). Changes in elemental concentrations are associated with early stages of apoptosis in human monocyte-macrophages exposed to oxidized low-density lipoprotein: An x-ray microanalytical study. *J Pathol* **188**(1): 100-6.

Slivka, A., LoBuglio, A. F. and Weiss, S. J. (1980). A potential role for hypochlorous acid in granulocyte-mediated tumor cell cytotoxicity. *Blood* **55**(2): 347-50.

Smit, M. J. and Anderson, R. (1992). Biochemical mechanisms of hydrogen peroxide- and hypochlorous acid-mediated inhibition of human mononuclear leukocyte functions in vitro: protection and reversal by anti-oxidants. *Agents Actions* **36**(1-2): 58-65.

Sohal, R. S. and Allen, R. G. (1985). Relationship between metabolic rate, free radicals, differentiation and aging: a unified theory. *Basic Life Sci* **35**: 75-104.

Sorimachi, H., Imajoh-Ohmi, S., Emori, Y., Kawasaki, H., Ohno, S., Minami, Y. and Suzuki, K. (1989). Molecular cloning of a novel mammalian calcium-dependent protease distinct from both m- and mu-types. Specific expression of the mRNA in skeletal muscle. *J Biol Chem* **264**(33): 20106-11.

Sorimachi, H., Ishiura, S. and Suzuki, K. (1993). A novel tissue-specific calpain species expressed predominantly in the stomach comprises two alternative splicing products with and without Ca(2+)-binding domain. *J Biol Chem* **268**(26): 19476-82.

Sorimachi, H., Ishiura, S. and Suzuki, K. (1997). Structure and physiological function of calpains. *Biochem J* **328**(Pt 3): 721-32.

Sorimachi, H., Saido, T. C. and Suzuki, K. (1994). New era of calpain research. Discovery of tissue-specific calpains. *FEBS Lett* **343**(1): 1-5.

Soszynski, M. and Bartosz, G. (1997). Decrease in accessible thiols as an index of oxidative damage to membrane proteins. *Free Radic Biol Med* **23**(3): 463-9.

Spencer, J. P., Whiteman, M., Jenner, A. and Halliwell, B. (2000). Nitrite-induced deamination and hypochlorite-induced oxidation of DNA in intact human respiratory tract epithelial cells. *Free Radic Biol Med* **28**(7): 1039-50.

Spottl, N., Wirleitner, B., Bock, G., Widner, B., Fuchs, D. and Baier-Bitterlich, G. (2000). Reduced pteridine derivatives induce apoptosis in human neuronal NT2/HNT cells. *Immunobiology* **201**(3-4): 478-91.

Spragg, R. G., Hinshaw, D. B., Hyslop, P. A., Schraufstätter, I. U. and Cochrane, C. G. (1985). Alterations in adenosine triphosphate and energy charge in cultured endothelial and P388D1 cells after oxidant injury. *J Clin Invest* **76**(4): 1471-6.

Springman, E. B., Angleton, E. L., Birkedal-Hansen, H. and Van Wart, H. E. (1990). Multiple modes of activation of latent human fibroblast collagenase: evidence for the role of a Cys73 active-site zinc complex in latency and a "cysteine switch" mechanism for activation. *Proc Natl Acad Sci U S A* **87**(1): 364-8.

Stary, H. C., Chandler, A. B., Dinsmore, R. E., Fuster, V., Glagov, S., Insull, W., Jr., Rosenfeld, M. E., Schwartz, C. J., Wagner, W. D. and Wissler, R. W. (1995). A definition of advanced types of atherosclerotic lesions and a histological classification of atherosclerosis. A report from the Committee on Vascular Lesions of the Council on Arteriosclerosis, American Heart Association. *Arterioscler Thromb Vasc Biol* **15**(9): 1512-31.

Steck, T. L. and Kant, J. A. (1974). Preparation of impermeable ghosts and inside-out vesicles from human erythrocyte membranes. *Methods Enzymol* **31**(Pt A): 172-80.

Steffens, S. and Mach, F. (2004). Inflammation and atherosclerosis. *Herz* **29**(8): 741-8.

Stridth, H., Kimland, M., Jones, D. P., Orennius, S. and Hampton, M. B. (1998). Cytochrome c release and caspase activation in hydrogen peroxide- and tributylin-induced apoptosis. *FEBS Lett* **429**: 351-5.

Sugiyama, S., Kugiyama, K., Aikawa, M., Nakamura, S., Ogawa, H. and Libby, P. (2004). Hypochlorous acid, a macrophage product, induces endothelial apoptosis and tissue factor expression: involvement of myeloperoxidase-mediated oxidant in plaque erosion and thrombogenesis. *Arterioscler Thromb Vasc Biol* **24**(7): 1309-14.

Sugiyama, S., Okada, Y., Sukhova, G. K., Virmani, R., Heinecke, J. W. and Libby, P. (2001). Macrophage myeloperoxidase regulation by granulocyte macrophage colony-stimulating factor in human atherosclerosis and implications in acute coronary syndromes. *Am J Pathol* **158**(3): 879-91.

Sun, J., Xu, L., Eu, J. P., Stamler, J. S. and Meissner, G. (2001). Classes of thiols that influence the activity of the skeletal muscle calcium release channel. *J Biol Chem* **276**(19): 15625-30.

Suzuki, K., Imajoh, S., Emori, Y., Kawasaki, H., Minami, Y. and Ohno, S. (1987). Calcium-activated neutral protease and its endogenous inhibitor. Activation at the cell membrane and biological function. *FEBS Lett* **220**(2): 271-7.

Tabas, I. (2005). Consequences and therapeutic implications of macrophage apoptosis in atherosclerosis: The importance of lesion stage and phagocytic efficiency. *Arterioscler Thromb Vasc Biol* **25**: 2255-64.

Tatsumi, T. and Fliss, H. (1994). Hypochlorous acid and chloramines increase endothelial permeability: possible involvement of cellular zinc. *Am J Physiol Heart Circ Physiol* **267**: H1597-H1607.

Tatzber, F., Rabl, H., Koriska, K., Erhart, U., Puhl, H., Waeg, G., Krebs, A. and Esterbauer, H. (1991). Elevated serum neopterin levels in atherosclerosis. *Atherosclerosis* **89**(2-3): 203-8.

Tavares, A. and Duque-Magalhàes, M. C. (1991). Demonstration of three calpains in the matrix of rat liver mitochondria. *Biomed Biochim Acta* **50**(4-6): 523-9.

Taylor, R. G., Geesink, G. H., Thompson, V. F., Koohmaraie, M. and Goll, D. E. (1995). Is Z-disk degradation responsible for postmortem tenderization? *J Anim Sci* **73**(5): 1351-67.

Thibodeau, M., Giardina, C. and Hubbard, A. K. (2003). Silica-induced caspase activation in mouse alveolar macrophages is dependent upon mitochondrial integrity and aspartic proteolysis. *Toxicol Sci* **76**(1): 91-101.

Thomas, E. L. and Fishman, M. (1986). Oxidation of chloride and thiocyanate by isolated leukocytes. *J Biol Chem* **261**(21): 9694-702.

Thomas, E. L., Grisham, M. B., Melton, D. F. and Jefferson, M. M. (1985). Evidence for a role of taurine in the in vitro oxidative toxicity of neutrophils toward erythrocytes. *J Biol Chem* **260**(6): 3321-9.

Thornberry, N. A. and Lazebnik, Y. (1998). Caspases: enemies within. *Science* **281**(5381): 1312-6.

Torgano, G., Cosentini, R., Mandelli, C., Perondi, R., Blasi, F., Bertinieri, G., Tien, T. V., Ceriani, G., Tarsia, P., Arosio, C. and Ranzi, M. L. (1999). Treatment of Helicobacter pylori and Chlamydia pneumoniae infections decreases fibrinogen plasma level in patients with ischemic heart disease. *Circulation* **99**(12): 1555-9.

Tremper-Wells, B. and Vallano, M. L. (2005). Nuclear calpain regulates Ca2+-dependent signaling via proteolysis of nuclear Ca2+/calmodulin-dependent protein kinase type IV in cultured neurons. *J Biol Chem* **280**(3): 2165-75.

Trollinger, D. R., Cascio, W. E. and Lemasters, J. J. (2000). Mitochondrial calcium transients in adult rabbit cardiac myocytes: inhibition by ruthenium red and artifacts caused by lysosomal loading of Ca(2+)-indicating fluorophores. *Biophys J* **79**(1): 39-50.

Tsuchiya, S., Yamabe, M., Yamaguchi, Y., Kobayashi, Y., Konno, T. and Tada, K. (1980). Establishment and characterization of a human acute monocytic leukemia cell line (THP-1). *Int J Cancer* **26**(2): 171-6.

Tuckey, N.P.L. (2008). Technologies for tissue preservation: the role of endogenous and exogenous antioxidants in preserving tissue function in Chinook Salmon, Oncorhynchus tshawytscha. *PhD thesis*.

Uberall, F., Werner-Felmayer, G., Schubert, C., Grunicke, H. H., Wachter, H. and Fuchs, D. (1994). Neopterin derivatives together with cyclic guanosine monophosphate induce c-fos gene expression. *FEBS Lett* **352**(1): 11-4.

Uemura, K., Adachi-Akahane, S., Shintani-Ishida, K. and Yoshida, K. (2005). Carbon monoxide protects cardiomyogenic cells against ischemic death through L-type Ca2+ channel inhibition. *Biochem Biophys Res Commun* **334**(2): 661-8.

Uhlig, S. and Wendel, A. (1992). The physiological consequences of glutathione variations. *Life Sciences* **51**: 1083-94.

Upston, J. M., Niu, X., Brown, A. J., Mashima, R., Wang, H., Senthilmohan, R., Kettle, A. J., Dean, R. T. and Stocker, R. (2002). Disease stage-dependent accumulation of lipid and protein oxidation products in human atherosclerosis. *Am J Pathol* **160**(2): 701-10.

Van Den Berg, J. and Winterbourn, C. C. (1994). Measurement of reaction products from hypochlorous acid and unsaturated lipids. *Methods in Enzymology* **233**: 639-49.

van den Dobbelsteen, D. J., Nobel, C. S., Schlegel, J., Cotgreave, I. A., Orrenius, S. and Slater, A. F. (1996). Rapid and specific efflux of reduced glutathione during apoptosis induced by anti-Fas/APO-1 antibody. *J Biol Chem* **271**(26): 15420-7.

van der Wal, A. C., Becker, A. E., van der Loos, C. M. and Das, P. K. (1994). Site of intimal rupture or erosion of thrombosed coronary atherosclerotic plaques is characterized by an inflammatory process irrespective of the dominant plaque morphology. *Circulation* **89**(1): 36-44.

Van Engeland, M., Nieland, L. J. W., Ramaekers, F. C. S., Schutte, B. and Reutelingsperger, C. P. M. (1998). Annexin V-affinity assay: A review on an apoptosis detection system based on phosphatidylserine exposure. *Cytometry* **31**(1): 1-9.

Verhagen, A. M., Ekert, P. G., Pakusch, M., Silke, J., Connolly, L. M., Reid, G. E., Moritz, R. L., Simpson, R. J. and Vaux, D. L. (2000). Identification of DIABLO, a mammalian protein that promotes apoptosis by binding to and antagonizing IAP proteins. *Cell* **102**(1): 43-53.

Vieira, H. L., Haouzi, D., El Hamel, C., Jacotot, E., Belzacq, A. S., Brenner, C. and Kroemer, G. (2000). Permeabilization of the mitochondrial inner membrane during apoptosis: impact of the adenine nucleotide translocator. *Cell Death Differ* **7**(12): 1146-54.

Vile, G. F., Rothwell, L. A. and Kettle, A. J. (2000). Initiation of rapid, P53-dependent growth arrest in cultured human skin fibroblasts by reactive chlorine species. *Arch Biochem Biophys* **377**(1): 122-8.

Vindis, C., Elbaz, M., Escargueil-Blanc, I., Augé, N., Heniquez, A., Thiers, J. C., Nègre-Salvayre, A. and Salvayre, R. (2004). Two distinct calcium-dependent mitochondrial pathways are involved in oxidized LDL-induced apoptosis. *Arterioscler Thromb Vasc Biol* **25**(3): 639-45.

Vissers, M. C., Day, W. A. and Winterbourn, C. C. (1985). Neutrophils adherent to a nonphagocytosable surface (glomerular basement membrane) produce oxidants only at the site of attachment. *Blood* **66**(1): 161-6.

Vissers, M. C., Lee, W. G. and Hampton, M. B. (2001). Regulation of apoptosis by vitamin C. Specific protection of the apoptotic machinery against exposure to chlorinated oxidants. *J Biol Chem* **276**(50): 46835-40

Vissers, M. C., Pullar, J. M. and Hampton, M. B. (1999). Hypochlorous acid causes caspase activation and apoptosis or growth arrest in human endothelial cells. *Biochem J.* **344**(Pt 2): 443-9.

Vissers, M. C., Stern, A., Kuypers, F., Van Den Berg, J. and Winterbourn, C. C. (1994). Membrane changes associated with lysis of red blood cells by hypochlorous acid. *Free Radic Biol Med* **16**(6): 703-12.

Vissers, M. C. and Thomas, C. (1997). Hypochlorous acid disrupts the adhesive properties of subendothelial matrix. *Free Radic Biol Med* **23**(3): 401-11.

Vissers, M. C. M., Carr, A. C. and Chapman, A. L. P. (1998). Comparison of human red cell lysis by hypochlorous and hypobromous acids: insights into the mechanism of lysis. *Biochem. J* **330**: 131-138.

Vissers, C. M. and Winterbourn, C. C. (1995). Oxidation of intracellular glutathione after exposure of human red blood cells to hypochlorous acid. *Biochem J* **307**: 57-62.

Wachter, H., Fuchs, D., Hausen, A., Reibnegger, G. and Werner, E. R. (1989). Neopterin as marker for activation of cellular immunity: immunologic basis and clinical application. *Adv Clin Chem* **27**: 81-141.

Wachter, H., Fuchs, D., Hausen, A., Reibnegger, G., Weiss, G., Werner, E. R. and Werner-Felmayer, G. (1992). Neopterin: Biochemistry-Methods-Clinical Application. New York, Walter de Gruyter.

Waddington, E. I., Puddey, I. B., Mori, T. A. and Croft, K. D. (2002). Similarity in the distribution of F(2)-isoprostanes in the lipid subfractions of atherosclerotic plaque and in vitro oxidised low density lipoprotein. *Redox Rep* **7**(3): 179-84.

Wagner, B. A., Buettner, G. R., Oberley, L. W., Darby, C. J. and Burns, C. P. (2000). Myeloperoxidase is involved in H2O2-induced apoptosis of HL-60 human leukemia cells. *J Biol Chem* **275**(29): 22461-9.

Wagner, D. K., Collins-Lech, C. and Sohnle, P. G. (1986). Inhibition of neutrophil killing of Candida albicans pseudohyphae by substances which quench hypochlorous acid and chloramines. *Infect Immun* **51**(3): 731-5.

Walle, A. J. and Wong, G. Y. (1989). Binding of acridine orange to DNA in situ of cells from patients with acute leukemia. *Cancer Res* **49**(13): 3692-5.

Wang, W. and Ballatori, N. (1998). Endogenous glutathione conjugates: occurrence and biological functions. *Pharmacol Rev* **50**(3): 335-56.

Wang, C. H., Chen, Y. J., Lee, T. H., Chen, Y. S., Jawan, B., Hung, K. S., Lu, C. N. and Liu, J. K. (2004). Protective effect of MDL28170 against thioacetamide-induced acute liver failure in mice. *J Biomed Sci* **11**(5): 571-8.

Wang, H., Yu, S. W., Koh, D. W., Lew, J., Coombs, C., Bowers, W., Federoff, H. J., Poirier, G. G., Dawson, T. M. and Dawson, V. L. (2004). Apoptosis-inducing factor substitutes for caspase executioners in NMDA-triggered excitotoxic neuronal death. *J Neurosci* **24**(48): 10963-73.

Watanabe, Y., Suzuki, O., Haruyama, T. and Akaike, T. (2003). Interferon-gamma induces reactive oxygen species and endoplasmic reticulum stress at the hepatic apoptosis. *J Cell Biochem.* **89**(2): 244-53.

Waterhouse, N. J., Ricci, J. E. and Green, D. R. (2002). And all of a sudden it's over: mitochondrial outer-membrane permeabilization in apoptosis. *Biochimie* **84**(2-3): 113-21.

Weber, H., Hühns, S., Lüthen, F., Jonas, L. and Schuff-Werner, P. (2005). Calpain activation contributes to oxidative stress-induced pancreatic acinar cell injury. *Biochem Pharmacol* **70**(8): 1241-52.

Weber, C. R., Piacentino, V. r., Ginsburg, K. S., Houser, S. R. and Bers, D. M. (2002). Na(+)-Ca(2+) exchange current and submembrane [Ca(2+)] during the cardiac action potential. *Circ Res* **90**(2): 182-9.

Wede, I., Widner, B. and Fuchs, D. (1999). Neopterin derivatives modulate toxicity of reactive species on Escherichia coli. *Free Radic Res* **31**(5): 381-8.

Weiss, G., Fuchs, D., Hausen, A., Reibnegger, G., Werner, E. R., Werner-Felmayer, G., Semenitz, E., Dierich, M. P. and Wachter, H. (1993). Neopterin modulates toxicity mediated by reactive oxygen and chloride species. *FEBS Lett* **321**(1): 89-92.

Weiss, S. J., Klein, P., Slivka, A. and Wei, M. (1982). Chlorination of Taurine by Human Neutrophils: evidence for hypochlorous acid generation *J. Clin Invest* **70**: 1341-1349.

Weiss, S. J., Peppin, G., Ortiz, X., Ragsdale, C. and Test, S. T. (1985). Oxidative autoactivation of latent collagenase by human neutrophils. *Science* **227**(4688): 747-9.

Weiss, S. J. and Slivka, A. (1982). Monocyte and granulocyte-mediated tumor cell destruction. A role for the hydrogen peroxide-myeloperoxidase-chloride system. *J Clin Invest* **69**(2): 255-62.

Werner-Felmayer, G., Werner, E. R., Fuchs, D., Hausen, A., Reibnegger, G. and Wachter, H. (1990). Neopterin formation and tryptophan degradation by a human myelomonocytic cell line (THP-1) upon cytokine treatment. *Cancer Res* **50**(10): 2863-7.

Werner, E. R., Fuchs, D., Hausen, A., Reibnegger, G. and Wachter, H. (1987). Simultaneous determination of neopterin and creatinine in serum with solid-phase extraction and on-line elution liquid chromatography. *Clin Chem* **33**(11): 2028-33.

Werner, E. R., Werner-Felmayer, G., Fuchs, D., Hausen, A., Reibnegger, G., Yim, J. J., Pfleiderer, W. and Wachter, H. (1990). Tetrahydrobiopterin biosynthetic activities

in human macrophages, fibroblasts, THP-1, and T 24 cells. GTP-cyclohydrolase I is stimulated by interferon-gamma, and 6-pyruvoyl tetrahydropterin synthase and sepiapterin reductase are constitutively present. *J Biol Chem* **265**(6): 3189-92.

Wernette, M. E., Ochs, R. S. and Lardy, H. A. (1981). Ca2+ stimulation of rat liver mitochondrial glycerophosphate dehydrogenase. *J Biol Chem* **256**(24): 12767-71.

Westermann, J., Thiemann, F., Gerstner, L., Tatzber, F., Kozak, I., Bertsch, T. and Kruger, C. (2000). Evaluation of a new simple and rapid enzyme-linked immunosorbent assay kit for neopterin determination. *Clin Chem Lab Med* **38**(4): 345-353.

Widner, B., Baier-Bitterlich, G., Wede, I., Wirleitner, B. and Fuchs, D. (1998). Neopterin derivatives modulate the nitration of tyrosine by peroxynitrite. *Biochem Biophys Res Commun* **248**(2): 341-6.

Whiteman, M., Armstrong, J. S., Cheung, N. S., Siau, J. L., Rose, P., Schantz, J. T., Jones, D. P. and Halliwell, B. (2004). Peroxynitrite mediates calcium-dependent mitochondrial dysfunction and cell death via activation of calpains. *FASEB J* **18**(12): 1395-7.

Whiteman, M., Chu, S. H., Siau, J. L., Rose, P., Sabapathy, K., Schantz, J. T., Cheung, N. S., Spencer, J. P. and Armstrong, J. S. (2007). The pro-inflammatory oxidant hypochlorous acid induces Bax-dependent mitochondrial permeabilisation and cell death through AIF-/EndoG-dependent pathways. *Cell signal* **19**(4): 705-714.

Whiteman, M., Jenner, A. and Halliwell, B. (1997). Hypochlorous acid-induced base modifications in isolated calf thymus DNA. *Chem Res Toxicol* **10**(11): 1240-6.

Whiteman, M., Rose, P., Siau, J. L., Cheung, N. S., Tan, G. S., Halliwell, B. and Armstrong, J. S. (2005b). Hypochlorous acid-mediated mitochondrial dysfunction and apoptosis in human hepatoma HepG2 and human fetal liver cells: role of mitochondrial permeability transition. *Free Radic Biol Med* **38**(12): 1571-84.

Widner, B., Mayr, C., Wirleitner, B. and Fuchs, D. (2000). Oxidation of 7,8-Dihydroneopterin by Hypochlorous Acid Yields Neopterin. *Biochemical and Biophysical Research Communications* **275**(2): 307-311.

Winrow, V. R., Winyard, P. G., Morris, C. J. and Blake, D. R. (1993). Free radicals in inflammation: second messengers and mediators of tissue destruction. *Br Med Bull* **49**(3): 506-22.

Winterbourn, C. C. (1985). Comparative reactivities of various biological compounds with myeloperoxidase-hydrogen peroxide-chloride, and similarity of the oxidant to hypochlorite. *Biochim Biophys Acta* **840**(2): 204-10.

Winterbourn, C. C. (2002). Biological reactivity and biomarkers of the neutrophil oxidant, hypochlorous acid. *Toxicology* **181-182**: 223-7.

Winterbourn, C. C. and Brennan, S. O. (1997). Characterization of the oxidation products of the reaction between reduced glutathione and hypochlorous acid. *Biochem J* **326**(Pt 1): 87-92.

Winterbourn, C. C., Garcia, R. C. and Segal, A. W. (1985). Production of the superoxide adduct of myeloperoxidase (compound III) by stimulated human neutrophils and its reactivity with hydrogen peroxide and chloride. *Biochem. J* **228**(3): 583-92.

Wirleitner, B., Baier-Bitterlich, G., Bock, G., Widner, B. and Fuchs, D. (1998). 7,8-Dihydroneopterin-induced apoptosis in Jurkat T lymphocytes: a comparison with anti-Fas- and hydrogen peroxide-mediated cell death. *Biochem Pharmacol* **56**(9): 1181-7.

Wirleitner, B., Czaputa, R., Oettl, K., Bock, G., Widner, B., Reibnegger, G., Baier, G., Fuchs, D. and Baier-Bitterlich, G. (2001). Induction of apoptosis by 7,8-dihydroneopterin: involvement of radical formation. *Immunobiology* **203**(4): 629-41.

Wirleitner, B., Schroecksnadel, K., Winkler, C., Schennach, H. and Fuchs, D. (2005). Resveratrol suppresses interferon-gamma-induced biochemical pathways in human peripheral blood mononuclear cells in vitro. *Immunol Lett* **100**: 159-163.

Wolf, B. B., Goldstein, J. C., Stennicke, H. R., Beere, H., Amarante-Mendes, G. P., Salvesen, G. S. and Green, D. R. (1999). Calpain functions in a caspase-independent manner to promote apoptosis-like events during platelet activation. *Blood* **94**(5): 1683-92.

Woll, E., Weiss, G., Fuchs, D., Lang, F. and Wachter, H. (1993). Effect of pteridine derivatives on intracellular calcium concentration in human monocytic cells. *FEBS Lett* **318**(3): 249-52.

Woodfield, K., Rück, A., Brdiczka, D. and Halestrap, A. P. (1998). Direct demonstration of a specific interaction between cyclophilin-D and the adenine nucleotide translocase confirms their role in the mitochondrial permeability transition. *Biochem J* **336**(Pt 2): 287-90.

Woods, A. A., Linton, S. M. and Davies, M. J. (2003). Detection of HOCl-mediated protein oxidation products in the extracellular matrix of human atherosclerotic plaques. *Biochem J* **370**((Pt 2)): 729-35.

Wu, G., Fang, Y. Z., Yang, S., Lupton, J. R. and Turner, N. D. (2004). Glutathione metabolism and its implications for health. *J Nutr* **134**(3): 489-92.

Wuttge, D. M., Zhou, X., Sheikine, Y., Wagsater, D., Stemme, V., Hedin, U., Stemme, S., Hansson, G. K. and Sirsjo, A. (2004). CXCL16/SR-PSOX is an interferon-gamma-regulated chemokine and scavenger receptor expressed in atherosclerotic lesions. *Arterioscler Thromb Vasc Biol* **24**(4): 750-5.

Xu, Q., Luef, G., Weimann, S., Gupta, R. S., Wolf, H. and Wick, G. (1993). Staining of endothelial cells and macrophages in atherosclerotic lesions with human heat-shock protein-reactive antisera. *Arterioscler Thromb* **13**(12): 1763-9.

Yamashima, T. (2004). Ca2+-dependent proteases in ischemic neuronal death: a conserved 'calpain-cathepsin cascade' from nematodes to primates. *Cell Calcium* **36**(3-4): 285-93.

Yap, Y. W., Whiteman, M., Bay, B. H., Li, Y., Sheu, F. S., Qi, R. Z., Tan, C. H. and Cheung, N. S. (2006). Hypochlorous acid induces apoptosis of cultured cortical neurons through activation of calpains and rupture of lysosomes. *J Neurochem* **98**(5): 1597-1609.

Yokota, M., Saido, T. C., Kamitani, H., Tabuchi, S., Satokata, I. and Watanabe, T. (2003). Calpain induces proteolysis of neuronal cytoskeleton in ischemic gerbil forebrain. *Brain Res* **984**(1-2): 122-32.

Yuan, X. M., Li, W., Brunk, U. T., Dalen, H., Chang, Y. H. and Sevanian, A. (2000). Lysosomal destabilization during macrophage damage induced by cholesterol oxidation products. *Free Radic Biol Med* **28**(2): 208-18.

Zdolsek, J. M., Olsson, G. M. and Brunk, U. T. (1990). Photooxidative damage to lysosomes of cultured macrophages by acridine orange. *Photochem Photobiol* **51**(1): 67-76.

Zhang, W., Li, D. and Mehta, J. L. (2004). Role of AIF in human coronary artery endothelial cell apoptosis. *Am J Physiol Heart Circ Physiol* **286**: H354-8.

Zhao, H., Kalivendi, S., Zhang, H., Joseph, J., Nithipatikom, K., Vásquez-Vivar, J. and Kalyanaraman, B. (2003). Superoxide reacts with hydroethidine but forms a fluorescent product that is distinctly different from ethidium: potential implications in intracellular fluorescence detection of superoxide. *Free Radic Biol Med* **34**(11): 1359-68.

Zheng, B., Cao, K. Y., Chan, C. P., Choi, J. W., Leung, W., Leung, M., Duan, Z. H., Gao, Y., Wang, M., Di, B., Hollidt, J. M., Bergmann, A., Lehmann, M., Renneberg, I., Tam, J. S., Chan, P. K., Cautherley, G. W., Fuchs, D. and Renneberg, R. (2005). Serum neopterin for early assessment of severity of severe acute respiratory syndrome. *Clin Immunol* **116**(1): 18-26.

Zhou, X., Paulsson, G., Stemme, S. and Hansson, G. K. (1998). Hypercholesterolemia is associated with a T helper (Th) 1/Th2 switch of the autoimmune response in atherosclerotic apo E-knockout mice. *J Clin Invest* **101**(8): 1717-25.

Zima, A. V., Copello, J. A. and Blatter, L. A. (2004). Effects of cytosolic NADH/NAD(+) levels on sarcoplasmic reticulum Ca(2+) release in permeabilized rat ventricular myocytes. *J Physiol* **555**(Pt 3): 727-41.

Zoratti, M. and Szabò, I. (1995). The mitochondrial permeability transition. *Biochim Biophys Acta* **1241**(2): 139-76.

ACKNOWLEDGEMENTS

I would like to dedicate this thesis to my beloved mum Ann Ma, my dad Jack Yang and my grandmother Ma Li Show Ching. I would like to express my deepest gratitude to them for giving me support, caring and cooking for me, and providing financial assistance throughout my PhD years.

I would like to thank my supervisor, Dr. Steven Gieseg, for all the assistance he has provided throughout my PhD. I am also grateful for the guidance provided by my co-supervisor, Professor Bill Davison. Special thanks to Professor Matt Whiteman from University of Exetor, UK for inspiring us to get into this area of research, for all the valuable advice throughout my PhD, and especially for many of the specific inhibitors and probes. I would also want to thank Dr Mark Hampton and Sarah Cuddihy for giving me guidance and for their gift of protease inhibitors and β-actin antibody to the Free Radical Biochemistry Laboratory; Professor Christine Winterbourn, Professor Tony Kettle and Stephanie Bozonet for their guidance and for allowing me to stay with their groups during the SFRRA conference in Melbourne. Special thanks to Dr Drusilla Mason for all the support and for sharing her biohazard hood and laboratory equipment, and Dr David Collings for his comments and advice on my fluorescence microscopy work. A big thank you also to Professor Barry Hick for his valuable advice.

Thanks to all the technical staff in the School of Biological Sciences. In particular, Claire Galilee and Maggie Tisch for their help with keeping the laboratory running smoothly; Jan Mckenzie for assistance with the fluorescence microscope; Franz Ditz and Nick Etheridge for maintaining the laboratory equipment; Jackie Healy for assistance with the SDS-PAGE analysis; Gavin Robinson for keeping the laboratory's gas cylinders well stocked and John Scott for solving computer problems.

This research would not have been possible without the steady supply of blood from the haemochromatosis patients; a big thank to all of the blood donors. Thanks also to the New Zealand Blood Service (Riccarton branch) for collecting the haemochromatosis blood. In addition, I wish to express my gratitude to Dr Barry Hock for his gift of IFN-γ and GMCSF to the Free Radical Biochemistry Laboratory. Special thanks to the National Heart Foundation of New Zealand for partially funding my research.

A big thank you to all the members of the Free Radical Biochemistry Laboratory, in particular Linzi, Carole, Anna, Nick, Zunika, Hanadi, Rebecca, Lucy, Anastasia, Raj and Elizabeth for the warm encouragement and support through all the good and bad times. Special thanks to Zunika and Hanadi for listening to my complaints and whining throughout my PhD, and special thanks to Lucy and Anastasia for proof-reading my thesis. I also want to express my gratitude towards my other friends, especially Sandi for helping with my poster making and keeping me from becoming a nerd in the laboratory.

I also want to say thank you to Bobby, Gloria, Casey, Steven and Bon for giving me support, playing Wii with me, and going to movies and karaoke with me. I also want to thank Keni for being patient with me when I am grumpy, for providing entertainment, and for fixing my computer whenever there is a problem. My PhD life would have been a living hell without you. I also want to give my deepest love to my beloved cat Evy for making me laugh and accompanying me when I was under tremendous pressure and crying.

[Frontiers in BIoscience 14, 1230-1246, January 1, 2009]
Macrophage antioxidant protection within atherosclerotic plaques
Steven P. Giesegt, David S. Leake[1]
, Elizabeth M. Flavant, Zunlka Amltt, Linzl ReIdt, Ya-Ting Yangl
[1] Free Radical Biochemistry Laboratory, School of Biological Sciences, University of Canterbury, Private bag 4800, Christchurch, New Zealand, [2] Biomolecular Sciences Section, School of Biological Sciences, University of Reading, Whiteknights, P.O. Box 228, *Reading, Berkshire, RG6 6AJ. U.K.*
TABLE OF CONTENTS

1. ABSTRACT
Macrophage cells within inflammatory lesions are exposed to a wide range of degrading and cytotoxic molecules including reactive oxygen species. Unlike neutrophils, macrophages do not normally die in this environment but continue to generate oxidants, phagocytose cellular remains, and release a range of cytoactive agents which modulate the immune response. It is this potential of the macrophage cell to survive in an oxidative environment that allows the growth and complexity of advanced atherosclerotic plaques. This review will examine the oxidants encountered by macrophages within an atherosclerotic plaque and describe some of the potential antioxidant mechanisms which enable macrophages to function within inflammatory lesions. Ascorbate, a-tocopherol, and glutathione appear to be central to the protection of macrophages yet additional antioxidant mechanisms appear to be involved y-Interferon causes macrophages to generate 7,8-dihydroneopterinlneopterin and 3-hydroxyanthranilic acid both of which have antioxidant properties. Manganese superoxide dismutase is also upregulated in macrophages. The evidence that these antioxidants provide further protection, so allowing the macrophage cells to survive within sites of chronic inflammation such as atherosclerotic plaques, will be described.

DOI: http://dx.doi.org/10.2741/3305